Regional Hydrology and Simulation of Flow of Stratified-Drift Aquifers in the Glaciated Northeastern United States

By ANGELO L. KONTIS, ALLAN D. RANDALL, *and* DAVID L. MAZZAFERRO

REGIONAL AQUIFER-SYSTEM ANALYSIS—NORTHEASTERN UNITED STATES

U.S. GEOLOGICAL SURVEY PROFESSIONAL PAPER 1415–C

U.S. DEPARTMENT OF THE INTERIOR

GALE A. NORTON, ***Secretary***

U.S. GEOLOGICAL SURVEY

Charles G. Groat, ***Director***

Reston, Virginia 2004

ISBN 0-607-95458-2

For sale by U.S. Geological Survey, Branch of Information Services, Box 25286, Federal Center, Denver, CO 80225

FOREWORD

THE REGIONAL AQUIFER-SYSTEM ANALYSIS PROGRAM

The Regional Aquifer-System Analysis (ASA) Program represents a systematic effort to study a number of the Nation's most important aquifer systems, which, in aggregate, underlie much of the country and which represent an important component of the Nation's total water supply. In general, the boundaries of these studies are identified by the hydrologic extent of each system and, accordingly, transcend the political subdivisions to which investigations have often arbitrarily been limited in the past. The broad objective for each study is to assemble geologic, hydrologic, and geochemical information; to analyze and develop an understanding of the system; and to develop predictive capabilities that will contribute to the effective management of the system. The use of computer simulation is an important element of the RASA studies to develop an understanding of the natural, undisturbed hydrologic system and the changes brought about in it by human activities, and to provide a means of predicting the regional effects of future pumping or other stresses.

The final interpretive results of the RASA Program are presented in a series of U.S. Geological Survey Professional Papers that describe the geology, hydrology, and geochemistry of each regional aquifer system. Each study within the RASA Program is assigned a single Professional Paper number beginning with Professional Paper 1400.

Charles G. Groat
Director

CONTENTS

ILLUSTRATIONS

TABLES

CONVERSION FACTORS

Multiply inch-pound unit	By	To obtain SI unit
	Length	
inch (in)	25.40	millimeter
foot(ft)	0.3048	meter
mile (mi)	1.609	kilometer
	Area	
square foot (ft^2)	0.09290	square meter
square mile (mi^2)	2.590	square kilometer
	Volume	
gallon (gal)	0.003785	cubic meter
million gallons (Mgal)	3,785	cubic meter
cubic foot (ft^3)	0.02832	cubic meter
	Flow	
foot per second(ft/s	0.3048	meter per second
foot per day (ft/d)	0.3048	meter per day
cubic foot per second (ft^3/s)	0.02832	cubic meter per second
cubic foot per second per square mile [(ft^3/s)/mi^2]	0.01093	cubic meter per second per square kilometer
gallon per minute (gal/min)	.06308	liters per second
gallon per minute per foot [(gal/min)/ft]	.2070	liters per second
million gallons per day (Mgal/d)	0.04381	cubic meter per second
	Temperature	
degree Fahrenheit (°F)	°C = 0.5556 (°F–32)	degree Celsius
	Hydraulic conductivity	
foot per day (ft/d)	0.3048	meter per day
foot per second (ft/s)	26,330	meter per day
	Transmissivity	
foot squared per day (ft^2/d)	0.09290	meter squared per day
	Leakance	
foot per day per foot [(ft/d)/ft]	1	meter per day per meter
foot per second per foot [(ft/s)/ft]	1	meter per second per meter
	Compressibility, Specific weight	
inches squared per pound (in^2/lb)	14.22	centimeters squared per kilogram
pounds per square inch per foot [(lb/in^2)/ft]	.231	kilograms per square centimeter per meter

VERTICAL DATUM

Sea Level: In this report "sea level" refers to the National Geodetic Vertical Datum of 1929 (NGVD of 1929)— a geodetic datum derived from a general adjustment of the first-order level nets of both the United States and Canada, formerly called "Sea Level Datum of 1929".

REGIONAL HYDROLOGY AND SIMULATION OF FLOW IN STRATIFIED-DRIFT AQUIFERS IN THE GLACIATED NORTHEASTERN UNITED STATES

BY ANGELO L. KONTIS, ALLAN D. RANDALL, AND DAVID L. MAZZAFERRO

ABSTRACT

The glaciated Northeast, which encompasses New England, New York, and northern parts of New Jersey, Pennsylvania, and Ohio, contains more than 5,000 aquifers composed of sand and gravel deposited by or in glacial meltwater. These stratified-drift aquifers are largely independent of one another but have similar hydraulic properties, similar modes of recharge and discharge, and similar interchange of water with regional streams that flow across them. Collectively, they are the principal source of ground water in this region, supplying about 1 billion gallons per day in 1987.

The first part of this paper summarizes knowledge of the hydrologic processes and properties that control the water resources of stratified-drift aquifers and the second part focuses on simulations of those aquifers. The paper includes regional maps of average precipitation, runoff, and evapotranspiration that are mutually consistent in that precipitation minus evapotranspiration equals runoff at all locations; each map reflects the spatial variation in both precipitation and runoff data. The low streamflows typical of late summer throughout the region reflect spatial variation in precipitation, in wetland area, and, most important, in properties of stratified-drift aquifers, chiefly their areal extent but also their hydraulic conductivity, specific yield, and topography. Large variations in annual precipitation between successive years or nearby basins are not accompanied by large variations in evapotranspiration. Ground-water evapotranspiration in the region is thought to decrease as depth to the water table increases beyond the reach of plant roots. In stratified drift, however, many trees send roots to depths of 20 feet or more. Seasonal changes in the relation of ground-water stage to base flow, which have been used to estimate ground-water evapotranspiration, can also be explained by seasonal variations in recharge resulting from variations in evapotranspiration from the unsaturated zone. Seasonal cycles in evapotranspiration and in river stage are the principal causes of water-table fluctuations in stratified-drift aquifers, but a persistent departure from average precipitation will cause a long-term net water-table rise or decline in stratified drift that is either remote from streams or somewhat fine-grained.

The horizontal hydraulic conductivity of stratified drift ranges from several feet per day for very fine sand to several thousand feet per day for gravel. Samples of clean, well-sorted sand, analyzed in the laboratory for the relation between grain size and hydraulic conductivity shows with remarkable consistency an upper limit of hydraulic conductivity, which increases as a log-linear function of median grain size. The hydraulic conductivity ranges over an order of magnitude below the upper limit in each grain-size class as a result of decreased sorting or increased silt content. Transmissivity of stratified drift has been estimated at many sites in the glaciated Northeast from aquifer tests, specific capacity tests, or the summing of estimated hydraulic conductivity values assigned to lithologic descriptions in borehole logs; where two or three of these approaches have been applied at the same sites, however, the results are only weakly correlated.

Stratified drift is found chiefly in valleys and includes three facies: (1) older sand and gravel, deposited along the sides and bedrock floor of the valley, (2) younger fine-grained sediment, and (3) still younger surficial sand and gravel. Each facies overlies parts of those deposited earlier, and each is discontinuously present in nearly every valley. Accordingly, a ground-water flow model of an entire valley fill would ordinarily require at least three layers, or a quasi-three-dimensional two-layer design that can implicitly account for a discontinuous fine-grained confining layer. Valley-fill aquifers are common throughout the glaciated Northeast. Headwater aquifers are valley-fill aquifers that are not crossed by large perennial streams, so withdrawals during periods of low streamflow would deplete streamflow downvalley by only a small fraction of the withdrawal. Less common aquifer types include outwash-plain, sand-plain, and hillside aquifers, all of which are inherently single surficial geologic units but could be simulated by two model layers to represent a typical decrease in grain size with depth or to test the common assumption that flow is virtually horizontal.

Stratified-drift aquifers are recharged not only by direct infiltration of precipitation but also by seepage losses from upland streams as they cross the aquifers, and by unchanneled surface and subsurface runoff from upland hillsides that border stratified drift. Where relief from valley floor to nearby hilltops exceeds 500 feet, upland runoff commonly provides more than half the recharge to valley-fill aquifers. A new method of simulating the components of recharge, termed the Variable-Recharge procedure, was developed for use with the U.S. Geological Survey modular three-dimensional finite-difference ground-water flow model. In this procedure, a quantity termed "water available for recharge" is applied uniformly to all model cells; it is generally calculated as monthly precipitation for the period of interest minus average monthly evapotranspiration (which, in turn, is calculated as the difference between average annual precipitation and runoff, distributed appropriately by months). The water available for recharge is accepted as recharge in any model cell only if the simulated head in that cell is lower than land surface. Thus, the Variable-Recharge procedure can simulate variations in recharge with time in response to changes in the configuration of the water table as well as changes in water available for recharge. If model boundaries are placed along topographic divides within uplands that border a valley-fill aquifer, the procedure will calculate the amount of water rejected as recharge and any simulated ground-water discharge from upland model cells, and will redistribute that water to adjacent margins of the valley-fill aquifer or to upland streams that drain across the aquifer.

An additional potential major source of recharge to most valley-fill aquifers is induced infiltration from streams. Streambeds are commonly conceptualized as a layer of sediment only a few feet thick that is less permeable than the underlying aquifer and restricts induced infiltration, although exceptions have been reported. Streambed leakance (vertical hydraulic conductivity of a streambed divided by streambed thickness) is probably less than 1 foot per day per foot for most large streams in the glaciated Northeast, but commonly

exceeds 1 foot per day per foot for small streams. Estimates of streambed leakance depend on accurate and spatially representative measurements of head difference across the streambed and of streamflow loss or downward infiltration velocity. Several methods of evaluating streambed leakance are reviewed. A range of plausible streambed leakance values calculated from different field data were incorporated in a set of alternative ground-water flow models of the Rockaway River valley at Dover, N.J. Each of the models at Dover could be calibrated equally well to head measurements in wells, and simulated streamflow loss near a riparian well field was proportional to the leakance specified in each model. Therefore, the calibration process could not discern which leakance value was most nearly correct. Knowledge of streamflow loss as well as head distribution is necessary to estimate streambed leakance by model calibration, just as with analytical methods. Calibration to a two-day flood event indicated that the storage coefficient of the valley fill was about 0.1, much less than specific yields commonly derived from laboratory tests but comparable to values commonly derived from aquifer tests, thus supporting use of storage coefficient values of about 0.1 for simulation of aquifer response to changes in stress of a few weeks or less duration.

Models of ground-water flow in stratified-drift aquifers in the Rockaway River valley at Dover, N.J. and in the Killbuck Creek valley at Wooster, Ohio were extended into adjacent uplands to demonstrate application of the Variable-Recharge procedure in simulating the upland contribution to valley recharge. For Killbuck Creek valley, a three-layer steady-state model was calibrated to water levels, pumpage, and streamflow gains or losses near two municipal well fields measured in the fall of 1984 and 1986. The model was tested by transient-state simulation of an 11-day episode of high runoff. For the Rockaway River valley, six alternative, two-layer transient-state models were calibrated to water levels, pumpage, and stream stage near a municipal well field over a two-year period; the six models encompassed plausible ranges in specified values of several hydraulic properties. Model design, inputs, and calibration are discussed in some detail, with emphasis on the requirements and results of the Variable-Recharge procedure. As simulated hydraulic conductivity in the uplands was increased, the upland water-table configuration became a progressively more subdued, smoother representation of land-surface topography, upland recharge increased and a larger proportion of ground-water flow paths were directed to the major valleys rather than to small upland streams. Upland runoff ranged from 12 to 28 percent of total recharge to the Rockaway River valley over the two-year simulation period when horizontal hydraulic conductivity of the uplands was 0.25 feet per day, but increased to 24 to 43 percent of valley recharge when horizontal hydraulic conductivity was increased to 4 to 6 feet per day. Upland runoff accounted for 63 percent of simulated steady-state recharge to Killbuck Creek valley, where relief was higher than along the Rockaway River. In both models, all of the simulated recharge on upland hillsides eventually recharged the valley-fill aquifer as lateral ground-water flow, whereas rejected recharge and upland discharge, routed as surface runoff to the margin of the aquifer by the Variable-Recharge procedure, did not all become recharge to that aquifer because at high rates of simulated surface runoff the water table in parts of the valley fill rose to or near land surface. Consequently, the magnitude of recharge to valley-fill aquifers from upland runoff can be expected to increase with increasing horizontal hydraulic conductivity (or vertical leakance) in the bordering uplands.

Few data were obtained for model input or calibration in the uplands bordering the Killbuck Creek and Rockaway River valleys, because the Variable-Recharge procedure and model extension into the uplands were not anticipated at the time of data collection. Nevertheless, a plausible distribution and range of upland recharge, surface runoff, and resultant recharge to the valley fill were achieved; the range of uncertainty could easily be reduced by modest amounts of upland data. The explicit inclusion of adjacent uplands in a valley-fill aquifer model and the application of the Variable-Recharge procedure increase the amount of model input required and the overall complexity of the model, but allow for study of a major component of aquifer recharge, simulation of upland runoff for multiple stress periods with minimal effort, and improved delineation of the upland contributing areas to well fields.

The Killbuck Creek and Rockaway River models incorporate several techniques in addition to the Variable-Recharge procedure that could be useful in simulations of stratified-drift aquifers:

1. If the magnitude or distribution of stresses on the day water levels are measured for model calibration differ appreciably from average stresses over the previous month, simulation of a month-long stress period followed by a 1-day stress period will facilitate calibration.

2. Calibration can be facilitated by interpolating simulated heads at a grid spacing finer than the model grid, such that the simulated heads are more representative of the observed heads used in model calibration.

3. The contact between a surficial stratified-drift aquifer and underlying fine-grained stratified drift, till, or bedrock is commonly treated as a zero-flow boundary, which is probably a valid assumption for most modeling purposes but a basal layer of uniform hydraulic properties can easily be added to the model to test this assumption.

INTRODUCTION

The U.S. Geological Survey has studied more than 24 regional aquifer systems throughout the United States as part of its Regional Aquifer-System Analysis (RASA) program. The purpose of this program is described in the Foreword of this report, and results of numerous RASA studies have been summarized or cited by Sun (1986), Sun and Weeks (1991), and Sun and Johnston (1994). Most RASA studies have investigated a single aquifer, or set of overlapping aquifers, that continuously underlies an area of a few hundred to a few thousand square miles, and have developed a single ground-water flow model of the entire aquifer system and(or) models of a few large subregions that collectively comprise the entire system. Other RASA studies, including this one, have investigated regions that contain only local aquifers that are largely independent of one another but are geologically and hydrologically similar. Detailed investigations and models of a few representative aquifers within such regions can establish hydrologic principles that could be applied to other aquifers in the same region.

This RASA study addresses the many aquifers composed of unconsolidated sand and gravel that overlie bedrock in the glaciated northeastern United States, an area of 122,000 mi^2 that includes the six New England States, New York, and parts of Ohio, Pennsylvania, and New Jersey (fig. 1). The northern boundary of this region (for the purposes of this report) is the border between the United States and Canada, and the southern boundary generally coincides with the southern extent of Pleistocene continental glaciation. Long Island, N.Y., Cape Cod, and the islands of Massachusetts were excluded from the study because their glacial deposits are surrounded by salt water and underlain by older unconsolidated sediments far more permeable than the bedrock elsewhere in the glaciated Northeast. The glaciated northeastern United States contains more than 5,000 distinct aquifers composed of stratified sand and gravel deposited by or in glacial meltwater. These sand-and-gravel aquifers, along with contemporaneous deposits of silt and clay that locally confine or impede ground-water flow, are collectively termed "stratified drift". Most of these aquifers underlie only a few square miles, occur within bedrock valleys, and are hydraulically

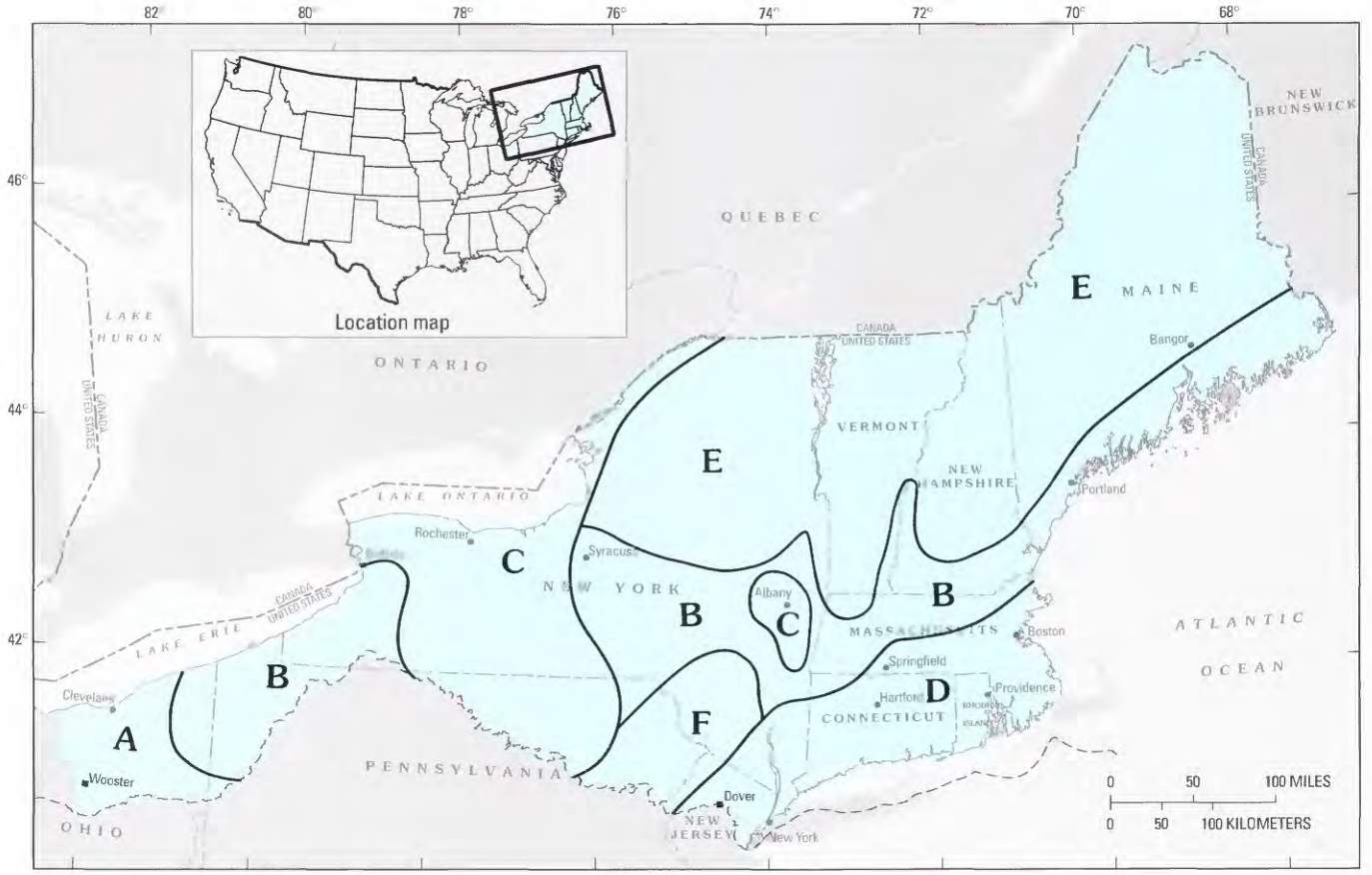

EXPLANATION

The glaciated Northeast, as described herein

E — Climatic region refered to in text

Southern limit of late Wisconsinan (Pleistocene) glaciation

Wooster — Location of ground-water flow model discussed in text

FIGURE 1.—Extent of the glaciated northeastern United States. The locations of ground-water flow models and climatic regions discussed in this report are also shown.

connected to streams. These aquifers are the principal source of ground water in the northeastern United States; many are individually capable of yielding more than 1 million gal/d, and collectively they supplied about 1 billion gal/d in 1987 (U.S. Geological Survey, 1990). The individual aquifers are generally not in contact with one another, and a single ground-water flow model that simulated all of these numerous, discontinuous aquifers, or even most of them, would be impossible to construct. Nevertheless, these aquifers can be viewed as a regional aquifer system in that they have a common mode of origin, have similar hydraulic characteristics, respond to recharge and pumping in similar ways, and commonly are hydraulically connected to the regional streams that flow across them. The approach used in this RASA study to characterize the stratified-drift aquifers in the glaciated Northeast was to investigate selected localities, review the literature on other localities, and present concepts, generalizations, representative values of aquifer properties, and simulation techniques that are applicable to individual aquifers throughout the region.

PURPOSE AND SCOPE

The principal findings of this RASA study are presented in three chapters of Professional Paper 1415. Chapter A (Haeni, 1995) describes several geophysical techniques that are well suited to delineation of stratified-drift aquifers. Chapter B (Randall, 2001) explains several geologic concepts that are widely applicable in interpreting the extent and satu-

rated thickness of stratified-drift aquifers, and presents capsule summaries of aquifer geometry in several subregions. Chapter C (this paper) reviews what is known about the magnitude of hydrologic processes and properties in stratified-drift aquifers, and suggests ways to facilitate simulation of these aquifers by ground-water flow models. The first part of this paper describes the hydrologic setting and processes that are common to most stratified-drift aquifers, and categorizes the aquifers into groups that have similar recharge potential and spatial position relative to bedrock, fine-grained glacial drift, and streams. It lists representative values of aquifer properties, and describes in general terms how ground-water flow systems function in this region. It also explains ways in which flow-system components may be simulated, the effects of lack of information on simulation results, methods for estimating the magnitude of certain hydraulic properties that are commonly used in simulation when site-specific data are unavailable, and a new method for simulating aquifer recharge. This new method, termed the Variable-Recharge procedure, allows explicit simulation of the uplands bordering a valley-fill aquifer to better represent recharge to the valley fill from upland sources. The second part of this paper illustrates various aspects of the simulation process, including the Variable-Recharge procedure, by describing models of ground-water flow that were designed during this study for two representative valley-fill aquifer systems, at Dover, N.J. and Wooster, Ohio.

PREVIOUS WORK

Many studies of individual aquifers or groups of aquifers in the glaciated Northeast have been published by the U.S. Geological Survey, by geological, environmental, and natural-resource agencies of the States in the region, and by others. A bibliography of literature relating to ground water of the glaciated Northeast (Wiltshire and others, 1986) catalogued 34 regional studies and more than 700 local or statewide investigations. A summary of the ground-water resources of each State in the region was included in a National Water Summary by the U.S. Geological Survey (1990), and the ground-water hydrology of New York and New England was summarized by Olcott (1995).

ACKNOWLEDGMENTS

The authors thank their U.S. Geological Survey colleague Forest P. Lyford for guidance and advice during early phases of the study, especially with regard to concepts underlying the development of the Variable-Recharge procedure. Appreciation is also extended to many individuals associated with the U.S. Geological Survey and Federal, State, and local agencies in the Northeast who provided data and offered suggestions on the conduct of the study and preparation of this report.

HYDROGEOLOGIC SETTING

The landscape of the glaciated Northeast can be divided into three broad physiographic categories:

1. Lowlands, where land surface is generally less than 500 feet above sea level (slightly higher in lowlands distant from the coast) and relief between hilltops and major valleys is generally less than 300 feet.
2. Plateaus, uplands, or hills, where land surface is generally less than 2,000 feet above sea level (slightly higher in southwestern New York) and relief between hilltops and major valleys is generally between 300 and 1,000 feet.
3. Mountains, where land surface is more than 2,000 feet above sea level in many places and ridges or peaks commonly rise more than 1,000 feet above the major valleys.

The distribution of these physiographic categories is shown in figure 2. The altitude and relief of the land surface had an effect on the distribution of proglacial water bodies and ice dynamics during deglaciation, thus constraining the distribution of stratified drift (Randall, 2001), and today influences the distribution of precipitation, runoff, and recharge to stratified-drift aquifers (Morrissey and others, 1988; Lyford and Cohen, 1988 and references therein) as discussed later in this paper.

REGIONAL GEOLOGIC UNITS

Earth materials in the glaciated Northeast include three fundamental geologic units—bedrock, till, and stratified drift. Bedrock, hard and consolidated, underlies the entire region, but is mantled nearly everywhere by unconsolidated glacial drift that includes till and(or) stratified drift. Till, a poorly sorted mixture of clay, silt, sand, and stones deposited directly from continental ice sheets, is the only unconsolidated material on most hills (fig. 3). Stratified drift, which consists of layered, sorted sediment, was deposited by meltwater in valleys or lowlands as the ice sheets retreated (Randall, 2001). Bedrock, till, and stratified drift are all tapped by wells. Sand and gravel deposits within the stratified drift are the only aquifers in which wells yielding hundreds of gallons per minute can generally be completed, but most of those stratified-drift aquifers are recharged by flow systems that include the adjacent till and bedrock (fig. 3). The geologic variability and aquifer potential of bedrock, till, and stratified drift are discussed briefly below. Hydraulic properties, recharge, and simulation of stratified-drift aquifers are discussed in greater detail in later sections.

BEDROCK

A variety of bedrock lithologies occur in the glaciated Northeast. The distribution of several lithologic categories that have hydrologic significance is shown in figure 4. All these categories are similar in that water movement is con-

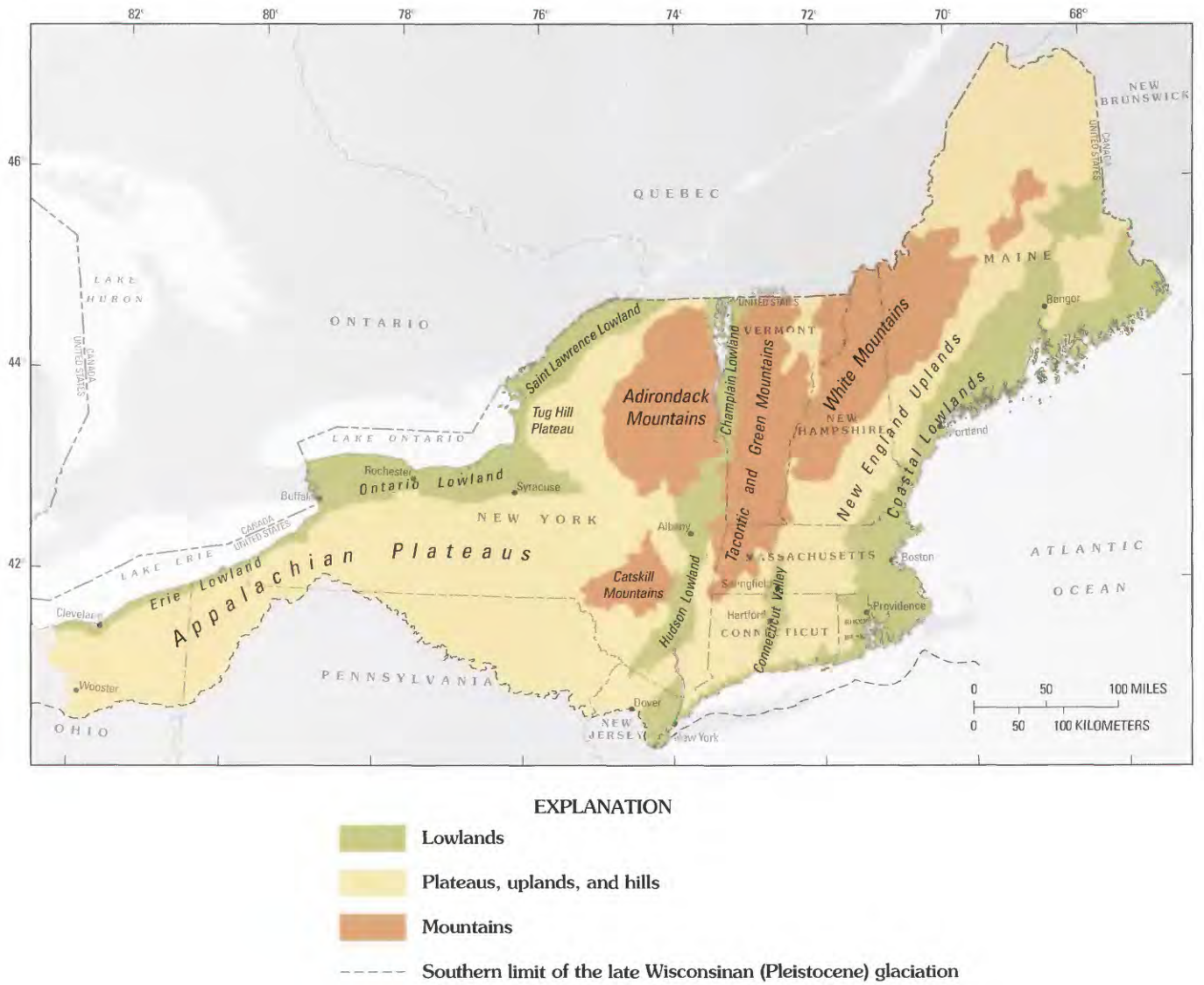

FIGURE 2.—Physiographic divisions of the glaciated Northeast (adapted from Denny, 1982, Cressy, 1966, and 1:250,000-scale topographic maps).

trolled by secondary permeability -- the joints or fractures that occur in all kinds of bedrock, are especially persistent along bedding planes in sedimentary bedrock, and have been locally enlarged by solution in carbonate and evaporite rock. The number and size of water-yielding fractures tend to decrease with depth; a variety of evidence that supports or fails to support this concept is cited and briefly summarized by Randall and others (1988a) and by Trainer (1988). A complementary conceptual model that considers fractures to occur chiefly at shallow depth in the Appalachian Plateau is presented by Wyrick and Borchers (1981).

Most bedrock in the region stores and transmits water only in fractures. The youngest sandstone formations, however, have retained some of their primary (intergranular) porosity (fig. 4). Although the porosity in these sandstones varies from place to place and contributes little to water-transmitting potential, water storage in intergranular pore space can make an appreciable contribution to aquifer yield. Porosity is progressively less important in rocks that are older, finer grained, and further east where metamorphic recrystallization was relatively intense.

In carbonate bedrock and in the evaporite-bearing shale of central New York, fractures and bedding planes that have been enlarged by solution are widely but unevenly distributed. Caves and conduits are common along the Helderberg escarpment of eastern and central New York (Baker, 1976; Palmer and others, 1991) but apparently are less abundant in most other areas of carbonate rock. Trainer and Salvas (1962) and Johnston (1964) provide detailed descriptions of dolomite aquifers in which ground-water flow is largely restricted

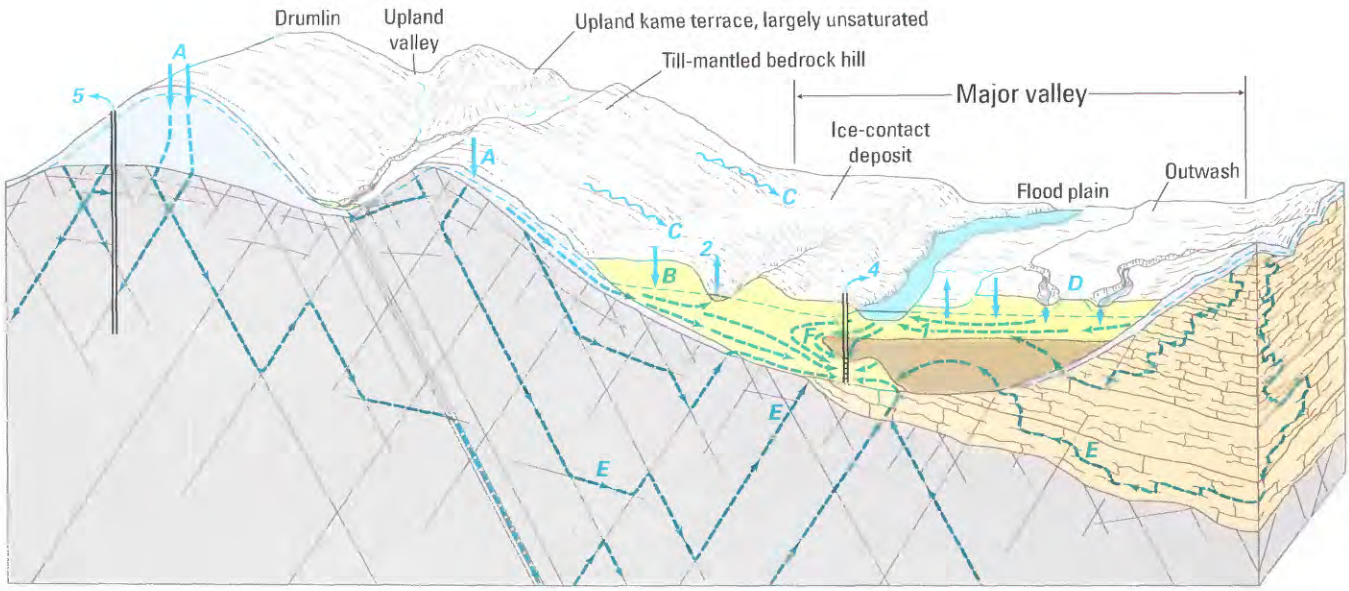

EXPLANATION

Geologic material in vertical section

- Till
- Sand, gravel
- Fine sand, silt, clay
- Porous bedrock
- Nonporous bedrock

Water table

Direction of ground-water flow

Well

Recharge to bedrock

A — Infiltration of precipitation through till in uplands

Recharge to stratified drift

B — Precipitation on valley floor, which infiltrates to water table unless diverted as evapotranspiration or as storm runoff from pavement or saturated soil

C — Runoff from adjacent till-covered hillsides at shallow depth through sandy till, through soil horizons, and (or) as surface rivulets

D — Continuous natural seepage losses from small tributaries not incised to the water table

E — Lateral and upward flow from deep circulation systems through bedrock

F — Induced infiltration from rivers near large-capacity wells where the water table is lowered by pumping

Discharge from stratified drift

1 — Seepage to river

2 — Ground-water evapotranspiration where the water table is shallow

3 — Underflow downvalley through stratified drift (not shown)

4 — Pumpage from well screened in stratified drift

Discharge from bedrock

5 — Pumpage from well that intersects fractures

FIGURE 3.—Idealized distribution of geologic units and ground-water flow in a valley-fill aquifer system. Not to scale; major valleys actually occupy only 5 to 30 percent of large basins (from Randall and others, 1988a, fig. 1).

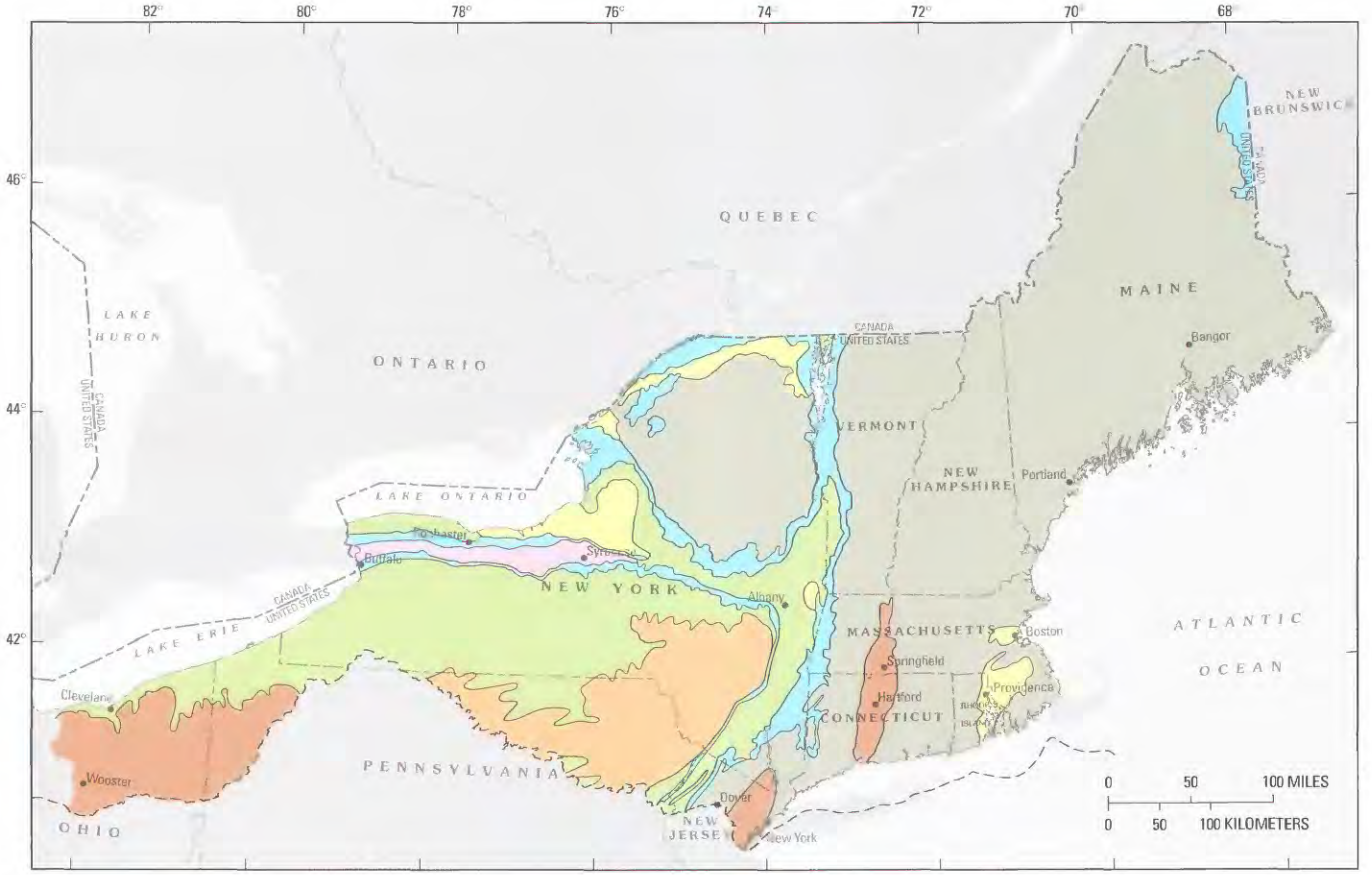

EXPLANATION

- Carbonates (limestone, dolomite, marble) locally interspersed with other lithologies
- Sandstone and shale, with some primary porosity
- Sandstone, indurated, nonporous
- Sandstone, coarse to fine, siltstone, and shale; nonmarine origin
- Shale, siltstone, fine sandstone; marine origin
- Shale with evaporites (gypsum, salt, anhydrite)
- Crystalline bedrock (metamorphic, igneous); nonporous
- Geologic contact
- Southern limit of late Wisconsinan (Pleistocene) glaciation

FIGURE 4.—Generalized distribution of bedrock lithology in the glaciated Northeast (adapted from Denny, 1982; Heath, 1964; Osberg and others, 1984; Fisher and others, 1970; Lloyd and Lyke, 1995; Meade, 1978; and other sources).

to solution-enlarged bedding planes that are separated by relatively impermeable rock little affected by solution. Other studies have shown that many wells penetrating carbonate bedrock have yields and depths of penetration that are indistinguishable from wells in nearby clastic or crystalline bedrock, indicating that no solution-enlarged fractures were penetrated (Frimpter, 1972, p. 56; Lloyd and Carswell, 1981, p.19). Water in carbonate bedrock is typically hard, and water in the shale-evaporite unit (fig. 4) can be highly mineralized.

Well Yields

The least productive bedrock in the glaciated Northeast is probably the shale that borders the south shores of Lakes Erie

and Ontario (Johnston, 1964; Richards and others, 1987; Lloyd and Lyke, 1995). Median well yield is only 2 gal/min in some localities. Water is obtained chiefly from fractures in the uppermost foot or so of bedrock, and where this zone is above the water table many holes yield virtually no water (Johnston, 1964). Elsewhere in the glaciated Northeast, 2 to 5 gal/min can be obtained from a well at almost any location, and yields of 10 to 30 gal/min are widely reported. In the extensive areas of nonporous fractured crystalline rock, shale, and indurated sandstones, yields greater than 100 gal/min have been obtained only in scattered localities, apparently where intense fracturing has increased transmissivity. Carbonate bedrock can yield several hundred gallons per minute where fractures are abundant or enlarged by solution, even though intervening areas are unproductive (Norvitch and Lamb, 1966; Johnston, 1964; Giese and Hobba, 1970). The porous sandstone and shale in central Connecticut and Massachusetts, southeastern New York, and northern New Jersey yield a few hundred gal/min to many deep municipal and industrial wells (Ryder and others, 1981; Perlmutter, 1959; Carswell and Rooney, 1976; Nemickas, 1976). Well yields as large as 100 gal/min have been forecast for some sandstone units in Ohio and western Pennsylvania (Rau, 1969; Schiner and Gallaher, 1979).

Bedrock aquifers are an important water resource in the glaciated Northeast because they are present everywhere, even though the yields available from individual wells in bedrock are generally much smaller than yields available from wells in stratified drift. In many upland localities, bedrock is the sole dependable source, or the most economical source, of potable water for homes, commercial establishments, and small public-supply systems. Water withdrawn from bedrock aquifers constitutes a significant percentage of total groundwater withdrawals throughout the region (table 1).

TABLE 1.—*Estimated amounts of ground water withdrawals in 1985, and amounts supplied by bedrock aquifers, in the glaciated northeastern United States*

[Data from U.S. Geological Survey, 1990; Ohio, Pennsylvania, and New Jersey are excluded because available data from those states do not distinguish withdrawals within the glaciated Northeast. Mgal/d, million gallons per day]

State	Ground-water withdrawals		
	Total (Mgal/d)	Amount from bedrock (Mgal/d)	Amount from bedrock, as percentage of total
Connecticut	144	60	42
Maine	66	21	32
Massachusetts[a]	299	no data	no data
New Hampshire	83	20[c]	24
New York[b]	631	257[c]	41
Rhode Island	27	5.5[c]	20
Vermont	37	13[c]	35
TOTAL	1,287		

[a] Excludes Cape Cod and islands.
[b] Excludes Long Island.
[c] Reduced 10 percent from number in cited source that includes withdrawals from till.

Hydraulic Properties

Median hydraulic conductivity and median specific capacity of wells completed in bedrock are reported in table 2 for several rock types and locations in the glaciated Northeast. Measurement conditions and environmental factors other than rock type can affect specific capacity and similarly affect estimates of hydraulic conductivity based on specific capacity. For example, specific capacity increases with well diameter and decreases with duration of pumping. It commonly decreases with magnitude of drawdown in fractured bedrock where large drawdowns can cause turbulent flow and where well head often falls below some fractures (Randall and others, 1966, fig. 37). Municipal, commercial, and industrial wells commonly have larger average specific capacity than domestic wells, because their diameters and depths are usually larger and because unsuccessful holes are abandoned and thus are not reflected in the computation of average values. Recharge from saturated sand and gravel overlying bedrock or from streams can stabilize specific capacity at values larger than would otherwise be obtained. Many of the sources cited in table 2 considered some of these factors, but because the numeric values in the table are qualified in such a variety of ways, no attempt is made in this paper to select a single representative value for each rock type. Nevertheless, the numeric values in table 2 are, as might be expected, generally higher for the porous sandstones and for the evaporite and carbonate bedrock units than for the crystalline and indurated clastic sediments that predominate in the glaciated Northeast.

Few data on storage properties of bedrock in the region are available. Randall and others (1988a) computed a median storage coefficient of 2×10^{-5} from pumping tests of 32 wells in crystalline bedrock. A median storage coefficient of 1.65×10^{-5} can be computed from pumping tests of 8 wells tapping dolomite in New York (Trainer and Salvas, 1962; Johnston, 1964). Carswell and Bennett (1963) recommend using a storage coefficient of 1×10^{-3} for porous sandstones in part of western Pennsylvania, on the basis of several pumping tests. The porous sandstones delineated in figure 4 have variable but apparently significant primary porosity; Perlmutter (1959) reports a median porosity of 0.098 in 11 samples from southeastern New York, and Heald (1956) reports a porosity

TABLE 2.—*Hydraulic conductivity of bedrock and specific capacity of wells penetrating bedrock in the glaciated Northeast*

[(gal/min)/ft, gallons per minute per foot; ft, feet; ft/d, feet per day; h, hour; in., inch. Dash means data for computation of median value not given in reference cited]

Bedrock type	Location	Median		Basis for computation	Reference
		Specific capacity [(gal/min)/ft]	Hydraulic conductivity (ft/d)[a]		
Crystalline	Northeastern Conn.	0.19	0.45	Specific capacity of 219 domestic wells	Randall and others, 1966
		0.30	0.6	Specific capacity of 28 commercial and industrial wells	do.
Crystalline	New England, Northern N.Y., Atlantic Canada	—	0.9	Pumping tests of 32 industrial and municipal wells; most intersect fracture zones	Randall and others, 1988a
Shale etc., marine	South-central N.Y.	0.46	—	180-day specific capacity of 66 wells, mostly in valleys. Median computed after excluding 11 low-yield wells	Hollyday, 1969
Sandstone etc., non-marine	Northeastern Pa.	0.25	—	Specific capacity of 101 domestic wells	Carswell and Lloyd, 1979
Siltstone	do.	0.18	—	Specific capacity of 32 domestic wells	do.
Shale	do.	0.28	—	Specific capacity of 27 domestic wells	do.
Sandstone, porous	Western Pa.	—	2.7	Pumping tests of 20 wells	Poth, 1963; Carswell and Bennett, 1963
Sandstone, porous	Northeastern Ohio				
(Berea)		1.5[b]	8.0[c]	Specific capacity of 319 wells	Rau, 1969
(Cussewago)		5.3[b]	20.0[b]	Specific capacity of 79 wells	do.
Sandstone, porous	Western Pa.				
(Berea)		.79	—	Specific capacity of 75 wells	Schiner and Gallaher, 1979
(Cussewago)		.96	—	Specific capacity of 276 wells	do.
(Sharpsville)		.74	—	Specific capacity of 135 wells	do.
Sandstone & shale, porous	Central Conn.	0.4	0.3	Specific capacity of 401 wells; median penetration of 200 ft assumed	Ryder and others, 1981
do.	Central Conn.	—	1.6	Pumping tests of 5 industrial-commercial wells	Randall, 1964; USGS unpublished
do.	Southeastern N.Y.	1.8	1.8	8-hour pumping tests of 7 municipal wells	Perlmutter, 1959
do.	Northern N.J.	1.7	—	Specific capacity of 62 municipal-industrial wells 6 to 8 in. diam.	Nemickas, 1976
do.	do.	3.1	—	Specific capacity of 59 municipal-industrial wells ≥12 in. diam.	do.
Shale with evaporites	Western N.Y.	29	108	8-h pumping tests of 9 industrial-commercial wells in 4 localities	LaSala, 1968; Kammerer and Hobba, 1967
Carbonate	Western N.Y.	8.3	186	Pumping tests of 10 industrial-commercial wells in 8 localities	LaSala, 1968; Johnston, 1964
Carbonate	Northeastern Pa.	0.38	—	Specific capacity of 10 domestic wells	Carswell and Lloyd, 1979
Carbonate (dolomite)	Northern N.Y.	—	21	Pumping tests of 13 test wells	Trainer and Salvas, 1962
do.	do.	1.0	—	Specific capacity of 80 wells	do.

[a] Transmissivity divided by length of borehole open to bedrock below the end of the casing; values represent an isotropic hemogenous medium hydraulically equivalent to the real unit, which is heterogenous and may be anisotropic, with flow limited to fractures that intersect a small fraction of borehole length.

[b] Mean rather than median.

[c] Median of mean values for 8 counties.

of 0.05 for sandstones of central Connecticut and Massachusetts. These values fall somewhat below the range for porosity of sandstones from random sites in the United States as measured in the laboratory (Morris and Johnson, 1967).

TILL

Till is an unsorted, unstratified mixture of sediment particles that can range in size from clay to boulders. It was deposited directly by glacial ice, rather than by meltwater, and occurs as a discontinuous layer mantling the bedrock throughout the glaciated Northeast. Till is the only unconsolidated sediment atop bedrock in most upland areas, where it is typically 10 to 30 feet thick but locally as thick as 200 feet. In mountainous areas, till is commonly thin and interrupted by many bedrock outcrops (Soller, 1993), but thick till can be found in some valleys (Stewart and MacClintock, 1969). In the Appalachian Plateau, till preferentially accumulated on the south sides of hills (Coates, 1966); these thick "till shadows" locally encroach into major valleys in the Catskill region (Randall, 2001). In areas of low to moderate relief, thick till accumulations are generally limited to drumlins (fig. 3) and similar streamlined, elliptical hills composed partly of bedrock but reshaped by moving ice (Mazzaferro and others, 1979; Randall and others, 1966; Bradley, 1964). Till that mantles bedrock in the major valleys or lowlands, beneath stratified drift, is typically less than 10 feet thick (Melvin and others, 1992, p.8; Randall, 2001). In many valleys along the northern fringe of the Appalachian Plateau, till is interlayered with fine-grained stratified drift as well as directly overlying bedrock, reflecting multiple glacial readvances (Randall, 2001).

Although ice sheets transported some rock fragments tens or hundreds of miles, till was derived predominantly from bedrock within a mile or so up-ice (northerly) from the site of deposition. Therefore, till is rich in silt and clay in regions underlain by shale bedrock, but sandier and commonly very stony in regions underlain chiefly by harder, coarser-grained rocks such as sandstone and many types of crystalline rock (fig. 4). In many upland localities in New England, weakly consolidated till of superglacial origin, characterized by crude stratification and a matrix of mostly sand, overlies compact, well-consolidated nonstratified basal till with a matrix of sand and some silt; some of the compact till is abundantly fractured, oxidized, and significantly older than the rest (Pessl and Schafer, 1968; Koteff and Pessl, 1985; Newman and others, 1990). Till layers along the north slope of the Appalachian Plateau are especially fine grained and nonstony, because ice readvancing in ponded water eroded and incorporated lake-bottom fines.

The water-transmitting capacity of till is chiefly a function of grain size and depositional setting (Stephenson and others, 1988). In general, hydraulic conductivity and specific yield are lower in till with a silt-clay matrix than in sandy till (Morris and Johnson, 1967). Till deposited at the base of a glacier is greatly compacted and commonly also fractured by the weight and stress of the ice; therefore, intergranular hydraulic conductivity is very low, but secondary (fracture) hydraulic conductivity can be two or three orders of magnitude higher. Till deposited in a superglacial setting is unfractured but less compacted and commonly coarser and better sorted as a result of meltwater activity, so can have intergranular hydraulic conductivity two orders of magnitude greater than basal till (Stephenson and others, 1988, p.306; Randall and others, 1966, table 23). The hydraulic conductivity of till in southern New England, derived primarily from crystalline rocks, ranges generally from 3 to 0.01 ft/d horizontally and 2 to 0.0001 ft/d vertically; primary porosity generally ranges from 30 to 40 percent for unweathered superglacial till in areas of crystalline bedrock, and from 20 to 30 percent for older basal till in areas of sedimentary bedrock (Melvin and others, 1992). In an intensively studied locality in western New York (Prudic, 1986) till has an average hydraulic conductivity of 0.0001 ft/d horizontally and vertically, and an average porosity of 32.4 percent.

Small water supplies, such as for a home, can be obtained from large-diameter dug wells penetrating till, especially where the till is sandy or includes sand lenses and is thick enough to remain partly saturated throughout the year. Withdrawals of water stored within such wells are replenished by slow seepage during non-pumping periods. Thin gravel deposits beneath till along the preglacial axes of some upland valleys have been tapped by drilled wells. Where till is several tens of feet thick in upland localities, it serves to protect water quality in the underlying bedrock.

STRATIFIED DRIFT

Stratified drift consists of layered sediments, sorted to varying degrees by glacial meltwater and deposited in bodies of ponded water that existed temporarily during deglaciation in valleys or lowlands all across the glaciated Northeast. Where the relatively coarse deposits of sand and gravel are sufficiently thick and saturated, they constitute productive aquifers. Although the northeastern United States was glaciated more than once, the most recent ice sheet generally scoured away any older drift in major valleys; thus, all the stratified drift in most major valleys today was deposited during the retreat of the last ice sheet, from about 21,000 to about 12,000 years ago. The stratified drift consists of three types (facies), each of which can be found in nearly every valley or lowland (Randall, 2001):

1. Proximal ice-contact deposits (dominantly gravel and sand), laid down beneath or beside ice when the ice still occupied most of the valley or lowland. The most extensive ice-contact deposits are generally in areas where bedrock

is relatively close to land surface, typically along the valley sides.

2. Distal fine-grained deposits (silt, clay, some very fine sand) formed in large lakes or the sea, later in time and farther from the ice margin than the ice-contact deposits—that is, at any particular moment they were being laid down in open water well beyond the ice margin, mantling or bordering ice-contact deposits formed earlier when the ice margin was nearby.
3. Surficial coarse-grained deposits (sand and gravel) laid down as deltas where tributary or meltwater streams entered large water bodies, and as channel deposits where tributary or meltwater streams flowed across lowlands after the proglacial water bodies had either drained or become filled with sediment. These surficial coarse deposits commonly form a thin, partly saturated cap on top of the distal fine-grained deposits.

Aquifer geometry, defined as the three-dimensional distribution of coarse sand and gravel within the glacial drift, is discussed in detail by Randall (2001), who also provides capsule descriptions of typical aquifer geometry in each of several hydrophysiographic regions in the glaciated Northeast (fig. 5). The most widespread terrain (region A of fig. 5) is characterized by distinct valleys that generally sloped away from the ice and contain stratified sediments that were laid down within a succession of small lakes according to the morphosequence concept of deposition described by Koteff (1974) and Koteff and Pessl (1981).

REGIONAL HYDROLOGIC PROCESSES

Hydrologic processes that affect flow through stratified-drift aquifers include precipitation, air temperature, evapotranspiration, ground-water evapotranspiration, and runoff. Their characteristics and regional distribution are summarized in the following sections.

PRECIPITATION AND AIR TEMPERATURE

Long-term mean annual precipitation (1951-80) in the glaciated Northeast ranges from less than 30 in. immediately south of Lake Ontario and in northeasternmost New York to more than 60 in. near several mountain or plateau summits (pl. 1). Areas along the eastern seaboard and in the Catskill, Adirondack, Green, and White mountains generally receive 44 in. or more in an average year, while several inland lowlands average from 32 to 40 in. Precipitation in a single year occasionally departs 10 in. or more from the long-term average. Plate 1 may slightly underrepresent precipitation in high-relief areas, as discussed in the section "Mean Annual Runoff".

Precipitation generally increases with altitude. Several authors (Knox and Nordenson, 1955; Hely and others, 1961; Ku and others, 1975) used regression analysis to demonstrate an increase in precipitation with altitude over large areas in the glaciated Northeast. Hendrick and deAngelis (1976) showed that monthly precipitation during winter and spring in northern Vermont typically increases about 1/2 in. per 1,000 ft of altitude above 600 ft, and Dingman (1981) calculated that mean annual precipitation in New Hampshire and Vermont increases about 9 in. per 1,000 ft of altitude. Seasonal variation in precipitation throughout the Northeast is small, commonly less than 35 percent from month to month (fig. 6), although most areas west of New England receive somewhat less precipitation in winter than during the rest of the year (fig. 6; Dethier, 1966).

Mean annual snowfall ranges from about 35 in. in the lowland areas of New Jersey, Pennsylvania, and Ohio to more than 100 in. in the mountainous areas of New York and New England (U.S. Environmental Data Service, 1968). Mean water equivalent of snowpack on March 1 is plotted in figure 7. Annual snowfall and snowpack accumulation has a significant effect on seasonal runoff patterns and the seasonal availability of water for recharge (Lyford and Cohen, 1988).

Mean annual air temperatures at selected weather stations in the region are also plotted in figure 7. Mean annual air temperatures range from about 40°F in northern Maine to about 50°F in the southern part of the region. Generally, coastal areas have somewhat higher average air temperatures than inland areas. In the absence of site data, the following expression, derived by Lee (1969), provides a means of estimating mean annual air temperature:

$$T = 133.65 - 1.981\,L - (0.002867)\,A, \qquad (1)$$

where T is mean annual air temperature, in degrees Fahrenheit,
L is latitude, in decimal degrees, and
A is altitude, in feet.

EVAPOTRANSPIRATION

Evapotranspiration is the process by which water is changed from the liquid or solid state into the vapor state and transpiration is the process by which water vapor escapes from living plants into the atmosphere (Langbein and Iseri, 1960). Thus, recharge to an underlying aquifer derived from precipitation can be reduced or delayed by evapotranspiration. Evapotranspiration that removes water from below the water table, thereby providing a means of ground-water discharge, is referred to as ground-water evapotranspiration. Methods of estimating these quantities for various time periods, and nominal rates for the glaciated Northeast, are as follows.

Annual Evapotranspiration

Mean annual evapotranspiration in the glaciated Northeast ranges from about 24 in. in lowlands of New Jersey near

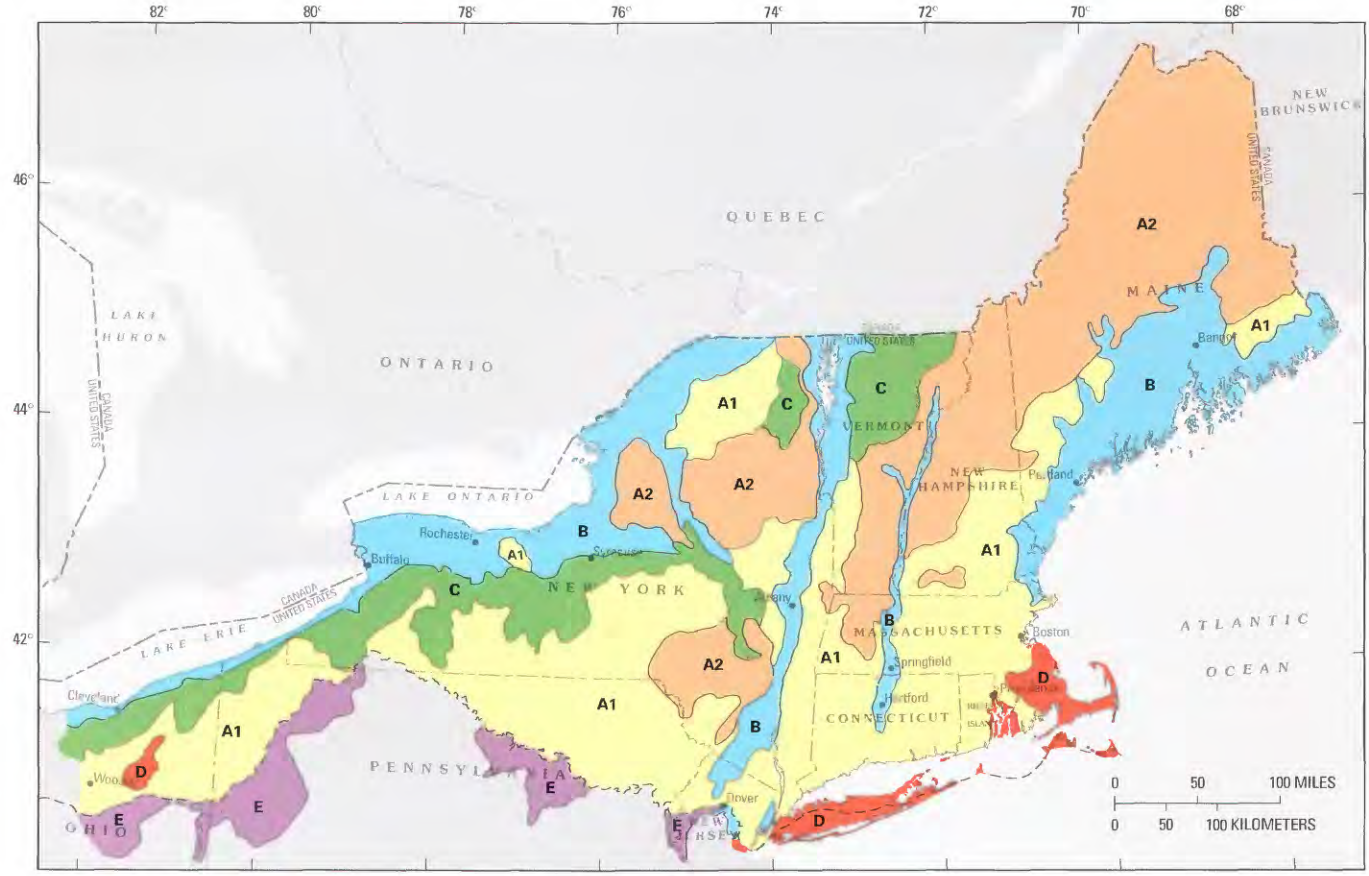

EXPLANATION

A	**Distinct valleys that generally drained away from ice; heterogenous stratified drift deposited in succesive small lakes**
A1	Extensive stratified valley fill
A2	Narrow or sparse stratified valley fill
B	**Broad lowlands innundated by large water bodies; extensive fines, locally extensive surficial sand plains and marginal deltas; little induced-recharge potential**
C	**Regions of high relief that drained toward the ice; thick drift, chiefly fines and (or) till**
D	**Extensive sandy outwash buries preglacial topography**
E	**Not recently glaciated; major valleys drained away from the ice and contain sandy outwash**
———	**Hydrophysiographic region boundary**
- - - - -	**Southern limit of the late Wisconsinan (Pleistocene) glaciation**

FIGURE 5.—Hydrophysiographic regions in the glaciated Northeast (simplified from Randall, 2001, pl. 1).

the southern limit of glaciation to about 16 in. in the mountains of northern New York and New England (pl. 1). The evapotranspiration rates on plate 1 were computed as the difference between mean annual precipitation and runoff for 1951-80 and compiled by a method described in the section "Mean Annual Runoff." Similar maps covering other time periods and different parts of the glaciated Northeast have been presented by Knox and Nordenson (1955), Hely and others (1961), and Church and others (1995, fig. 5*a*).

Another approach to estimating annual evapotranspiration was developed by Langbein and others (1949), who related mean annual evapotranspiration (*ET*), in inches, to mean annual air temperature (*T*), in degrees Fahrenheit, by the equation:

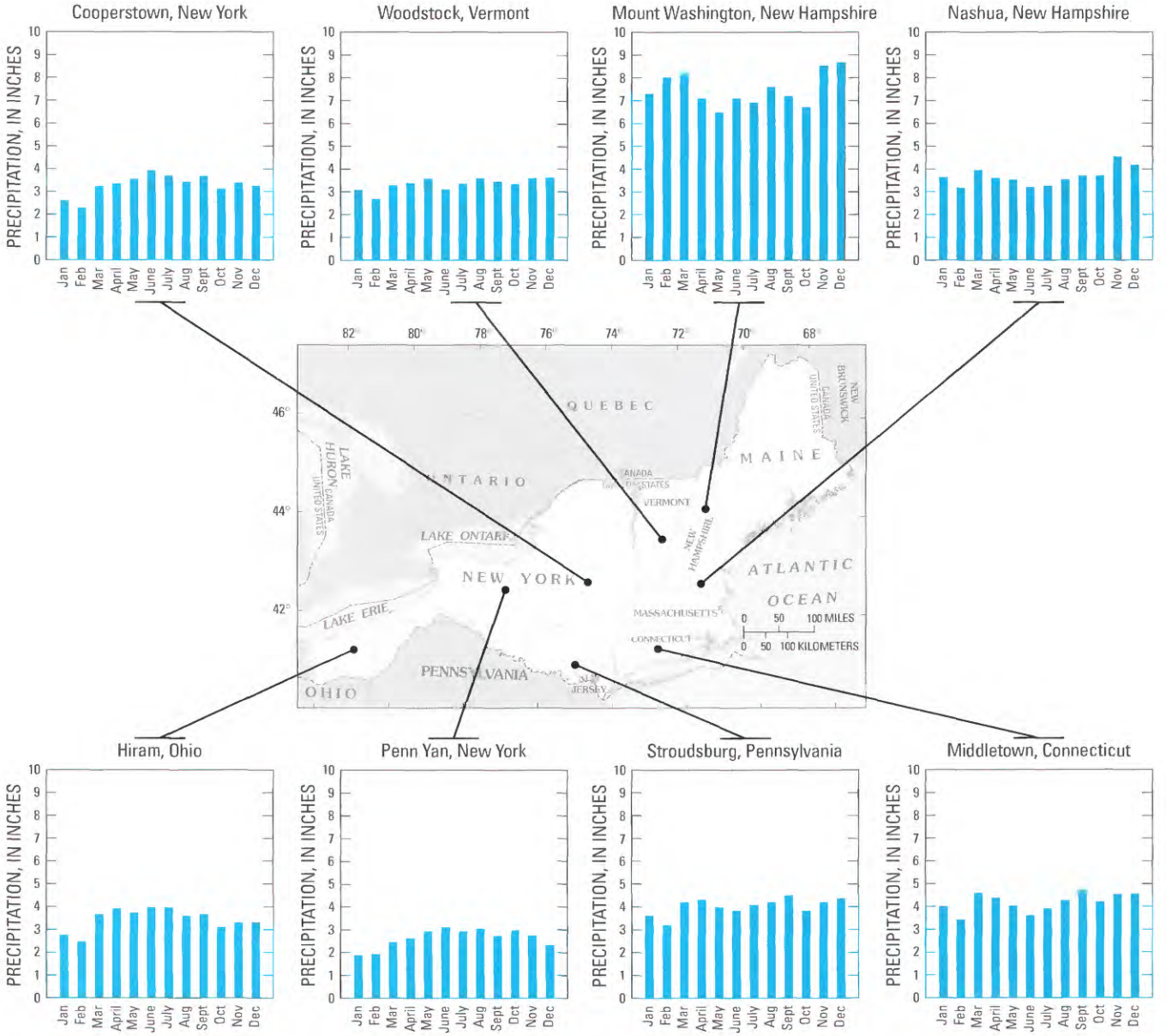

FIGURE 6.—Monthly mean precipitation values at eight stations in the glaciated Northeast, for 1951–80 (data from National Oceanic and Atmospheric Administration, 1985a,b).

$$ET = 0.73\,T - 12. \quad (2)$$

Combining equations 1 and 2 results in an expression that can be used to approximate evapotranspiration from latitude and altitude:

$$ET = 85.57 - 1.45\,L - 0.0021\,A. \quad (3)$$

Annual evapotranspiration in humid regions is constant or increases only slightly with increased precipitation (Johnstone and Cross, 1949, p. 105). The standard deviation of mean annual air temperature at sites in the glaciated Northeast has ranged from 1 to 1.5° F during 1931-80 (National Oceanic and Atmospheric Administration, 1981). Accordingly, equation 2 suggests that the standard deviation of mean annual evapotranspiration is on the order of 1 in. By contrast, the standard deviation of mean annual precipitation at sites in the glaciated Northeast has ranged from 4.5 to 7.5 in. during the same period (National Oceanic and Atmospheric Administration, 1981). Large variations in annual precipitation between successive years or nearby watersheds in the Northeast are typically accompanied by variations of similar magnitude in runoff, which requires that any variation in evapotranspiration with precipitation must be slight (Thomas,

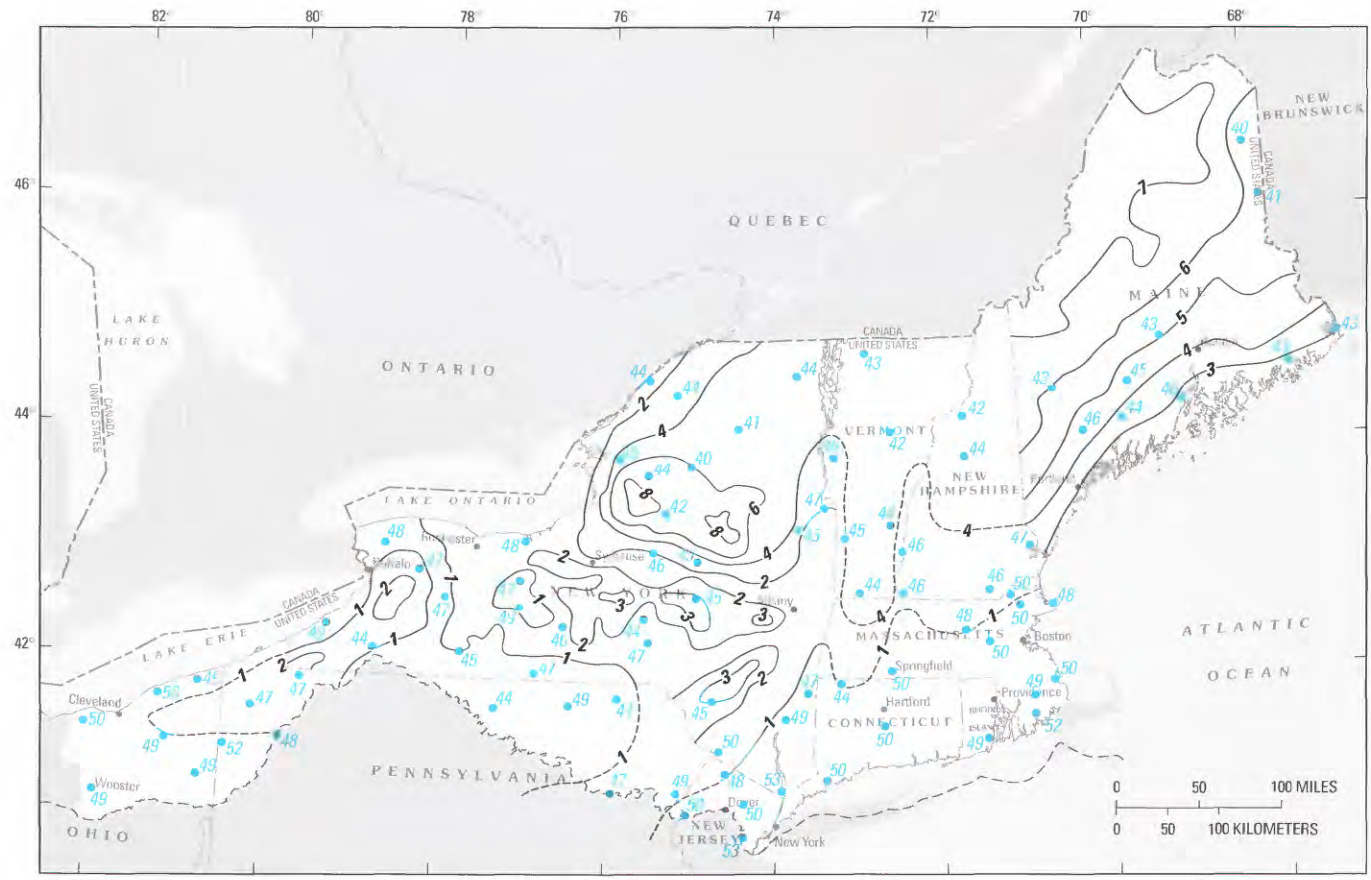

EXPLANATION

Line of water equivalent of snowcover on March 1, in inches, based on snow surveys (Hayes, 1972; Allen and Barnes, 1985). Contour interval is variable

Line of water equivalent of snowcover on March 1, in inches, estimated from temperature data. Contours represent 1-inch and 4-inch depths

Southern limit of the late Wisconsinan (Pleistocene) glaciation

Mean annual air tempreature, in degrees Fahrenheit (data from National Oceanic and Atmospheric Administration, 1985a and b)

FIGURE 7.—Mean water equivalent of snowpack on March 1 (calculated over varying time periods) and mean annual temperature (1951–1980) at selected stations in the glaciated Northeast (modified from Lyford and Cohen, 1988).

M.P. and others, 1967; Likens and others, 1977; Carswell and Lloyd, 1979).

Short-Term Variation in Evapotranspiration

Although mean evapotranspiration for periods of several years can be calculated with reasonable accuracy from long-term precipitation and runoff records alone, calculation of evapotranspiration for periods of weeks or months by water-balance methods requires information that is more difficult to acquire, such as changes in the amounts of water stored in streams, in aquifers, on land surface as snow, and above the water table as soil moisture. Such methods have been proposed by Thornthwaite (1948), Thornthwaite and Mather (1955, 1957), Palmer (1965), and Thomas (1981), among others; each is typically applied to compute both evapotranspiration and runoff, after which computed runoff is compared with streamflow records to verify the computation (Crain, 1974) or to calibrate by iterative procedures certain parameters required in the computation (Alley, 1984). A simpler alternative approach relies on the fact that short-term evapotranspiration rates are generally proportional to air temperature and the length of daylight during the growing season (Olmsted and Hely, 1962; Cruff and Thompson, 1967; Hamon, 1961); they are also proportional to, but somewhat lower than, pan-evaporation rates (Mustonen and McGuin-

ness, 1968; McGuinness and Bordne, 1972). Consequently, monthly evapotranspiration can be estimated by first computing mean annual evapotranspiration for a long-term period from suitable precipitation and runoff records, then assuming that annual evapotranspiration in each year of interest does not vary greatly from year to year and therefore is virtually the same as the long term mean annual evapotranspiration. The long term annual evapotranspiration is then distributed month by month over the year(s) of interest in proportion to the product of monthly mean temperature and percentage of annual daylight (Olmsted and Hely, 1962; Randall, 1986) or to monthly pan evaporation (Lyford and Cohen, 1988). This approach is applicable for estimating water available for recharge to stratified-drift aquifers, as explained in the section "Recharge from Direct Infiltration of Precipitation" further on. Other specialized techniques for estimating evapotranspiration that do not involve water-balance methods are summarized by Dingman (1994, p. 256-302).

Ground-Water Evapotranspiration

Ground-water evapotranspiration rates presumably decrease as depth to the water table increases, for two reasons:

1. The amount of water available for evaporation and transpiration from any given depth interval of soil decreases as the water table and the tension-saturated capillary fringe drop below that interval, especially in sandy soils (Prill and others, 1965). Evaporation from tanks 4.5 ft deep filled with unvegetated clay loam was found to decrease from about 25 percent to less than 10 percent of pan evaporation when the water table dropped from about 1 to 3 ft below land surface (White, 1932; Todd, 1980, p 6.12).
2. Transpiration is intuitively assumed to be proportional to the abundance of plant roots, which ordinarily diminishes with depth.

The foregoing evidence suggests that ground-water evapotranspiration could be expected to occur at a maximum rate equal to potential evapotranspiration or free-water-surface evaporation when and where the capillary fringe is at land surface, but to decline as the capillary fringe declines and to be zero when and where the capillary fringe is below some depth. In ground-water models this depth is termed the extinction depth and has commonly been taken to be 6 to 8 ft (McDonald and Harbaugh, 1988, p. 10-5). In woodland areas underlain by sand and gravel, however, ground-water evapotranspiration can occur even if the saturated zone is 15 to 20 ft below land surface. Stone and Kalisz (1991) argue that although water uptake by plants from a given soil volume requires the presence of roots, it does not increase in proportion to the abundance of roots, citing Gardner (1964) among others. Also, many studies of tree-root distribution that report penetration of only a few feet were conducted in localities where bedrock, unweathered till, fragipan layers, permafrost, or saturation at depths of a few feet greatly restricted further root penetration or hindered the examination of possible penetration at greater depth. Several studies have reported deeper root penetration on well-drained sandy soils than elsewhere (Stone and Kalisz, 1991, p.88). For example, Stout (1956) observed that 4 trees growing on a gravel terrace in southern New York sent roots deeper than any of 21 trees growing on till-covered hillsides nearby. An extensive literature survey (Stone and Kalisz, 1991) revealed that some tree roots extended to depths greater than 10 ft at about 50 percent of the sites investigated in soils described as sand, sandy or gravely loam, sandy clay, alluvium, or coarse, as summarized in the following table that excludes tropical species.

	Number of sites investigated at which maximum depth of roots was		
Tree variety	10 feet or less	greater than the maximum depth investigated, which was less then 10 feet	greater than 10 feet, as much as 25 feet
Gymnosperms (pine, spruce, fir, juniper, cypress)	20	6	27
Angiosperms (maple, birch, beech, oak, hickory, elm, tulip tree, catalpa, fruit trees)	16	5	17

Some plants, termed phreatophytes, habitually obtain water from below the water table and are generally capable of extending roots to depths of 15 ft or more to reach the water table; such plants have been extensively studied in arid regions (Robinson, 1958) but the prevalence of similar behavior in humid regions is less well documented.

Basinwide mean rates of ground-water evapotranspiration ranging from 1 to 8 in/yr have been computed for a few localities in the glaciated Northeast. These rates, like basinwide mean rates of ground-water discharge to streams, are of little significance in evaluating stratified-drift aquifers because any basinwide statistic obscures major differences between areas of till and areas of stratified drift in each basin. Furthermore, the accuracy of the computed rates is questionable. A comprehensive basinwide water-balance analysis by Meinzer and Stearns (1929) is conceptually reasonable, but ground-water evapotranspiration was calculated as a residual that incorporated any errors in other terms in the water-balance equation. A technique based on seasonal changes in the relation of ground-water stage to ground-water discharge, described by

Schicht and Walton (1961) and Olmstead and Hely (1962), was applied to compute ground-water evapotranspiration in studies by Frimpter (1974), Randall and others (1966), Allen and others (1966) and in several subsequent water-resource appraisals in Connecticut and Rhode Island. This technique requires determination of the mean (or median) ground-water stage in one or more wells within a watershed for each month of the year. Ideally, the relation between mean ground-water stage and mean base flow (ground-water discharge) in the stream draining that watershed will resemble the ground-water rating curve in figure 8. Data points for typical winter months, when ground-water evapotranspiration is virtually zero, define a straight line. The leftward displacement of other months from the winter line is taken to represent ground water discharged by evapotranspiration rather than by seepage to streams. If long-term mean ground-water evapotranspiration is sought, long-term mean values of ground-water stage and base flow for each month would be plotted. The idealized seasonal cycle shown in figure 8 could be explained not only by seasonal variation in ground-water evapotranspiration, however, but also by variation in recharge resulting from seasonal change in evapotranspiration from the unsaturated zone. For a given aquifer stage, ground-water discharge during a period of recharge is greater than ground-water discharge during a period without recharge, as demonstrated analytically by Rorabaugh (1964) and confirmed by F.P. Lyford (U.S. Geological Survey, written commun., 1985) who was able to replicate the form of the rating curve in figure 8 by a ground-water flow model of an idealized valley-fill aquifer in which alternating 6-month periods of steady recharge and zero recharge were simulated. Many studies have reported that total evapotranspiration (evapotranspiration from above the water table as well as below) exceeds normal rainfall in summer in most of the glaciated Northeast, resulting in zero recharge for several months in most years (Lyford and Cohen, 1988, table 1; Crain, 1974). Thus, the assumption that seasonal displacement of the relation of ground-water stage to ground-water discharge is entirely the result of ground-water evapotranspiration may not be valid.

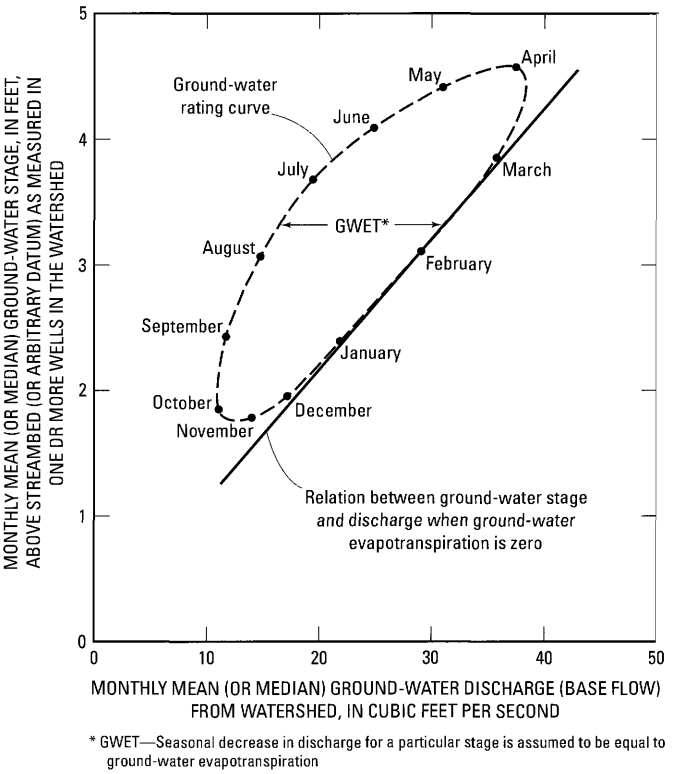

FIGURE 8.—Idealized seasonal change in the relation of ground-water stage to ground-water discharge.

RUNOFF

Runoff has been defined as that part of precipitation that appears in streams (Langbein and Iseri, 1960), and has been conceptualized as consisting of surface runoff (overland flow), subsurface stormflow (interflow), and ground-water runoff (base flow). Surface runoff is the component that moves across the land surface when the soil is saturated or is impermeable. (Saturation can occur when rainfall intensity exceeds infiltration capacity or where the water table or capillary fringe rises to land surface.) Subsurface stormflow follows shallow flow paths above the water table, including flow paths within temporary perched saturated zones where surface soils are much more permeable than underlying materials, or those through macropores such as mole runs, frost cracks, or cavities left as roots decay. Ground-water runoff is precipitation that infiltrates to the water table, becomes part of the ground-water flow system, then discharges into a stream channel. The magnitude of the total runoff is a function of the magnitude of precipitation and evapotranspiration, whereas the relative magnitudes of the individual runoff components are a function of various factors, including climate, degree of vegetation, land use, hydraulic properties of the soil and underlying rock or glacial deposits, rainfall intensity, and topography. Runoff is generally taken as equal to streamflow from gaged watersheds, and runoff components have been quantified by separation of streamflow hydrographs through various methods that are somewhat inexact and not rigorously related to the source components they are inferred to represent (Hall, 1968).

Although the foregoing concepts are generally applicable, they ignore the fact that some watersheds and watershed segments lose appreciable quantities of water underground, as ground-water outflow that has not yet discharged to streams and may never do so; that is, it may discharge to the ocean, or to production wells, or to ground-water evapotranspiration, or to streams at some point downgradient from the region under consideration. Accordingly, runoff from a region can be more generally defined as "the total amount of liquid water leaving a region", which is equal to streamflow plus ground-water

outflow (Dingman, 1994, p.16) and ground-water runoff can be defined as including not only ground-water discharge to streams but also ground-water outflow. Annual runoff per unit area from a particular watershed, even if it consists largely of surface runoff and subsurface stormflow, can be used to estimate the amount of water that is potentially available for ground-water recharge and is likely to become recharge in localities underlain by surficial sand and gravel; such an estimate would be conservative in that it would not include any ground water that has been discharged as ground-water evapotranspiration but might be captured by wells if the water table were lowered by pumping. Lyford and Cohen (1988) and later sections of this paper explain how water available for recharge can be estimated and used to simulate actual recharge to valley-fill aquifers.

Ground-Water Runoff

Most ground-water runoff is ultimately discharged to streams, except along the coast where ground water discharges directly into the ocean. Because ground-water runoff per square mile is several times greater from stratified drift than from till, the percentage of stratified drift in a watershed has a powerful influence on the magnitude of low streamflow (Thomas, 1966; Ku and others, 1975; Cervione and others, 1982; Barnes, 1986). Ground-water runoff other than discharge to streams may be significant locally, as discussed below.

Underflow Through Stratified Drift In Valleys.—Most large streams in the glaciated Northeast, and some small streams, follow valleys that are filled in part with stratified-drift aquifers. Some ground water flows downvalley through the stratified drift, driven by a component of the potentiometric gradient that parallels and roughly equals the downvalley slope of the floodplain; this ground water crosses beneath the watershed perimeter as delineated from topographic maps and leaves the watershed as underflow. If the head distribution were precisely known, the true watershed perimeter within the valley fill could perhaps be delineated along ground-water flow lines such that no underflow would cross beneath that perimeter, although contrasting flow directions in deep and shallow ground water might make this task difficult (Modica and others, 1997). Underflow is generally a negligible fraction of annual mean streamflow, except in a few broad valleys drained only by small headwater streams, but underflow can be significant relative to low streamflow. Rates of underflow through stratified drift have been calculated as 0.33 ft^3/s in a valley 400 ft wide (Jacob, 1938) and 4.1 ft^3/s in a valley 3,500 ft wide (Randall and others, 1988b)

Outflow Along Regional Flow Systems.—Throughout the glaciated Northeast, ground-water flow is most vigorous at shallow depth, through permeable stratified drift in valleys and through the few feet of weathered till or sandy ablation till that overlie less permeable basal till or bedrock in uplands. Accordingly, local flow systems predominate, directed toward points of discharge along nearby streams and entirely encompassed by local watersheds. A small fraction of ground-water flow, however, may follow longer regional flow systems from broad upland regions to more distant major streams. Dingman (1981) reported that differences between mean annual precipitation (computed from an equation he developed) and measured mean annual streamflow tends to increase with altitude in New Hampshire and Vermont, whereas evapotranspiration (computed from published equations based on radiation and temperature) decreases with altitude. He pointed out that one possible explanation for the discrepancy is that an appreciable fraction of precipitation on high-altitude watersheds may be lost to ground-water outflow along regional flow systems. Most bedrock in the glaciated Northeast has small permeability, however, and seems incapable of transmitting an appreciable fraction of annual runoff. Likens and others (1977) present evidence that ground-water flow out of certain mountain watersheds in New Hampshire is negligible. Studies by Wandle and Randall (1994) and Dingman (1978) indicate that low flows of streams in high-relief areas of central New England increase with altitude; this would not be expected if ground-water outflow along regional flow systems were appreciable, because such outflow should reduce discharge to local streams more severely during low flow than at times of mean flow.

Mean Annual Runoff

The variation in mean annual runoff across the glaciated Northeast is shown on plate 2. This map is based primarily on records of streamflow from 503 gaged watersheds, nearly all of which are less than 500 mi^2, and 60 percent are less than 100 mi^2. Recorded streamflows were corrected for any significant diversions. Values of mean annual runoff from 486 of these watersheds for 1951-80 were compiled as part of a study by Krug and others (1990), in which any streamflow record that did not include the entire 30-year period was extended by regression with the record from a nearby station by the method of Matalas and Jacobs (1964). Mean annual runoff values from eight watersheds in northeastern Ohio and nine in Canada near the United States border, all of which were gaged continuously during 1951 through 1980, were compiled as part of the present study. The perimeter of each watershed was drawn on a base map of 1:1,000,000 scale, and the mean annual runoff was written within or near it to facilitate contouring. These measured values of watershed runoff were supplemented by estimates of runoff at 419 precipitation stations in the United States and 64 in Canada, which were obtained as follows: Precipitation at each station was partitioned into point estimates of evapotranspiration and runoff, which were constrained such that the evapotranspiration estimates varied smoothly across the region and decreased with increasing altitude and latitude, and runoff estimates were

consistent with measured runoff from nearby watersheds. A point estimate of runoff was judged to be consistent if it equaled average runoff from a nearby watershed, or if it were somewhat higher (or lower) and a compensating departure from average watershed runoff could reasonably be inferred in distant parts of the watershed from altitude or regional trends. Bishop and Church (1992, 1995) also computed point estimates of runoff at precipitation stations to supplement runoff from gaged watersheds for use in contouring annual runoff, although their partitioning procedures differed somewhat from those described above.

Plate 2 differs appreciably in detail from a map of mean annual runoff drawn by Krug and others (1990) from nearly the same runoff data, but the two maps are generally similar and of comparable accuracy. Krug and others (1990, table 4) excluded 5 percent of the watersheds in their data set, selected at random, before drawing their runoff map; then, as a test of map accuracy, they estimated runoff from their map for each of the excluded watersheds and compared the estimates with runoff compiled from gaging-station records. A total of 38 watersheds within the glaciated Northeast were excluded. The same 38 watersheds were excluded from the initial draft of plate 2, and runoff for each excluded watershed was estimated from that map by the weighted-average method described by Krug and others (1990). The runoff estimates from plate 2 were found to be more accurate than estimates from the map by Krug and others (1990) for 21 of the 38 watersheds, equally accurate for 3, and less accurate for 14. The mean absolute deviation from observed runoff for the 38 watersheds was 1.42 in. for plate 2, and 1.72 in. for the map by Krug and others (1990). Both maps slightly underestimated runoff; mean deviation for both maps was about -0.5 in. Subsequently, the accuracy of plate 2 was improved by incorporating data from Canada and from the 38 watersheds initially excluded.

After revision of the runoff map, a map of mean annual precipitation (pl. 1) was drawn such that precipitation contours parallel runoff contours and are consistent with the point precipitation data. Differences between runoff and precipitation on these two maps correspond to the evapotranspiration that had been estimated by partitioning of precipitation at each station into regionally consistent point runoff and evapotranspiration values. Evapotranspiration is shown on plate 1 as 1-in. zones of uniform evapotranspiration rather than as contours because evapotranspiration at each precipitation station was estimated only to the nearest inch during the partitioning process. Finally, as a means of quality control, Geographic Information Systems software was used to create a three-dimensional surface from the runoff contours, and a similar surface from the precipitation contours, by the Delaunay method of triangulation (ESRI, 1991, p. 2-11). These surfaces were resampled to generate lattices having a spacing of 4 mi. between lattice points, and runoff was subtracted from precipitation in each lattice block. Discrepancies between the array of evapotranspiration values thus computed and the original evapotranspiration zones led to correction of several mislabeled contours and minor misinterpretations in placement of contours.

Maps of precipitation and runoff that were drawn independently of each other appear together in several publications (for example, Lyford and others, 1984; Olcott, 1995; Moody and others, 1986). Such maps tend to be mutually inconsistent in that they commonly indicate precipitation and runoff to increase in different directions, that may differ by as much as 90 degrees in some localities, which is inherently implausible and which results in large, anomalous differences between adjacent areas in evapotranspiration as computed by subtracting runoff contours from precipitation contours. Although extreme differences in evapotranspiration might be expected between adjacent local terrains as different as a bare bedrock slope and a swamp, spatial variability should be small and gradual when evapotranspiration is estimated from runoff averaged over watersheds encompassing several square miles or more, as suggested by evapotranspiration maps by Knox and Nordenson (1955) and Hely and others (1961). Plates 1 and 2 are mutually consistent in that precipitation minus evapotranspiration equals runoff at all locations, and precipitation and runoff increase together.

The reference period 1951-80 was adopted because sets of runoff and precipitation data that had already been adjusted to that period were available. Increases in runoff and possible decreases in evapotranspiration from 1940 or 1950 through 1988 have been reported (Lins and Michaels, 1994); such trends were not considered in this study.

Plate 1 may slightly underrepresent mean precipitation and correspondingly underrepresent evapotranspiration in areas of high relief, as inferred from the following evidence. A small-scale map of evapotranspiration by Knox and Nordenson (1955) indicates smaller decreases in evapotranspiration with increased altitude than shown on plate 1. A few records, some discontinuous (Iorio, 1972; Bishop and Church, 1992) suggest that precipitation on mountain peaks may generally exceed values indicated on plate 1. At high altitudes fog drip and rime augment the moisture recorded by rain gages (Dingman, 1981). Research in Switzerland suggests that precipitation-gage networks in mountainous areas underestimate area-averaged precipitation by 10 to 20 percent (Diaz, 1995). Differences between runoff from small upland watersheds, large watersheds, and point runoff partitioned from precipitation required that runoff (and precipitation) be depicted as increasing with altitude in many areas of high relief on plates 1 and 2, but most precipitation stations in such areas are near population centers in valleys, so the contours are not precisely controlled by point data at high altitudes.

Plate 2 may slightly underestimate runoff in that all data were derived from or adjusted to streamflow records and therefore do not include any ground-water underflow that bypasses gaging stations. Underflow is probably an insignifi-

cant fraction of mean annual runoff at most gaging stations, however, and is smaller than measurement error. In extensive areas of stratified drift, where runoff occurs chiefly as ground-water runoff, plate 2 may substantially underrepresent local streamflow but should reasonably represent total runoff. Thus, plates 1 and 2 may be used to estimate recharge to aquifers, as discussed further on.

Maps of precipitation, runoff, and evapotranspiration more detailed and accurate than plates 1 and 2 could be prepared by a more comprehensive approach that first quantified the relation of precipitation to altitude and other orographic factors, before mutually adjusting the inferred distribution of precipitation, runoff, and evapotranspiration, as done in this study, to ensure consistency. Knox and Nordenson (1955) adopted such a comprehensive approach, but mapped only part of the glaciated Northeast, used data from 1921-50, and did not document their computations. Hely and others (1961) comprehensively mapped the Delaware River basin and presented graphical relations of precipitation to orographic factors. Bishop and Church (1995) described preparation of runoff maps of eastern United States based on the runoff data of Krug and others (1990) and a numerical model under development that computes precipitation distribution from altitude and slope orientation.

Temporal Variation in Runoff

In general, runoff varies through time as a function of regular seasonal cycles each year and less regular, longer-term fluctuations in precipitation. Seasonal cycles in solar radiation and temperature govern storage of moisture as snow (fig. 7) and frozen ground in winter, release of that moisture in the spring, and depletion of soil moisture and ground-water recharge in summer. As a result, streams throughout the glaciated Northeast follow a seasonal pattern in which the minimum mean monthly runoff occurs in August or September and is typically only 5 to 20 percent of maximum mean monthly runoff, which occurs in March or April. Cycles in precipitation are such that several successive months or years can be much wetter or dryer than average, and a particular drought or wet period typically varies in intensity across the region (Barksdale and others, 1966).

Several reports have quantified seasonal cycles of precipitation, evapotranspiration, and runoff in parts of the glaciated Northeast for long-term average conditions (Lyford and Cohen, 1988; Handman and others, 1986, like earlier reports in the Connecticut Water-Resources Inventory series) or for specific years (Meinzer and Stearns, 1929). Lyford and Cohen (1988) identified six climatic regions (fig. 1) based on annual snow accumulation, runoff, and monthly streamflow hydrographs. Representative hydrographs of watersheds from each region are shown in figure 9. Each watershed was gaged for at least 10 years; most are smaller than 30 mi^2 and contain negligible sand and gravel. In climatic regions A and D, where snowpack usually does not greatly affect runoff, mean monthly runoff increases gradually during winter to a maximum in March. In regions B, C, and F, mean monthly runoff generally decreases slightly during the winter, when some water is stored as snow, and increases markedly in March and April, when snowmelt is a significant component of runoff. In region E, runoff is depressed from December through March, relative to other regions, and snowmelt runoff continues into May. In region F, runoff is less abundant in spring and greater in summer than in other regions, possibly because water may be stored in sandstone in winter and slowly released in summer, and(or) because precipitation is relatively abundant in summer. Summer flows in region C are lower than elsewhere, probably because summer precipitation is consistently less than evapotranspiration.

Spatial Variation in Seasonal Low Runoff

The magnitude of streamflow during periods of low runoff in late summer or fall reflects the spatial variations in mean annual precipitation and evapotranspiration depicted on plate 1, but is also affected by other watershed properties, chiefly the extent of surficial sand and gravel relative to till, as illustrated by flow-duration curves for streams in Connecticut (fig. 10). For example, according to figure 10, streamflow equaled or exceeded 99 percent of the time from a watershed underlain entirely by coarse-grained stratified drift would be about 20 times greater than that from a watershed of the same size in which 90 percent of the surface sediment was till or fine-grained lake-bottom deposits and only 10 percent was coarse stratified drift. In a watershed underlain entirely by till, streams would be dry 7 percent of the time. The effect of spatial variation in precipitation was also incorporated in figure 10, by adjusting all data to a mean annual runoff of 1.8 $(ft^3/s)/mi^2$. Accordingly, daily flows per square mile estimated from figure 10 must be multiplied by the ratio of mean annual runoff from the watershed of interest to 1.8 $(ft^3/s)/mi^2$, and by watershed area, to obtain daily flows in cubic feet per second from that watershed (mean annual runoff in inches, estimated from plate 2, can be multiplied by 0.074 to obtain cubic feet per second per square mile.) Figure 10 also shows that (1) surficial geology has little effect on daily streamflows exceeded 25 to 35 percent of the time, which are close to the mean annual runoff (Hunt, 1967), and (2) daily streamflows that are seldom exceeded increase as percent of the watershed underlain by coarse stratified drift decreases.

Regression equations developed for several regions in the glaciated Northeast (table 3) indicate that most of the variation in low streamflow from one place to another is attributable to three factors—water availability (water input), area of surficial sand and gravel, and area of lakes, swamps, and other wetlands. The spatial extent of surficial sand and gravel commonly exceeds the extent of stratified-drift aquifers, but in general the two are nearly equivalent. Wetland area corre-

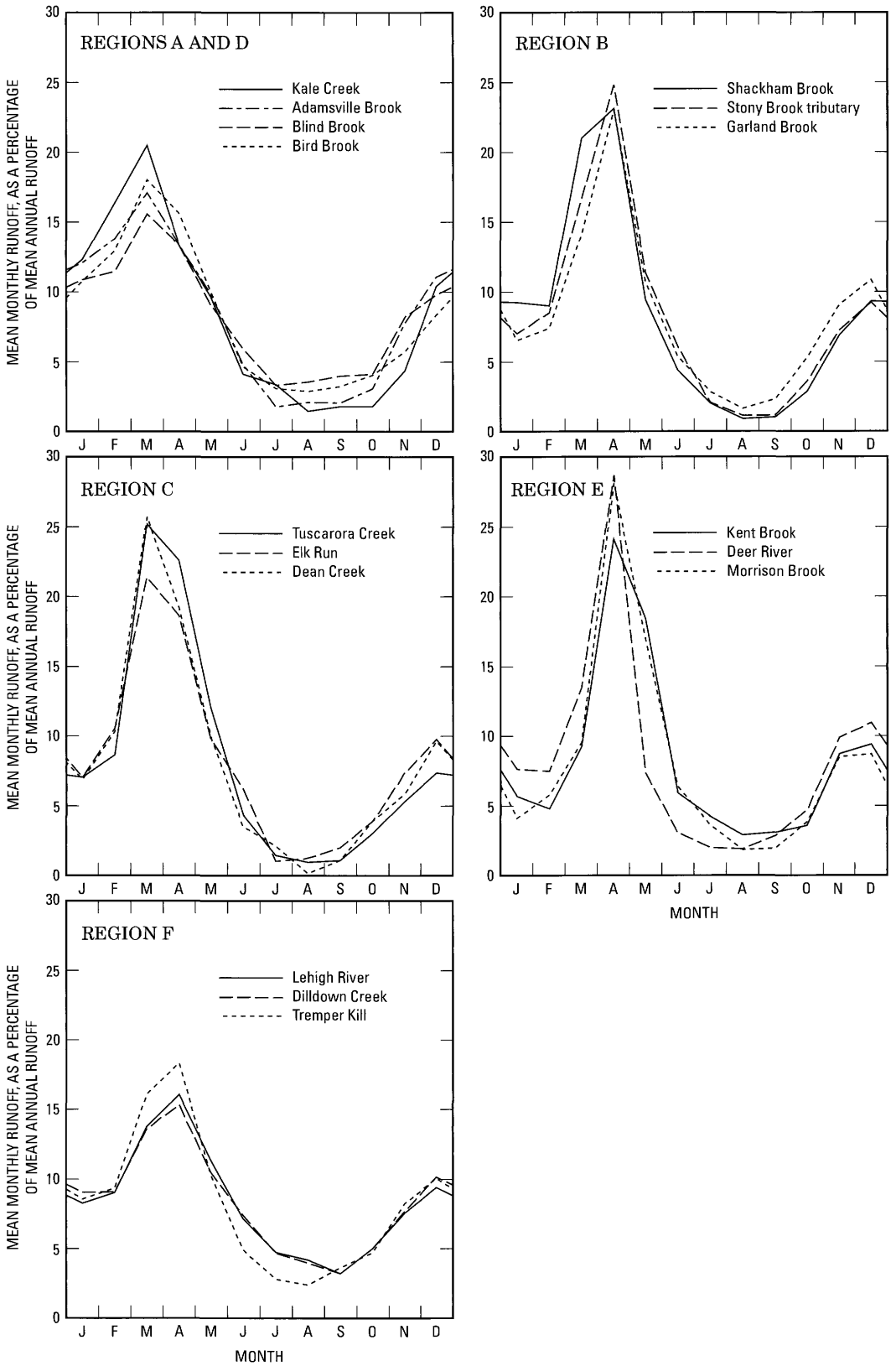

FIGURE 9.—Mean monthly runoff as a percentage of mean annual runoff for representative upland basins in the glaciated Northeast (from Lyford and Cohen, 1988, fig. 7). Location of climatic regions A–F are shown in figure 1. Locations, drainage area, mean annual runoff, and period of record for these and other basins are given in Lyford and Cohen (1988).

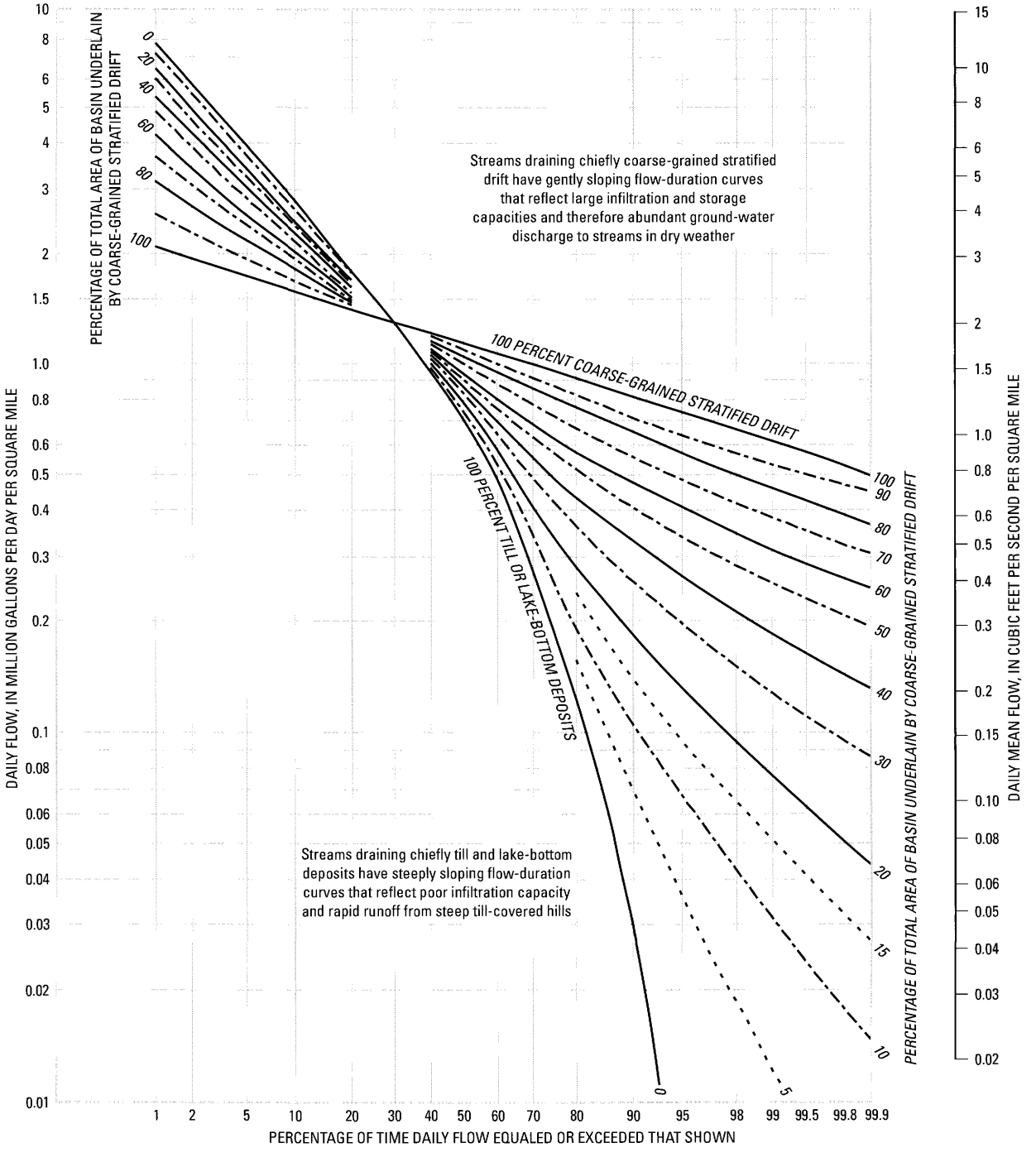

FIGURE 10.—Duration curves of daily mean streamflow showing effect of surficial geology. Curves are based on data for 1930–60 from 26 gaging stations on unregulated streams in and near Connecticut, exclusive of a region of relatively high relief in northwestern Connecticut, and are adjusted to a mean annual flow of 1.8 cubic feet per second per square mile (modified from Weiss and others, 1982, fig. 15; first developed by Thomas, 1966).

TABLE 3.—*Equations developed to predict low streamflow in the glaciated Northeast from surficial geology and other drainage-basin properties*

[Areas are in square miles, altitudes in feet, runoff in cubic feet per second (ft^3/s), stream length in miles. Modified from Randall and Johnson, 1988]

Region	Dependent variable[a]	Regression constant	Independent variables: Surficial geology[b]		Independent variables: Water input[c]		Independent variables: Wetlands	Coefficient of determination (R^2 adjusted)	Standard error (ft^3/s)
Connecticut and vicinity[d]	7Q10	= 0	+ 0.72 (area underlain by sand & gravel) + 0.05 (area underlain by till)		not tested	–	0.72 (area of wetlands)	not reported	0.96
Eastern New England (areas of low relief)[e]	$(7Q10)^{0.75}$	= –0.20	+ 2.58 (area underlain by sand & gravel / stream length) (mean runoff) + 0.021 (area underlain by till + fines) (mean runoff)			–	15.7 (area underlain by alluvium + area wetlands in sand & gravel) / (drainage area)	93.7[f]	1.57[f]
Western and northern New England (areas of higher relief)[e]	$(7Q10)^{0.6}$	= –1.20	+ 0.38 (area underlain by sand & gravel – area underlain by alluvium) + 0.024 (area underlain by till + fines)	+	0.0011 (mean basin altitude)	–	0.7 (area of wetlands)	95.7[f]	1.43[f]
Susquehanna River basin, N.Y.[g]	7Q10	= +0.049	+ 0.51 (area underlain by sand & gravel)	+	0.028 [(mean runoff/drainage area) –1.85] (drainage area)	–	0.93 (area of wetlands in sand & gravel)	.99	0.55
Lower Hudson River basin, N.Y.[h]	7Q10 / drainage area	= –0.03	+ 0.47 (area underlain by sand & gravel excluding wetlands) / (drainage area)	+	0.000013 (mean basin altitude)	[i]		not reported	0.63[j]

[a] 7Q10 is a statistical index of low streamflow, defined as the average flow over 7 consecutive days that occurs as the lowest such flow in the year once in 10 years, on average.
[b] Areas include any wetlands within the boundaries of sand and gravel or till, except as noted in this column.
[c] May be represented by mean annual runoff, mean annual precipitation, or elevation, all three of which are correlated with one another in many regions and can be regionalized independently of low flow. (For Eastern New England, mean runoff appears in the "surficial geology" column because the equation requires the areas of surficial geologic units to be multiplied by mean runoff).
[d] Modified from Cervione and others (1982) by L.A. Weiss and R.L. Melvin (U.S. Geological Survey, written commun., 1983).
[e] Wandle and Randall (1994).
[f] Computed after detransformation of predicted low flows to cubic feet per second.
[g] Modified from Ku and others (1975) by A.D. Randall (U.S. Geological Survey, written commun., 1991).
[h] Barnes (1986).
[i] Not significant as an independent variable, probably because area of wetlands in sand and gravel is incorporated, negatively, in surficial geology term.
[j] Predicted values of dependent variable (7Q10 per unit area) multiplied by drainage area, then standard error computed.

lates negatively with low streamflow (table 3), presumably because evapotranspiration from riparian wetlands consumes ground water that would otherwise emerge as low streamflow. Many studies other than those cited in table 3 have also demonstrated the importance of one or more of these three factors. For example, Tasker (1972) and Male and Ogawa (1982) demonstrated that low streamflow was a function of the water transmitting potential of surficial earth materials, which they represented by a term roughly proportional to transmissivity. Dingman (1978, 1981) recognized the increase in water availability with altitude as an influence on low flow in mountainous regions of northern New England, but was unable to consider the effect of surficial geology because few suitable maps were available. Johnson (1970) showed that mean annual runoff and area of wetlands correlated with low flow in uplands of northern Vermont. Coates (1971) found that differences in low flow between the Delaware and Susquehanna River basins of New York were largely a function of differences in area of valley-bottom stratified drift between these adjacent basins. Lapham (1988) found that streamflows that were exceeded 90 to 99.9 percent of the time in southeastern Massachusetts were strongly correlated with the extent of stratified drift.

In general, ground-water discharge to streams is influenced by aquifer properties and dimensions. The 2-dimensional, 3-layer ground-water flow model depicted in figure 11 illustrates the interaction of some of the factors that control ground-water discharge to streams during periods of low flow. The model represents a vertical slice through half of an idealized watershed, from ridgetop to midvalley. The layering and hydraulic properties of the upland hillside were designed to be generally representative of the Susquehanna River basin of south-central New York, and were held constant for a series of transient-state simulations in which width, hydraulic conductivity and specific yield of the valley fill were varied. Each simulation consisted of 6 months of steady recharge followed by 4 months without recharge. Stream stage during the zero-recharge period was lowered a total of 1.7 ft in monthly increments, to approximate the typical seasonal recession of stream stage. Ground-water evapotranspiration was simulated at rates that varied seasonally and became zero when the water table was deeper than 5 ft below land surface. Simulated discharge to the stream at the end of the 4-month recession (fig. 12) represents low-flow conditions, and was affected by the following valley-fill properties:

1. *Hydraulic conductivity.*—The lowest hydraulic conductivity value simulated for the valley fill (1.1 ft/d, fig. 12) is comparable to the values simulated for the till layers (1.7 and 0.17 ft/d, fig. 11). As the hydraulic conductivity of the valley fill was progressively increased, stream discharge at the end of the recession increased initially, then decreased. At large hydraulic conductivity values, typical of clean gravel, or at narrow valley widths, discharge to the stream approached 0.37×10^{-4} ft^3/s, which is the simulated rate of discharge from the upland. Thus, at either condition the valley fill serves only as a conduit from upland to stream at times of low flow. Ground-water discharge to streams at the end of the simulated period of low flow was greatest where hydraulic conductivity of the valley fill was equivalent to that of fine sand (in valleys with a half-width of about 0.25 mi.) or medium sand (in valleys with a half-width of about 0.5 mi.) (fig. 12). Much larger hydraulic conductivity values have been reported for some aquifers (Randall, 1977; Reynolds, 1987; Bergeron, 1987); figure 12 suggests that such productive aquifers may contribute less water to streams during periods of low flow than fine-sand aquifers that drain more slowly. Such an inverse correlation between hydraulic conductivity of surficial sand and magnitude of low flows has been observed in the coastal plain of Delaware, where surficial fine to coarse sand (comparable to the valley component of figure 11) underlies entire watersheds (Johnston, 1971).
2. *Specific yield.*—Specific yield of the valley fill was 0.2 for all simulations depicted in figure 12. A reduction in specific yield (not shown in figure 12) to 0.035, a value similar to that of weathered till, raised the water table in the valley fill initially and thus increased ground-water discharge early in the simulated recession. Discharge at the end of the recession was less than discharge for a specific yield of 0.2, however, because the water table had earlier declined nearly to stream grade and the small remaining gradient toward the stream yielded little discharge.
3. *Area.*—Figure 12 shows that the maximum rate of ground-water discharge to the stream increased in proportion to valley-fill width (and thus in proportion to area, inasmuch as the model represents a unit length of valley). At low hydraulic conductivity, however, this relation of discharge to width was masked by effects of topography and ground-water evapotranspiration, as explained below.
4. *Topography and ground-water evapotranspiration.*—The altitude of most of the valley floor in the model was more than 40 ft above stream stage (fig. 11), and simulated ground-water evapotranspiration was generally small. When hydraulic conductivity was decreased to values typical of upland till, however, the water table rose close to land surface, resulting in an increase in ground-water evapotranspiration and a corresponding decrease in discharge to the stream. Thus, one reason for large low-flow yields from areas of permeable stratified drift is the deep water table and minimal ground-water evapotranspiration typical of many such areas.

For many years, hydrologists have recognized that the magnitude of seasonal low streamflow can be used to evaluate the hydraulic properties of aquifers (Cross, 1949; Schneider, 1957, 1965; Paulson, 1965). The studies described or cited in this section have demonstrated that the converse is

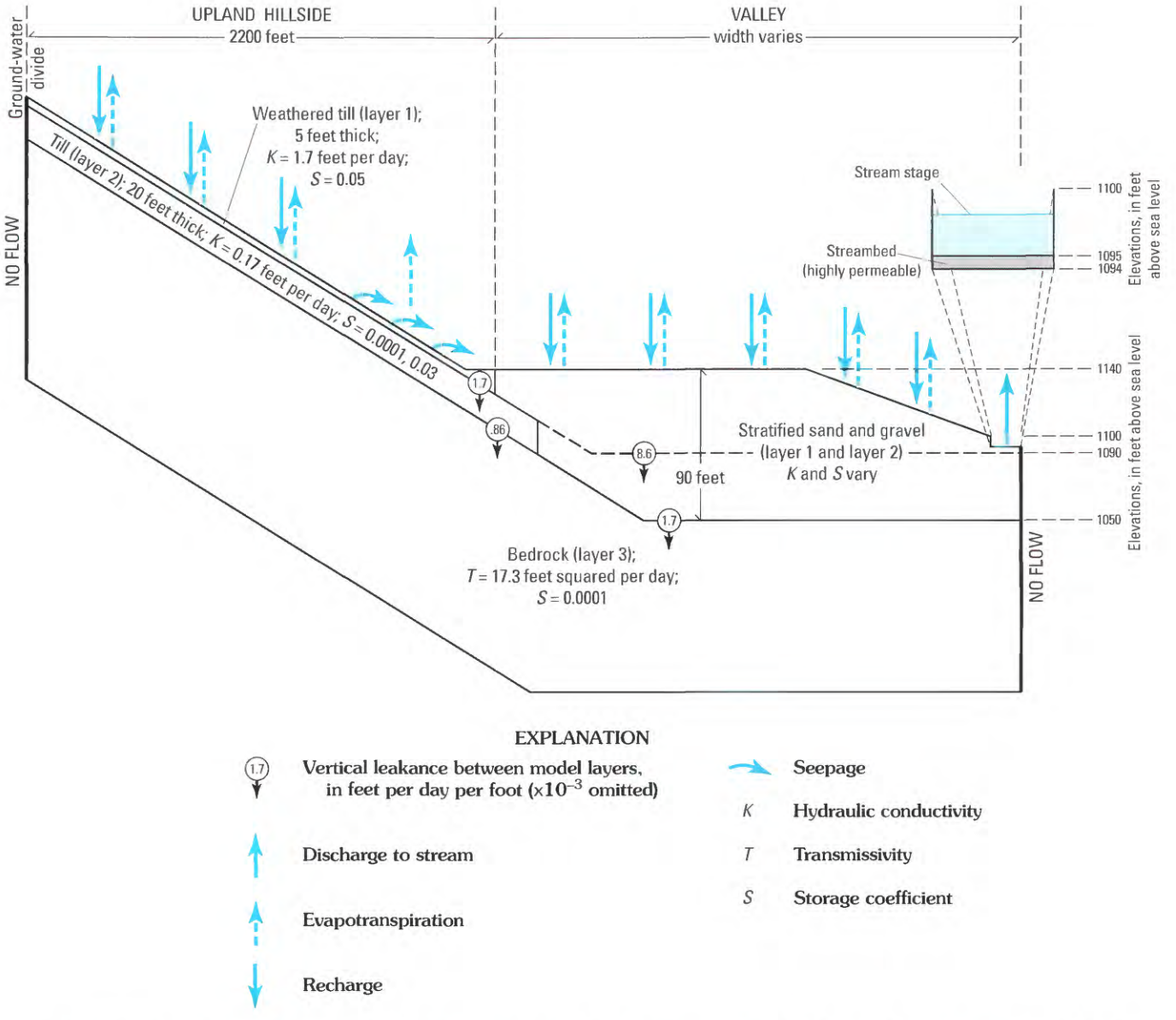

FIGURE 11.—Dimensions and properties of a 2-dimensional model that represents an idealized vertical section across a valley and the adjacent upland hillside. The model was developed to simulate factors affecting ground-water discharge to streams.

also true in the glaciated Northeast: stratified-drift aquifers are the principal source of ground-water discharge that sustains streamflow under drought conditions and limit flood extremes by storing excessive precipitation and runoff for gradual release later. Therefore, the relative extent of such aquifers can be used to predict the magnitude of low or high streamflows, as illustrated in figure 10 and table 3.

WATER-TABLE FLUCTUATIONS

The fluctuations in solar radiation, temperature, precipitation, and evapotranspiration that shape annual runoff cycles also cause water-table fluctuations. The water table normally rises irregularly from late fall through early spring, then declines during the growing season, as illustrated in figure 13 and elsewhere (for example, Meinzer and Stearns, 1929; Maevsky, 1976; U.S. Geological Survey, 1997). Frimpter (1980) and Socolow and others (1994) present methods for estimating the range of water-table fluctuation at any site of interest, based on correlation of a single water-level measurement at the site to long-term records of fluctuation in observation wells.

Patterns of water-level fluctuation differ from place to place as a function of hydraulic conductivity of the aquifer and distance from the nearest stream. In many valleys, the water table in stratified drift is generally within a few feet of stream stage, and rises or falls with the stream. Annual mini-

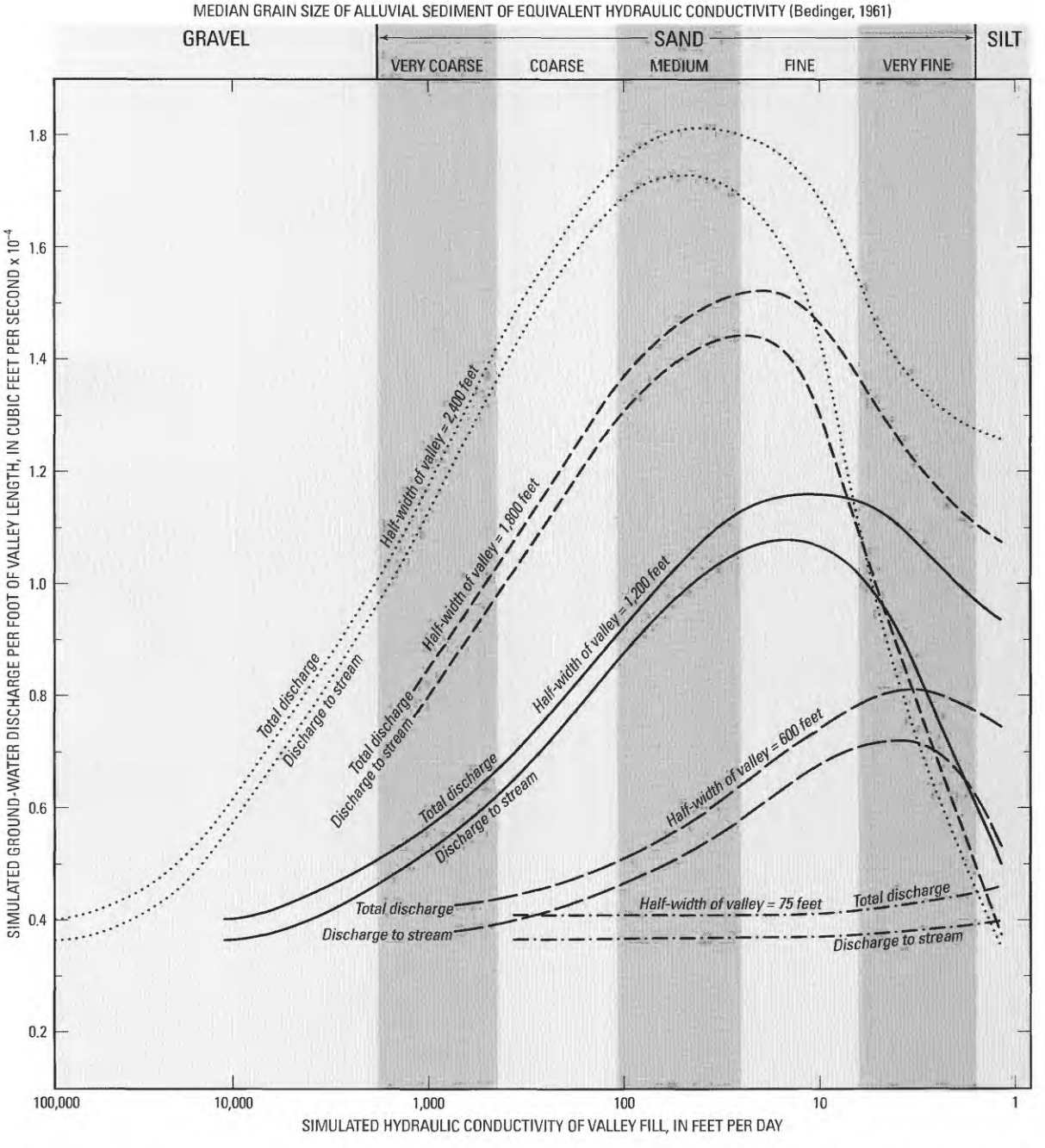

FIGURE 12.—Simulated ground-water discharge from idealized upland/valley-fill system after 4 months without recharge as a function of valley half-width, hydraulic conductivity of valley-fill materials, and ground-water evapotranspiration. Half-width of valley is the distance from the base of the adjacent hillside to a stream flowing along the axis of the valley. Total discharge for each half-width is ground-water discharge to the stream plus ground-water evapotranspiration.

mum water levels in wells near streams or in highly permeable stratified drift are nearly the same every year, because minimum stream stage is controlled by riffles in the channel, whose elevations seldom change appreciably; whereas annual maximum water levels in these wells reflect flood peaks whose magnitude and timing can differ appreciably from year to year. Wells OT7 and W533 (fig. 13*C*) illustrate this pattern; the latter is 800 ft from the nearest stream. By contrast, in stratified drift that is distant from streams and(or) sufficiently fine-grained to maintain a water table several feet above the stream, annual cycles of water-level fluctuation are commonly superimposed on rising or falling trends caused by longer-term fluctuations in precipitation. That is, during a succession of relatively wet years the annual maximum and the annual minimum are both higher each year than the previous year, reflecting increased storage in the stratified drift as

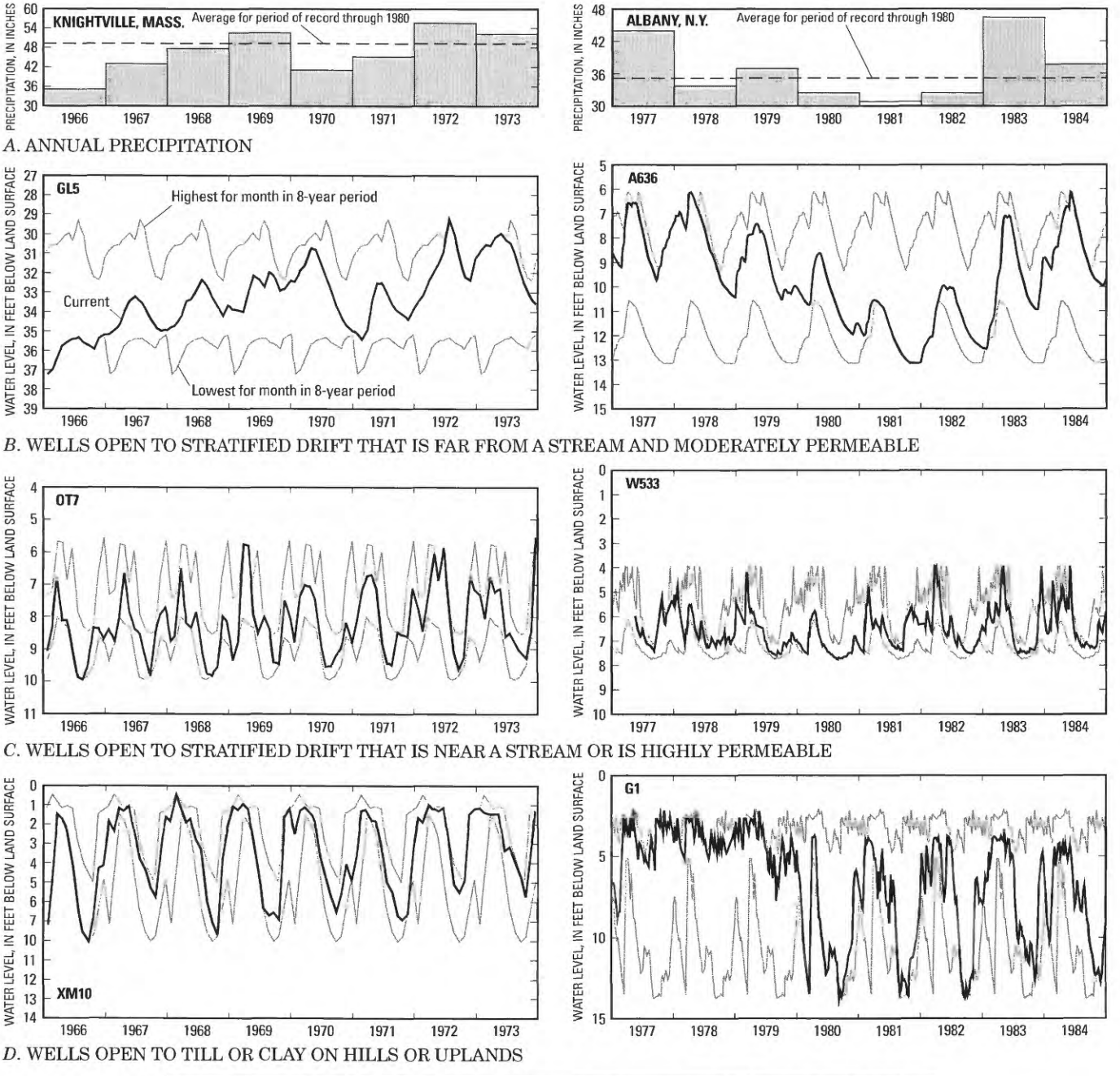

A. ANNUAL PRECIPITATION

B. WELLS OPEN TO STRATIFIED DRIFT THAT IS FAR FROM A STREAM AND MODERATELY PERMEABLE

C. WELLS OPEN TO STRATIFIED DRIFT THAT IS NEAR A STREAM OR IS HIGHLY PERMEABLE

D. WELLS OPEN TO TILL OR CLAY ON HILLS OR UPLANDS

Site	Town or city, state	Distance to nearest stream (feet)	Distance to precipitation site cited (miles)
Knightville	Westhampton, Mass.	- -	0
GL5	Granville, Mass.	1,100	14.8
OT7	Otis, Mass.	165	14.0
XM10	Wilmington, Mass.	980	90.0
Albany	Colonie, N.Y.	- -	0
A636	Albany, N.Y.	3,000	4.8
W533	Salem, N.Y.	800	38.0
G1	New Baltimore, N.Y.	800	24.8

FIGURE 13.—Hydrographs of water-table fluctuation representative of upland till, stratified drift distant from streams, and stratified drift near a stream. Data from National Oceanic and Atmospheric Administration (1966–84) and U.S. Geological Survey unpublished records.

hydraulic gradients steepen to accommodate the increased flux. Wells GL5 and A636 (fig. 13*B*) illustrate this pattern. Well GL5 penetrates a terrace of stratified drift that fills a small valley, stands 40 ft above the nearest stream, and probably consists of deltaic sand whose grain size becomes finer with depth. Well A636 penetrates a deltaic sand plain several miles wide in which surficial medium to fine sand grades downward to silt and clay. A different pattern is typical of many wells that penetrate till or lacustrine silt and clay on hills or uplands; commonly annual maximum water levels are nearly the same each year, only a few feet below land surface, because the sediment saturates nearly to land surface every spring, whereas annual minima vary more widely, presumably in response to variations in the amount of rainfall during the summer (fig. 13*D*). Well XM10 penetrates till on a gentle hill that rises only 15 feet above stream grade, whereas well G1 penetrates lacustrine silt and clay that may overlie till at shallow depth, on a ridge that stands 100 ft above the nearby stream.

The typical annual cycle of water-table fluctuation observed throughout the Northeast demonstrates that groundwater recharge occurs primarily during the non-growing season, from November through April, in most years. Water-balance studies and isotope data support this generalization. Computations of the amount of water available for recharge in successive months by water-balance methods (precipitation, minus evapotranspiration as estimated either from pan evaporation or from temperature and length of daylight) consistently indicate recharge predominantly during the non-growing season, as a long-term average and in individual years (Lyford and Cohen, 1988; Crain, 1974; Randall, 1986). The stable isotope content of ground water in stratified drift at sites in Ohio and New Jersey (Dysart, 1988) and Connecticut (J.E. Dysart, USGS unpublished records) was nearly constant and similar to that of streamflow in winter and early spring, but was isotopically lighter than streamflow during the growing season. This pattern is readily explained by the occurrence of most ground-water recharge in winter or early spring (Dysart, 1988, p.152).

STRATIFIED-DRIFT AQUIFERS OF THE GLACIATED NORTHEAST

The glaciated Northeast contains many deposits of stratified drift that are physically discontinuous but geologically similar, and that collectively form one of the most important sources of water supply in the region. They are generally found in the principal valleys and are hydraulically connected to perennial streams. Thick and extensive outwash deposits that bury pre-existing hills as well as valleys occur in a few localities. Plate 3 shows the location and extent of all tracts of coarse-grained stratified drift that are large enough to be discernable at the 1:1,500,000 scale of the plate and that have generally been designated in published reports as having a saturated thickness of at least 10 ft and(or) being capable of yielding at least 10 gal/min to individual wells. Altogether, the stratified-drift aquifers on plate 3 represent 12.6 percent (15,400 mi^2) of the 122,000 mi^2 area of the glaciated Northeast. Plate 3 also depicts the following information on aquifer yield:

1. Location of well fields where pumpage has averaged at least 5 mgal/d.
2. Aquifers judged capable of sustained yields of at least 5 mgal/d.
3. Aquifers judged especially suitable for large seasonal withdrawals without causing substantial concurrent depletion of streamflow by induced infiltration, including headwater, outwash-plain, and sand-plain aquifers as defined in the plate explanation and in the text section "Aquifer Types."

Plate 3 was compiled by Geographic Information System techniques from a variety of maps whose scales range from 1:24,000 to 1:500,000; each source map (or the earliest map in each series of maps) is cited on the plate. The areal extent of the aquifers shown on plate 3 is not necessarily proportional to aquifer yield and is unrelated to well yield. Many of the larger tracts are broad sand plains containing thin or fine-grained surficial sand over lake-bottom silt and clay, or deltaic aprons perched above stream grade along mountain fronts, deeply incised and therefore largely unsaturated. Plate 3 is intended to illustrate the abundance, widespread distribution, and local extent of stratified-drift aquifers in the glaciated Northeast. It indicates that large, continuous withdrawals are possible in many places, particularly along the larger streams where abundant induced infiltration can occur, and that aquifers suitable for use as storage reservoirs for large seasonal withdrawals are also scattered widely across the region. Local hydrologic studies, such as those cited on plate 3, should be consulted with regard to selecting sites for large-capacity wells and estimating their yields.

COMMON CHARACTERISTICS

The stratified-drift aquifers share several common geohydrologic features despite their scattered, discontinuous distribution.

1. They consist largely of sand and gravel, deposited by or in glacial meltwater, that can range widely in grain size and stratification over distances as small as a few tens of feet.
2. Aquifer recharge originates as precipitation that falls on the surface of the aquifer and adjacent uplands.
3. Most of the aquifers are hydraulically connected to a perennial stream or a lake that crosses or borders the aquifer.
4. Ground water stored within, and moving through, the aquifers is unconfined in most places, although confined or

semiconfined conditions occur where aquifers are buried beneath fine-grained stratified drift.

5. The aquifer systems are dynamic in that water is continuously passing through them. Recharge and discharge can occur simultaneously, at varying rates such that storage is either increasing or decreasing.
6. Individual aquifers are generally independent of one another, in that pumping from one aquifer rarely causes drawdown in others. Large withdrawals from an aquifer commonly deplete the flow of the stream to which it is hydraulically connected, however, and thereby reduce the amount of water potentially available to a downstream aquifer during periods of low flow. Also, a regional drought that reduces recharge over a large area can result in decreased yields from all sand and gravel aquifers in the affected area.
7. Saturated thickness of sand and gravel is at most a few hundred feet and commonly ranges from 10 to 150 ft. Many wells that tap the aquifers are less than 100 ft deep.
8. The surficial sediments are generally highly permeable; therefore, most of these aquifers are vulnerable to immediate contamination from spills or burial of liquids or soluble substances that could be leached by infiltrating precipitation.
9. Natural changes in storage, as evidenced by fluctuations in the water table, generally follow seasonal patterns. These include short, relatively well-defined periods in the spring and fall when recharge greatly exceeds discharge, and longer, less well defined periods in the summer and winter when discharge generally exceeds recharge.
10. The high permeability of sand and gravel aquifers allows large water supplies to be obtained from a relatively small number of wells with large individual yields.

AQUIFER TYPES

The stratified-drift aquifers of the glaciated Northeast can be classified according to their location within the drainage system, recharge and discharge patterns, boundaries, and dimensions. Six aquifer types can be identified: valley fill, headwater, sand plain, hillside, outwash plain, and buried. Their principal characteristics are described below, in figure 14, and in table 4. The design of ground-water flow models to simulate each of these aquifer types is discussed in the section "Simulation of Aquifer Types" further on.

1. Valley-fill aquifers (fig. 14*A*) are the principal type of stratified-drift aquifer in the glaciated Northeast in terms of abundance and water-supply potential. They occur in valleys and are crossed by major perennial streams from which they can receive significant induced infiltration. They also receive considerable amounts of recharge from adjacent uplands. Valley fill typically includes from 10 to 150 ft of saturated sand and gravel that may be underlain, bordered, or in part overlain by fine-grained stratified drift, and is always bordered on 2 sides and underlain by relatively impermeable bedrock. A variety of valley-fill aquifers having different configurations of sand and gravel relative to fine-grained stratified drift are depicted in figure 14*A*.
2. Headwater aquifers (fig. 14*B*) also occur in valleys; they are similar in dimensions and composition to other valley-fill aquifers (fig. 14*A*) but are not crossed by major perennial streams that originate elsewhere. They are recharged by direct infiltration of precipitation and by runoff from adjacent uplands, and are drained by small streams whose upper reaches may cease flowing seasonally. Many are only moderately thick (25 to 75 ft) and consist of coarse, heterogeneous ice-contact sand and gravel.
3. Sand-plain aquifers (fig. 14*C*) are typically found in areas that were once occupied by large proglacial lakes. These aquifers are relatively thin (20-50 ft), consist of fine to medium sand, and are recharged primarily by direct infiltration of precipitation. They are typically underlain by clay and silt that limit downward ground-water movement. Streams associated with sand-plain aquifers typically penetrate the full thickness of the aquifer and are incised into the underlying clay and silt. As a consequence, the streams function as aquifer drains rather than as sources of induced infiltration and have virtually no potential for induced infiltration.
4. Hillside aquifers (fig. 14*D*) are found along the sides of major valleys where bedrock is near land surface. These aquifers typically consist of ice-contact sand and gravel, range from 10 to 150 ft in thickness, and are thinly saturated because much of the sand and gravel is above stream grade. Perched hillside aquifers are chiefly important as contributors of ground-water discharge to springs, streams, or adjacent valley-fill aquifers.
5. Outwash-plain aquifers (fig. 14*E*) formed chiefly in areas of low relief at or near the margins of the continental ice sheet, where thick (50-150 ft) accumulations of sand and gravel largely buried the former topography. Scattered till hills rise above some outwash plains and contribute some upland runoff, but most recharge is from direct infiltration of precipitation. This natural recharge cannot generally be augmented by induced infiltration, because most outwash plains are crossed only by small streams that rise within the outwash plain and that are fed by local ground-water discharge.
6. Buried aquifers (fig. 14*A*) are confined or semi-confined by fine-grained sediment. Many are delta-fed; that is, near the side of the valley they are overlain in part by coarse-grained deltaic sediments that extend upward to land surface and constitute an avenue through which direct precipitation and seepage losses from tributary streams can reach the buried aquifers. Others are isolated, such that

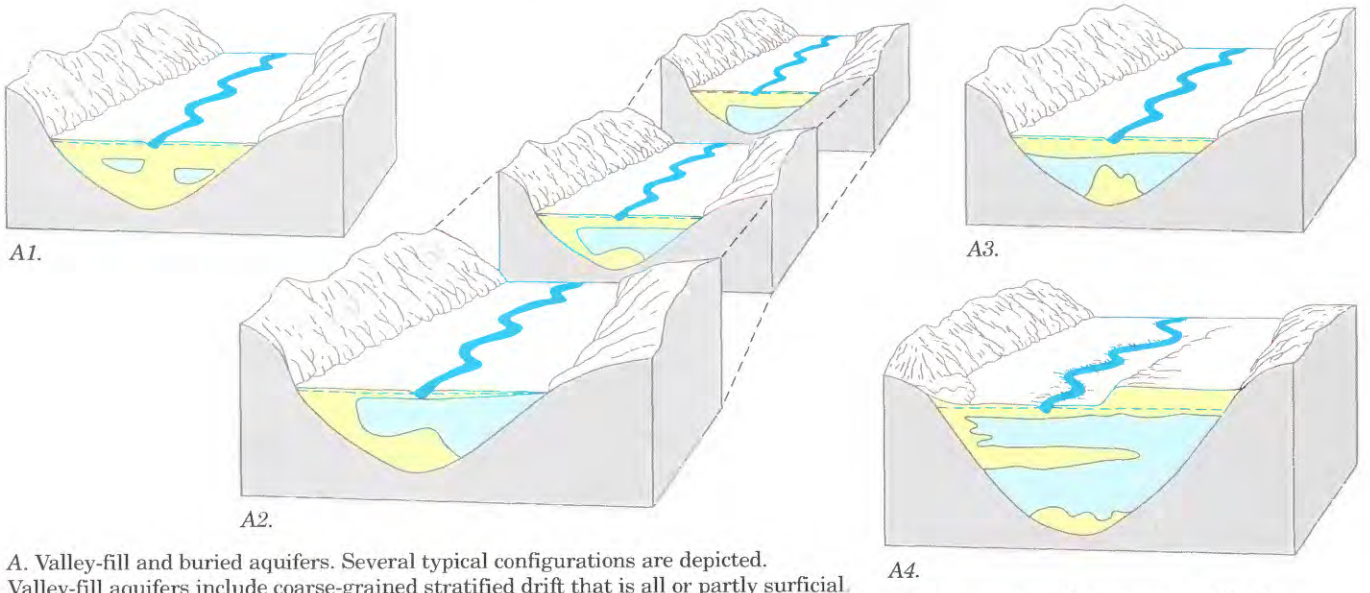

A. Valley-fill and buried aquifers. Several typical configurations are depicted.
Valley-fill aquifers include coarse-grained stratified drift that is all or partly surficial.
Buried aquifers are either isolated beneath fines (A3, A4) or can be recharged from land surface near the valley margins (A2, A4).

B. Headwater aquifers. Same forms shown in *A*, but no major stream along the valley axis.

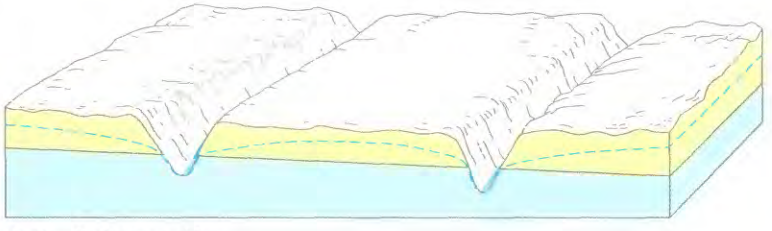

C. Sand-plain aquifer

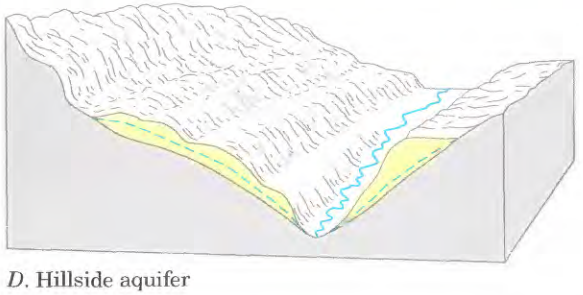

D. Hillside aquifer

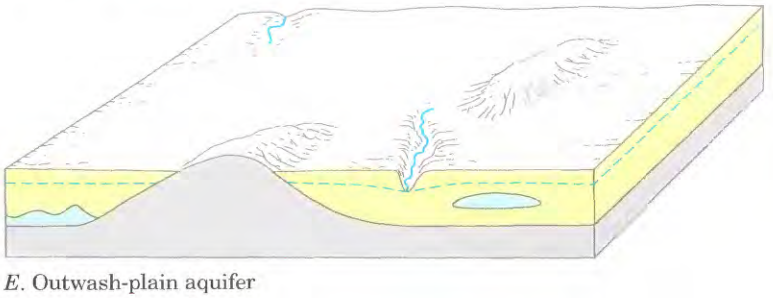

E. Outwash-plain aquifer

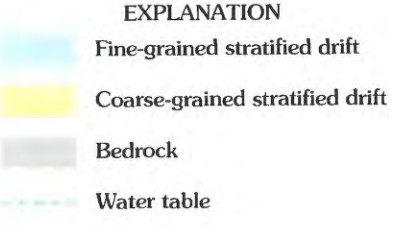

FIGURE 14.—Idealized types of stratified-drift aquifers that differ in their relations to hydraulic boundaries and recharge sources (modified from Randall, 2001, fig.38).

TABLE 4.—*Classification of stratified-drift aquifers in the glaciated Northeast and summary of their chief hydrologic characteristics*

[>, greater than; <, less than; "Direct" refers to recharge from precipitation on the aquifer]

Aquifer type	Estimated abundance among all stratified-drift aquifers (percent)	Typical topographic or geohydrologic setting	Principal sources of recharge	Function of principal stream
Valley fill	>80	Major and secondary river valleys	Direct, unchanneled flow from uplands, leakage from tributary streams, induced recharge.	Receives discharge from aquifer under nonpumping conditions, is a source of induced recharge under pumping conditions.
Headwater	5 to 10	Upper reaches of broad valleys	Direct, unchanneled flow from uplands, leakage from tributary streams.	Receives discharge from aquifer; flow is small, may go dry seasonally.
Hillside	<5	Sides of valleys in areas of high relief	Direct, minor unchanneled flow from uplands.	Receives discharge from aquifer under most conditions.
Outwash plain	<5	Areas of low relief near persistent former ice margins (outwash areas)	Direct, minor unchanneled flow from isolated hills surrounded by outwash.	Receives discharge from aquifer under nonpumping conditions; originates within aquifer; downstream reaches can be sources of limited induced recharge under pumping conditions.
Sand plain	<5	Sites of former glacial lakes	Direct, minor unchanneled flow from hills.	Receives discharge from aquifer under all conditions.
Buried (delta-fed)	<5	Major valleys and lowlands, near tributaries	Leakage from stream-supplied deltaic deposits, flow from adjacent formations.	Tributaries provide recharge to deltaic deposits that supply the buried aquifer; master stream not in contact with aquifer.
Buried (isolated)	<1	Major valleys and lowlands	Flow from adjacent formations.	No streams are in contact with aquifer.

they receive recharge only from adjacent fine-grained sediment and bedrock.

Many prominent headwater aquifers and a few large outwash-plain or sand-plain aquifers are identified as such on plate 3; smaller examples exist but are not identified, as indicated in the map explanation. No attempt was made to distinguish the other types of aquifers on plate 3. Randall (2001) presents more information on the distribution of outwash-plain, sand-plain, and buried aquifers and briefly describes another uncommon type of aquifer, the isolated aquifer, which consists of a body of sand and gravel that is surrounded and overlapped by fines deposited in a large proglacial water body.

NATURAL FLOW SYSTEM

The principal components of the natural flow system of a stratified-drift aquifer—those that control the amount of water that an individual aquifer is capable of supplying over the long term—are as follows:

1. Direct recharge from precipitation: Water that enters a stratified-drift aquifer as a consequence of rain and snow falling on the land surface directly above the aquifer.
2. Recharge from streams: Water that seeps into an aquifer from the channels of principal streams or tributaries.
3. Inflow from (or outflow to) adjacent areas: Water that enters an aquifer as (a) unchanneled surface or near-surface flow from adjacent uplands, (b) predominantly horizontal subsurface flow from adjacent uplands, and (c) flow from stratified drift upstream along the valley (underflow); or that leaves the aquifer as flow to stratified drift downstream along the valley (outflow).
4. Flow from (or to) underlying formations: Water that enters (or leaves) an aquifer as primarily vertical subsurface

flow from (or to) underlying formations. In general, these formations are bedrock, or till overlying bedrock.

5. Ground-water discharge: Water that discharges naturally to surface-water bodies such as streams, lakes, and wetlands.
6. Ground-water evapotranspiration: Water that discharges to the atmosphere through the combined processes of evaporation and transpiration.

Under natural conditions, some of the components of recharge to and discharge from stratified-drift aquifers undergo predictable temporal variations similar to those of runoff depicted in figure 9. For example, recharge from precipitation normally occurs during the fall, winter, and spring, particularly just before and just after the growing season. Ground-water discharge, underflow, inflows from adjacent uplands and inflows from the underlying bedrock are normally continuous, although the rate and direction of flow are not constant. For example, rates of ground-water discharge to streams and of infiltration from streams are in part a function of the difference in hydraulic head between the aquifer and stream, both of which can vary seasonally.

RECHARGE

The spatial and temporal variation of recharge to stratified-drift aquifers is a key determinant of the long-term availability of water and one of the more important elements required for simulation of flow in these aquifers. Under natural conditions, recharge to stratified drift can originate from several sources: (1) precipitation (rain and snow melt) that falls directly on the land surface above the stratified drift and infiltrates to the saturated zone, (2) unchanneled runoff from upland hillsides immediately adjacent to the stratified drift, flowing as surface or shallow subsurface runoff during and after storms, (3) ground water from adjacent till or bedrock, the product of flow systems that originate in part from the adjacent hillsides and in part from more distant uplands, and (4) infiltration from the channels of upland streams that cross the stratified drift. Under developed conditions, recharge is generally also available from (5) infiltration from major streams, induced by pumping, and (6) return of waste water after use. All but the last of these sources are diagrammed in figure 3. Valley-fill aquifers may also receive some recharge by underflow from upvalley under natural conditions, and also from downvalley under developed conditions.

Procedures for estimating recharge have evolved over the years along with the conceptualization of recharge sources. Early studies focused on computing basinwide average recharge, which can be equated to the sum of ground-water discharge to streams (base flow) plus underflow, any pumpage not returned to the aquifer after use, and ground-water evapotranspiration, plus or minus net changes in ground-water and soil-moisture storage over the period of study. Ground-water discharge to streams can be estimated by separation of streamflow hydrographs at gaging stations into base flow and storm runoff components, through a variety of graphical techniques (Hall, 1968; Schicht and Walton, 1961; Knisel, 1963; Meinzer and Stearns, 1929) or computerized procedures (Pettyjohn and Henning, 1979; Rutledge, 1993). In a few studies in the glaciated Northeast, nearly all components of the ground-water budget were calculated from measurements within the watershed (Meinzer and Stearns, 1929); more commonly underflow and net pumpage were judged to be negligible, net change in storage was minimized by selecting periods of a year or longer over which the net change in water level was small, and ground-water evapotranspiration was ignored (thereby resulting in a conservative underestimate of recharge). Annual or monthly recharge rates thus computed are presented in several reports (Meinzer and Stearns, 1929; Randall, 1964; Rosenshein and others, 1968; Allen and others, 1966) but are of little value as an index to potential ground-water withdrawals because each represents a basin wide average of small rates of recharge to till-mantled uplands and much larger rates of recharge to stratified-drift aquifers in valleys.

Rates of recharge to stratified drift and to till have been estimated by analysis of basinwide average annual recharge rates in several basins in and near Connecticut. The methodology was developed in a series of water-resource appraisals for segments of that state, and finalized by Mazzaferro and others (1979). Ground-water discharge to streams was computed by hydrograph-separation techniques for an individual year in each of several basins with different proportions of stratified drift. A graph of the results (fig. 15) indicates that annual ground-water discharge ranges from about 35 percent of runoff in areas underlain entirely by till to about 95 percent of runoff in areas underlain entirely by stratified drift. The scatter in the data is probably due to changes in storage in some years, imprecision in hydrograph-separation techniques and in delineation of the areal extent of till and stratified drift, and minor ground-water discharge by pumping (Cervione and others, 1972, p.47). Natural recharge to any stratified-drift aquifer can then be conservatively estimated as the sum of recharge from precipitation on the aquifer (the product of total runoff for the period of interest times 0.95 times area of stratified drift) plus ground-water runoff from adjacent upland hillsides that slope toward the aquifer (the product of total runoff for the period of interest times 0.35 times area of adjacent hillsides.) This recharge conceptualization and computation technique has been widely used, in Connecticut water-resource appraisals (Handman and others, 1986, and predecessors) and in several ground-water flow models in New England (Haeni, 1978; Morrissey, 1983; Olimpio and de Lima, 1984; Mazzaferro, 1986a; Dickerman and Ozbilgin, 1985). A similar methodology was applied by Taylor (1988) to a much smaller array of basins in south-central New York. Nevertheless, this approach does not fully account for natural

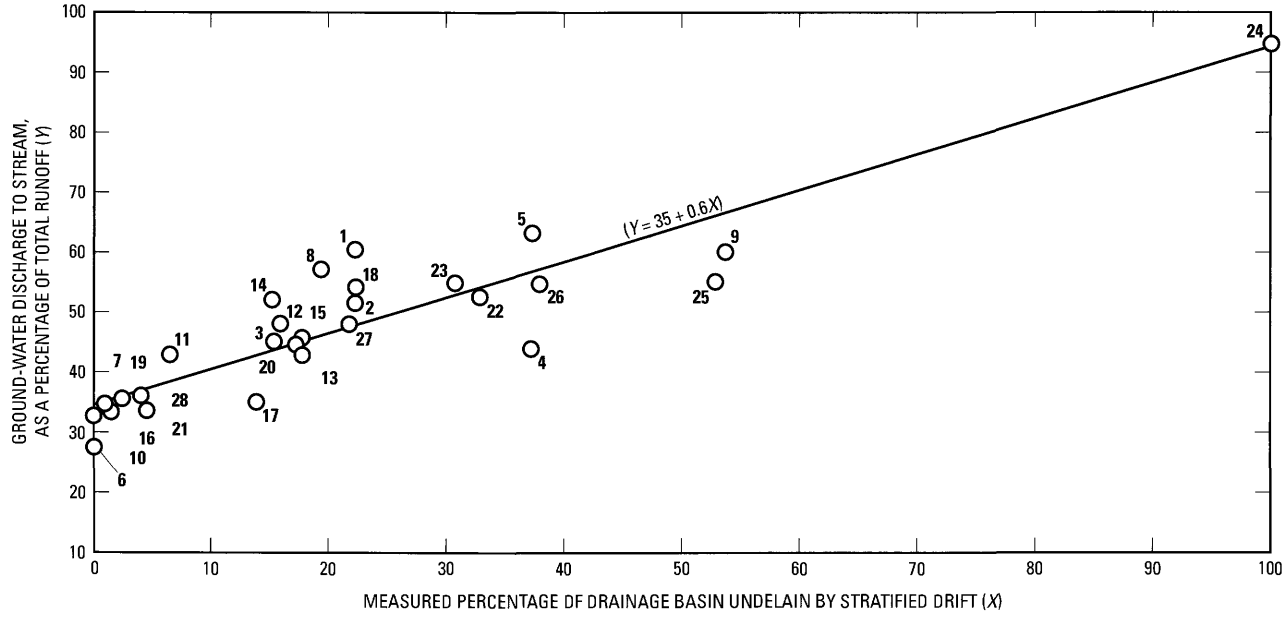

IDENTIFICATION OF DATA VALUES

Data value	Drainage basin	Time period [W.Y., Water Year]	Reference
1	Salmon Brook	1950 W.Y.	Randall, 1964
2	Salmon Brook	1953 W.Y.	do.
3	Pomperaug River	1914–1916	Meinzer and Stearns, 1929
4	Pequabuck River	1953 W.Y.	La Sala, 1964
5	Pequabuck River	1957 W.Y.	do.
6	Ash Brook	May 1963–April 1964	Thomas and others, 1967
7	Safford Brook	May 1963–April 1964	do.
8	Skungamaug River	May 1963–April 1964	do.
9	Denison Brook	August 1962–July 1963	Randall and others, 1966
10	Lowden Brook	August 1962–July 1963	do.
11	Mashamoquet Brook	August 1962–July 1963	do.
12	Little River	August 1962–July 1963	do.
13	East Branch Saugatuck River	1966 W.Y.	Ryder and others, 1970
14	Norwalk River	1966 W.Y.	do.
15	Poquonock River	1966 W.Y.	do.
16	Little River	1966 W.Y.	do.
17	Blackberry River at Canaan	1968 W.Y.	Cervione and others. 1972
18	Blackberry River at West Norwalk	1968 W.Y.	do.
19	Whiting River	1968 W.Y.	do.
20	Salmon Creek	1968 W.Y.	do.
21	Factory Brook	1968 W.Y.	do.
22	Salmon Creek (adjusted)	1968 W.Y.	Unpublished Connecticut data
23	Ipswich River, Massachusetts	1939 W.Y.–1959 W.Y.	Baker and others, 1964
24	Several basins, Long Island, N.Y.	- -	Pluhowski and Kantrowitz, 1964
25	Quinnipiac River	1970 W.Y.	Mazzaferro and others, 1979
26	Misery Brook	1970 W.Y.	do.
27	Mill River	1970 W.Y.	do.
28	Race Brook	1970 W.Y.	do.

FIGURE 15.—Relation between ground-water discharge to streams and percentage of drainage basin underlain by coarse-grained stratified drift (from Weaver, 1987, as modified from Mazzaferro and others, 1979). All drainage basins are in Connecticut except as noted; see cited references for locations.

recharge from upland runoff to stratified-drift aquifers, especially in areas of high relief, as explained in the next section.

RECHARGE FROM UPLAND RUNOFF

Several investigators (Crain, 1974; MacNish and Randall, 1982; Randall, 1986; Tepper and others, 1990) have proposed that where stratified drift is bordered by upland hillsides, all or nearly all unchanneled runoff from the hillsides will infiltrate into the stratified drift, including surface or shallow-depth storm runoff as well as ground-water flow through deeper levels of till and bedrock. Detailed hydrologic and geochemical studies (Sklash and Farvolden, 1982; Martinec, 1975) suggest that ground water constitutes a much larger fraction of runoff from upland hillsides than commonly inferred from hydrograph separation. Calibration of a ground-water flow model (Haeni, 1978) to observed water levels required more recharge along the valley margins than was indicated as being available from the computation technique described in the previous paragraph (F.P. Haeni, USGS, oral commun. 1988). Caldwell and others (1987) showed that a stratified-drift aquifer in southwestern New Hampshire received significant recharge as unchanneled runoff from adjacent hillsides.

Upland runoff in the channels of tributary streams also can recharge valley-fill aquifers. In the Appalachian Plateau of New York, small upland tributaries go dry seasonally where they enter larger valleys; this loss of flow was noted as a source of recharge to the valley fill by Wetterhall (1959) and was described as being typical of the region by Ku and others (1975). Seepage losses from tributaries on alluvial fans adjacent to the walls of Cassadaga Creek valley in southwestern New York were shown by Crain (1966) to be a major source of recharge to a gravel aquifer beneath 100 ft of silt and clay in midvalley. The magnitude and distribution of seepage loss from tributary streams of the Susquehanna River basin in south-central New York was investigated by Randall (1978), who found that loss rates were small near the edges of the main valley, but were at least 1 ft^3/s per 1,000 ft of channel several hundred feet downstream. Similar loss rates from tributaries were measured by Williams (1991) in Marsh Creek valley of north-central Pennsylvania, and by Johnson and others (1987) and Tepper and others (1990) in the Saco River valley in eastern New Hampshire. A few stream reaches in each locality showed little or no loss because they are underlain by fine-grained deposits, rather than the typical alluvial gravel. In general, recharge from channeled upland runoff is a function of the hydraulic conductivity of the streambed and underlying materials, and the difference between stream stage and head in the aquifer. At times, recharge may be further constrained by the limited amount of streamflow entering the valley, which could be determined from streamflow measurements or estimated from regional runoff maps or from tabulated streamflow data from similar geographic and geologic settings.

The estimated magnitudes of recharge from channeled and unchanneled upland runoff to several valley-fill aquifers, some of which are affected by pumping, are given in table 5. The table indicates that recharge derived from upland sources can be a significant percentage of total valley-fill recharge. Similar results were obtained by Riser and Madden (1994) from a simulation of ground-water flow in an idealized valley-fill aquifer. Morrissey and others (1988) concluded that the percentage of recharge derived from upland sources tends to increase with increasing upland topographic relief and with decreasing valley width. Width is significant merely because the volume of recharge from precipitation on the valley floor necessarily decreases as valley width decreases, whereas upland runoff is unaffected by valley width. Relief is significant because most tributary streams in areas of high relief have steep gradients such that the tributary channels near the valley sides are at much higher elevation than the master stream, a condition that favors seepage of substantial amounts of water from the tributaries to the valley fill. By contrast, the elevation and gradient of tributaries in areas of low relief tend to be low, and seepage losses under natural conditions are probably minimal.

Average monthly amounts of channeled or unchanneled runoff from any upland hillside or watershed may be estimated by multiplying the average annual runoff for that locality (from pl. 2) by the average percentage of annual runoff in each month (from fig. 9, for the climatic regions delineated in fig. 1). To convert the resulting average monthly runoff in inches to cubic feet per second, multiply the result by the area, in square miles, of the upland hillside or watershed of interest and by a conversion factor selected from the table below.

Number of days in month	Conversion factor
28	0.960
29	.927
30	.896
31	.867

For example, if annual runoff is 20 inches, and 20 percent of the runoff is in March, the March runoff is 4 inches. If the upland area of interest is 2 mi^2, the runoff is 4 x 2 x 0.867 = 6.94 ft^3/s. More precise values of the percentage of annual runoff in each month for 37 unregulated streams, including the 16 streams illustrated in figure 9, may be obtained from Lyford and Cohen (1988, table 3). The same procedure can be used to estimate channeled or unchanneled runoff for any particular period of time if concurrent records of streamflow at a suitable site along a typical upland stream are available. The

TABLE 5.—*Upland sources of recharge to selected valley-fill aquifers in the glaciated Northeast*

[>, greater than; ft., feet; ft^3/s, cubic feet per second; mi^2, square miles. Data compiled in part from Morrissey and others (1988) and Williams and Morrissey (1996).]

Location of aquifer (and original data source)	Conditions[a]	Channeled upland runoff: Basis and method of computation	Recharge (ft^3/sec)	Percent of total recharge	How simulated[b]	Unchanneled upland runoff: Basis and method of computation	Recharge (ft^3/sec)	Percent of total recharge	How simulated[b]	Total from upland runoff: Recharge (ft^3/sec)	Percent of total recharge
Relief greater than 500 feet from valley flow to nearby hilltops											
Killbuck Creek Wooster, Ohio (this paper)	CP*	Model simulation, based on streamflows and streambed properties estimated from several measurements or computed by Variable-Recharge procedure	3.2	26	SV	Annual water available for recharge estimate as 1.0 $(ft^3/s)/mi^2$, by water-balance method; upland runoff computed by Variable-Recharge procedure	4.6	37	V	7.8	63
Catatonk Creek Candor, N.Y. (MacNish and Randall, 1982)	L	Higher of (a) estimated streamflow, or (b) 1 ft^3/s per 1,000 ft of channel (for channels with slope >1%	1.95	36	N	Annual recharge in uplands estimated to average 0.6 $(ft^3/s)/mi^2$ based on literature cited[c], generally equivalent to 0.25 ft^3/s per mile of valley wall	1.2	22	N	3.2	58
Fly Creek, Pleasant Brook Smyrna, N.Y. (Reynolds and Brown, 1984)	L	1 ft^3/s per 1,000 ft of channel with slope >1%	5.5	24	N	Annual recharge in uplands estimated to average 0.6 $(ft^3/s)/mi^2$ based on literature cited[c], generally equivalent to 0.25 ft^3/s per mile of valley wall	4.6	20	N	10.1	44
Susquehanna River Broome County, N.Y. (Randall, 1986)	CP	Estimated from several measurements of stream loss or from generalized loss of 1 ft^3/s per 1,000 ft of channel with slope >1%	15.1	36	F	Unchanneled upland runoff (and direct recharge) estimated from current monthly precipitation minus average monthly evapotranspiration as 1.4 $(ft^3/s)/mi^2$, reduced to 1.1 $(ft^3/s)/mi^2$ during model calibration	6.6	16	F3	21.7	52
Harford valley Harford, N.Y. (Randall and others, 1988b)	C	Recharge from upland runoff (channeled plus unchanneled) computed as underflow leaving valley reach (average of two methods) minus direct recharge (from water-balance analysis)	—	—	F	Included with channeled runoff	—	—	I	2.6	60

TABLE 5.—*Upland sources of recharge to selected valley-fill aquifers in the glaciated Northeast*—Continued

[>, greater than; ft., feet; ft^3/s, cubic feet per second; mi^2, square miles. Data compiled in part from Morrissey and others (1988) and Williams and Morrissey (1996).]

Location of aquifer (and original data source)	Conditions[a]	Channeled upland runoff: Basis and method of computation	Recharge (ft^3/sec)	Percent of total recharge	How simulated[b]	Unchanneled upland runoff: Basis and method of computation	Recharge (ft^3/sec)	Percent of total recharge	How simulated[b]	Total from upland runoff: Recharge (ft^3/sec)	Percent of total recharge
Relief greater than 500 feet from valley flow to nearby hilltops (continued)											
Marsh Creek north-central Penna. (Williams and Morrissey, 1996)	CP*	Model simulation; upland runoff based on gaged flow of two tributaries, recharge calibrated against several measurements of stream loss	9.8	80	S	Runoff from gaged tributaries averaged 1.4 $(ft^3/s)/mi^2$ during 3-month calibration period. (Direct recharge assumed to be the same)	1.6	13	F1	11.4	93
Saco River, Conway, N.H. (Tepper and others, 1990)	LP	Several measurements of stream losses	10.8	16.5	F	Runoff from two nearby gaged watersheds averaged 2.4 $(ft^3/s)/mi^2$	24.5	37.5	F1	35.3	54
Relief less than 500 feet from valley floor to nearby hilltops											
Ela River, New Durham, N.H.	L[d]	Model simulation	0.3	4.5	R	Runoff from a nearby gaged	2.0	33	F2	2.3	37.5
Cocheco River, Farmington, N.H. (Mack and Lawlor, 1992)	L[d]	Model simulation	0.3	3.5	R	watershed averaged 1.45 $(ft^3/s)/mi^2$ for 1966–77	4.5	50	F2	4.8	53.5
Farmington River, Farmington, Conn. (Mazzaferro, 1989)	L*	Not considered[e]	—	—	—	Ground-water recharge in uplands averages 0.52 $(ft^3/s)/mi^2$ (7 inches)[f]	20	31	F1	20	31
Lower Wood River, southwestern R.I. (Dickerman and others, 1990)	L	Runoff from two nearby gaged watersheds averaged 2.0 $(ft^3/s)/mi^2$ during 1941–76	2.2	8	F	Same as for channeled runoff	8.1	27	F1	10.3	35
Rockaway River, Dover, N.J. (this paper)	LCP	Not considered[e]	—	—	—	Average seasonal amounts of water available for recharge estimated by water-balance method; upland runoff computed by Variable-Recharge procedure[g]	3.5	57	V	3.5	57

Footnotes for this table appear on the following page.

TABLE 5.—*Upland sources of recharge to selected valley-fill aquifers in the glaciated Northeast*—Continued

[Footnotes]

[a] L based on data averaged over 10 or more years.
C based on current data for 1 to 24 months during period of study, generally claimed to approximate average conditions.
P part of ground-water discharge is to pumped wells.
* rates for periods of above-average and below-average recharge also estimated in cited reference.

[b] Method of simulating recharge from this source in ground-water flow model:
F Specified flux, applied to cells at or downstream from the point at which tributary stream begins to cross aquifer.
F1 Specified flux representing each unchanneled hillside, divided equally among model cells along adjacent margin of aquifer.
F2 Same as F1, but divided in proportion to upland area contributing to each model cell along margin of aquifer.
F3 Specified areal recharge rate applied to all model cells, multiplied by area of each cell within aquifer, plus (only for cells along aquifer margin) area of unchanneled hillside upslope from that cell.
I Unchanneled upland runoff not differentiated; simulated as part of channeled runoff.
N No ground-water flow model.
R River package (McDonald and Harbaugh, 1988).
S Stream package (Prudic, 1989).
V Variable-Recharge procedure, explained in this paper.

[c] These estimates, derived from two cited references, may be conservative. Kantrowitz (1970, p. 67) estimated that 25 percent of precipitation on upland hillsides directly tributary to valley-fill aquifers becomes storm runoff that recharges these aquifers, but apparently ignored ground-water runoff from the hillsides. Randall (1977, p. 61) calculated an annual water budget for a valley-fill aquifer that included 8 inches of unchanneled runoff from upland hillsides where urban development may have diverted much of the runoff to storm sewers.

[d] Direct recharge was estimated as 50 percent of average precipitation. This generalization, although approximately true in many places, is invalid in principle (Johnstone and Cross, 1949, p. 105) and in practice in the glaciated Northeast with respect to variation from place to place (compare pls. 1 and 2) or from year to year (see section on evapotranspiration).

[e] Tributaries that cross aquifer are few, small, and ephemeral, and (or) follow low-gradient valleys underlain by stratified drift and, hence, are unlikely to be sources of appreciable recharge under average conditions.

[f] Source and time period not stated in Mazzoferro (1989); may represent average ground-water runoff from uplands (Mazzoferro and others, 1979, fig. 38) and, if so, underestimates unchanneled upland runoff.

[g] Recharge values presented are average for the four seasons.

most suitable sites for measurement of the flow of upland streams are narrow valley reaches where the streams flow on till or bedrock, so that all runoff passes the gaging station as surface flow.

Ground water that flows to valley-fill aquifers from bedrock in bordering hillsides is included in estimates of unchanneled runoff from those hillsides. Ground water that flows through bedrock to major valleys along deep, regional flow systems from more distant intervening upland areas is difficult to quantify, but is thought to be small because (1) bedrock is much less permeable than stratified drift, and (2) hydrologic budgets and ground-water flow models of valley-fill aquifers can usually be satisfied without calling for more recharge than is reasonably estimated to be available from other sources. In the Appalachian Plateau of southwestern New York, northeastern Ohio, and northwestern Pennsylvania, water in the bedrock at or slightly below the base of the valley fill is commonly saline, and saline water is also found locally in the lower part of the drift (Crain, 1974; Randall, 1972, 1979; LaSala, 1968). This saline water presumably constitutes discharge from regional flow systems. Geochemical contrasts between water in bedrock and water in the upper part of the stratified drift have been used to estimate bedrock contribution to individual pumped wells (Breen, 1988, Dysart, 1988, Breen and others, 1995) or to streams (LaSala, 1967; Archer and others, 1968). In most of the glaciated Northeast, however, the mineralogy of drift resembles that of nearby bedrock, and although water in bedrock is geochemically more evolved than that in drift because its residence time is greater, the geochemical characteristics of water in bedrock and drift are similar (Rogers, 1989).

RECHARGE FROM DIRECT INFILTRATION OF PRECIPITATION

Natural recharge (R) to stratified drift by direct infiltration of precipitation to the saturated zone over a particular time period can be described by the water-balance relation (modified from Lyford and Cohen, 1988), in which all terms are expressed as a depth of liquid water over the area of interest:

$$R = P - ET + SN_m - SN_s - SR \pm SM \qquad (L) \qquad (4)$$

where P is precipitation
ET is evapotranspiration of moisture above the water table,
SN_m is snowmelt,
SN_s is accumulation of snow held in storage,
SR is surface runoff, and
SM is the change in soil moisture content.

As implied by the relation in figure 15, surface runoff is generally negligible in areas underlain by stratified drift. Therefore, direct recharge can be calculated from equation 4 in five steps. The method of calculation for mean monthly recharge is illustrated in table 6 for an aquifer at Cooperstown, New York, in climatic region B (fig. 1), using long-term average data values.

1. Determine from local records the precipitation for each month (or other appropriate time increment) in the year(s) of interest. (Item 1, table 6). If long-term mean recharge is to be calculated, but no long-term precipita-

TABLE 6.—*Example of water-balance computation of long-term mean monthly recharge to stratified drift from direct infiltration of precipitation*

[All values in inches, except as noted. Dashes indicate values assumed to be zero or not part of computation. Minor imbalance in some totals results from rounding of monthly evapotranspiration. (Computation is based on equation 4 (p. C36 of this paper), for a site at Cooperstown, N.Y., and is modified from an example computation by Lyford and Cohen, 1988)]

Item no.	Water-balance term	Month												Annual total
		Jan	Feb	Mar	Apr	May	June	July	Aug	Sept	Oct	Nov	Dec	
1	Precipitation[1]	2.57	2.29	3.24	3.37	3.50	3.89	3.65	3.39	3.66	3.13	3.38	3.21	39.28
2	Evapotranspiration[2]				(9.5)	(14.9)	(18.3)	(19.9)	(17.0)	(12.0)	(8.1)			(100)
		—	—	—	−1.81	−2.83	−3.48	−3.78	−3.23	−2.28	−1.54	—	—	−19.0
3	Snow storage (−) or snow melt (+)[3]	−1.4	−0.4	+3.2	0	0	0	0	0	0	0	0	−1.4	—
4	Soil moisture:[4] depletion (+) or addition (−)	—	—	—	—	—	—	+0.13 (0.13)	−0.13 (0)	—	—	—	—	—
5	Mean monthly recharge	1.17	1.89	6.44	1.56	0.67	0.41	0	0.03	1.38	1.59	3.38	1.81	20.33

[1] Long-term (1951–80) means (National Oceanic and Atmospheric Administration, 1985a; Lyford and Cohen, 1988, table 1).
[2] Upper values (in parentheses) are percentage of mean annual pan evaporation from April through October based on mean monthly pan evaporation (1956–70) at Aurora Research Farms, N.Y. (Lyford and Cohen, 1988, table 2). Lower values represent pan-evaporation percentages multiplied by mean annual evapotranspiration of 19 inches, from plate 1.
[3] Based on long-term (1930–60) data from Hanover, N.H. (Lyford and Cohen, 1988, fig. 6 and table 1).
[4] Lower values (in parentheses) are accumulated soil-moisture deficit. The amount by which evapotranspiration exceeds precipitation in July produces a soil-moisture deficit. In August only 0.13 inches of water is needed to remove the accumulated soil-moisture deficit.

tion records are available close to the site of interest, estimate mean annual precipitation from a regional map such as plate 1, then multiply mean monthly values from the nearest long-term precipitation station by the ratio of estimated mean annual precipitation at the site to mean annual precipitation at the nearest station.

2. Estimate mean annual evapotranspiration directly from plate 1, or by subtracting mean annual runoff (pl. 2) from mean annual precipitation (pl. 1). Distribute evapotranspiration by months in proportion to pan evaporation (item 2, table 6), as described by Lyford and Cohen (1988), or in proportion to the product of percent daylight times mean monthly air temperature, as described by Olmsted and Hely (1962). Evapotranspiration values thus generated should be representative of any individual year as well as of an average year, as discussed in the section "Short-term variation in evapotranspiration". Slightly more accurate results could probably be obtained by adjusting monthly and annual values in proportion to deviations from the mean in pan evaporation or temperature during the year(s) of interest.
3. Estimate the amount of snow accumulation or snowmelt for each month (item 3, table 6) from local climate records, or use long-term mean values from Lyford and Cohen (1988, fig. 6, table 1).
4. Calculate changes in soil-moisture content (item 4, table 6) from the foregoing data. If precipitation plus snowmelt (SN_m), or minus snow accumulation (SN_s), for a particular month exceeds evapotranspiration (as occurs from September to June, table 6), soil moisture does not change. Depletion of soil moisture results when evapotranspiration exceeds precipitation (as in July, table 6). This depletion is replenished when precipitation again exceeds evapotranspiration (as in August, table 6).
5. Calculate recharge (R) as the algebraic sum of items 1 - 4 in table 6.

This water-balance method is simple to apply but gives only approximate values, not only because estimates of individual items may be in error, but also because the assumptions of negligible surface runoff and areally uniform evapotranspiration may not be warranted everywhere. The method would overestimate direct recharge to the extent an aquifer is overlain by wetlands or by paved, sewered areas in which precipitation cannot infiltrate to become recharge. It would probably underestimate direct recharge to stratified drift in which the water table is consistently 10 to 20 ft or more below land surface naturally or as a result of pumping, because evapotranspiration (particularly ground-water evapotranspiration) in such areas is likely to be less than values depicted on plate 1, which are based on water-balance calculations averaged over large watersheds that include many areas of shallow water table in uplands and valleys.

A quantity termed "water-available-for-recharge" was proposed by Lyford and Cohen (1988) as an alternative to

simulating actual recharge in ground-water flow models. Water-available-for-recharge (*WAFR*) is equal to recharge, as described by equation 4, plus surface runoff. Where the water table is a few feet or more below land surface, *WAFR* would readily infiltrate to the water table and become recharge. By contrast, where low topography or low vertical permeability results in seasonal or perennial saturation to land surface, part or all of the *WAFR* would become surface runoff. Accordingly, use of *WAFR* would result in more accurate estimation of recharge in stratified-drift aquifers that contain extensive wetlands and also in adjacent till-mantled uplands, where the water table commonly approaches land surface seasonally. The use of *WAFR* would be especially advantageous in transient-state simulations in which stresses cause significant changes in the water-table configuration over time. These concepts are discussed in detail further on, in the section on the Variable-Recharge procedure, where they are incorporated into a method for simulating direct recharge and the distribution of channeled and unchanneled upland runoff to a valley-fill aquifer.

RECHARGE FROM MAJOR STREAMS

Under natural conditions, the principal or master stream in each major valley normally gains water continually from stratified drift aquifers, although some reaches may lose flow, especially during dry periods (for example, Frimpter, 1974, p. 48). Streams that normally gain flow can become sources of recharge during periods of rising stage; recharge by this mechanism is referred to as temporary bank storage because much of the recharged water returns to the stream as the stage drops.

Pumping ground water often reverses the natural hydraulic gradient and induces infiltration from nearby streams. The magnitude of streamflow losses depends on the magnitude of the pumping, locations of pumping wells, hydraulic properties of the streambed and aquifer, and rate of flow to the well from other recharge sources. Estimation of infiltration from streams is discussed in the section "Flow between Streams and Aquifers".

HYDRAULIC PROPERTIES

Hydraulic properties of stratified drift that are required for the simulation of ground-water flow include saturated thickness, hydraulic conductivity and(or) transmissivity, and storage coefficient. These properties can vary significantly among aquifers and over the extent of a single aquifer. Nevertheless, certain regional generalizations with regard to magnitude and range of variations can be inferred. In the following pages, reference is made to small and large valleys. These terms denote the lower and upper ends of the range of valley widths (about 1,000 to 10,000 ft) typical of the glaciated Northeast.

SATURATED THICKNESS

Saturated thickness of unconsolidated sediment is a useful guide to potential well yield in small valleys of the glaciated Northeast. Depth to bedrock is generally less than 100 ft and averages less than 50 ft, and much of the valley fill consists of coarse-grained stratified drift (Mazzaferro and others, 1979; Crain, 1966). In such valleys, transmissivity is roughly proportional to total saturated thickness. Areas where saturated thickness exceeds about 10 ft are potential sources of ground water. Well yield can be expected to increase as saturated thickness increases.

In large valleys, total saturated thickness of unconsolidated sediment is not a useful guide to potential well yield. Fine-grained sediment of lacustrine origin increases in volume as valley depth and width increase, and is commonly more abundant than coarse-grained sediment; therefore, thickness of the coarse-grained sediment can be considerably less than total saturated thickness. For example, in large valleys of south-central New York, where depth to bedrock ranges from about 70 to 500 ft, thickness of saturated, coarse-grained deposits generally ranges from 10 to 150 ft (MacNish and Randall, 1982).

Fine-grained confining units, whose saturated thickness exceeds 300 ft in some localities and averages more than 100 ft over large areas, typically vary from very fine sand to silt to clay, but locally may include fine sand. Fine sand deposits can readily transmit water to wells screened in underlying or adjacent coarse stratified drift, and could themselves support screened wells yielding as much as 100 gal/min, although few such wells have been constructed in the glaciated Northeast because more productive aquifers are widely available. Meade (1978) inferred that extensive deposits of fine to very fine sand, silt, and clay in Connecticut are capable of yielding 1 to 100 gal/min to individual wells.

HYDRAULIC CONDUCTIVITY

Hydraulic conductivity of stratified drift is governed principally by the size, shape, and arrangement of individual grains, and the continuity of pore spaces between grains. In general, materials with large interconnected pore spaces have higher hydraulic conductivity than materials with small poorly connected pore spaces. Hydraulic conductivity is highest in clean, well-sorted, well-rounded gravel, and is significantly diminished by smaller grain size, subangular grains, poor sorting, and high silt content.

Published Values

The hydraulic conductivity of stratified drift varies widely, with large differences commonly occurring over distances of only a few hundred feet laterally and a few feet vertically. Values determined from aquifer tests at wells completed in coarse-grained stratified drift typically range from about 50 to 500 ft/d (Randall and others, 1966; Myette

and others, 1987; Hansen and Lapham, 1992; Dickerman, 1984), although higher values are not uncommon for very coarse-grained well-sorted material (Sammel and others, 1966; Giese and Hobba, 1970; Silvey and Johnston, 1977; Hill and Pinder, 1981; Hill and others, 1992). Hydraulic conductivity values on the order of 10,000 ft/d have been reported for few localities where unusually large flows of meltwater deposited clean gravel beds several hundreds of feet wide (Winslow and others, 1965; Yager, 1986). Reported hydraulic conductivity values for sand-plain aquifers that consist mostly of fine to medium sand range from about 50 to 100 ft/d (Snavely, 1983; Heath and others, 1963). Many studies that report estimates of hydraulic conductivity or transmissivity of specific stratified drift aquifers in the glaciated Northeast are cited in table 7.

Fine-grained stratified drift can range in size from clay to fine sand. In general, silt and clay were deposited chiefly in deep valleys and broad lowlands occupied by extensive bodies of water during deglaciation; narrow valleys in which meltwater flow was more rapid contain little sediment finer than very fine sand. Few data are available on the hydraulic conductivity of fine-grained sediment in the glaciated Northeast. Laboratory determinations of hydraulic conductivity ranging from 0.0001 to 2.7 ft/d, based on a few samples of fine-grained sediment, were reported by Allen and others (1966), Randall and others (1966), Sammel and others (1966) and Hill and others (1992). Prudic (1986) obtained a median of 0.0057 ft/d from slug tests of five piezometers tapping lenses of lacustrine silt and sand within till; Yager (1986) obtained a median of 0.34 ft/d from three similar tests of valley-fill sand and silt. Several modeling studies resulted in the following estimates of vertical hydraulic conductivity of fine-grained confining layers: 0.042 ft/d (Meisler, 1976), 0.004 ft/d (Randall, 1979), 0.0013 ft/d (Bergeron, 1987), and 0.0001 ft/d (Randall, 1986).

Vertical Anisotropy

Most stratified-drift aquifers are hydraulically anisotropic chiefly because they contain many layers whose individual hydraulic conductivities differ appreciably. Horizontal hydraulic conductivity of individual layers can range from a few feet per day or less for silt and clay strata, to several thousand feet per day for some gravels. Because layering is horizontal or gently dipping in most stratified drift, vertical hydraulic conductivity is significantly less than horizontal hydraulic conductivity, commonly by a ratio of 1:10 or greater. Dickerman (1984) analyzed 18 pumping tests from a predominantly coarse-grained stratified-drift aquifer in Rhode Island and reported that the ratio of vertical to horizontal hydraulic conductivity ranged from 1:5 to 1:80 and averaged about 1:10. Cervione and others (1972) assumed vertical-to-horizontal hydraulic conductivity ratios of 1:2 to 1:25 in estimating transmissivity of stratified drift in the upper Housatonic River basin in Connecticut. Yager (1986) calculated an average ratio of about 1:425 from tests of stratified-drift aquifers at five sites along the Susquehanna River in Kirkwood, N.Y., and Conklin, N.Y.

Anisotropy in hydraulic conductivity can significantly decrease the long-term yields of wells that tap stratified-drift aquifers, as demonstrated in table 8 for a series of simulations of four idealized aquifers by a method described in Mazzaferro and others (1979). The four aquifers have identical hydraulic properties, which are representative of stratified-drift aquifers in small valley settings, but have different boundary conditions. For most boundary conditions, simulated well yield decreases about 30 percent (from about 3 to 2 Mgal/d) as vertical anistropy increases from 1:1 (isotropic) to 1:100. For the aquifer with two impermeable boundaries, yield was less, as was the decrease in yield relative to isotropic conditions.

Estimation of Hydraulic Conductivity

Hydraulic conductivity of a stratified-drift aquifer can be estimated from analysis of samples whose hydraulic conductivity has been individually measured by laboratory methods or estimated from grain-size analysis by empirical relations, as discussed below. Because many stratified-drift aquifers are heterogenous, both laterally and vertically, large numbers of samples would be needed to completely characterize the hydraulic conductivity of such aquifers. Average hydraulic conductivity at a site can also be derived from estimates of transmissivity obtained through field procedures discussed further on. Because different techniques of estimating hydraulic conductivity use differing volumes of porous material, the resulting estimates of hydraulic conductivity can be scale dependent, as discussed by Bradbury and Muldoon (1990). For example, hydraulic conductivity values based on laboratory methods or grain-size analysis are representative of small volumes. Hydraulic conductivity values derived from measurements in a pumped well (such as specific capacity) or from pumping tests represent the region near the pumped well or within a network of nearby observation wells. Hydraulic conductivity values obtained from calibrated ground-water flow models or flow-net analysis are usually representative of relatively large volumes of stratified drift.

Laboratory methods.—Hydraulic conductivity can be determined with great precision from permeameters, devices that measure the rate of flow of water through samples of earth materials. The samples tested may not be representative of the portion of aquifer from which they were obtained, however, because they can be disturbed during collection or transit. Samples collected by methods in which disturbance is likely are commonly repacked mechanically in the laboratory before testing. Morris and Johnson (1967) reported that hydraulic conductivity and porosity of individual samples of water-laid sand and gravel were generally higher after

TABLE 7.—*Areas in the glaciated Northeast where values of hydraulic conductivity and(or) transmissivity of stratified drift have been estimated*

[Some sources give areal appraisals; most only give values at tested wells]

Area of investigation	Data source
Connecticut	
Lower Connecticut River basin	Weiss and others, 1982
Farmington	Mazzaferro, 1980, 1989
Farmington River basin	Handman and others, 1986
Lower Housatonic River basin	Wilson and others, 1974
Upper Housatonic River basin	Cervione and others, 1972
Pomperaug River basin	Mazzaferro, 1986a
Pootatuck River valley	Haeni, 1978
Quinebaug River basin[1]	Randall and others, 1966
Quinnipiac River basin	Mazzaferro and others, 1979
Shetucket River basin	Thomas and others, 1967
Southwestern Connecticut	Weaver, 1987
Southwestern Conn. coastal basins	Ryder and others, 1970
Storrs	Rahn, 1968
Titicus River valley	Grady and others, 1992
Maine	
Little Androscoggin River valley	Morrissey, 1983
Saco River valley	Tepper and others, 1990
Massachusetts	
Hudson, Sudbury	Perlmutter, 1962
Ipswich River basin	Sammel and others, 1966
Ipswich River basin (upper part)	Baker and others, 1964
Mattapoisett River valley	Olimpio and deLima, 1984
Merrimack River valley	Delaney and Gay, 1980
Millers River basin	Collings and others, 1969
Nashua River basin	deLima, 1991
Nashua and Souhegan River basins	Brackley and Hansen, 1977
Plymouth-Carver area	Hansen and Lapham, 1992
Southeastern Mass. coastal basins	Williams and Tasker, 1974a, b
Shawsheen River basin	Delaney and Gay, 1980
Taunton River basin	Williams and others, 1973
Taunton River basin	Lapham, 1988
Woburn	Myette and others, 1987
Woburn	deLima and Olimpio, 1989
New Hampshire	
Bellamy, Cocheco, and Salmon River basins	Mack and Lawlor, 1992
Exeter, Lamprey, and Oyster River basins	Moore, 1990
Lower Merrimack River and coastal basins	Stekl and Flanigan, 1992
Middle Merrimack River basin	Ayotte and Toppin, 1995
Nashua Regional Planning area	Toppin, 1987
New Jersey	
Delaware River near Walpack	Wright Associates, 1982
Essex and Morris Counties	Meisler, 1976
Flat Brook valley	Wright Associates, 1982
Long Valley	Hill and Pinder, 1981
Morris County	Gill and Vecchioli, 1965
Morris County, Berkshire and Pequannock valleys	Canace and others, 1983
Morristown	Vecchioli and Nichols, 1966
Musconetcong River valley	Hill and Pinder, 1981
Pequest River valley near Great Meadows	Hutchinson, 1981
Rahway River and Arthur Kill	Anderson, 1968
Ramapo River near Mahwah	Hill and others, 1992
Rockaway River valley near Dover	(this report)
Rockaway River valley near Dover	Geraghty and Miller, 1968, 1969, 1972
Upper Rockaway River basin	Gordon, 1993

TABLE 7.—*Areas in the glaciated Northeast where values of hydraulic conductivity and(or) transmissivity of stratified drift have been estimated*—Continued

[Some sources give areal appraisals; most only give values at tested wells]

Area of investigation	Data source
New York	
Binghamton, Johnson City	Randall, 1977
Champlain-Upper Hudson River basins	Giese and Hobba, 1970
Chemung River basin	Reisenauer, 1977
Chemung River valley near Corning	Ballaron, 1988
Cortland, Otter Creek and Tioughnioga River valleys	Reynolds, 1987
Cortland, Otter Creek valley	Cosner and Harsh, 1978
Croton valley	Leggette and Jacob, 1938
Dale valley	Randall, 1979
Erie-Niagara basin	LaSala, 1968
Jamestown area	Crain, 1966
Milton area, Saratoga County	Mack and others, 1964
Eastern Oswego River basin	Kantrowitz, 1970
Western Oswego River basin	Crain, 1974
Owego	Reynolds and Garry, 1990
Pine Bush area, Albany County	Snavely, 1983
Saranac River valley	Giese and Hobba, 1970
Saratoga National Park	Heath and others, 1963
Eastern Schenectady County	Winslow and others, 1965
Susquehanna River valley, southcentral Broome County	Yager, 1986
Susquehanna River valley, southwestern Broome County	Randall, 1986
Smyrna, North Norwich	Reynolds and Brown, 1984
Woodbury Creek valley	Frimpter, 1972
Ohio	
Dayton area[2]	Norris and Spieker, 1966
Dayton area[2]	Norris, 1970
Dayton area[2]	Fidler, 1975
Killbuck Creek valley near Wooster	Miller, 1975, 1976
Killbuck Creek valley near Wooster	Miller and Associates, 1981
Killbuck Creek valley near Wooster	Jones and others, 1958
Killbuck Creek valley near Wooster	Springer, 1990
Killbuck Creek valley near Wooster	(this report)
Six buried valleys in northeastern Ohio	Ohio Drilling Co., 1971
Pennsylvania	
Western Crawford County	Schiner and Gallaher, 1979
Mercer quadrangle	Poth, 1963
Williamsport region, Lycoming County	Lloyd and Carswell, 1981
Wyoming valley, Luzerne County	Hollowell, 1971
Rhode Island	
Beaver River-Pasquiset Brook	Dickerman and Ozbilgin, 1985
Blackstone River area	Johnston and Dickerman, 1974a
Branch River basin	Johnston and Dickerman, 1974b
Chipuxet River basin	Dickerman, 1984
Upper Pawcatuck River basin	Allen and others, 1966
Lower Pawcatuck River basin	Gonthier and others, 1974
South Kingston	Silvey and Johnston, 1977
Potowomut-Wickford area	Rosenhein and others, 1968
Lower Wood River basin	Dickerman and others, 1990
19 sites throughout the State	Lang and others, 1960
Vermont	
Winooski River valley, E. Montpelier; Dog River valley, Northfield	Hodges and others, 1976a
Upper Winooski River basin	Hodges and others, 1977
White River Junction	Hodges and others, 1976b

[1] Obsolete "bailer method" of analysis used for some tests; data (Thomas and others, 1966) can be reanalyzed by current methods.
[2] West of glaciated Northeast as delineated on figure 1.

TABLE 8.—*Simulated well yield as a function of vertical anisotropy for four idealized aquifer-boundary conditions*

[Simulated yields tabulated below are from a single well at the end of 180 days of continuous pumping and no recharge. Well yield is defined as the maximum pumping rate that can be sustained without drawing water levels below top of well screen. ft^2/d, feet squared per day. Mgal/d, million gallons per day]

Hydraulic properties and well characteristics for all simulations

Effective well radius	1.0 feet	Specific yield	0.2
Saturated thickness	75.0 feet	Screen length	18.75 ft (25 percent of saturated thickness)
Transmissivity	20,000 ft^2/d		

Run no.	Vertical anisotropy*	Yield (Mgal/d)	Reduction in yield (percent)
Condition A: Two line-source (recharge) boundaries 200 feet from well			
1	1:1	3.056	0
2	1:2	2.874	6
3	1:5	2.639	14
4	1:10	2.485	19
5	1:20	2.355	23
6	1:50	2.207	28
7	1:75	2.149	30
8	1:100	2.108	31
Condition B: No boundaries (infinite aquifer)			
1	1:1	2.693	0
2	1:2	2.539	6
3	1:5	2.351	13
4	1:10	2.226	17
5	1:20	2.111	22
6	1:50	1.976	27
7	1:75	1.924	29
8	1:100	1.892	30
Condition C: One line-source boundary and one impermeable-barrier boundary, each 200 feet from well			
1	1:1	2.971	0
2	1:2	2.758	7
3	1:5	2.557	14
4	1:10	2.417	19
5	1:20	2.291	23
6	1:50	2.149	28
7	1:75	2.088	26
8	1:100	2.050	31
Condition D: Two impermeable-barrier boundaries, each 200 feet from well			
1	1:1	1.353	0
2	1:2	1.304	4
3	1:5	1.244	8
4	1:10	1.204	11
5	1:20	1.168	14
6	1:50	1.126	17
7	1:75	1.110	18
8	1:100	1.099	19

* Ratio of vertical to horizontal conductivity.

repacking, but Wolf and others (1991) found no statistically significant difference in hydraulic conductivity between intact and repacked samples of glacial outwash from Cape Cod, Mass.

Point values of hydraulic conductivity derived from laboratory or field tests are perhaps most useful when correlated with grain-size distribution determined from precise sieve analysis or visual description, to develop graphs or equations that can be used to extrapolate hydraulic conductivity data on the basis of more widely available lithologic logs. Several such extrapolation techniques that have been applied in the glaciated Northeast are described in the following paragraphs.

Grain-size analysis.—The hydraulic conductivity of earth materials is a function of grain diameter, as initially suggested by Hazen (1892) and verified by several investigators. Many published empirical relations have the general form:

$$K = cD^x, \tag{5}$$

where K is hydraulic conductivity of the material,
D is some characteristic grain diameter, and
c and x are coefficients.

The median grain size (*D50*) has been widely used as an index of grain diameter, and is relatively easy to estimate from semiquantitative lithologic descriptions of samples. The "effective size", a particle of such diameter that 10 percent of the grains are smaller and 90 percent are larger, has also been widely used for this purpose. Shepherd (1989) analyzed 19 published data sets, regressing *D50* against laboratory-determined values of hydraulic conductivity, and calculated coefficients c and x of equation 5 for each data set. For any particular median grain size, the spread of the predicted hydraulic conductivity derived from the various regressions was about 1 order of magnitude. Other investigators have developed relations between median grain size and hydraulic conductivity that also take into account the effects of sorting (Krumbein and Monk, 1942; Masch and Denny, 1966; Ayotte and Toppin, 1995).

Median grain size for each of 51 samples, as determined from sieve separations, is plotted in figure 16 against hydraulic conductivity, as measured by laboratory permeameters. The selected samples are of three types: (1) 24 undisturbed samples of stratified drift from southern New England, oriented horizontally (Randall and others, 1966; Thomas and others, 1967; Cervione and others, 1968; Baker and others, 1964; Wilson and others, 1968), (2) 9 split-spoon samples from drill cores in outwash on Cape Cod, oriented vertically (Olney, 1983), and (3) 18 samples of outwash from outside the glaciated Northeast, initially separated into several grain-size fractions by sieving, then recombined in measured proportions to produce 9 samples with uniform median grain size but differing sorting and 9 samples with differing median grain size but uniformly well sorted (Krumbein and Monk, 1942). The samples from Connecticut, many of which were selected as examples of especially well-sorted materials (Randall and others, 1966, p. 51), define with remarkable consistency an upper limit of hydraulic conductivity within each grain-size class. The 9 samples of uniformly well-sorted outwash assembled by Krumbein and Monk (1942) generally fall along the same trend line of maximum hydraulic conductivity (line UL, fig. 16). Within each grain-size class, the data range over about 1 order of magnitude in hydraulic conductivity below the maximum values, presumably reflecting decreased sorting or increased silt content, although hydraulic conductivity of the Connecticut samples does not consistently decrease with increasing uniformity coefficient (a measure of sorting, defined as the ratio of *D60* to *D10*), as shown by Mazzaferro and others (1979, fig. 35). A similar observation was made by Rose and Smith (1957). The four samples whose D50 exceeds 2 mm all contain 32 to 35 percent sand and silt; their hydraulic conductivities are probably near the maximum for sandy gravel, but the hydraulic conductivity of rare openwork gravel lenses could exceed 10,000 ft/d (as estimated from upward extrapolation of line UL).

Lines representing five published empirical relations of hydraulic conductivity to median grain size, developed from various data sets, are included in figure 16, in addition to the trend line of maximum hydraulic conductivity previously mentioned. Two of these relations were developed by Masch and Denny (1966) for poorly-sorted and well-sorted sand, derived from synthetically assembled test samples of washed Colorado River sands with controlled statistical distributions. Another linear relation, developed by Shepherd (1989), represents "texturally immature" channel deposits that are roughly equivalent to sand-size stratified drift. The remaining two lines were developed as follows by Ayotte and Toppin (1995) to represent poorly and well-sorted sands in southern New Hampshire. They determined grain-size distributions by sieve analysis for 454 samples of stratified drift, and calculated the inclusive standard deviation for each sample as an index of sorting. On the basis of this index the samples were classified into poorly sorted, moderately sorted, and well sorted subsets. The hydraulic conductivity of each sample was then estimated from the following empirical equation of Olney (1983) based on the *D10* grain size:

$$K = 2100\,(D10)^{0.65}\ .$$

This equation was developed by regression analysis of hydraulic conductivity from laboratory permeameter tests and *D10* grain size, based on eight samples of Cape Cod outwash, one sample of beach sand from Massachusetts, and 20 samples of the aforementioned Krumbein and Monk (1942) data. (Hydraulic conductivity values for most of these 29 samples are plotted against *D50* grain size in figure 16.) The final step in the analysis by Ayotte and Toppin (1983) was to develop regression equations relating hydraulic conductivity thus estimated to *D50* grain size for each of their three data subsets; the equations for the poorly and well-sorted data subsets are represented by lines T and A in figure 16. Their line for well-sorted material (line A) is similar to the average relation developed by Bedinger (1961) from Arkansas River sands.

The scatter of points on figure 16 shows that hydraulic conductivity can vary widely within every category of grain size from fine sand to fine gravel. Samples from the glaciated Northeast whose grain-size distribution and hydraulic conductivity have been determined are still few in number, so it is not surprising that a comprehensive and reliable method of estimating hydraulic conductivity from grain-size distribution remains to be developed. Figure 16 provides a reasonable basis for estimating the upper limit of hydraulic conductivity as a function of median grain size in sand and very fine gravel. The empirical relations cited and illustrated in figure 16 can serve as a guide to reducing such estimates to the extent that the materials considered depart from being clean and well sorted.

TRANSMISSIVITY

The preceding discussion of hydraulic conductivity emphasized estimation of water-transmitting capacity on a

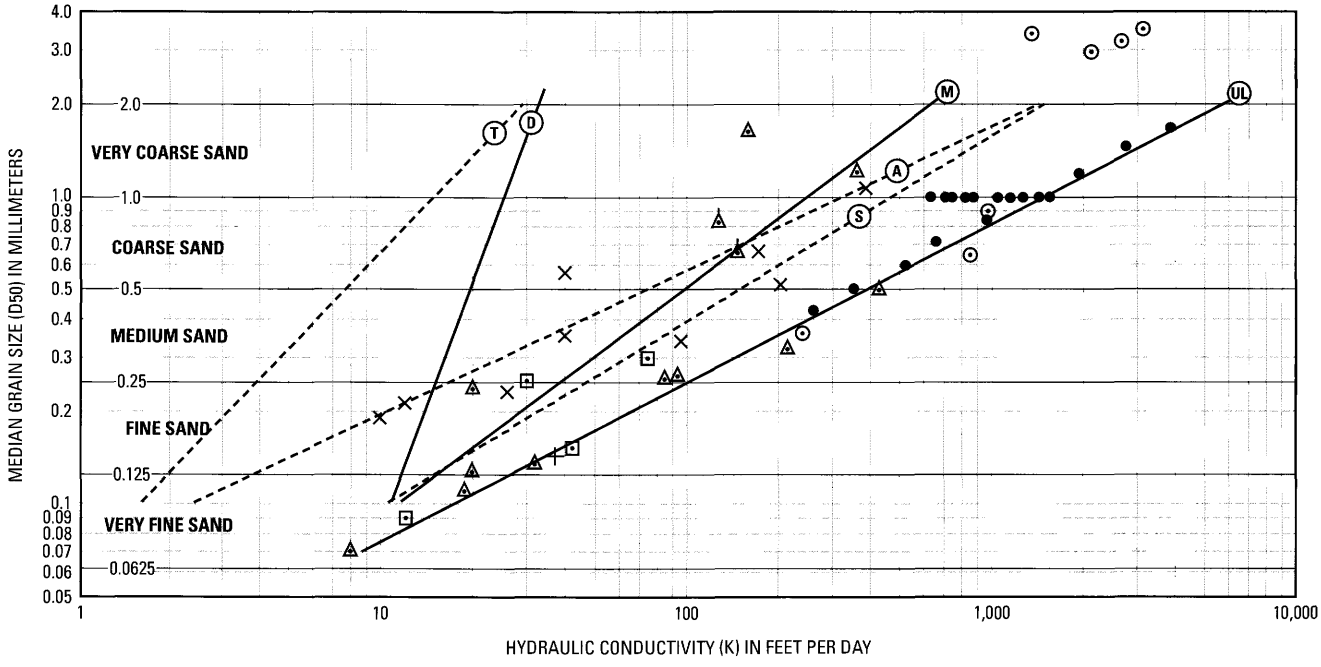

EXPLANATION

Undisturbed samples, oriented horizontally

⊙ Quinebaug River basin, Connecticut (Randall and others, 1966)

△ Shetucket River basin, Connecticut (Thomas and others, 1967)

△ Southern Connecticut, tributary to Thames River or ocean (Cervione and others, 1968)

⊡ Upper Ipswich River basin, Massachusetts (Baker and others, 1964)

\+ Beacon Hill Brook valley, Connecticut (Wilson and others, 1968)

Split-spoon samples, oriented vertically

× Cape Cod and Singing Beach, Massachusetts (Olney, 1983)

Recombined sieve separates of glacial outwash

● Location unspecified; 9 samples have median grain size of 1 millimeter but varied standard deviation; 9 have uniform standard deviation but varied grain sizes (Krumbein and Monk, 1942)

Linear equations relating hydraulic conductivity to median grain size, developed from various data sets as cited— Equation representing each line is given

—(UL)— Approximate upper limit of hydraulic conductivity for clean, well-sorted sand (based on data plotted in this figure); $K = 1{,}500(D50)^{1.9}$

Subsets of 454 samples of stratified drift from southern New Hampshire (Ayotte and Toppin, 1995)

--(A)-- Well-sorted subset; $K = 323.6(D50)^{2.12}$

--(T)-- Poorly-sorted subset; $K = 15.1(D50)^{0.97}$

--(S)-- Immature channel deposits (Shepherd, 1989); $K = 467(D50)^{1.65}$

Colorado River sands; grain-size fractions separated and reassembled so as to have controlled statistical distributions (Masch and Denny, 1966, fig. 8)

—(M)— Well-sorted subset; $K = 250(D50)^{1.38}$

—(D)— Poorly-sorted subset; $K = 25(D50)^{0.48}$

FIGURE 16.—Laboratory-determined hydraulic conductivity as a function of median grain size for samples of stratified drift from the glaciated Northeast, and several empirical relations based on other data sets.

small scale, one sample or layer at a time. Transmissivity, or the water-transmitting capacity of the entire aquifer thickness, is more important and ranges even more widely than hydraulic conductivity. Saturated thickness of stratified-drift aquifers generally ranges over less than an order of magnitude, whereas hydraulic conductivity can range over several orders of magnitude. Consequently, hydraulic conductivity has a correspondingly greater effect on transmissivity than does saturated thickness. As discussed earlier, the saturated thickness of coarse-grained stratified drift in small river valleys generally is less than 100 ft and averages less than 50 ft, whereas saturated thickness of coarse-grained materials in large river valleys is generally somewhat greater but rarely exceeds 150 ft. If average saturated thickness is taken to range from 50 to 100 ft, and average hydraulic conductivity is taken to range from 50 to 500 ft/d, then the transmissivity of most aquifers can be anticipated to fall between 2,500 and 50,000 ft^2/d.

Published Values

Transmissivity values ranging from 1,000 to 50,000 ft^2/d have been calculated from aquifer tests at wells tapping coarse-grained stratified drift in many parts of the glaciated Northeast, as documented in many of the references cited in table 7. Values of 100,000 ft^2/d or more have been calculated for a few localities in New York (Yager, 1986; Randall, 1977,1986; Winslow and others, 1965; Kantrowitz, 1970; Crain, 1974).

Reported transmissivity values for fine-grained stratified drift are sparse and typically range from a few hundred to about 2,000 ft^2/d. Grady and others (1992) reported a transmissivity of less than 1,000 ft^2/d for a predominantly fine-grained aquifer in the Titicus River valley of southwestern Connecticut. Toppin (1987) reported transmissivity less than 2,000 ft^2/d for an extensive area along the Merrimack River near Nashua, N.H. in which saturated thickness ranged from 10 to 100 ft. The potential yield of individual wells in such relatively thick but fine-grained aquifers is unlikely to exceed 250 gal/min.

Estimation of Transmissivity

Transmissivity of stratified drift at many sites in the glaciated Northeast has been estimated, mostly from three types of data: (1) aquifer-test results, (2) specific-capacity values (both 1 and 2 are based on pumping of large-capacity wells and, therefore, possibly biased toward above-average transmissivity), and (3) hydraulic conductivity values estimated for individual units in geologic logs, then multiplied by unit thickness and summed to obtain transmissivity. Each of these methods is discussed below.

Aquifer Tests.—Many graphical or analytical techniques are available for estimating aquifer transmissivity from aquifer tests, as described by Theim (1906), Theis (1935), Wenzel (1942), Hvorslev (1951), Ferris and others (1962), Jacob (1963), Boulton (1963), Cooper and others (1967), Todd (1970, 1980), Lohman (1972), Walton (1970, 1987), Neuman (1975), Bennett (1976), Bear (1979), Bouwer and Rice (1976), Freeze and Cherry (1979), Driscoll (1986), and Kruseman and de Ridder (1990). Applications in the glaciated Northeast are too numerous to mention, but detailed examples are presented by Heath and others (1963), Perlmutter (1962), Lang and others (1960), and Hill and others (1992).

Most analytical methods are based on the nonequilibrium equation of Theis (1935), and assume that (1) the aquifer is confined, homogeneous, isotropic, of uniform thickness and of infinite areal extent, (2) the pumped well fully penetrates the aquifer and is of infinitesimal diameter, and (3) water removed from storage is discharged instantaneously with decline in head. These assumptions are seldom met completely in stratified-drift aquifers, which are typically heterogeneous, unconfined, variable in thickness, bounded by bedrock valley walls and tapped by partially penetrating wells. These inconsistencies complicate the analytical interpretation of aquifer-test results and have led some investigators to estimate the distribution of transmissivity near production wells by calibrating ground-water flow models to head data from the aquifer test (for example, Randall, 1979; Yager, 1986; Rutledge, 1993; Reilly and Harbaugh, 1993).

Specific Capacity.—Transmissivity can be estimated from specific capacity of production wells by simple but approximate graphs or equations (Walton, 1962, 1970; Driscoll, 1986; Razack and Huntley, 1991), or by more complex relations (Jacob, 1947; Theis and others, 1963; Hurr, 1966; Walton, 1962, 1970). Results can be adjusted for partial penetration, dewatering, and well loss (Butler, 1957; Turcan, 1963; Walton, 1962, 1970). Specific capacity data are much more abundant than aquifer-test data and have been used to estimate transmissivity in many investigations. For example, Mazzaferro and others (1979) calculated transmissivities ranging from 200 to 32,800 ft^2/d by the method of Theis and others (1963), from specific capacities of 64 wells in south-central Connecticut. In this analysis, application of a method to adjust specific capacity for partial penetration (Butler, 1957) increased the majority of measured specific capabilities by factors of 2 to 3, thereby increasing the resultant estimates of transmissivity.

Geologic Logs.— A method for estimating transmissivity from geologic logs, developed by Bedinger (1961), has been widely applied in the glaciated Northeast (for example, Ryder and others, 1970; Randall, 1977, Ayotte and Toppin, 1995). In this procedure, hydraulic conductivity values are assigned to the lithologic descriptions commonly used in geologic logs. Transmissivity can then be computed from any geologic log by summing the thickness-weighted hydraulic conductivity values for all layers penetrated. The assigned hydraulic conductivity values are sometimes refined by comparison of

transmissivities computed from several geologic logs with transmissivities computed from aquifer tests or specific capacities of the same wells. Then, a revised transmissivity is recomputed from each geologic log.

Although many investigators in the glaciated Northeast have applied multiple techniques to estimate transmissivity, few have published or compared estimates obtained by different techniques at individual sites. Weiss and others (1982) presented transmissivity estimates based on geologic logs and on specific capacity values for 47 sites in south-central Connecticut. The mean of the transmissivity estimates based on geologic logs was nearly identical to the mean based on specific-capacity data (table 9), but the simple Spearman rank correlation coefficient for the 47 pairs of values was only 0.28. (This coefficient measures the correlation between pairs of values ranked according to size; it minimizes the effect of outliers and is appropriate for data sets that may not have a normal distribution.) Aquifer-test data also were available at four of the 47 sites, and the transmissivities derived from the three methods are significantly different (table 9). Randall (1977) evaluated the transmissivity distribution within a small aquifer in south-central New York. Individual values estimated from geologic logs and specific-capacity data varied widely at some sites (table 9), and the Spearman rank correlation coefficient for 28 pairs of transmissivity values was only 0.61. For both data sets, transmissivity estimates based on specific capacity had a much wider range than those based on geologic logs, and results of both methods differ appreciably from results of aquifer-test analysis from 10 sites (table 9). The weak correlation between the geologic log and specific capacity values may result, in part, from difficulty in estimating the hydraulic conductivity of gravel layers, which can vary by an order of magnitude or more, depending on sand and silt content.

Transmissivity values estimated by the foregoing methods at the sites of individual production wells or drillholes are commonly contoured to show the inferred distribution of transmissivity within an aquifer. In parts of the aquifer that lack data sites, contours may be constrained to some extent by saturated thickness or geologic interpretation. Transmissivity values for stratified drift along the Susquehanna River in south-central New York were contoured in this manner, then re-evaluated by flow-net analysis (Randall, 1977) and ground-water flow model calibration (Randall, 1986). Both of these integrated areal methods indicated aquifer transmissivity to be about half as large as estimated by contouring individual data points, especially near production wells, where aquifer tests and specific capacity had indicated large transmissivity values. This contrast could be explained by steeply dipping, thin, poorly sorted or fine-grained beds of low hydraulic conductivity being scattered through the aquifer; such beds would not significantly reduce transmissivity calculated from borehole logs or specific capacity, but would serve as barriers to lateral flow and thereby reduce overall aquifer transmissivity.

TABLE 9.—*Transmissivity estimates derived from geologic logs, specific-capacity data, and aquifer tests for sites in lower Connecticut River basin (A) and in Binghamton-Johnson City, N.Y. (B)*

[All values are in feet squared per day. Dashes indicate no aquifer tests for most sites]

Statistic	Method		
	Geologic logs	Specific capacity	Aquifer test
***A.* Values based on 47 sites in lower Connecticut River basin (Weiss and others, 1982)**			
Maximum	33,000	68,000	—
Minimum	620	50	—
Mean	10,600	10,100	—
Values based on 4 of the 47 sites			
Maximum	17,000	68,000	40,100
Minimum	7,800	16,000	10,700
Mean	11,700	41,450	23,050
***B.* Values base on 28 sites in Clinton Street-Ballpark aquifer in Binghamton and Johnson City, N.Y. (Randall, 1977)**			
Maximum	80,000	205,000	—
Minimum	5,000	3,000	—
Mean	37,800	47,500	—
Values based on 10 of the 28 sites			
Maximum	60,000	133,500	61,500
Minimum	5,000	3,000	10,500
Mean	37,000	54,500	24,900

POROSITY AND STORAGE COEFFICIENT

The most widely used indices of water-filled pore space in stratified-drift aquifers are porosity (total pore space per unit volume of sediment) and storage coefficient (volume of water released per unit area per unit decline in head). Storage coefficient can vary greatly with time and test conditions or methods, as described below.

Porosity.—The porosity of 20 samples of sand or gravel from the stratified drift of New England ranged from 27 to 45 percent, median 37 percent (Allen and others, 1966; Baker and others, 1964; Bradley, 1964). Porosity of 15 samples of

silt to very fine sand from the same areas ranged from 27 to 44 percent, median 40 percent. These results are typical of alluvial sediments and "washed drift" throughout the United States (Morris and Johnson, 1967).

Storage coefficient, unconfined conditions.—The specific yield or long-term unconfined storage coefficient can be determined in the laboratory by measuring the volume of water that ultimately drains by gravity from a known volume of saturated sediment (a process that can take several months or more) or by a centrifuge procedure that yields equivalent results promptly (Johnson, 1967). Laboratory determinations of specific yield for 54 samples of sand or gravel from New England ranged from 24 to 47 percent, median 33 percent, and for 24 samples of predominantly silt to very fine sand ranged from 16 to 41 percent, median 33 percent (Baker and others, 1964; Allen and others, 1966; Randall and others, 1966; Thomas and others, 1967; Thomas and others, 1968; Bradley, 1964; Weigle and Kranes, 1966). Such values may be appropriate for use in calculations or model simulations of dewatering over long periods (Neuman, 1987). Although the New England reports cited also present grain-size distributions for the samples tested, none attempt to relate specific yield to grain size or sorting as done in several studies outside the glaciated Northeast summarized by Johnson (1967).

Unconfined storage coefficients may also be estimated in the field, by the volume-balance method in which the storage coefficient is taken to be the ratio of the cumulative volume of water pumped to the volume of the resultant cone of depression (Nwankwor and others, 1984) or by the water-budget method in which precipitation, runoff, and changes in water-table elevation within a small watershed are carefully measured, and monthly differences between precipitation and runoff are partitioned between evapotranspiration and changes in storage, constrained by the seasonal cycle of evapotranspiration and by whatever estimated storage coefficient minimizes error (Rasmussen and Andreasen, 1959). Storage coefficients thus calculated generally apply to periods of several days or weeks, and may be termed "gravity yield" (Rasmussen and Andreasen, 1959). These methods have apparently not been applied in the glaciated Northeast. They are subject to significant imprecision in estimation of some inputs, notably the extent of the cone of depression in the volume-balance method (Neuman, 1987,1988) and evapotranspiration and changes in soil-moisture content in the water-budget method.

Storage coefficient from pumping tests.—Storage coefficient is commonly computed, along with transmissivity, from aquifer-test data through a variety of curve-matching procedures (for example, Ferris and others, 1962; Walton, 1962, 1970, 1987; Lohman, 1972; Todd, 1980). In tests of stratified-drift aquifers, transmissivity near the pumped well is commonly estimated from the earliest drawdown or recovery measurements, before the water-level response to pumping is affected by heterogeneities within the aquifer or by aquifer boundaries along the valley sides. Storage coefficients calculated from early data are commonly smaller than the usual range for unconfined conditions, even in surficial aquifers that lack any obvious fine-grained confining layers, presumably because (1) gravity drainage occurs slowly in response to head changes and (2) anisotropy and partially penetrating production wells can result in vertical flow components within the aquifer that are inconsistent with analytical assumptions. Type-curve methods have been developed that consider delayed gravity drainage (Boulton, 1963, Prickett, 1965, Neuman, 1972, 1975, Moench, 1995). Storage coefficients estimated by these methods are consistently in the range of 0.03 to 0.13 and clearly reflect unconfined conditions, but nevertheless tend to be lower than the specific yield as determined from volume-balance and laboratory methods (Nwankwor and others, 1984). Storage coefficients computed from pumping tests are probably appropriate for use in calculations or model simulations where the focus is on the response of an unconfined aquifer to variations in stress (Neuman, 1987).

Storage coefficient, confined conditions.—The storage coefficient for a confined stratified-drift aquifer can be estimated by multiplying specific storage times aquifer thickness. From the following generalized properties and equation 20 of Lohman (1972), specific storage was calculated to be about 10^{-4} per foot for fine-grained stratified drift and 10^{-6} per foot for coarse sand and gravel:

Specific weight of water: 0.434 $(lb/in^2)/ft$

Compressibility of water: 3.3×10^{-6} in^2/lb

Compressibility of silt and fine sand: 7×10^{-4} in^2/lb

Compressibility of coarse sand and gravel: 7×10^{-6} in^2/lb (Freeze and Cherry, 1979, p. 55)

Porosity: 0.4 for silt and fine sand, 0.3 for coarse sand and gravel.

Storage coefficients reported for confined stratified-drift aquifers in the glaciated Northeast range from 10^{-2} to 10^{-4} (Crain, 1966; Lang and others, 1960; Meinzer and Stearns, 1929; Meisler, 1976; Randall, 1979; Schiner and Gallaher, 1979).

FLOW BETWEEN STREAMS AND AQUIFERS

The exchange of water between streams and the underlying stratified-drift aquifers is an important aspect of the hydrology of this region. Ground water is discharged primarily to streams under natural conditions, but streams can also be significant sources of natural or induced recharge. The exchange of water between stream and aquifer is commonly conceptualized and simulated in ground-water flow models as vertical flow through a distinct streambed layer that is ordinarily less permeable than the underlying aquifer. For example, the USGS modular ground-water flow model (MODFLOW) of McDonald and Harbaugh (1988) represents

the flow, *QRIV*, between stream and aquifer, over a stream reach within model cell i, j, k, as:

$$QRIV = \frac{KLW}{m}(HRIV - h_{i,j,k}), \quad h_{i,j,k} > RBOT \quad (L^3/T) \tag{6a}$$

$$QRIV = \frac{KLW}{m}(HRIV - RBOT), \quad h_{i,j,k} \leq RBOT \tag{6b}$$

where *HRIV* is the head in the stream,
$h_{i,j,k}$ is the head in the aquifer,
RBOT is the elevation of the bottom of the streambed,
K is the vertical hydraulic conductivity of the streambed,
m is streambed thickness, and
LW is streambed area (of length *L* and width *W*).

In equation 6, *K*/*m* is termed streambed leakance and *KLW*/*m* is termed streambed conductance. Input to the model consists of the three quantities: streambed conductance, bottom elevation, and head in the stream. Of these, bottom elevation, head in the stream, and the streambed-area component of streambed conductance can usually be determined fairly accurately, whereas the streambed-leakance component is typically poorly known. Streambed thickness is not an explicit input value but is required for estimation of streambed bottom elevation.

The prevailing concept of a distinct streambed layer of relatively low hydraulic conductivity is based chiefly on observations of silty gravel or organic-rich silt lenses within modern alluvium, and unsaturated conditions beneath streams in some localities near production wells. Moore and Jenkins (1966) described a thin layer of silty alluvium beneath a stream channel in Colorado. Haeni (1978) described alluvium of a small river in Connecticut to be poorly sorted sand and gravel, and collected two samples whose vertical hydraulic conductivities were 1.3 and 3.9 ft/d. DeLima (1991) reported that a brook in northern Massachusetts was underlain by 0.75 ft of fine sand that contained organic matter and was less permeable than the underlying medium-sand aquifer. Burkham (1970) reported that in the unstable alluvial channels of ephemeral streams in the southwestern United States, grain size commonly decreases upward to silt, which is deposited as flow decreases during flood recession. Others have speculated that thin silt layers may settle temporarily in large pools along the gravel-bed streams in the glaciated Northeast. The concept of a silty streambed layer, however, is not universally applicable. For example, seepage losses from tributary streams in the Appalachian Plateau are controlled by hydraulic conductivity of thick alluvial-fan deposits and(or) underlying sediment, rather than by a thin streambed layer (Randall, 1978; Williams, 1991). The Beaver River in Rhode Island flows on loose sandy gravel that appears more permeable than the underlying aquifer (Dickerman and Ozbilgin, 1985).

Some authors, who lacked measurements of head immediately below the streambed or had evidence that the vertical hydraulic conductivity of the streambed equals or exceeds that of the underlying aquifer, have adopted a formulation in which the head difference and vertical distance between the stream and a well(s) open to the underlying aquifer are used to calculate or simulate an average vertical conductance (Reilly and others, 1983; Tepper and others, 1990; Dickerman and others, 1990). Such a value is mathematically equivalent to the harmonic mean of the streambed conductance and the vertical conductance of the underlying aquifer, and may be substituted for streambed conductance in ground-water flow models.

TEMPORAL VARIATIONS IN STREAMBED HYDRAULIC PROPERTIES

The hydraulic properties of a streambed can vary over time as a function of stream temperature. Water temperature fluctuates seasonally from 0°C to about 25°C in many streams in the glaciated Northeast (Ku and others, 1975; Lapham, 1989). An increase in temperature from 0° to 25°C will result in a 50-percent decrease in water viscosity, and a consequent doubling of hydraulic conductivity in the streambed (Winslow and others, 1965; Bouwer, 1978, p. 43). The resulting increase in infiltration from losing stream reaches to the underlying aquifer may be of lesser magnitude, however, in that the vertical hydraulic conductivity of the underlying aquifer may constrain infiltration, and temperature anomalies may be dissipated by heat exchange along vertical flow paths. Seasonal temperature ranges of 12°C or more have commonly been observed several hundred feet from rivers near riparian well fields (Winslow and others, 1965; Norris and Spieker, 1962; Randall, 1977, 1986; Dysart and Rheaume, 1999).

Fluctuations in stream stage, and hence in hydraulic gradient across a streambed, cause fluctuations in the rate of vertical seepage loss. Infiltration can occur through the banks as well as the bottom of the stream, and lateral hydraulic conductivity of streambank channel deposits can substantially exceed vertical hydraulic conductivity of the streambed. The potential for lateral infiltration as stream stage increases might result in effective values of streambed leakance that increase with stream stage at some sites. Streambed leakance is commonly estimated from data collected during periods of low stream stage, when seepage loss as estimated from streamflow can be most accurately measured. Such leakance estimates would result in an underestimate of infiltration at high stream stage. Evidence for the importance of lateral seepage is illustrated in figure 17, which shows that seepage loss per unit length of channel from two tributaries in north-

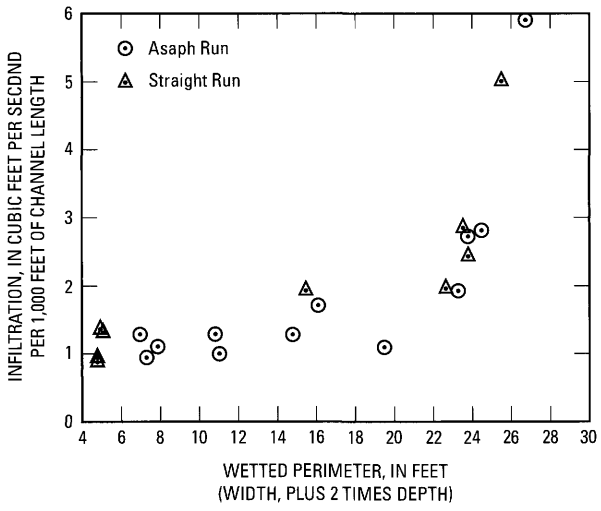

FIGURE 17.—Seepage losses on the alluvial fans of two tributaries within the broad valley of Marsh Creek in north-central Pennsylvania (fromWilliams, 1991, fig. 18). Average width and depth of these tributaries are 15 feet and 0.4 feet, respectively.

central Pennsylvania increased only slightly as channel wetted perimeter (width of stream plus twice the depth of water) increased from 4 to 22 ft, mostly by widening. Seepage loss then increased rapidly as wetted perimeter increased further, mostly by deepening. These results imply that downward flow through the streambed could be much less than lateral flow away from the stream. In a 2.2-mile reach of a small stream in Massachusetts, measured streamflow decreased by 10 times the vertical seepage loss through the streambed as measured by infiltrometers (deLima, 1991), which also suggests that streambank lateral conductivity may greatly exceed vertical conductivity of the streambed. Induced infiltration from the Mohawk River near Schenectady, N.Y. decreases greatly each fall when regulated river stage is lowered and streambanks are less deeply inundated (Winslow and others, 1965).

Streambed properties can be permanently altered by accumulation or excavation of sediment. The persistent downward flux in areas of induced infiltration or natural seepage loss may result in gradual clogging of the streambed with suspended sediment, as reported from recharge-augmentation schemes (Berend and others, 1967). By contrast, excavation and backfilling of streambeds can eliminate natural fine-grained laminations and result in rapid induced infiltration near well fields (Randall, 1970). The effects of changes in temperature, stream stage, or sediment on transmission of water through a streambed can be simulated in transient-state ground-water flow models by allotting additional stress periods in which variation in streambed leakance or stream stage is specified.

METHODS OF ESTIMATING STREAMBED LEAKANCE

Values of streambed leakance (K/m), as estimated for several streams in the glaciated Northeast from a variety of methods, are given in table 10. Most of the reported streambed leakance values for large streams are 1 (ft/d)/ft or less. In the absence of specific site data, this value is a reasonable initial estimate for use in simulation. Values of streambed leakance higher than 1 (ft/d)/ft are mostly associated with tributary streams flowing on alluvial fans. The following review of methodologies is based largely on several studies conducted as part of this RASA project to obtain representative values of streambed hydraulic properties and develop estimation methods.

Model Calibration

Most streambed leakance values in table 10 were estimated from calibration of ground-water flow models. If all other hydraulic properties and stresses are known, streambed leakance can be derived by calibration of such a model to measured heads. In general, however, all other hydraulic properties and stresses are seldom known, in which case model calibration will yield streambed leakance values that are not narrowly constrained (Yager, 1993; Kontis, 1999). Accordingly, values in table 10 that are based on calibration of ground-water flow models that lack stream-loss data are at best rough approximations. The following methods of measuring rates of stream loss or vertical flux can be used in conjunction with measurements of head distribution beneath the streambed to calculate average streambed leakance, directly (equation 6) or through model calibration.

Paired Streamflow Measurements

The difference between streamflow measurements at the upstream and downstream ends of a stream reach, divided by streambed area, yields an integrated average rate of seepage loss from that reach. Measurement precision is crucial to the successful application of this method. If streamflow measurements are made by current meter, extraordinary care is necessary, including selection of similar measurement sites, careful grading of the streambed, multiple replicate measurements, and adjustments of measurements at different sites over several hours to an exactly uniform stream stage (Dysart and Rheaume, 1999). If a continuous record of stage can be obtained for several days at carefully designed weirs, net loss can be precisely determined over a range of fluctuating flow conditions (Rahn, 1968).

Vertical Temperature Profiles

Rates of ground-water flow between a stream and the underlying sediments can be estimated from vertical profiles of water temperature beneath the stream, together with measured or readily estimated physical and thermal properties

TABLE 10.—*Published values of streambed leakance at sites in the glaciated Northeast, and the methods by which they were derived*

[Streambed leakance (K/m) is defined as the ratio of vertical hydraulic conductivity, K, to thickness, m, of sediment over which head difference prevails. K is in feet per day, and m is in feet]

Location and hydrogeologic setting (setting is valley-fill stratified drift except where otherwise described)	Method	Estimated streambed leakance (feet per day per foot)
Rockaway River near Dover, N.J. (Dysart and Rheaume, 1999)	Paired streamflow measurements	0.21 (0.35 maximum plausible)
	Dissolved oxygen tracer	0.28
	Vertical temperature profile (Lapham, 1989)	0.68
	Mass balance of environmental isotopes	0.68
Norwalk River near Cannondale, Conn. (D. Mazzaferro, U.S. Geological Survey, written commun., 1991)	Paired streamflow measurements	2.6*
Farmington River near Farmington, Conn. (Mazzaferro, 1989)	Calibration of ground-water flow model; K/m unchanged from initial assumed value	0.5
Susquehanna River near Kirkwood, N.Y. (Yager, 1993)	Calibration of ground-water flow model, re-evaluated through parameter estimation.	0.1 (or less)
	Constant-head permeameter measurements on 5 samples of silty materials	0.001*
Muscoot River near Mt. Kisco, N.Y. (S. Wolcott, U.S. Geological Survey, written commun.), upland stream flowing on alluvium and minor amounts of stratified drift	Calibration of ground-water flow model	1.0
Mattapoisett River, Plymouth County, Mass. (Olimpio and deLima, 1984)	Calibration of ground-water flow model; K/m unchanged from initial assumed value	0.75
Chemung, Tioga, and Cohocton Rivers near Corning, N.Y. (Ballaron, 1988)	Calibration of ground-water flow model	.09–.55
Streams tributary to Chemung River near Corning, N.Y. (Ballaron, 1988)	Calibration of ground-water flow model	1.2–4.3
Black and Rockaway Rivers, Long Valley, N.J. (Hill and Pinder, 1981)	Calibration of ground-water flow model	0.76
Beacon Hill Brook-tributary to Naugatuck River-lower Housatonic River basin, Conn. (Wilson and others, 1974)	Paired streamflow measurements	0.95
Little Androscoggin River valley, Oxford County, Maine (Morrissey, 1983)	Calibration of ground-water flow model	1.0**
Aberjona River near Woburn, Mass. (deLima and Olimpio, 1989)	Calibration of ground-water flow model	2.0**
Gulf Brook, Pepperell, Mass. (deLima, 1991); small stream	Paired streamflow measurements. 3 streambed infiltrometers	3.6 0.37
Morse Brook, Shirley, Mass. (deLima, 1991); small stream on sand plain	Paired streamflow measurements. Calibration of ground-water flow model	4.1 2.0

TABLE 10.—*Published values of streambed leakance at sites in the glaciated Northeast, and the methods by which they were derived*—Continued

[Streambed leakance (K/m) is defined as the ratio of vertical hydraulic conductivity, K, to thickness, m, of sediment over which head difference prevails. K is in feet per day, and m is in feet]

Location and hydrogeologic setting (setting is valley-fill stratified drift except where otherwise described)	Method	Estimated streambed leakance (feet per day per foot)
Pootatuck River near Newtown, Conn. (Haeni, 1978)	Paired streamflow measurements, supported by calibration of ground-water flow model	1
Scioto River, southeast Franklin County, Ohio (Weiss and Razem, 1980; Razem, 1983***)	Aquifer tests and calibration of ground-water flow model	0.38*
Tioughnioga River, Cortland County, N.Y. (Cosner and Harsh, 1978), headwater reach of broad valley, only small streams	Calibration of ground-water flow model	0.02–0.08
Ramapo River near Mahwah, N.J. (Hill and others, 1992)	Paired streamflow measurements, supported by calibration of ground-water flow model	3 (for streambed thickness of 10 ft)
Tioughnioga River, Cortland, N.Y. (Reynolds, 1987)	Paired streamflow measurements	0.7
Beaver River-Pasquiset Brook, Rhode Island (Dickerman and Ozbilgin, 1985)	Aquifer tests that give effective vertical hydraulic conductivity of streambed and aquifer combined	0.4*–15.2*
Lower Wood River, southern R.I. (Dickerman and others, 1990)	Calibration of ground-water flow model	2.7–4
Great Miami River near Dayton, Ohio (Fidler, 1975)***	Paired streamflow measurements	0.06–5.0
Potowomut River basin, Rhode Island (Rosenhein and others, 1968)	Variable-head permeameter measurements at 11 sites	0.09* to 15* (average of 1.1 for streambed thickness of 2 ft)
Saco River valley, North Conway, N.H. (Tepper and others, 1990)	Calibration of ground-water flow model	2.5
Lamprey River, N.H. (Moore, 1990)	Assumed value in uncalibrated ground-water flow model	1.0
North and South Branch Sugar River, N.H. (Moore and others, 1994)	Assumed value in uncalibrated ground-water flow model	1.0
Marsh Creek, north-central Penna., and Asaph and Straight Runs (tributary streams) (Williams and Morrissey, 1996; J.H. Williams, USGS, written commun., 1996)	Calibration of ground-water flow model do.	0.73 3.3 and 10
Ware River near Hardwick, Mass. and near New Braintree, Mass. (Lapham, 1989)	Vertical temperature profile do.	0.004 0.15–1.0
Killbuck and Apple Creeks near Wooster, Ohio (Breen and others, 1995). Little Killbuck and Clear Creeks (tributary streams) (Breen and others, 1995)	Calibration of ground-water flow model do.	0.01*–1* 2*–10*

* No information on streambed thickness; given value is based on streambed thickness of 1 foot.
** Initial assumed value; final value(s) after calibration not specified in report.
*** Outside glaciated Northeast.

(Lapham, 1989). This method is based on a numerical solution of the equation that describes one-dimensional vertical flow of fluid and heat in saturated sediments. Water-temperature measurements are made at depth intervals of 1 or 2 ft in wells or closed pipes 1 to 2 inches in diameter. The measurements are repeated every few hours for several days to define diurnal temperature fluctuations, or every few weeks for a year or more to define seasonal fluctuations. The method can be applied in gaining or losing reaches. Specific discharge (flow per unit area) is determined precisely at each site, but several sites in each stream reach would be required before an average specific discharge or total loss rate could be estimated with confidence. The method is economical, independent of streamflow, and therefore suitable for estimation of streambed hydraulic properties in large streams.

Dissolved-Oxygen Tracer Method

Dysart and Rheaume (1999) describe and apply a method for estimating specific discharge by comparing the timing and magnitude of diurnal dissolved-oxygen fluctuations in a stream and in piezometers finished immediately below the streambed. Water from the stream and the piezometer(s) is pumped at a low rate to an in-line flow-through cell in which dissolved oxygen is measured every few hours over several days.

Geochemical Mass-Balance Method

In this method, the amounts of conservative dissolved chemical constituents or environmental isotopes in river water and native ground water are compared with the amounts in water from production wells or nearby observation wells, to calculate by proportions the amount of induced infiltration passing a particular observation well or captured by a particular production well. The method was used by Breen (1988), Breen and others (1995), Dysart (1988) and Dysart and Rheaume (1999) to estimate the amount of recharge from bedrock to stratified drift as well as the amount of induced infiltration from streams.

ACCURACY OF STREAMBED LEAKANCE ESTIMATES

The accuracy of streambed leakance values for a stream reach obtained by any of the foregoing methods depends as much on accurate determination of the head difference between stream and aquifer as on accurate seepage-loss or specific-discharge measurements. Consider an idealized stream reach (fig. 18) with a distinct streambed of area LW, spatially varying streambed thickness $m(x,y)$ and streambed vertical hydraulic conductivity $K(x,y)$ assumed to vary over (x,y) but not vertically across the streambed. At any point $P(x,y)$ on the surface of the streambed, the vertical flow between the stream and underlying aquifer through the streambed is described by the specific discharge $q(x,y)$:

$$q(x,y) = \frac{K(x,y)}{M(x,y)}\Delta h(x,y) \sim \frac{K(x,y)}{m(x,y)}\Delta h(x,y), \quad (7)$$

where $\Delta h(x,y)$ is head in the stream minus the head at a point beneath the streambed open to a piezometer, and

$M(x,y)$ is the distance from the top of the streambed to the point at which the head is measured and is assumed to be the same as the streambed thickness $m(x,y)$; that is, the base of the postulated streambed is assumed to be known and the piezometer placed near the base.

At each piezometer, head is measured in the aquifer beneath the streambed, and also in the stream around the piezometer casing. The difference between these two measurements, $\Delta h(x,y)$, represents a discrete point on a continuous two-dimensional head-difference surface between the ends of the idealized stream reach at measurement sections a and b (fig. 18). The net stream gain or loss, denoted by $\Delta Da,b$, is the difference in stream discharge between sections a and b and is the sum of the specific discharges over the area LW; that is,

$$\Delta Da,b = Da - Db = \int_0^L \int_0^W q(x,y)dxdy = \int_0^L \int_0^W \frac{K(x,y)}{m(x,y)}\Delta h(x,y)dxdy \quad (L^3/T) \quad (8)$$

If the streambed hydraulic conductivity $K(x,y)$ and the thickness $m(x,y)$ are essentially constant over the reach a–b, then

$$\Delta Da,b = \frac{K}{m}\int_0^L \int_0^W \Delta h(x,y)dxdy \quad , \text{or}$$

$$\frac{K}{m} = \frac{\Delta Da,b}{\int_0^L \int_0^W \Delta h(x,y)dxdy} \cdot \quad (L/T)/L .$$

Thus, for these conditions, the accuracy of the streambed leakance, K/m, is dependent not only on the stream loss ($\Delta D_{a,b}$) but also on the sum of the head differences over the area LW (that is, the volume beneath the head-difference surface). If K and m are, in fact, virtually constant over the extent of the area LW, then Δh should also be virtually constant so that,

$$\int_0^L \int_0^W \Delta h(x,y)dxdy = \Delta h^* LW ,$$

where Δh^* is the vertical head-difference assumed to be constant over the area LW, so that

$$K/m = (\Delta Da,b)/(\Delta h^* LW). \quad (9a)$$

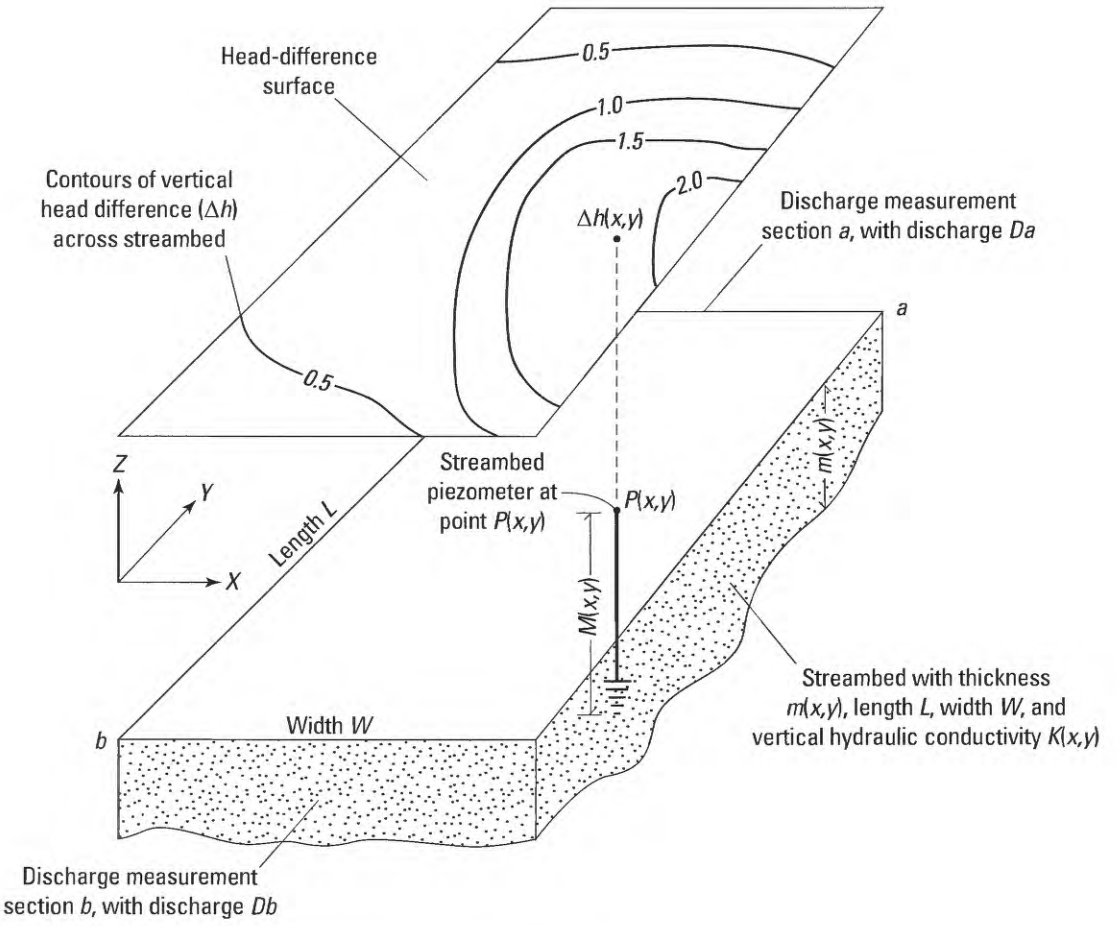

FIGURE 18.—Idealized streambed showing terms in equations 7–9 used to calculate streambed leakance (K/m) from stream-discharge measurements (Da and Db) and vertical head differences $\Delta h(x,y)$, as measured with streambed piezometers at points $P(x,y)$ over a stream reach of length L and width W.

In reality, there is probably some variation in the head difference, but if a large number of streambed piezometers are suitably distributed over the area of reach a–b, Δh^* can be accurately calculated as the average of the head measurements at all piezometers. In practice, however, only a few piezometer measurements are made; thus, only an estimate of Δh^* is available. In addition, the measured streamflow loss is only an approximation of actual loss so that an estimate of streambed leakance $(K/m)'$ is available. That is

$$(K/m)' = \Delta D'a,b/\Delta\bar{h}LW\,, \qquad (9b)$$

where $\Delta\bar{h}$ is the estimated head difference, an average of the piezometer head-difference measurements,

$\Delta D'a,b$ is the estimated stream loss based on available measurements, and

$(K/m)'$ is the estimated streambed leakance of the stream reach.

If the error in estimating stream loss is P_1 and the error in estimating the head-difference is P_2, where P_1 and P_2 are each expressed as a percent of the true value divided by 100, then

$$\Delta D' = \Delta D + P_1\Delta D\,,$$

$$\Delta\bar{h} = \Delta h^* + P_2\Delta h^*\,,$$

and

$$(K/m)' = \frac{\Delta D}{\Delta h^*}\left(\frac{1+P_1}{1+P_2}\right)\frac{1}{LW} = (K/m)\left(\frac{1+P_1}{1+P_2}\right), \qquad (10a)$$

where the error P_1 or P_2 is positive for overestimates and negative for underestimates. Because ΔD and Δh^* are defined as positive when the stream is losing, they cannot be underestimated by more than 100 percent; consequently P_1 and P_2 cannot be less than -1.0, and the expressions $(1+P_1)$ and $(1+P_2)$ in equation 10a cannot be negative. The expression $(1 + P_1) / (1 + P_2)$ equation 10a, is termed the "error factor"; it

is a measure of the uncertainty in streambed leakance due to errors in estimating the stream loss and the average head difference across the streambed. The error factor for error-free estimates of stream loss and head loss would have a value of unity.

The effects of errors in ΔD and(or) Δh^*, from 0 to 100 percent, on streambed leakance are illustrated in figure 19 by several curves that relate the magnitude of the error factor (denoted by f) to variations in P_1 and P_2. The two dotted curves show how varying percentage error in stream loss (P_1) affects the error factor if the head difference is accurate ($P_2 = 0$); one of these curves represents $f = 1 + P_1$ (stream loss is overestimated), the other represents $f = 1 - P_1$ (stream loss is underestimated). The two dashed curves show the effect of percentage error in head difference on the error factor if stream loss is accurate ($P_1 = 0$) and $f = 1/(1 \pm P_2)$. These four curves show that the effects of underestimation of stream loss or head difference are greater in magnitude than the effects of overestimation. For example, if stream loss is measured with no error ($P_1 = 0$) and Δh^* is overestimated by 50 percent ($P_2 = 0.5$), then $f = 2/3$, and the estimated streambed leakance (K/m) would be 2/3 of its actual value, whereas if Δh^* is underestimated by 50 percent ($P_2 = -0.5$), then $f = 2$ and $(K/m)'$ would be twice its actual value. If the absolute value of the percentage error in estimating ΔD and Δh^* is the same, that is $|P_1| = |P_2| = P$, then the maximum and minimum estimates of streambed leakance are:

$$(K/m)'_{max} = (K/m)\frac{(1+P)}{(1-P)}, \text{ and} \qquad (10b)$$

$$(K/m)'_{min} = (K/m)\frac{(1-P)}{(1+P)}. \qquad (10c)$$

Equation 10b assumes that ΔD is overestimated and Δh^* is underestimated, whereas equation 10c assumes that ΔD is underestimated and Δh^* is overestimated. The two solid curves in figure 18 depict the error factors in equations 10b and 10c, $f = (1 + P) / (1\text{-}P)$ and $f = (1 - P) / 1{+}P)$. These curves show, for example, that if the uncertainty in both ΔD and Δh^* is 20 percent, the maximum and minimum estimates of K/m would be 1.5 and 2/3 times the actual value, respectively. If the uncertainty in both estimates is 50 percent, the maximum and minimum estimates of streambed leakance would be 3 and 1/3 times the actual value, respectively.

AQUIFER SIMULATION

If the flow system of a stratified-drift aquifer is to be simulated by a ground-water flow model, the information that must be obtained or inferred includes: (1) the three-dimensional spatial configuration of the aquifer and of any non-aquifer materials in the model area; (2) the magnitude and spatial distribution of hydraulic properties (hydraulic conductivity and storage) of the aquifer and non-aquifer materials; (3) the magnitude and distribution, in time and space, of natural and manmade sources and sinks (inflow and outflow) of water within the model area; (4) the magnitude and direction of ground-water flow across the boundaries of the model; and (5) the hydraulic head at a sufficient number of locations to allow calibration, and the temporal variation of head at each location if the simulation is time-dependent.

Given this information, the ground-water flow system can be simulated by any of several available modeling codes, such as those described by van der Heijde and others (1988), Appel and Reilly (1988), McDonald and Harbaugh (1988), or Anderson and Woessner (1992). Although the MODFLOW code of McDonald and Harbaugh is used in the example simulations described further on, the following discussion applies equally well to other model codes. The discussion addresses the placement and nature of model boundaries and the spatial discretization of the model and then considers the application of these aspects of model design to the several types of stratified-drift aquifers previously identified (fig.14, table 4). Finally, a new procedure for the simulation of recharge is described that is well suited for systems in which water levels are near land surface.

MODEL BOUNDARIES

An important aspect of model design is delineating the perimeter of the model and the boundary conditions along that perimeter. As discussed by Franke and Reilly (1987) and Franke and others (1987), defining the spatial limits of a model is analogous to defining the natural hydraulic boundaries of an aquifer. Model boundaries, however, need not coincide with aquifer boundaries. For example, consider figure 20, which depicts an idealized drainage basin consisting of a valley-fill aquifer and bordering uplands. At least three alternative boundary configurations could be used to model this aquifer system. Commonly, model boundaries are specified to coincide with the geologic contact between the valley fill and the till-covered bedrock upland, at or near the base of the valley wall (boundary C, fig. 20). The uplands are excluded from the model because (1) the bedrock and till are much less permeable than the coarse-grained stratified drift in the valley fill, so ground-water flow within the upland is assumed to be negligible, and(or) (2) the hydraulic properties of the bedrock and till are poorly known and therefore cannot be accurately simulated, and(or) (3) inclusion of the uplands would result in a model that is unduly large and complex for the intended purpose. Any flow of water into the valley fill from the uplands must be estimated and represented by applying appropriate boundary conditions to valley cells adjacent to the model boundaries.

Alternatively, the model boundaries could be specified to coincide with the perimeter of the topographic drainage basin

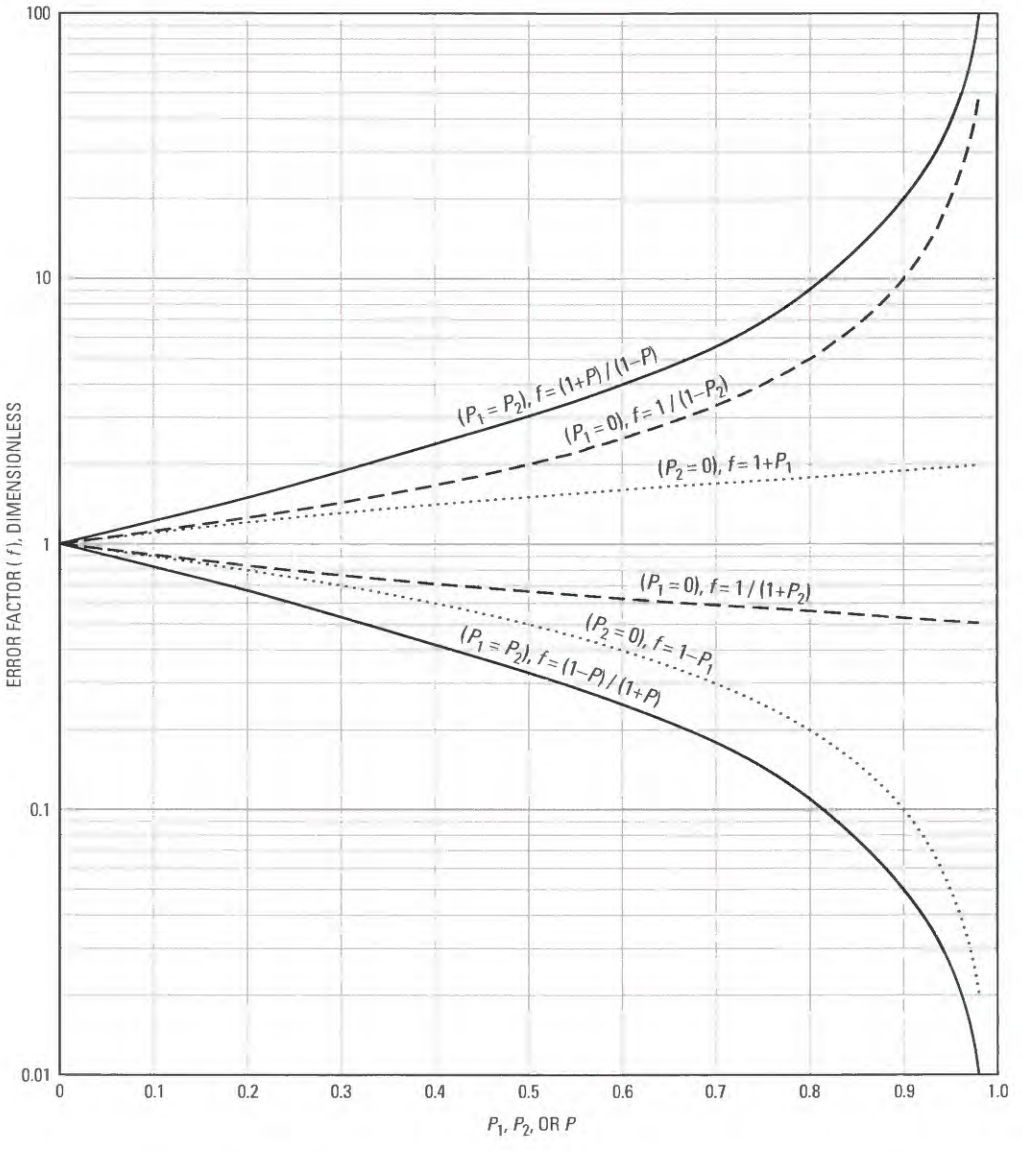

EXPLANATION

P_1	**Error in estimation of loss of streamflow over losing reach of stream**—In percent divided by 100
P_2	**Error in estimation of the mean value of the vertical head loss, across the streambed, over the losing reach of stream**—In percent divided by 100
P	**Is the absolute value of P_1 and P_2 when P_1 equals P_2**
$1+P, 1+P_1, 1+P_2$	**Denote overestimation of value**
$1-P, 1-P_1, 1-P_2$	**Denote underestimation of value**
f	**Error factor**—Expresses the error in streambed leakance, as defined for each curve and used in equations 10a, 10b, and 10c

FIGURE 19.—Error in estimated streambed leakance as a function of errors in stream loss and in vertical head difference between stream and aquifer, assuming uniform streambed hydraulic conductivity and thickness.

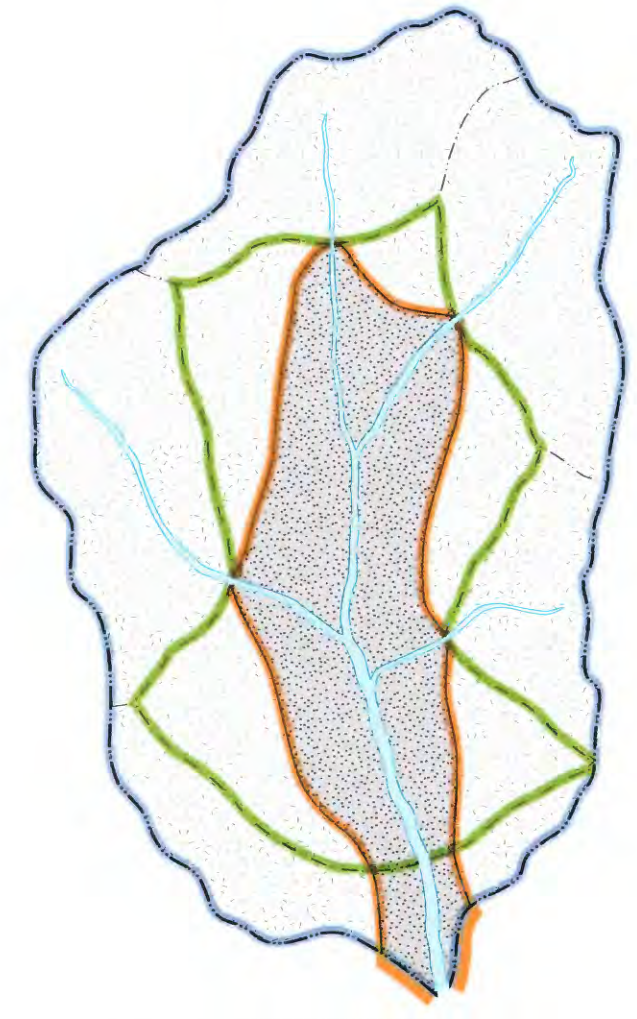

FIGURE 20.—Alternative model-boundary configurations in relation to a typical valley-fill aquifer and the drainage basin that surrounds it.

(boundary A, fig. 20). Such boundaries are commonly natural ground-water divides as well as surface-water divides, and could be simulated as zero-flow boundaries. The model would incorporate the entire ground-water and surface-water flow system, much of which originates in the uplands beyond the valley-fill stratified drift. A simpler alternative would be to extend the model outward from the valley fill only to the nearest upland subbasin divides, which could also be simulated as zero-flow boundaries (boundary B, fig. 20). Upland basins drained by tributary streams would be excluded from the model, but runoff from such basins could be estimated and treated as a potential source of seepage losses where the simulated tributary channels cross the valley-fill aquifer. Upland hillsides that slope toward the valley fill would be included in the model; lateral subsurface flow and any unchanneled surface runoff from these areas would be simulated.

Inclusion of part or all of the adjacent uplands in the model (alternatives A and B, fig. 20) can be advantageous in studies where knowledge of the upland flow system is important, such as in delineation of the contributing area to wells pumping from the valley fill. It also allows the model to compute flux across the margin of the stratified drift for both steady-state and transient conditions, an approach that is more convenient and possibly more accurate than independently estimating boundary flows as required by alternative C. Although knowledge of the magnitude and spatial variability of the hydraulic properties of the uplands is limited in most places, order-of-magnitude estimates can generally be made. In those few localities where thick morainal deposits or unusually permeable bedrock allow subsurface flow beneath basin divides, alternatives A or B may be inappropriate. The advantages and disadvantages of including the adjacent uplands in a ground-water flow model are considered further in the ensuing discussion of example models of the Rockaway River valley near Dover, N. J., and the Killbuck Creek valley near Wooster, Ohio.

The lower boundary of a model, like the lateral boundaries, is commonly placed at the geologic contact that separates the stratified-drift aquifer from poorly permeable material, such as lacustrine silt and clay, till, or bedrock. The effect of excluding the material beneath the aquifer from a simulation can be readily determined by model-sensitivity analysis, as discussed further on.

The upper boundary of any aquifer system is the water table. Most models of stratified-drift aquifers simulate this boundary, and can incorporate several model subroutines that have been developed to simulate natural processes occurring at the water table, including recharge from infiltrating precipitation, discharge in the form of ground-water evapotranspiration, seepage to or from surface-water bodies, and outward seepage where the water table intersects land surface. Models that represent only a confined aquifer can incorporate the effects of the saturated zone above that aquifer by boundary

conditions that approximate vertical flow through the overlying confining unit, as in Meisler (1976), Randall (1979), and Olimpio and deLima (1984).

At upvalley and downvalley margins of a model, a specified flux or general head boundary condition is commonly used to simulate underflow through the valley fill. Less commonly, where coarse-grained stratified drift thins or is truncated, or where a ground-water divide occurs under natural conditions within a valley, a zero-flow boundary is appropriate. These boundaries should be far enough from the area of interest that (1) model stresses will have a minimal affect on the flow and head near the boundary and (2) the magnitude of flow at the boundary will have a minimal effect on flow and head in the area of interest. Each of these boundary conditions are used in the ground-water flow models of the Rockaway River near Dover, N.J. and the Killbuck Creek near Wooster, Ohio, discussed further on.

SPATIAL DISCRETIZATION

In designing any ground-water flow model, the model cell spacing and number of layers are selected to represent the known or inferred spatial variability of the hydraulic properties and head distribution throughout the system and the nature of the problem, hypothesis, or technique that the model is intended to test. Most ground-water systems, including those of the glaciated Northeast, are inherently three-dimensional. Nevertheless, many surficial stratified-drift aquifers have been simulated by two-dimensional (single layer) models on the assumption that any vertical flow is small relative to horizontal flow and can therefore be neglected, or because little information is available on the magnitude and distribution of head and hydraulic properties of the stratified drift with depth. The assumption that flow is virtually horizontal could readily be tested, however, by simulating the aquifer with two or more model layers and applying the anticipated stresses over a plausible range of anisotropy or hydraulic conductivity variation with depth. If the simulated flow is indeed virtually horizontal over the range of variations, this behavior can be presented as a conclusion with some degree of confidence, rather than as an assumption. Other uncertainties in model design, such as the position of a boundary or the possible heterogeniety in some locale, can be similarly addressed by designing the model to be as general as feasible and testing model sensitivity to alternative hypotheses.

As previously discussed, the stratified drift can be generally classified into three depositional facies: (1) heterogeneous gravel and coarse sand deposited near the margin of the ice sheet as it retreated; (2) fine-grained sediment deposited later in open water, when the ice margin was farther away; and (3) surficial sand and some gravel deposited still later atop the fines by meltwater or postglacial streams. Although each of these facies is discontinuous, many valleys are characterized by a widespread surficial aquifer of variable thickness and origin, extensive bodies or lenses of fine-grained sediment at intermediate depths, and a deeper aquifer that is locally absent but in some places constitutes the entire thickness of the valley fill. This three-facies, two-aquifer stratigraphy has been conceptualized in many studies, including those described by Ballaron (1988), Crain (1966, 1974), Exarhoulakos and others (1992), Frimpter (1972), Mazzaferro (1986a), Mazzaferro and others (1979), Meade (1978), Moore (1990), MacNish and Randall (1982), Olimpio and DeLima (1984), Randall (1979, 1986), Randall and others (1966), Reynolds and Brown (1984), and Toppin (1987).

Depending on the purposes of a particular simulation, the three facies can be treated in several ways:

1. The entire stratified-drift section can be simulated, with intercalated fine-grained sediment assigned to a particular model layer or implicitly simulated by low values of vertical leakance between aquifer layers (for example, Hill and others, 1992; Randall, 1986; Exarhoulakos and others, 1992: Breen and others, 1995).
2. The deep stratified-drift aquifer can be ignored and only the surficial aquifer simulated, from the water table down to the top of fine-grained stratified drift or bedrock, whichever constitutes the base of the surficial aquifer in any given region of the modeled area (for example, Snavely, 1983; Kontis, 1999; Reynolds 1987). Bergeron (1987) simulated an extensive surficial aquifer, but used a 2-layer model with low values of vertical leakance where that aquifer is separated into two aquifers by localized fine-grained lenses.
3. If the surficial aquifer is thin or irrelevant to the purpose of the model, only the buried aquifer, and any windows that allow recharge from above, can be simulated (for example, Randall, 1979).

AQUIFER TYPES

The principal geohydrologic characteristics of each of six generalized types of stratified-drift aquifers found in the glaciated Northeast are described in the following sections, along with possible approaches for their simulation. Sandplain, outwash-plain, and hillside aquifers are inherently single surficial geologic units, overlying differently configured bedrock or fine-grained sediments. Buried aquifers are also generally single layers within or beneath fine-grained sediments. These four types of aquifers could be simulated by 1-layer, 2-dimensional models, although the three surficial types commonly consist of deltaic deposits that become finer with depth and thus could be simulated by two layers of differing hydraulic conductivity. Valley-fill and headwater aquifers, by contrast, are commonly conceptualized as incorporating the entire valley fill, which may include extensive layers of fine-grained sediment, such that multi-layer models are needed.

Valley-Fill Aquifers

Valley-fill aquifers, the predominant type of stratified-drift aquifer in the glaciated Northeast, are found in major and secondary valleys and are hydraulically connected to a perennial master stream. The geometry, sediment distribution and sources of recharge typical of valley-fill aquifers are depicted in figures 21*A* and 21*B*. These aquifers commonly consist chiefly of ice-contact stratified drift that was deposited on or against abundant glacial ice, but also may include surficial deltaic or fluvial sand and gravel deposited later in deglaciation when most of the ice had melted. The valley fill also commonly contains lenses or bodies of fine-grained sediment that can be simulated as part of the model or treated as a boundary depending on their thickness and extent. The coarse-grained sediments (sand and gravel) were commonly deposited where depth to bedrock was least, along the valley sides or near midvalley knolls, resulting in modest saturated thicknesses today. Valley-fill aquifers are recharged from five principal sources: (1) direct infiltration of precipitation where the aquifer crops out, (2) unchanneled surface and subsurface runoff from adjacent upland areas, (3) leakage from tributary streams, (4) induced infiltration from the master stream draining the valley, and (5) upward leakage from the bedrock.

The master streams associated with typical valley-fill aquifers are seldom sources of recharge under natural (nonpumping) conditions, because water levels in the aquifers are usually above stream grade and the streams act as drains. During extended periods of little or no recharge, water levels in local, highly transmissive aquifers may fall below the grade of the master stream temporarily, resulting in recharge from the stream to the aquifer. During brief periods of rising stream stage, recharge in the form of bank storage may also occur temporarily. Under stressed (pumping) conditions, stream reaches adjacent to pumping centers can become major sources of recharge if water levels in the aquifer are drawn below the stream stage. This induced infiltration has the potential to greatly increase aquifer yields and is often a primary consideration in the evaluation of the long-term yield potential of valley-fill aquifers. One of the consequences of induced infiltration is a reduction in streamflow.

Valley-fill aquifers are bordered by uplands of relatively low permeability, where surface-water and ground-water drainage divides are generally coincident. The uplands are part of the hydraulic system of the valley fill in that flow emanating from the uplands is a source of recharge to the valley fill. Unchanneled subsurface and surface runoff infiltrates into the valley-fill sands and gravels at and beneath the base of upland hillsides, and tributary streams flowing across the valley fill contribute recharge wherever stream-surface elevations are higher than hydraulic head in the valley fill under natural conditions or as a result of pumping. In regions of substantial topographic relief, upland sources typically can account for more than 50 percent of total recharge to valley-fill aquifers (table 5; Morrissey and others, 1988).

A three-layer model design suitable for simulation of many valley-fill aquifers is illustrated in figure 21*C*. Vertical discretization and zones of similar hydraulic conductivity correspond to the typical three-facies aquifer geometry illustrated in figure 21*B*. The fine-grained sediment is simulated as part of model layers 2 and 3, an appropriate design when that sediment is fine sand to silt that may not constitute a distinct, nearly impermeable confining layer. Vertical leakance between layers is computed as the harmonic mean of the vertical hydraulic conductivities of adjacent layers divided by average layer thickness (McDonald and Harbaugh, 1988, p.5-12). Figure 21*C* also illustrates two options for simulation of the upland: one option is to extend each model layer laterally into the bedrock (or till) beneath the upland as far as the nearest divide (as in boundary position A of figure 20), then estimate values for hydraulic properties and recharge in the upland; the second option is to place the model boundary along the edge of the stratified-drift aquifer (as in boundary position C of figure 20), then estimate recharge from the uplands to the valley fill and apply it as a boundary condition.

A two-layer, quasi-three-dimensional model design also suitable for simulation of many valley-fill aquifers is illustrated in figure 22. A geologic section (fig. 22*A*) depicts the three typical valley-fill facies plus two postglacial units (facies 4 and 5, fig. 22*A*) that complicate the stratigraphy in a few localities. The various geologic units are classified in figure 22*B* into an upper aquifer and a lower aquifer locally separated by an implicitly simulated confining layer. Outwash (facies 3, fig. 22*A*) is generally the surficial aquifer, but where it is downwarped it can be treated as the lower aquifer, or part thereof. In the corresponding model design (fig. 22*C*), the discontinuous fine-grained deposits (facies 2 and 4) are not explicitly modeled, but their effect is simulated by using low values of vertical leakance where the two aquifers are separated by fine-grained lake beds, and high values of vertical leakance where the surficial aquifer directly overlies the deeper aquifer or is downwarped to become the deeper aquifer. Although the stratified drift terminates against bedrock (or till) along the valley bottom and sides (fig. 22*A*) the two model layers could be extended laterally into the adjacent bedrock (fig. 22*C*) and a third model layer could be added to represent bedrock below the valley fill.

MODFLOW is capable of simulating the effects of tributary streams and the perennial main stream associated with typical valley-fill systems by means of two procedures, the Stream Package (Prudic, 1989) and the River Package (McDonald and Harbaugh, 1988, chap. 6). Either package can be used to simulate perennial streams, in which only the flow between stream and aquifer is important. The Stream Package can be used to simulate the component of recharge that originates as upland channeled runoff. In this procedure, the magnitude of streamflow can be specified as model input, at the

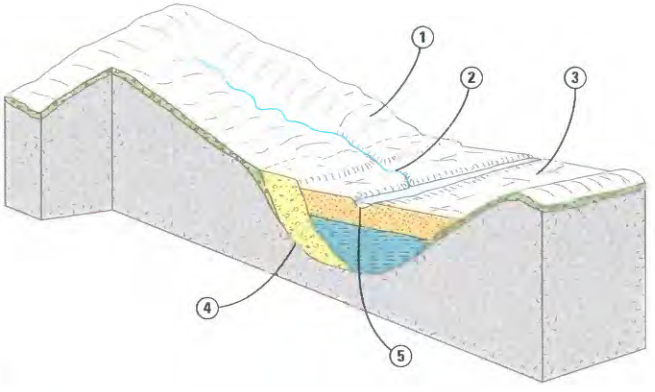

A.

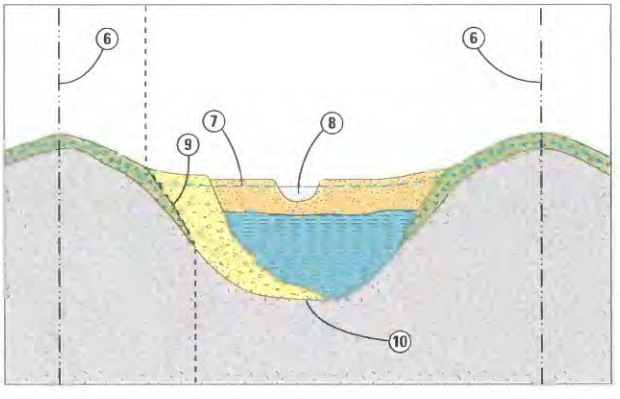

B.

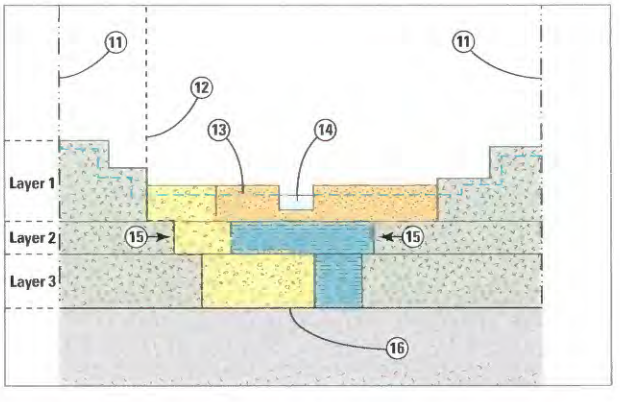

C.

(1) A significant amount of water can recharge the aquifer as unchanneled runoff from adjacent upland areas.

(2) A significant amount of water can recharge the aquifer as seepage from tributary streams draining the uplands.

(3) Some water recharges the aquifer directly from precipitation.

(4) Small amounts of water may recharge the aquifer as subsurface flow from bedrock.

(5) Perennial streams flowing across valley fill have the potential to be major sources of recharge under pumping conditions when ground-water levels fall below the stream.

(6) Drainage divide: a boundary between adjacent drainage basins. Ground-water and surface-water divides usually conicide.

(7) Water table is typically above stream surface.

(8) Master stream is typically perennial and receives discharge from the aquifer flow system. It has the potential to be a major source of recharge to the aquifer.

(9) Lateral contact of stratified drift against till or bedrock, which have markedly smaller hydraulic conductivity. If the small subsurface flow into the valley fill can be approximated, this is an appropriate lateral aquifer boundary.

(10) Basal contact of stratified drift atop bedrock. Data on the magnitude of flows across this contact are sparse, but for most purposes the flow can be treated as zero.

(11) Model boundary: simulated as zero flow.

(12) Alternative model boundary: simulated as specified flux into valley fill.

(13) Water table: typically above stream surface.

(14) River: simulated as leaky confining bed.

(15) Minor flow into valley fill.

(16) Model boundary: simulated as zero flow.

EXPLANATION

Lithology	Hydraulic conductivity
Very fine sand, silt, clay	Low
Sand	Medium
Gravel and sand	Medium to high
Till	Low
Till and (or) bedrock	Low
Bedrock	Very low

FIGURE 21.—Valley-fill aquifer: (*A*) Physical setting and sources of recharge; (*B*) a typical sediment distribution and natural boundaries in a vertical section corresponding to (*C*) a possible model configuration.

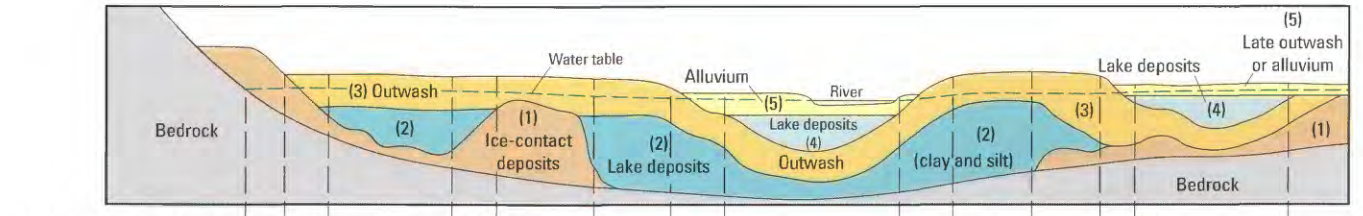

A. GEOLOGIC CONFIGURATION

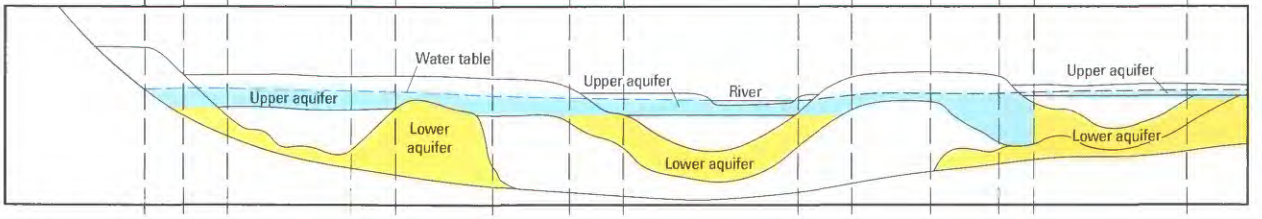

B. WATER-BEARING UNITS

MODEL ELEMENT	FLOW DIRECTION	RELATIVE WATER-TRANSMITTING CAPACITY														
LAYER 1	→ ← Horizontal	Low	Med.	Med.	Medium	Med.	Medium	Medium	Med.	Medium	Med.	Low	High	Med	Low	Medium
LEAKANCE	↑ ↓ Vertical	Low	Low	High	Low	Low	High	Low	High	Low	High	Low	Low	High	Low	High
LAYER 2	→ ← Horizontal	Low	Low	Med.	Low	Med.	High	Nil	Med.	High	Med.	Nil	Medium	Med.	High	High

Extension of model layers into bedrock

C. MODEL

FIGURE 22.—Idealized valley-fill aquifer and corresponding ground-water flow model geometry: (*A*) Geologic units; (*B*) classification of geologic units into aquifers and confining layers; and (*C*) model representation of aquifers and confining layers. Numbers in parentheses are facies numbers, see text. Vertical dashed lines indicate alignment of equivalent segments of *A*, *B*, and *C* (modified from Randall, 1986).

valley wall where a tributary leaves the upland and begins to cross the valley-fill aquifer; the model then computes vertical flow between stream and aquifer in each stream cell, and augments or depletes the simulated streamflow by the amount of seepage gain or loss within each cell. If a stream loses a sufficient amount of water, it may go dry as it flows across the stratified drift. In simulations where the model boundary is at the edge of the stratified drift, runoff from each tributary watershed at that point could be computed from daily or monthly upland runoff at some nearby gaging station that represents upland terrain, or from long-term average monthly upland runoff, as illustrated in figure 9 for several representative basins and as described by Lyford and Cohen (1988). In simulations where the uplands are an active part of the model, and the Variable-Recharge procedure (discussed further on) is used to simulate areal recharge, the quantity of upland channeled runoff and, therefore, the magnitude of streamflow appearing at the valley wall in tributary streams, need not be specified in the model input but can be determined by the model as a function of the upland head distribution.

Models of individual valley-fill aquifers in the glaciated Northeast have been described in some detail in reports by Cosner and Harsh (1978), Randall (1979, 1986), Bergeron (1987), Mazzaferro (1986a), Yager (1986, 1993), Morrissey (1983), Haeni (1978), Olimpio and de Lima (1984), Hill and Pinder (1981), Hill and others (1992), Kontis (2001), Tepper and others (1990), Ballaron (1988), Reynolds (1987), deLima and Olimpio (1989), Dickerman and Ozbilgin (1985), Dickerman and others (1990).

Headwater Aquifers

Headwater aquifers are similar to valley-fill aquifers, except that they lie close to drainage divides and are not crossed by large perennial streams. Some headwater aquifers occupy broad valleys floored with stratified drift that was deposited when meltwater flowed across watershed divides during deglaciation; the modern drainage divides cross these through-valley floors, which are now drained only by small headwater streams (fig. 23*A1*). Other headwater aquifers occupy enlarged reaches near the heads of ordinary valleys, bordered by narrow uplands that rise to the watershed divide (fig. 23*A2*). A general characteristic of headwater aquifers is that the ratio of valley-floor area to upland area within the

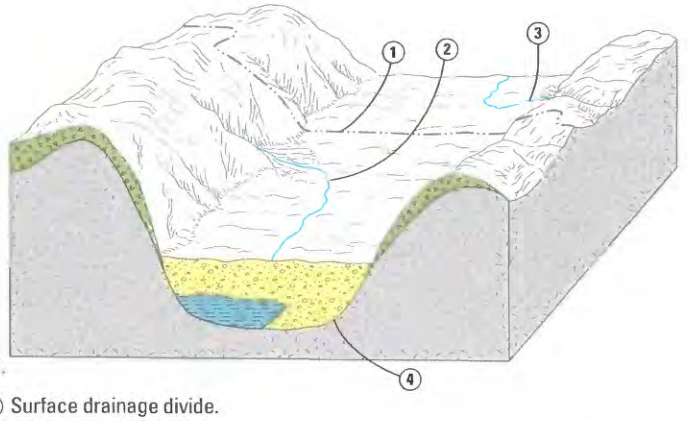

A1.

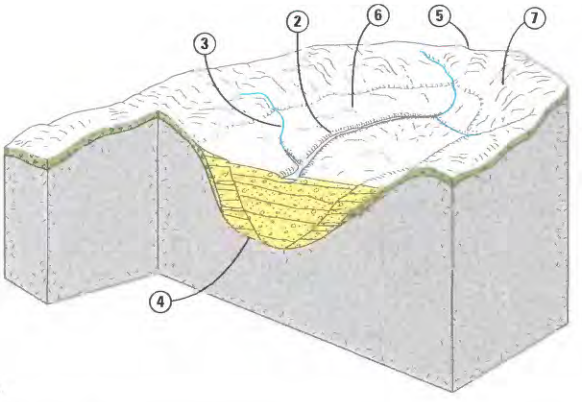

A2.

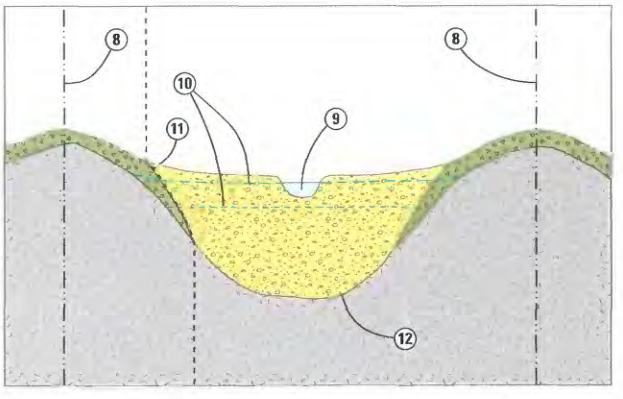

B.

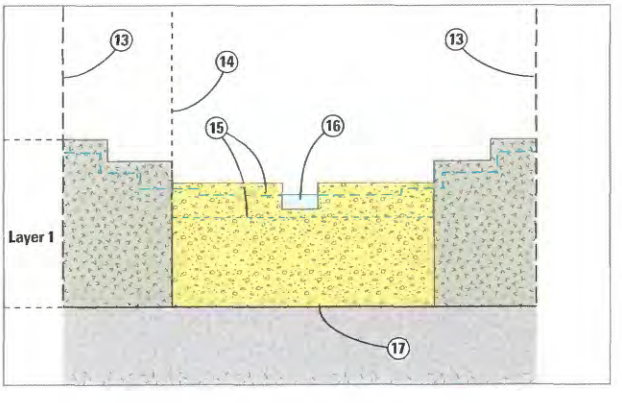

C.

① Surface drainage divide.

② Upland runoff that reaches the main channel can seep into the aquifer, except when the water table rises above the channel and ground water discharges there.

③ Upland runoff in tributary channels seeps into the aquifer.

④ Small amounts of water flow from the bedrock into the aquifer.

⑤ Natural ground-water divides and surface-water divides in upland areas normally coincide.

⑥ Precipitation on the valley floor recharges the aquifer.

⑦ Unchanneled runoff and subsurface flow from adjacent upland areas recharge the aquifer.

⑧ Drainage divide: a boundary between adjacent drainage basins. Ground-water and surface-water divides usually coincide.

⑨ Master stream: invariably small; dry or a source of recharge from upland runoff when water table is below channel; receives discharge and is a minor potential source of induced recharge when water table is above channel.

⑩ Water table: large seasonal fluctuation likely.

⑪ Lateral contact of stratified drift against till or bedrock, which have markedly smaller hydraulic properties. If the small subsurface flow into the valley can be approximated, this is an appropriate lateral aquifer boundary.

⑫ Basal contact of stratified drift atop bedrock. Data on the magnitude of flows across this contact are sparse, but for most purposes the flow can be treated as zero.

⑬ Model boundary: simulated as zero flow.

⑭ Alternative model boundary: simulated as specified flux into valley fill.

⑮ Water table.

⑯ Stream: simulated as a leaky confining bed or drain.

⑰ Model boundary: simulated as zero flow.

EXPLANATION

Lithology	Hydraulic conductivity
Very fine sand, silt, clay	Low
Gravel and sand	Medium to high
Till	Low
Till and (or) bedrock	Low
Bedrock	Very low

FIGURE 23.—Headwater aquifer: (*A*) Typical physical settings, a through valley (*A1*) and a broad upper reach of an ordinary valley (*A2*); (*B*) aquifer boundaries and a typical sediment distribution in a vertical section corresponding to (*C*) a possible model configuration.

watershed is unusually large, and upland tributaries correspondingly small. Throughout much of a normal year, the upland tributaries go dry shortly below the point where they begin to cross the valley floor, and streamflow along the valley axis begins wherever the volume of recharge from upland runoff and direct precipitation on the valley floor exceeds the capacity of the stratified drift to transmit water downvalley. Upland streamflow may reach the valley axis after heavy rain, however, and in winter or spring the water table in the valley fill may rise to the point that ground water discharges to the stream channel all along the valley axis. Because headwater aquifers are not associated with large perennial streams that originate elsewhere, they have little or no potential for recharge by induced infiltration, except perhaps along their downvalley margins where either (a) the headwater valley joins another valley that contains a large stream, or (b) the aquifer changes gradually from a headwater type to a valley-fill type as drainage area increases. Headwater aquifers are uniquely suitable as potential sources of seasonal or emergency water supplies, because the absence of induced infiltration allows large volumes of water to be withdrawn during seasonal or occasional episodes of low flow with little depletion of streamflow downvalley, as illustrated in figure 24.

Aquifer geometry and grain-size distribution in headwater aquifers are generally the same as in valley-fill aquifers; coarse-grained deposits predominate, but lenses or bodies of fine-grained lacustrine sediment commonly occur as well. Thus, the geologic sections in figure 23*A*,*B* and 21*A*,*B* are interchangeable. Model designs suitable for valley-fill aquifers may also be used for headwater aquifers, with the following qualifications:

1. The River Package of McDonald and Harbaugh (1988) is inappropriate for simulating these small streams, because it does not allow streams to go dry and therefore the emphemeral nature of streamflow and aquifer recharge cannot be simulated. A small, ephemeral master stream that heads within the aquifer could be simulated with the Drain Package of McDonald and Harbaugh (1988). The Drain Package allows flow to the stream when aquifer head is above the streambed and prevents flow from the stream to the aquifer when aquifer head drops below the streambed. Alternatively, a stream could be simulated with the Stream Package (Prudic, 1989).
2. Where a drainage divide crosses a headwater aquifer, its position is highly sensitive to the effects of pumping so that the model must extend upvalley and downvalley far beyond the divide to some natural boundary or perhaps to a general (head-dependent) flux boundary.

Appraisals of several individual headwater aquifers are presented by Weaver (1987) and Randall and others (1988b). A ground-water flow model of one such aquifer indicated that 10.8 million gal/d could be withdrawn in July and August each year, and that during those two months streamflow downvalley would be reduced by only 14 percent of the amount pumped (Randall and others, 1988b). Low flows of the Paskamanset River in southeastern Massachusetts were reduced by an amount equal to average pumpage from four municipal wells along the river banks but were unaffected by comparable pumpage from three municipal wells in a small headwater aquifer within the same watershed (Bent, 1995, table 7). Uncalibrated, idealized ground-water flow models were developed by Wright Associates (1982) for four valley reaches in New York and New Jersey, one of which extends downstream from a headwater aquifer identified on plate 3 and contains an unusually small master stream relative to the size of the valley; trial simulations suggest that seasonal withdrawal of 14 million gal/d per mi^2 from this valley reach would reduce streamflow by only 9 percent of the volume pumped, whereas comparable schemes in valleys occupied by larger streams would result in far greater induced infiltration.

Hillside Aquifers

Hillside aquifers (fig. 25) are of minor importance as sources of water to wells in the Northeast but can be significant as sources of water to streams or valley-fill aquifers downgradient. Hillside aquifers consist of ice-contact materials that were deposited along valley margins, where the underlying bedrock (or till) is generally above stream grade; consequently, even though these deposits can range up to 150 ft in thickness, their saturated thickness is small unless they are predominantly fine-grained and poorly permeable, so they seldom constitute productive aquifers. Examples have been mapped or briefly described east of Berlin, N. H. (Gerath and others, 1985), in Ackworth, N. H. (Caldwell, 1986) and in Mendon, Vt. (Willey and Butterfield, 1983). Where hillside aquifers are hydraulically connected to valley-fill aquifers, they gradually release stored water as recharge to the valley fill. Where they are isolated by stream incision, they discharge through springs and are a source of base flow in streams.

Selection of hydraulic boundaries for a hillside aquifer is usually straightforward (fig. 25*C*). A zero-flow boundary can reasonably represent the ground-water divide that coincides with the drainage divide upslope from the aquifer. Zero-flow boundaries can also represent the upvalley and downvalley lateral aquifer margins, which would approximately coincide with flow lines directed downslope. Where a hillside aquifer merges with a valley-fill aquifer, its downslope margin can be represented by a specified-flux or specified head boundary; where the hillside aquifer is incised downslope and discharges as springs, specified heads to represent the springs or seepage faces are appropriate.

Outwash-Plain Aquifers

Outwash-plain aquifers typically consist of sand and gravel that, during deglaciation, were deposited as extensive

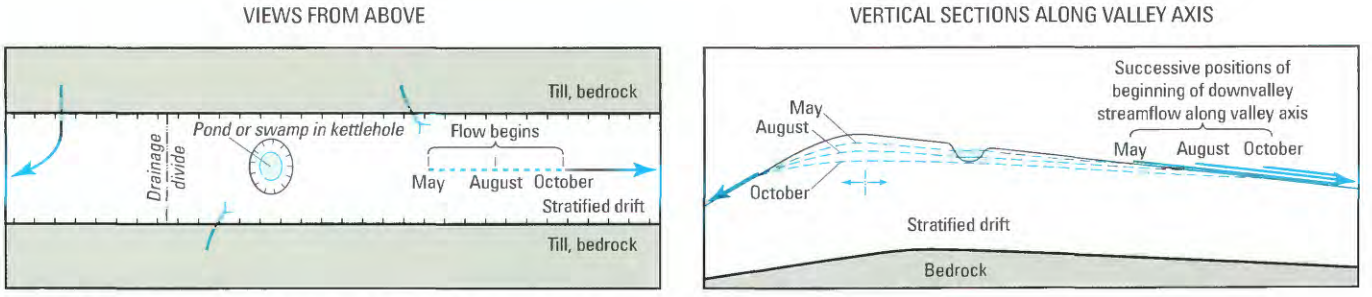

A. IN SUMMER, UNDER NATURAL (NON-PUMPING) CONDITIONS

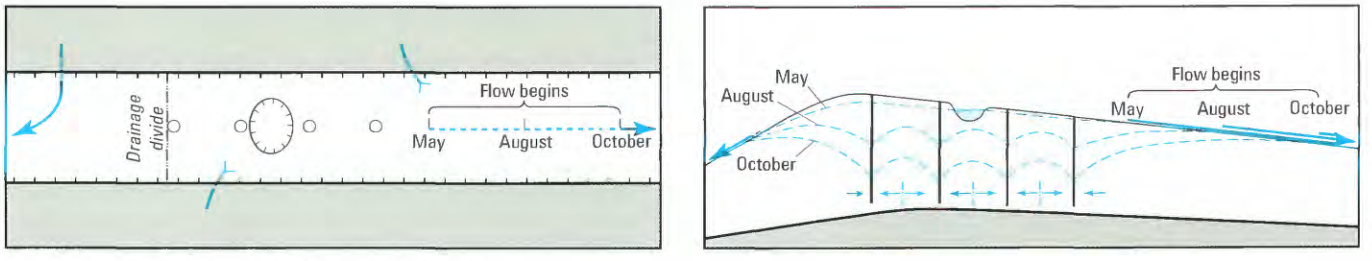

B. IN SUMMER, WITH SEASONAL PUMPING

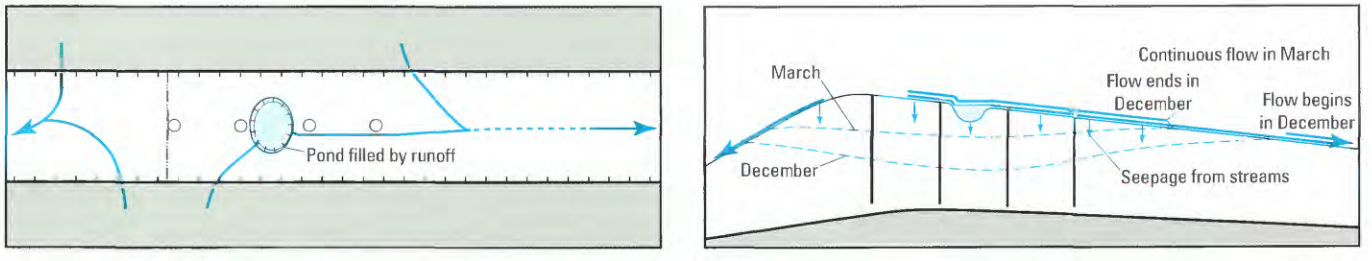

C. IN WINTER, AFTER CESSATION OF PUMPING

EXPLANATION

Views from above

- Well
- Stream—Flow continues beyond arrow. Dashed where channel is dry during part of the season
- Stream goes dry
- Valley wall

Vertical sections

- Well
- Land surface
- Stream—Flow continues beyond arrow
- Stream goes dry
- Water table
- Direction of ground-water flow

FIGURE 24.—Water-table positions, directions of ground-water flow, and surface-water features in an idealized through-valley headwater aquifer (modified from Randall and others, 1988b, fig. 3).

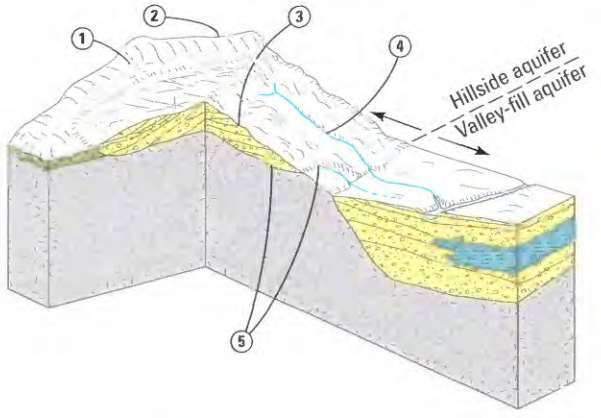

A.

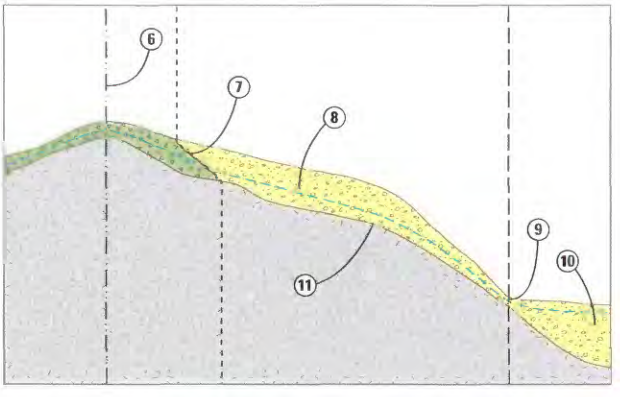

B.

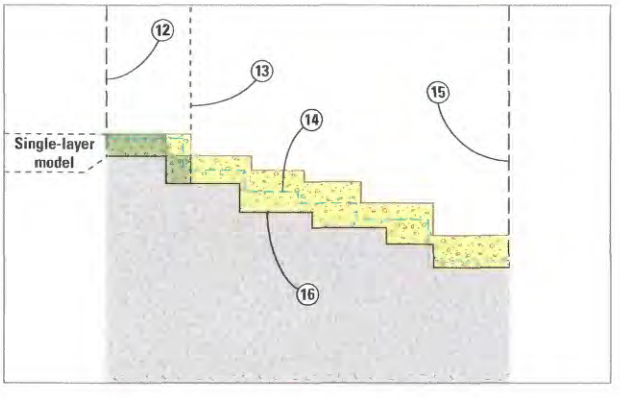

C.

(1) Small amounts of unchanneled surface or subsurface runoff from till-mantled upland further upslope may recharge hillside aquifer.

(2) Drainage divide.

(3) Most recharge is derived from precipitation directly on the aquifer.

(4) Streams draining hillside deposits are rarely sources of recharge. When water table rises above stream channel, the stream acts as a drain. When the water table falls below the stream channel, streamflow ceases.

(5) Heads generally decline with depth, so the hillside aquifer discharges to underlying bedrock; ground water also flows downslope to discharge as springs at the toe of the hillside aquifer, or as lateral flow into an adjacent valley-fill aquifer.

(6) Drainage divide: a boundary between adjacent drainage basins. Ground-water and surface-water divides usually coincide.

(7) Lateral contact of stratified drift against till or bedrock, which have markedly smaller hydraulic properties. If flow across the contact can be approximated, it is an appropriate lateral aquifer boundary.

(8) Water table.

(9) Boundary between hillside and valley-fill aquifers. Stratified-drift thickness may be small or zero here because of non-deposition or stream erosion.

(10) Valley-fill stratified drift aquifer: water from hillside aquifer flows to, and recharges, the valley-fill aquifer downgradient.

(11) Basal contact of stratified drift atop bedrock.

(12) Model boundary: simulated as zero flow.

(13) Alternative model boundary: simulated as specified flux into hillside aquifer.

(14) Water table.

(15) Model boundary: simulated as specified flux out of hillside aquifer.

(16) Model boundary: simulated as zero flow.

EXPLANATION

Lithology	Hydraulic conductivity
Very fine sand, silt, clay	Low
Gravel and sand	Medium to high
Till and (or) bedrock	Low
Bedrock	Very low

FIGURE 25.—Hillside aquifer: (*A*) Physical setting and sources of recharge; (*B*) sediment distribution and natural boundaries in a vertical section oriented in the direction of hillside slope, corresponding to (*C*) a possible model configuration.

deltas or fluvial outwash (fig. 26). They occur in areas of low relief and are typically thick enough (50 to 150 ft) that they bury all or most preglacial topographic features. A decrease in grain size with depth is fairly common, but thin sandy outwash that overlies silt and clay would be classified as a sand-plain aquifer, described in the next section. Outwash-plain aquifers receive most of their recharge by direct infiltration of precipitation, but also can receive small amounts of recharge as runoff from scattered hills of till or bedrock that protrude through the outwash deposits or lie along the margins. Streams are generally small and widely spaced; induced infiltration is possible locally, but because most streams originate within the outwash plain, the process of induced infiltration is essentially a transfer of water from one part of the aquifer to another, not an augmentation of supply. Recharge from bedrock is probably negligible because the hydraulic conductivity of the bedrock is low, and relief is also low. The outwash-plain aquifer in the Plymouth-Carver area of southeastern Massachusetts is described by Hansen and Lapham (1992), and the outwash-plain aquifer in Cape Cod, Mass. is described by Guswa and LeBlanc (1985). Outwash-plain aquifers that are more than 1 mi^2 in extent are identified on plate 3, except for the large outwash-plain aquifers on Long Island, N. Y. and Cape Cod which are outside the study area.

Watershed boundaries within outwash plains are ground-water divides, which seldom coincide with topographic divides (fig. 26*B*) and can shift in response to pumping. That is, large ground-water withdrawals from a well near a boundary can cause the boundary to migrate outward, resulting in a temporary increase in the size of the watershed being tapped and a decrease in the size of the adjacent watershed. The base of most outwash-plain aquifers is the contact between the outwash and the underlying bedrock.

Zero-flow boundaries can be placed at ground-water divides when an outwash-plain aquifer is being modeled under natural conditions (fig. 26*C*). If pumping stresses that have the potential to reach those boundaries are modeled, however, model boundaries must be placed beyond the natural ground-water divides. A general head boundary placed beyond a natural divide could simulate natural flow from the divide to the model boundary, and the reversal of flow if heads decline near the divide. The margins of outwash-plain aquifers that are in contact with permanent bodies of water, such as a large stream or the ocean, can be represented by specified-head or specified-flux boundaries. Streams that originate within the outwash plain are small and likely to dry up if the water table falls below stream stage naturally or as a result of pumping. The Stream Package (Prudic, 1989) of MODFLOW is designed to simulate this behavior and is an appropriate method of modeling outwash-plain streams.

Sand-Plain Aquifers

Sand-plain aquifers typically consist of medium to fine sand or silty sand that overlies extensive clay and silt deposited in former glacial lakes (fig. 27). The surficial sand is typically 20 to 50 ft thick and is recharged chiefly by direct infiltration of precipitation, but may also receive as recharge some upland runoff from adjacent hills or ridges. Many of the streams that cross sand-plain aquifers are incised through the aquifers into the underlying silt and clay. These streams function primarily as drains and have little or no potential as sources of recharge. Where the contact of surficial sand over silt or clay is abrupt, water discharges from the sand as a series of springs or seeps along the stream channel. Where the contact is gradational, the surficial sand aquifer may be dewatered near streams as water seeps downward and laterally through the underlying finer sediment to the incised channels.

Lateral boundaries of ground-water flow models are commonly placed at the physical limits of the sand-plain aquifer (fig. 27*C*). That is, specified-head boundaries can represent the margins of the sand plain along scarps or ravines cut by postglacial streams, and specified-flux boundaries can represent the margins along bedrock hills that locally border the sand plain; alternatively, zero-flow boundaries can be placed along the crests of those hills. In models that incorporate only part of a sand plain, zero-flow or general-head boundaries can be placed along ground-water divides between minor watersheds, which need not coincide with topographic divides. Such boundaries may migrate as a function of stresses imposed by pumping from wells or by climatic cycles, in which case general-head boundaries are the appropriate choice. A zero-flow bottom boundary can be placed where surficial sand directly overlies silt and clay, whereas simulation of an additional, basal model layer(s) of smaller hydraulic conductivity would be appropriate where the base of the aquifer is gradational. Problems involving movement of contaminants may require incorporation of the underlying fine-grained section in the model. Streams that flow within the sand plain can be simulated with the Stream Package (Prudic, 1989). Streams that cannot lose water to the aquifer because they are incised nearly to the base of the sand or into the underlying silt and clay could be simulated as drains; alternatively, the spring discharge could be modeled with specified heads, set equal to the average elevation of the springs or any seepage faces that may be present (fig. 27*C*), or set equal to stream-surface elevation where the stream is above the base of the lowest model layer and equal in width to the cells in the finite-difference grid.

Buried Aquifers

Buried aquifers are deposits of saturated sand and gravel that are covered by lacustrine silt and clay (figs. 28, 29). Some are completely covered or isolated, such that they can receive recharge only as flow from or through the bedrock,

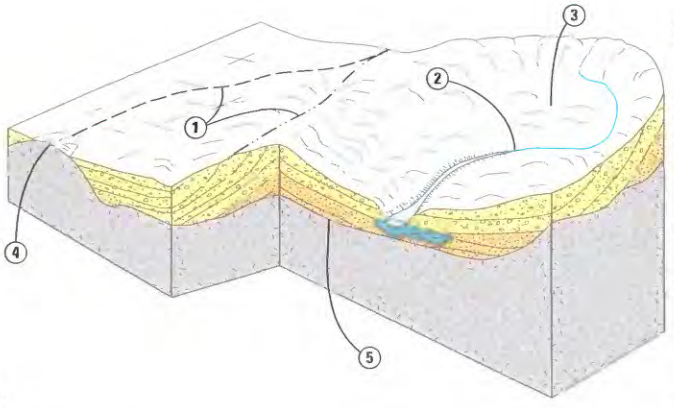

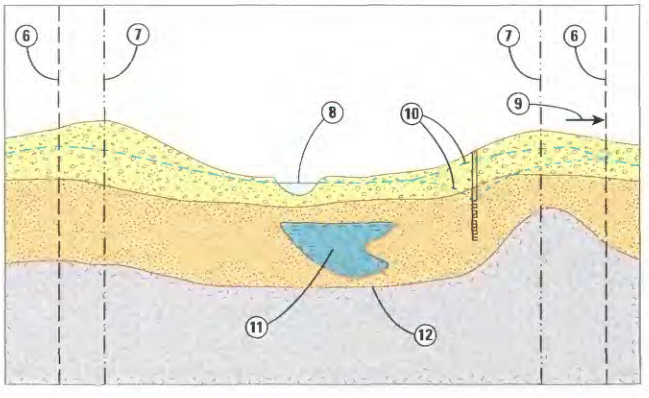

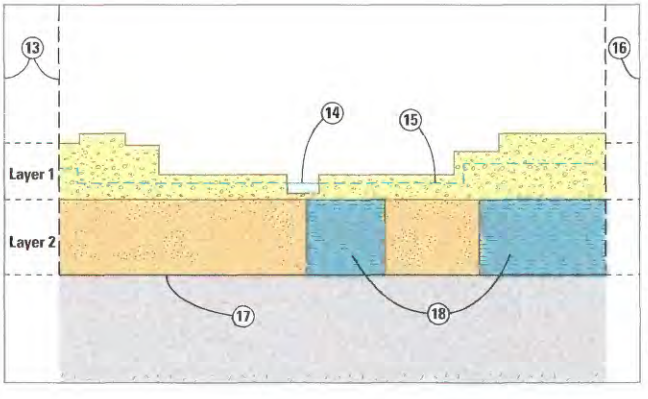

① Surface drainage divides(— · —) rarely coincide with ground-water divides (— — —), which are affected by variation in hydraulic conductivity, bedrock topography, and stream spacing.

② Streams draining an outwash plain are sustained entirely by ground-water discharge. Streamflow in upper reaches ceases seasonally when water table falls below stream channel.

③ All natural recharge is from precipitation.

④ A few bedrock hills are not entirely buried by outwash.

⑤ Small amounts of water may interchange between the aquifer and bedrock.

⑥ Ground-water divide.

⑦ Topographic drainage divide.

⑧ Outwash-plain stream: intermittent in upper reaches, perennial in lower reaches. Acts as a discharge zone when water table is above stream channel.

⑨ Large withdrawals of ground water, especially near ground-water divide, may cause divide to shift outward.

⑩ Water table, lowered by pumping.

⑪ Lenses of fine-grained material can significantly impede ground-water flow.

⑫ Contact between stratified drift and bedrock. For most purposes, flows across this contact can be treated as zero.

⑬ Model boundary: may be simulated as zero flow at ground-water divide (right) or as a general-head boundary beyond ground-water divide (left).

⑭ Stream: simulated by a leaky confining bed or as a drain.

⑮ Water table.

⑯ Model boundary: may be simulated as a general-head boundary beyond the effects of pumping.

⑰ Model boundary: simulated as zero flow.

⑱ Low transmissivity to account for fine-grained material in section and for thin aquifer above bedrock knoll.

EXPLANATION

Lithology	Hydraulic conductivity
Very fine sand, silt, clay	Low
Sand	Medium
Gravel and sand	Medium to high
Bedrock	Very low

FIGURE 26.—Outwash-plain aquifer: (*A*) Physical setting; (*B*) sediment distribution and aquifer boundaries in a vertical section corresponding to (*C*) a possible model configuration.

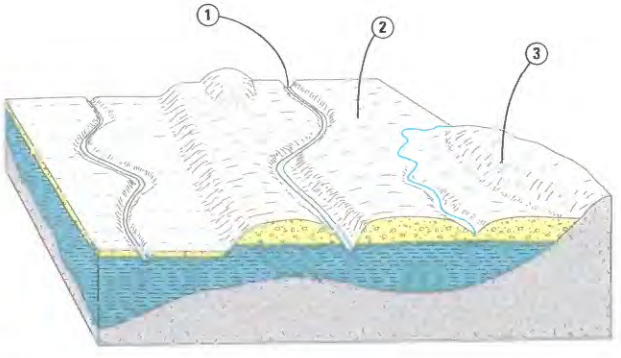

A.

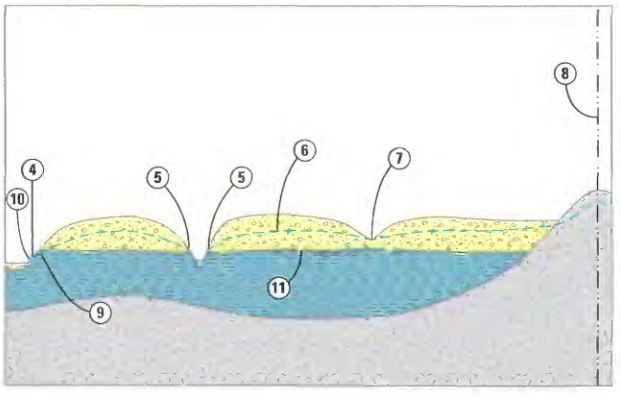

B.

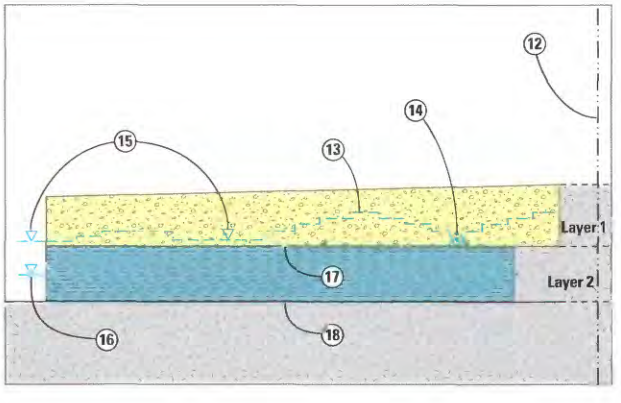

C.

① Most streams draining sand-plain aquifers are incised into the underlying fines.

② Precipitation on the aquifer is the principal source of recharge.

③ Runoff from hills is a minor source of recharge.

④ Scarp: aquifer removed by postglacial erosion.

⑤ Ground-water discharge by springs or seeps along stream incised through aquifer.

⑥ Water table.

⑦ Ground-water discharge by seepage to small stream incised nearly to base of aquifer.

⑧ Ground-water divide locally coincides with topographic drainage divide on bedrock hill.

⑨ Where aquifer is underlain by silt and very fine sand, it can be dewatered by downward flow near scarps or incised streams.

⑩ Seepage face.

⑪ Base of sand-plain aquifer is effective base of flow system where aquifer is underlain by silt and clay.

⑫ Ground-water divide may be treated as a zero-flow boundary.

⑬ Water table.

⑭ Stream simulated as a drain.

⑮ Specified heads equal to average altitude of seepage face where aquifer is cut out by erosion.

⑯ Specified head if layer 2 is simulated and silt is partly dewatered.

⑰ Zero-flow boundary if only layer 1 is simulated.

⑱ Zero-flow boundary if layer 2 is simulated.

EXPLANATION

Lithology	Hydraulic conductivity
Very fine sand, silt, clay	Low
Gravel and sand	Medium to high
Bedrock	Very low

FIGURE 27.—Sand-plain aquifer: (*A*) Physical setting and sources of recharge; (*B*) sediment distribution and aquifer boundaries in a vertical section corresponding to (*C*) a possible model configuration.

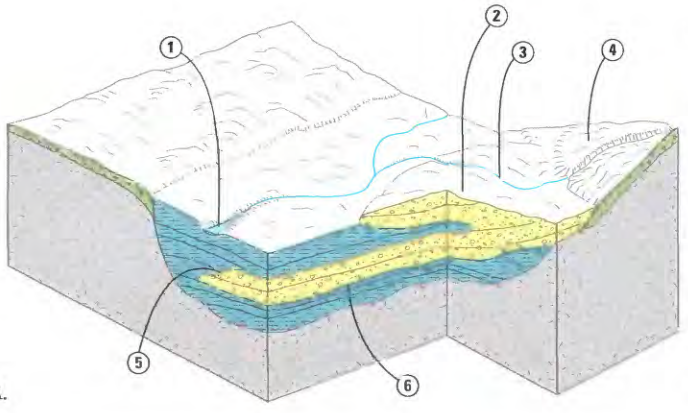

A.

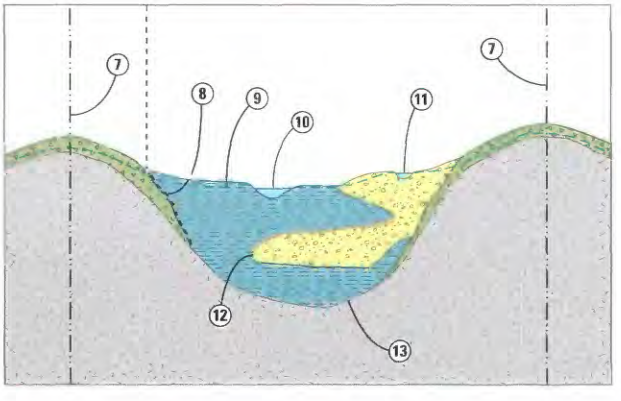

B.

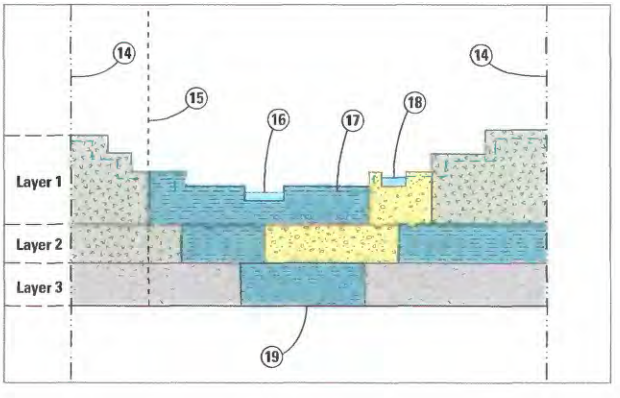

C.

(1) Little or no water recharges the buried aquifer from streams flowing across the fine-grained deposits in the main valley.

(2) Precipitation on deltaic deposits (but not on the valley floor) recharges the buried aquifer.

(3) Tributary streams flowing across deltaic deposits are potentially the largest source of water for the buried aquifer. Seepage losses from these streams increase when water levels in the deltaic deposits decline in response to pumping from the buried aquifer.

(4) Some subsurface flow and unchanneled runoff from upland areas recharge deltaic deposits that then recharge the buried aquifer.

(5) Some water may recharge the buried aquifer as subsurface flow from adjacent fine-grained stratified drift.

(6) Some water may recharge the buried aquifer as subsurface flow from underlying silt or bedrock.

(7) Drainage divide: a boundary between adjacent drainage basins. Ground-water and surface water divides in uplands are coincident.

(8) Lateral contact between fine-grained stratified drift and till or bedrock. Flow across this contact is quite small.

(9) Water table.

(10) Perennial main stream has little or no potential as a direct source of recharge to the buried aquifer.

(11) Tributary stream flowing across deltaic deposits, potentially a major source of recharge to the buried aquifer.

(12) The adjacent fine-grained stratified drift can provide some recharge when the aquifer is pumped.

(13) Contact between fine-grained stratified drift and bedrock. For most purposes, the flow across this boundary can be treated as zero.

(14) Model boundary: simulated as zero flow.

(15) Alternative model boundary: simulated as zero flow or small specified flux.

(16) Main stream channel not simulated.

(17) Water table.

(18) Tributary stream in delta area: simulated as leaky confining unit.

(19) Model boundary: simulated as zero flow.

EXPLANATION

Lithology	Hydraulic conductivity
Very fine sand, silt, clay	Low
Gravel and sand	Medium to high
Till	Low
Till and (or) bedrock	Low
Bedrock	Very low

FIGURE 28.—Buried (delta-fed) aquifer: (*A*) Physical setting and sources of recharge; (*B*) sediment distribution and boundaries in a vertical section corresponding to (*C*) a possible model configuration.

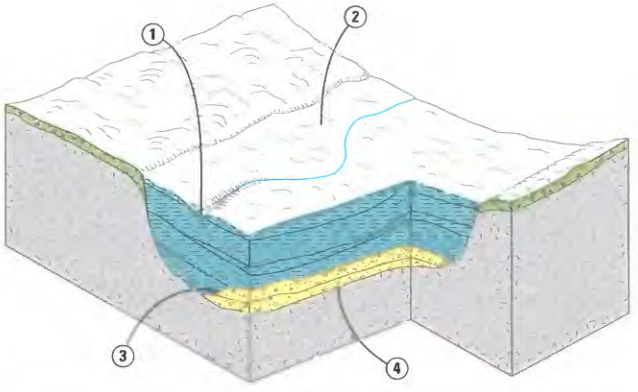

A.

① No water recharges the buried aquifer directly from streams flowing across the fine-grained deposits in the valley.

② No water recharges the buried aquifer directly from precipitation.

③ Most recharge to the buried aquifer occurs as subsurface flow from adjacent fine-grained stratified drift.

④ Some water recharges the buried aquifer as subsurface flow from underlying bedrock.

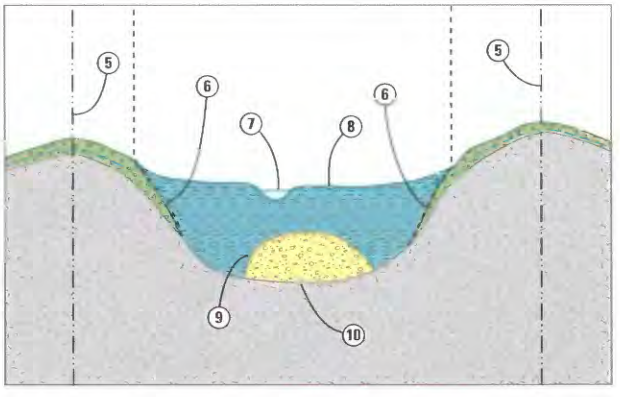

B.

⑤ Drainage divide: a boundary between adjacent drainage basins.

⑥ Lateral contact between fine-grained stratified drift and till or bedrock. Flow across this contact is quite small.

⑦ Main stream has little or no potential as a direct source of recharge to the buried aquifer.

⑥ Water table.

⑨ The adjacent fine-grained stratified drift can provide some recharge when the aquifer is pumped.

⑩ Contact between buried stratified-drift aquifer and bedrock. For most purposes, flow across this boundary can be treated as zero.

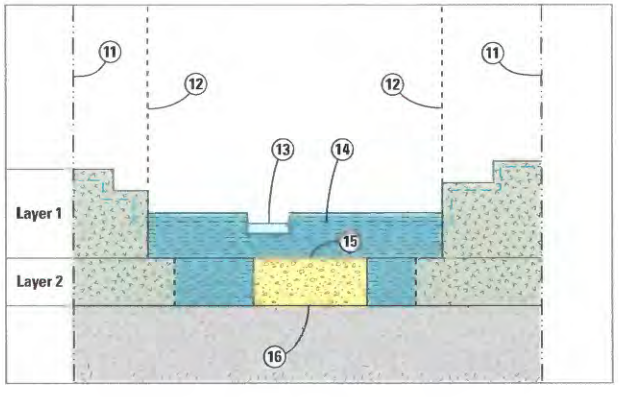

C.

⑪ Model boundary: simulated as zero flow.

⑫ Alternative model boundary: simulated as specified flux in second layer.

⑬ Stream: not simulated.

⑭ Water table: simulated as specified head.

⑮ Recharge to buried aquifer simulated by vertical leakance.

⑯ Model boundary: simulated as zero flow.

EXPLANATION

Lithology	Hydraulic conductivity
Very fine sand, silt, clay	Low
Gravel and sand	Medium to high
Till	Low
Till and (or) bedrock	Low
Bedrock	Very low

FIGURE 29.—Buried (isolated) aquifer: (*A*) Physical setting and sources of recharge; (*B*) sediment distribution and boundaries in a vertical section corresponding to (*C*) a possible model configuration.

till, and fine-grained stratified drift that surround them (fig. 29). Others are covered by fine-grained sediment that is locally interrupted by deltas or subaquatic fans of gravel and sand deposited by upland tributaries where they entered the valley that contains the buried aquifer; these "windows" of permeable sediment can readily transmit recharge from precipitation and tributaries to the buried aquifer (fig. 28). Establishing the extent and degree of isolation of buried aquifers requires considerable subsurface data such as borehole logs, geophysical and geochemical information, and records of the response of water levels to stress. For example, Crain (1966) used geologic logs and water-level records to show that a heavily pumped buried aquifer near Jamestown, N. Y. was not isolated but was in fact hydraulically connected to and recharged from several tributary deltas. Delta-fed buried aquifers in the Little Tonawanda Creek valley in western New York and in the Connecticut River basin of Massachusetts have been appraised in some detail by Randall (1979) and Talkington and O'Brien (1991). Buried aquifers were identified and mapped in many localities within the Appalachian Plateau and Ontario lowland of New York during reconnaissance studies (MacNish and Randall, 1982; Crain, 1974; Kantrowitz, 1970) that, generally, did not establish whether the buried aquifers were isolated or delta-fed. The distribution of sediments within a valley fill can be sufficiently complex that a buried aquifer in one locality is merely a downwarped segment of an aquifer that is surficial in an adjacent locality, in which case the entire mass of sediments is probably best analyzed as a valley-fill aquifer.

The hydraulic boundaries of buried aquifers (figs. 28*B*, 29*B*) are virtually the same as those of valley-fill aquifers, except for the upper surface; consequently, any differences with regard to modeling pertain to how the surficial materials are simulated. Figure 28*C* depicts a delta-fed buried aquifer whose upper model boundary is placed at the water table; fine-grained sediments above the buried aquifer are explicitly represented as a separate model layer (or layers), and the simulation is the same as that of a valley-fill aquifer. The Killbuck Creek buried aquifer (discussed further on) is modeled in this manner. If the upper model boundary were placed at the base of the fine-grained material that overlies the buried aquifer, however, vertical flow at the top of the aquifer must be simulated by applying appropriate boundary conditions. A boundary condition suitable for steady-state simulations is to specify an upper model layer in which any cell that represents fine-grained sediment is assigned a specified head equal to the local water-table altitude (fig. 29*C*). Any cell containing surficial coarse deltaic deposits associated with a stream may be treated as active. The buried aquifer can be simulated as a layer that converts from confined to unconfined conditions if the hydraulic head falls below the base of the confining unit. Another, and perhaps simpler, approach is to simulate the buried aquifer as a single layer (layer 2 of fig. 28*C* or 29*C*) and apply specified fluxes along the top of that layer to simulate recharge from overlying sediments.

VARIABLE-RECHARGE PROCEDURE

Four of the aquifer types discussed above (valley-fill, headwater, hillside, and buried aquifers), have adjoining uplands that can provide considerable recharge to the aquifers as (1) unchanneled ground-water inflow and surface runoff, and (2) channeled runoff (in tributaries that recharge the stratified drift through seepage). A procedure for simulating recharge and the contribution of the uplands to stratified drift, termed the Variable-Recharge (V-R) procedure (Kontis, 2001), was developed in this study and applied (Kontis, 1999; Breen and others, 1995) to the two models described further on. The procedure is designed primarily for valley-fill aquifers bordered by uplands that transmit water to the valley fill at rates that can differ widely depending on (1) upland topography, (2) the composition of upland and valley-fill materials, and (3) the relation of hydraulic head in those materials to land surface. Applications in which the V-R procedure can be useful include (1) simulations in which the extent and distribution of areas with head at or above land surface may vary significantly as a function of seasonal or annual variations in precipitation and evapotranspiration, (2) simulations of the advective migration of contaminants originating in uplands, (3) simulations of recharge to wetlands and(or) aquifer response to pumping near wetlands and ephemeral streams, and (4) simulations of valley-fill aquifers bordered by uplands composed of poorly permeable bedrock or till.

CONCEPTUALIZATION

Simulation of recharge in MODFLOW with the Recharge Package (McDonald and Harbaugh, 1988, p. 7-1) entails specifying the *areal distribution of recharge* and applying it to specified active model cells, irrespective of the model head distribution, whereas simulation of recharge with the V-R procedure entails specifying the *amount of water available for recharge* (*WAFR*, defined further on in eq. 11) and applying it to specified active model cells. Whether this water becomes recharge depends, in part, on the model-head distribution. The basic premise of the procedure is that where the hydraulic head is at or above land surface, precipitation cannot be accepted as recharge, and discharge (outward seepage) from the aquifer may occur. Thus, the method is conceptually similar to (1) the "variable-source area" overland-flow concept of Dunne and Black (1970), which postulates that overland flow occurs when soils are saturated by a rising water table, and (2) the ground-water model code of Potter and Gburek (1987), wherein outward seepage is calculated once the water level reaches land surface. Where recharge is rejected or outward seepage occurs in upland areas, the rejected recharge and outward seepage become surface runoff

that may eventually become recharge to a valley-fill aquifer at the base of the upland hillsides, either as channeled flow in tributaries that cross the valley fill, or as unchanneled runoff that infiltrates when it reaches the valley fill. The land surface areas within which recharge, rejected recharge and outward seepage occur may vary spatially as a function of temporal variations in *WAFR*.

INPUT INFORMATION

The V-R procedure was designed for use with MODFLOW (McDonald and Harbaugh, 1988) and requires the following information when the uplands are explicitly simulated and upland surface runoff (channeled and unchanneled) is distributed to specified parts of the modeled area. If the uplands are not explicitly simulated or upland surface runoff is not distributed to other parts of the model, only items 1 and 6 are required.

1. Average land-surface elevation of each active model cell that receives *WAFR*.
2. Division of the entire model area into a V-R zone array. These zones differentiate (a) upland topographic subbasins for which surface runoff is calculated and redistributed to other parts of the model and (b) topographically low areas in which surface runoff is not redistributed. The topographically low areas will usually include the main valley-fill aquifer being evaluated but may also include some upland valleys in which surface runoff enters streams whose flow does not cross the aquifer being evaluated. These lowland areas, if specified in items 4 and 5, may receive water from the uplands. Each upland subbasin is assigned a unique non-zero zone number whereas all topographically low areas are collectively designated zone zero.
3. The proportion of upland runoff (rejected recharge plus outward seepage) that reaches the valley floor as channeled flow in each upland subbasin. This quantity can be estimated from the topographic configuration of the subbasin as the percentage of the subbasin area that slopes toward channels whose valley-floor reaches are explicitly simulated, as described in item 4.
4. The location of each model cell that contains a channel in which upland runoff simulated by the V-R procedure reaches the valley floor, if interaction of that channeled runoff with an aquifer is to be simulated. For each of these cells, the streambed conductance, stream stage, and elevation of the top and bottom of the streambed in the cell is specified.
5. The location of each model cell along the valley wall that receives upland runoff in areas where the upland runoff reaches the valley floor as unchanneled runoff.
6. The estimated quantity of water available for recharge (*WAFR*) for each time period simulated. This quantity can be computed from the equation:

$$WAFR = P - ET + SN_m - SN_s \pm SM \quad (L), \qquad (11)$$

where terms on the right hand side are as defined in equation 4 and all terms represent depths of accumulation. If evapotranspiration of soil moisture (*ET*) exceeds precipitation (*P*), *WAFR* is zero, and soil moisture (*SM*) is depleted. If precipitation exceeds evapotranspiration, then soil moisture addition occurs. This addition cannot become *WAFR* until any soil-moisture deficits accumulated over time have been replenished. The value of *WAFR* can be calculated by equation 11 for the entire modeled area and then modified for all cells within any subbasin by specifying a multiplicative factor for the subbasin. A method by which equation 11 can be applied to aquifers in the glaciated northeastern United States is given in Lyford and Cohen (1988).

Input to the model consists of *WAFR* expressed as a flow rate. The flow rate, *Rwa*, for any finite-difference cell with location indices (fig. 30) *i*, *j*, *k* is

$$Rwa_{i,j,k} = \left(\frac{WAFR}{t}\Delta r\Delta c\right)_{i,j,k} \quad (L^3/T), \qquad (12)$$

where Δr and Δc are the cell dimensions in the row and column directions respectively, $\Delta r\Delta c$ is the area of the cell *i*, *j*, *k*, and *t* is the length of the time period for which *WAFR* is computed. In the MODFLOW indexing system for finite-difference cells, if *I*, *J*, *K* are the total number of model rows, columns, and layers, respectively, then $i = 1,2,\ldots I$; $j = 1,2,\ldots J$ and $k = 1,2,\ldots K$. In the V-R procedure, the layer index (*k*) is the model layer to which *Rwa* is applied.

FORMULATION

The V-R procedure is implemented in MODFLOW each time the finite-difference equation is formulated (that is, at each iteration). At each iteration, the simulated hydraulic head in each cell receiving *WAFR* is compared with land-surface elevation. The *WAFR* value is partitioned into recharge, rejected recharge, or both, depending on the elevation of the simulated hydraulic head (H_a) relative to land surface (H_s) or to a pseudo-land surface H'_s defined to be $H_s - df$, where *df* (a depth factor) is a specified distance below land surface (fig. 30). The pseudo-land surface and depth factor, as explained below, are computational devices used to minimize numerical instabilities. Three alternative recharge conditions (eqs. 13a, 13b, and 13c) are simulated by the V-R procedure, as illustrated in figure 30. For each condition, the amounts of recharge (*R*), rejected recharge (*REJ*), outward seepage (*OS*), and surface runoff (*SR*) at each finite-difference cell *i*, *j*, *k* receiving *WAFR* is described in equations 13a, 13b, and 13c. In these equations, the cell location *i*, *j*, *k* is implicit.

Condition 1 (full recharge, no rejected recharge, no surface runoff, no outward seepage):

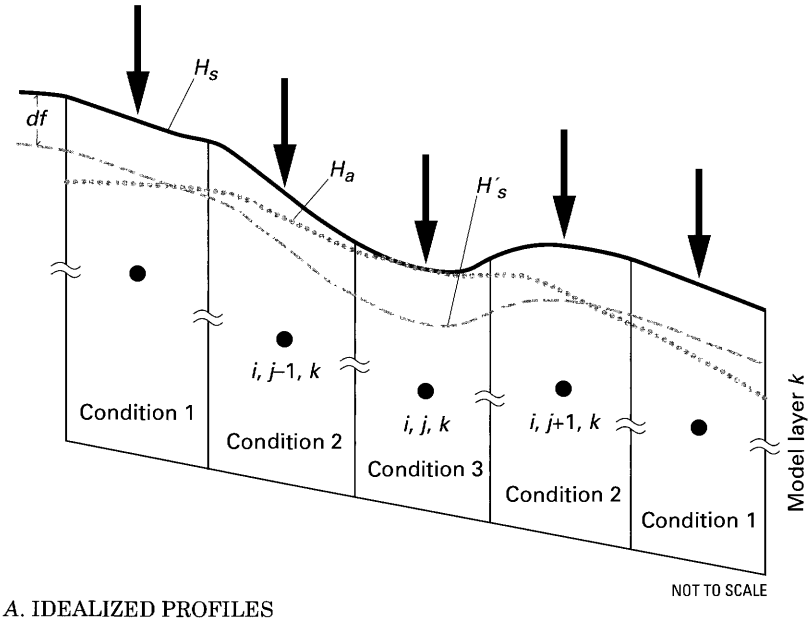

A. IDEALIZED PROFILES

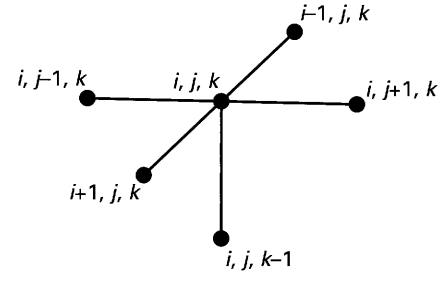

B. FINITE-DIFFERENCE COMPUTATION STENCIL

EXPLANATION

Rate of water available for recharge (*Rwa*) applied to each uppermost model cell

Land surface (H_s)

df **Depth of pseudo land surface below land surface, usually 1 foot or less**

Pseudo land surface (H'_s, equals $H_s - df$)

Water level (H_a)

● **Center of cell**

i, j, k **Indices of finite-difference model node located at i^{th} row, j^{th} colmn, k^{th} layer**

Condition

1	$H_a \leq H'_s$	(Full recharge)
2	$H'_s < H_a < H_s$	(Partial recharge)
3	$H_a \geq H_s$	(No recharge)

FIGURE 30.—Idealized profiles of land surface, psuedo land surface, and potentiometric surface along ground-water flow model finite-difference row *i* showing three recharge conditions defined in the Variable-Recharge procedure. Also shown is the finite-difference computation stencil used to compute flow between node *i, j, k*, and 5 adjacent nodes for Variable-Recharge condition 3 of equation 13 (modified from Kontis, 2001, fig. 4).

$$\left.\begin{aligned} R &= Rwa \\ REJ &= 0 \\ SR &= 0 \\ OS &= 0 \end{aligned}\right\} \text{if } H_a \le H'_s \quad (L^3/T). \tag{13a}$$

Condition 2 (partial recharge, partial rejected recharge, surface runoff, no seepage):

$$\left.\begin{aligned} R &= Rwa\frac{H_s - H_a}{df} \\ SR &= REJ = Rwa - R \\ OS &= 0 \end{aligned}\right\} \text{if } H'_s < H_a < H_s, \text{ and } df > 0. \tag{13b}$$

Condition 3 (no recharge, full rejected recharge and surface runoff, possible outward seepage):

$$\left.\begin{aligned} R &= 0 \\ REJ &= Rwa \\ SR &= REJ + OS = Rwa + OS \end{aligned}\right\} \text{if } H_a \ge H_s. \tag{13c}$$

The V-R procedure occasionally gives rise, during the iteration process, to numerical instabilities that prevent convergence to a suitable solution for head; therefore, the pseudo-land surface (H'_s) and depth factor (df) are introduced to minimize such instability. These terms have no physical meaning, but the manner in which the depth factor affects recharge is related to a physical process in some hydrologic settings. For example, if the actual land surface represented by a model cell contains microtopography with relief similar to the depth factor, a water-level rise to the elevation of the low places will prevent further recharge in these places and will result in rejected recharge, outward seepage and formation of surface rills. Recharge can still occur in the areas between the low places but will tend to be less than if the microtopography were absent, and the total amount will decrease as the water table continues to rise. Similarly, where the water rises to or above the pseudo-land surface, as described by equation 13b, the amount of recharge is reduced. In general, the partition of *WAFR* into recharge and surface runoff will vary as a function of the depth factor. During testing of the V-R procedure, use of a nonzero depth factor of 1 ft or less in equations 13a and 13b generally minimized numerical instabilities, and variations in recharge and runoff over this range were relatively small. If the depth factor is zero, then $H_s = H'_s$, and only conditions 1 and 3 (eqs. 13a and 13b) apply.

Outward seepage, OS in equation 13c, is assumed to occur if the sum of the ground-water flows between the cell i, j, k and the five adjacent cells depicted in fig. 30 is positive. This is determined from the provisional quantity OS^* for cell i, j, k, defined as

$$OS^* = q_{i,j-1/2,k} + q_{i,j+1/2,k} + q_{i-1/2,j,k} + q_{i+1/2,j,k} + q_{i,j,k+1/2} \quad (L^3/T), \tag{13d}$$

in which the q terms represent ground-water flows between cell i, j, k and the 5 adjacent cell (eqs. 10-13 and eq. 15 of McDonald and Harbaugh, 1988). If OS^* is positive, the net ground-water flow from adjacent areas is into the cell and this net inflow is designated as outward seepage by setting $OS = OS^*$. In addition, the cell in question is set to a constant head, equal to land-surface elevation; that is, $H_a = H_S$ if $OS^* > 0$. If the net ground-water flow between the cell i, j, k, and adjacent cells is zero or away from the cell ($OS^* \le 0$) outward seepage does not occur, and the cell continues to be active and the provisional term OS^* is not used.

If a cell converts to a constant-head seepage cell it becomes a constant-head cell in all MODFLOW packages in which the cell had been active. If the effect of a particular MODFLOW package in a simulation is to induce a lowering of head in one or more cells (as may result from a discharging well), those cells will probably always be active, but if the effect of a package is to cause head in one or more cells to rise (as may result from a recharging well) and the value of equation 13d is positive, the effect of that package could change in unintended ways when head reaches land surface and the cells become constant head. If the flow between a seepage cell and adjacent cells is reversed (from positive to negative) in response to changing hydraulic conditions, the constant-head condition is removed and the cell becomes active.

The amount of surface runoff from each subbasin is calculated at each iteration, as the sum of the rejected recharge and outward seepage for all cells within that upland subbasin (Variable-Recharge zone), and is distributed to the adjacent valley floor according to the information specified in items 3, 4, and 5 above. The unchanneled runoff from each subbasin is divided equally among all valley cells designated to receive runoff from that subbasin and is applied as additional WAFR to these cells. The channeled runoff from each subbasin is divided equally among all streams draining that subbasin that are explicitly simulated in the V-R procedure, and is applied as the initial streamflow in the upstream cell of each stream, at the edge of the valley floor. The streams may gain or lose water as they flow across the valley floor, depending on the relation between stream-surface altitude and the hydraulic head in the aquifer beneath the stream.

LIMITATIONS

Some of the conceptual and programming limitations of the V-R package are as follows:

1. The V-R procedure code has no provision to transfer flow from the downstream end of a stream explicitly simulated with the V-R procedure to a receiving stream that is simulated with the Stream Package.
2. If the *ET* estimate that was used to calculate *WAFR* (eq. 1) includes ground-water evapotranspiration (gwet), and if gwet is explicitly simulated by the Evapotranspiration Package, gwet will be overestimated, and flow in the aquifer will be underestimated. One way to minimize this potential overestimation of gwet would be to include code in MODFLOW to calculate gwet at each iteration, then convert gwet to an average gwet rate over the model area, and subtract this average rate from the *WAFR* rate.
3. Channeled and unchanneled upland surface runoff calculated by the V-R procedure is instantaneously applied to the valley; that is, the travel time of surface water from areas of runoff generation to cells along the valley wall is not accounted for.

BUDGET TERMS

In the Variable-Recharge procedure, some or all of the *WAFR* to the uplands eventually becomes recharge to the valley fill. The processes by which this occurs may be described and summarized by an upland budget, each component of which is calculated in the Variable-Recharge procedure in units of volume/time. Budget terms are calculated for each upland subbasin, for the entire upland area modeled, and for the upland contributions to valley recharge.

Terms for Each Upland Subbasin

The relative amounts of recharge and surface runoff for each cell are characterized by the *WAFR* flow rate (*Rwa*), rejected recharge (*REJ*), and outward seepage (*OS*).When these terms are summed over cells within each upland subbasin, which is referred to as a Variable-Recharge zone, the zonal sums *WAFRZ*(*i*), *REJZ*(*i*) and *OSZ*(*i*), are generated for each upland zone *i*, *i* = 1, 2,... *NZ*, defined as:

$$WAFRZ(i) = \omega(i)\sum_{u} Rwa, \tag{14a}$$

$$REJZ(i) = \sum_{u} REJ \Big| H_a \geq H_s + \sum_{u} REJ \Big| H'_s < H_a < H_s, \tag{14b}$$

and

$$OSZ(i) = \sum_{u} OS. \tag{14c}$$

The factor $\omega(i)$ $(0 \leq \omega(i) \leq 1)$ in equation 14a allows the modeler to modify the calculated rate of *WAFR* of each zone, if the rate of *WAFR* is postulated to vary spatially and(or) for sensitivity analysis. The ω factor, for each zone *i*, is read in as part of the input data and applied to each of the cells in zone *i*. $\sum_{u}$ denotes summation over all cells within zone *i*, and *Rwa*, *REJ*, H_a, H_s, H'_s, and *OS* are as defined in equations 12 and 13.

Surface runoff is the sum of rejected recharge and outward seepage, direct recharge is the flow rate of *WAFR* minus rejected recharge, and net recharge is the flow rate of *WAFR* minus surface runoff. The surface runoff (*SRZ*(*i*)), direct recharge (*DRZ*(*i*)), and net recharge (*NRZ*(*i*)) for upland zone *i* are defined as:

$$SRZ(i) = REJZ(i) + OSZ(i), \tag{14d}$$

$$DRZ(i) = WAFRZ(i) - REJZ(i), \text{ and} \tag{14e}$$

$$NRZ(i) = WAFRZ(i) - SRZ(i). \tag{14f}$$

In some locations, part of the surface runoff from an upland basin may be unavailable to recharge the adjacent valley fill because it is diverted; for example, it could be intercepted by storm drains that discharge to surface water. Consequently, the amount of surface runoff that is available to recharge the valley could be less than the amount indicated by equation 14d. The available surface runoff (*ASRZ*(*i*)) to the valley from zone *i*, for some estimated proportion $\rho(i)$, $(0 \leq \rho(i) \leq 1)$ is denoted by

$$ASRZ(i) = \rho(i)SRZ(i). \tag{14g}$$

If $\varepsilon(i)$, $(0 \leq \varepsilon(i) \leq 1)$ is the estimated proportion of available surface runoff that becomes channeled runoff in zone *i*, then the channeled runoff (*ACRZ*(*i*)) and unchanneled runoff (*AURZ*(*i*)) available to recharge the valley from zone *i* are

$$ACRZ(i) = \varepsilon(i)ASRZ(i), \text{ and} \tag{14h}$$

$$AURZ(i) = (1 - \varepsilon(i))ASRZ(i). \tag{14i}$$

The proportion terms ω, ρ, and ε in equations 14a, 14g, 14h and 14i are part of the V-R procedure input (Kontis, 2001).

Terms for Entire Upland Area Modeled

The zonal values explained above when summed over all upland zones constitute the upland water budget for the entire model. Budget values calculated by the V-R procedure are defined as follows:

Total *WAFR* flow rate; $TWAFR = \sum_i WAFRZ(i)$, (14j)

Total rejected recharge; $TREJ = \sum_i REJZ(i)$, (14k)

Total outward seepage; $TOS = \sum_i OSZ(i)$, (14l)

Total surface runoff;

$$TSR = TREJ + TOS = \sum_i SRZ(i), \quad (14m)$$

Total direct recharge; $TDR = \sum_i DRZ(i)$, (14n)

Total net recharge; $TNR = TDR - TOS = \sum_i NRZ(i)$, (14o)

Total available surface runoff; $TASR = \sum_i ASRZ(i)$, (14p)

Total available channeled runoff;

$$TACR = \sum_i ACRZ(i), \text{ and} \quad (14q)$$

Total available unchanneled runoff;

$$TAUR = \sum_i AURZ(i), \quad (14r)$$

where $\sum_i$ denotes summation over all upland zones i, $i = 1, 2, \ldots NZ$.

Terms for Upland Contribution to Valley Recharge

The *WAFR* applied to the uplands eventually recharges the valley fill in three forms—subsurface groundwater flow, recharge from unchanneled runoff and recharge from channeled runoff. The budget terms that pertain to these sources are defined as follows.

Subsurface flow—that is, the total lateral ground-water flow (*TLF*) from the uplands to the valley as determined at the valley wall between upland and valley cells—is

$$TLF = TNR + \sum_U (St + Q), \quad (14s)$$

where St denotes upland flow in or out of storage,
Q represents any other additional upland sources and sinks, and
$\sum_U$ denotes summation over all upland cells.

The total lateral flow, under steady-state conditions, is equivalent to the total net recharge (*TNR*) if no upland sources or sinks are present.

The amount of available channeled and unchanneled runoff that actually recharges the valley depends on (1) the relation between aquifer head and stream-surface elevation in cells containing streams, and (2) the relation between aquifer head and land-surface elevation in cells designated to receive unchanneled runoff. The total channeled recharge (*TCR*) and total unchanneled recharge (*TUR*) are defined as,

$$TCR = \sum_i \delta(i) ACRZ(i), \quad (14t)$$

$$TUR = \sum_i \gamma(i) AURZ(i), \quad (14u)$$

where $\delta(i)$ $(0 \le \delta(i) \le 1)$ symbolizes the proportion of available channeled runoff that actually recharges the valley from zone i in the form of stream losses, and $\gamma(i)$ $(0 \le \gamma(i) \le 1)$ symbolizes the proportion of available unchanneled runoff from zone i that recharges valley cells adjacent to the uplands. The δ and γ factors are neither specified as input nor calculated in the V-R procedure, but are included in equations 14t and 14u to emphasize that only a part of the available runoff may recharge the valley. The recharge from these sources will depend on the simulated hydraulic head distribution in the aquifer relative to corresponding stream surface and land surface elevations. All streamflow that does not become recharge is discharged to the main stream of the entire modeled system, and is calculated as *TSF*, where

$$TSF = TACR - TCR. \quad (14v)$$

The total recharge to the valley from all upland sources (TR_{u-v}) is the sum of total lateral flow (eq. 14s), total channeled recharge (eq. 14t) and total unchanneled recharge (eq. 14u), that is

$$TR_{u-v} = TLF + TCR + TUR. \quad (14w)$$

The terms of equation 14a-14w and how they can be used to analyze the valley recharge components originating in the uplands are discussed in detail in the following two examples of stratified-drift aquifer simulation.

EXAMPLES OF STRATIFIED-DRIFT AQUIFER SIMULATIONS

Ground-water flow models of two valley-fill systems were constructed to (1) demonstrate application of the Variable-Recharge procedure as a method of simulating areal recharge and calculating the upland-derived components of recharge to a valley fill aquifer, (2) demonstrate the effects of simulating the uplands explicitly, (3) test model sensitivity to selected hydraulic properties, and (4) illustrate several modeling

approaches and techniques that may be useful in the simulation of systems similar to those described here. The two models represent the valley-fill aquifers beneath the Rockaway River near Dover, N.J. and the buried-valley aquifer beneath Killbuck Creek near Wooster, Ohio. These areas are typical of several varieties of valley-fill aquifers and, from a simulation point of view, contain the elements that must be addressed in the modeling of most valley-fill systems. An abridged documentation of both models is given herein; the complete documentation for the Dover model is given in Kontis (1999); that for the Wooster model is given in Breen and others (1995).

Model boundaries of both areas were selected to coincide, where feasible, with natural hydraulic boundaries; however, water-level records and detailed information regarding the hydraulic properties of the valley fill were limited primarily to regions in and around municipal well fields. Thus both models include areas, primarily in the uplands but also within the valleys, in which pertinent information such as the lateral and vertical distribution of hydraulic properties and water levels was limited.

In general, the range in the magnitude of hydraulic properties that may be specified during model calibration is relatively narrow in areas containing reliable data, even though the spatial continuity of data between points of known values may be uncertain. In areas where data are widely spaced or absent, the specified magnitude of the hydraulic properties is guided by hydrogeologic plausibility. Model calibration entails selection of hydraulic values such that their combined effect produces simulated heads and flow patterns that conform to observed head and flow patterns. A reasonable statistical match can usually be obtained, however, from many combinations of hydraulic properties. Additional data are generally needed to decrease the number of feasible combinations. In some settings, glacial and glaciofluvial hydrogeologic facies models (Anderson, 1989) can be incorporated to aid in the interpretation of large-scale spatial trends and, in turn, the assignment of hydraulic properties.

For the Dover area, six transient-state models were developed to show the response of head and flow patterns to (1) imprecisely known hydraulic properties in certain areas, and (2) several alternative hypotheses of materials distribution.

The Wooster model was used to analyze the sources of water that recharge the stratified drift and to investigate model sensitivity to variations in upland horizontal and vertical hydraulic conductivity, tributary streambed leakance, and the presence of a poorly permeable layer beneath the valley fill.

VALLEY-FILL AQUIFER BENEATH THE ROCKAWAY RIVER NEAR DOVER, NEW JERSEY

The valley-fill aquifer that underlies the Rockaway River near Dover in northeast Morris County, N.J. supplies water for a population of about 20,000 and lies along the terminal moraine that marks the southern extent of Wisconsin-age glaciation (fig. 1). The hydrogeology of the area is described in Gill and Vecchioli (1965), Canace and others (1983, 1993), Stanford (1989) and Dysart and Rheaume (1999). Hill and Pinder (1981) developed a ground-water flow model of a part of the Rockaway River valley upstream from Dover. Gordon (1993) constructed a ground-water flow model with a uniform grid spacing of 500 ft that represents valley-fill aquifers in the upper Rockaway River basin and includes the valley reach described herein.

HYDROLOGIC SETTING

In general, northeast Morris County is characterized by northeast-trending metamorphic and igneous bedrock and narrow valleys containing morainal and stratified-drift deposits. The ridges have a maximum altitude of about 1,000 ft and are generally 200 to 300 ft above the valley floor. The unconsolidated sediments that mantle the bedrock range in thickness from less than 20 ft to 150 ft.

Proglacial lakes (glacial lakes Dover and Wharton) formed in the Rockaway River valley as advancing late Wisconsinan ice blocked the valley at or near Dover, as described by Stanford (1989). Fine-grained lake-bottom sediments and sandy deltas were deposited in these lakes and capped by morainal deposits. After the ice retreated, meltwater cut through the moraine along the present course of the Rockaway River and deposited coarse-grained outwash. According to this interpretation, deltaic sand and(or) lake-bottom fines may underlie the morainal deposits depending on location. The surficial geology of the area near Dover, N.J. is shown in figure 31. The bedrock-surface altitude, approximated from seismic-refraction data and a few deep wells, is depicted in figure 32 and indicates that a trough in the bedrock lies about 1,000-2,000 ft east or northeast of the present valley axis.

The stratified drift near the Dover municipal production wells is about 100 ft thick (fig. 33). The upper 20 to 30 ft consists of poorly sorted outwash gravel and is underlain by 40 to 50 feet of sand and gravel; the lower 35 ft consists of lake-bottom sediments of silt, fine sand, and some clay. The average combined pumping rates from the three production wells was about 2.1 ft^3/s in 1975 and about 4.9 ft^3/s in 1984. Pumping of this magnitude is sufficient to induce infiltration from the nearby Rockaway River, as documented by Dysart and Rheaume (1999), who calculated by various methods estimates of streambed leakance (K/m, eqs. 6 and 7), ranging from 0.21 to 0.68 (ft/d)/ft (table 10) that were used by Kontis (1999) to constrain the Dover ground-water flow models.

MODELING STRATEGY

A finite-difference ground-water flow model was constructed to represent a 2.5-mile reach of the Rockaway River valley and adjacent uplands. As previously discussed, data on

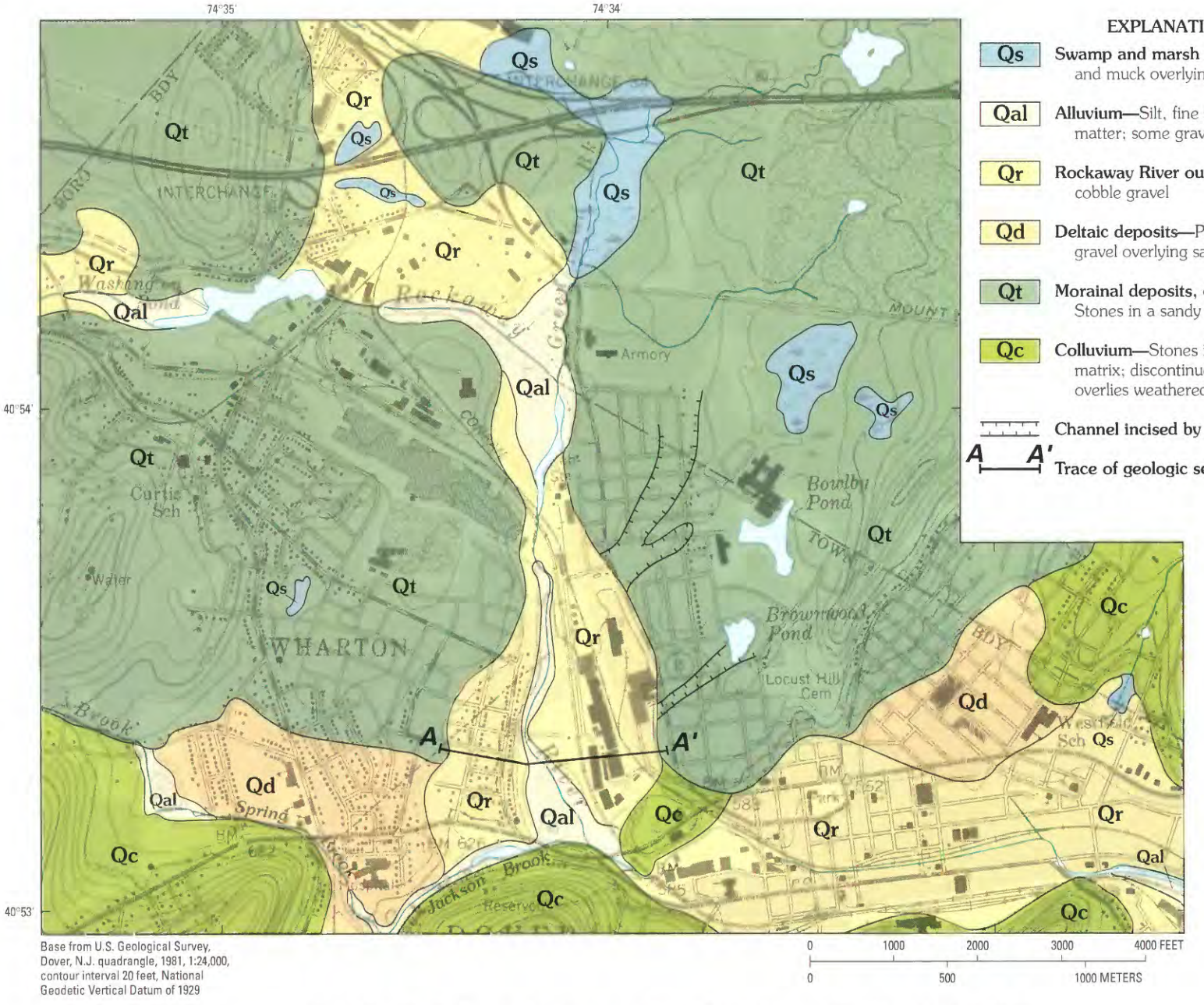

FIGURE 31.—Surficial geology and topography near Dover, N.J. (modified from Stanford, 1989).

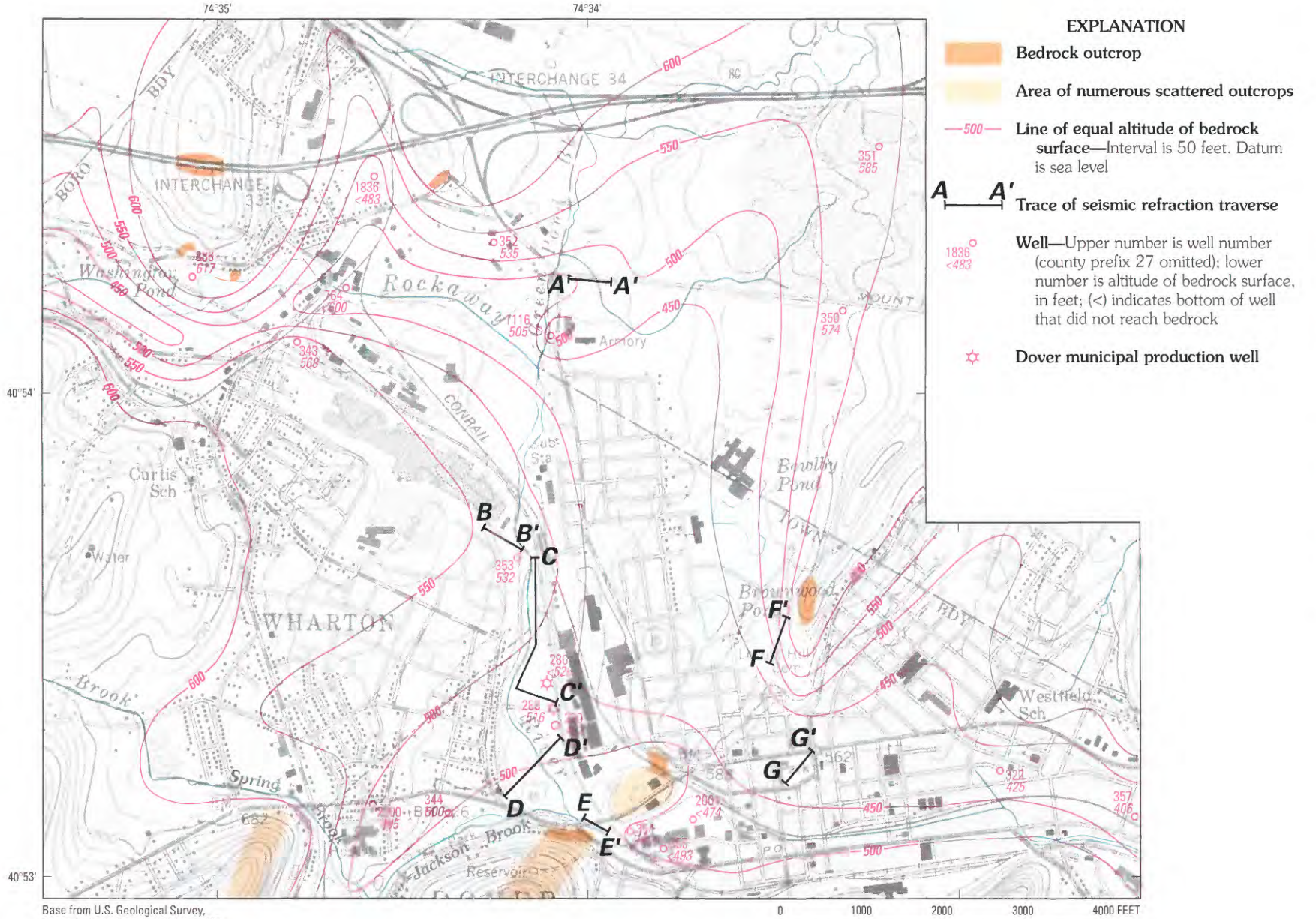

FIGURE 32.—Generalized configuration of the bedrock surface near Dover, N.J. (From Dysart and Rheaume, 1999, fig. 5. Logs of wells given in tables 20 and 21 of Dysart and Rheaume, 1999. Results of geophysical surveys furnished by P. Lacombe, U.S. Geological Survey, written commun., 1985. Outcrops and interpretation of bedrock surface in part after Stanford, 1989).

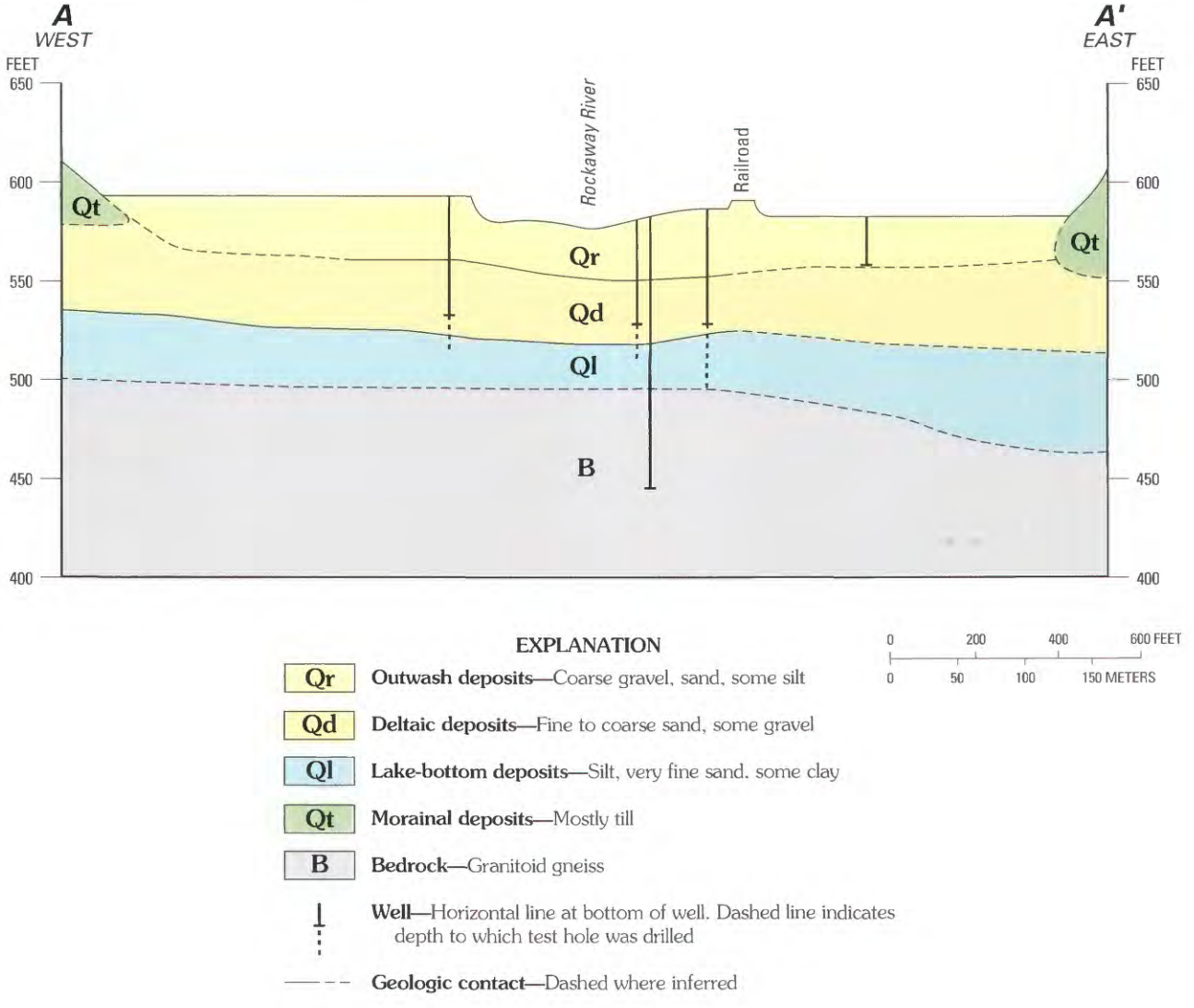

FIGURE 33.—Generalized geologic section across the Rockaway River through Dover well field. Line of section is shown in figure 31 (from Dysart and Rheaume, 1999, fig. 7; records and locations of wells given in Dysart and Rheaume, 1999).

the types of valley-fill deposits and their hydraulic properties were minimal in the model area outside of a 0.16 mi^2 subregion surrounding the Dover well field (fig. 34). Therefore, six model designs were developed in which a range of hydraulic conductivity values were tested, and in which the vertical leakance of the Rockaway River streambed was varied over its estimated range. All six models were identical in dimensions, time span simulated, applied *WAFR*, and pumping-rate distributions. Five models differed appreciably in their simulated values of streambed leakance and hydraulic conductivity values for the uplands and parts of the valley fill, but the statistical fit of simulated to observed heads achieved in each model was virtually the same. Alteration of specific yield resulted in significantly improved model fit for the sixth model. The sensitivity of one of the Dover models to several hydrologic factors was investigated, including the magnitude of unchanneled runoff from the uplands, the presence of a poorly permeable layer beneath the valley fill, heterogeneity of streambed hydraulic properties, and the temporal distribution of pumping rates.

MODEL DESIGN AND PROCEDURES

The unequally spaced model grid (consisting of 34 rows and 41 columns) and the locations of river cells, constant-head cells and zero-flow cells are shown in figure 34. Model cell dimensions range from 75 to 500 ft. Cells simulated with the River Package of MODFLOW (river cells) were located along reaches of the Rockaway River and its tributaries (fig. 34). The specified-head cells of figure 34 represent upland ponds located east of the Rockaway River (fig. 32).

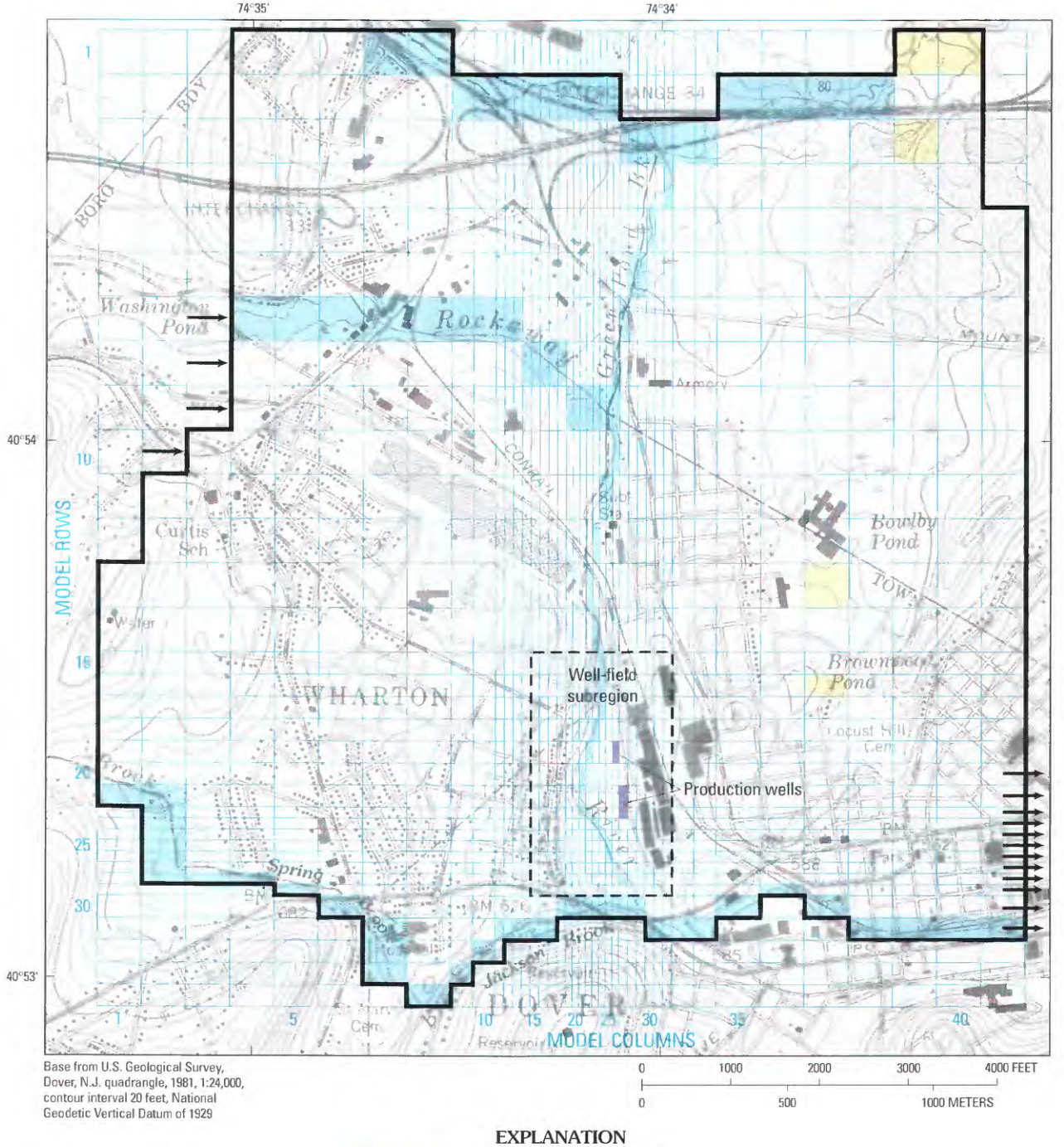

FIGURE 34.—Dover model grid, location of river and specified-head nodes, boundary fluxes, and well-field subregion (from Kontis, 1999, fig. 24).

Geologic Discretization

The Dover models consist of two layers. The top layer (layer 1) represents the surficial coarse sand and gravel deposited along the Rockaway River as outwash and alluvium; elsewhere it represents other surficial geologic units—till, bedrock, and proglacial deltaic deposits (fig. 31). This top layer was treated as unconfined.

Layer 2, which was treated as being confined, represents fine to coarse deltaic sand or lacustrine-fan sand and gravel that underlies surficial outwash along the Rockaway River valley. The Dover municipal production wells are open to this unit, which well logs indicate to be somewhat more permeable than the overlying outwash in the vicinity of the well field (Dysart and Rheaume, 1999). In some places, the lower sand and gravel is overlain by till, rather than outwash. Whether this unit is continuous south of Brownwood Pond beneath the morainal till that blocks the deep bedrock valley reach east of the Dover municipal wells (fig. 32) is unknown because the number and distribution of deep wells is insufficient to define its extent and continuity. Consequently, two model designs were developed: in one design it was assumed that the coarse deposits in the Dover well field area are continuous to the east beneath the till, and in the second it was assumed that they are absent beneath the till, such that the coarse deposits are discontinuous in this vicinity. Because the extent of the coarse sand and gravel beneath outwash or morainal deposits within the bedrock valley north of well 353 in Wharton (fig. 32) is also uncertain, layer 2 in this area was treated as sandy till rather than sand and gravel in some models. Elsewhere, layer 2 represents till and bedrock.

Model Boundaries

Reaches of Green Pond Brook, Spring and Jackson Brooks, and the Rockaway River along the northern and southern parts of the model were treated as lateral zero-flow boundaries (fig. 31). Most of the western model boundary is aligned to coincide with the upland surface drainage divide and was also treated as a zero-flow boundary. A specified nonzero flow boundary in the vicinity of Washington Pond (fig. 34) represents eastward underflow within the Rockaway River valley. The northern two-thirds of the eastern edge of the model, part of which coincides with a surface drainage divide, was treated as a zero-flow boundary.

The southeastern corner of the modeled area is separated from the Dover well field by a surface drainage divide (fig. 32) but is included as an active part of the model because the continuity of the sand and gravel of layer 2 beneath the divide is uncertain. Cells along the southeastern model boundary that represent stratified drift were assigned eastward directed nonzero specified fluxes (fig. 34 and table 11) computed by Darcy's law from representative values of hydraulic conductivity and head gradient.

TABLE 11.—*Boundary fluxes specified for models of groundwater flow in the Rockaway River valley at Dover, N.J.*

[Fluxes are in cubic feet per second. Positive flux values represent flow into model, minus (–) sign denotes flow out of model. Locations of cells where fluxes are applied are show in fig. 34. Fluxes are the same in all stress periods and in all six models except as footnoted]

Location in model		Boundary flux	
Row	Column	Layer 1	Layer 2
7	4	0.40	0.40*
8	4	.02	0.40*
9	4	.02	0.40*
10	3	.02	0.02
20	41	–0.05	–0.05
21	41	–0.05	–0.05
22	41	–0.04	–0.04
23	41	–0.04	–0.04
24	41	–0.04	–0.04
25	41	–0.04	–0.04
26	41	–0.04	–0.04
27	41	–0.04	–0.04
28	41	–0.04	–0.04
29	41	–0.04	–0.04
30	41	–0.04	–0.04
31	41	–0.075	–0.04

* 0.02 in models 5 and 6.

Vertical flow between layer 2 and underlying till or crystalline bedrock was assumed to be small; therefore the bottom of layer 2 was treated as a no flow boundary. The significance of this assumption is examined in the later section "Addition of a Third Model Layer".

Time Discretization and Stress Periods

Transient-state simulations of the 2 years from September 1983 through September 1985 were conducted to encompass the period over which water levels were measured. Initial conditions for these simulations were obtained from transient-state simulations of four seasonal stress periods in which the applied stresses were representative of long-term averages for each season (Kontis, 1999). The simulations were repeatedly cycled through the four seasons until steady state was achieved, and were terminated at the end of the summer season. These initial-condition simulations are referred to as the long-term average models.

Water levels in observation wells in and around the Dover well field were measured from May 1984 through November 1985 at intervals ranging from several weeks to several months. Sets of water levels measured in 1984 on May 18, July 7, and September 20 and in 1985 on January 19-24, May 28, and September 19 (table 22 of Dysart and Rheaume, 1999) were selected for calibration of the 2-year transient-state simulations. Each of the time intervals between the

selected sets of observed water levels were divided into a relatively long stress period followed by one or two relatively short stress periods, to give a total of 14 stress periods (table 12) for the 2-year period. Discretizing the interval between calibration times into long and short stress periods can be useful if stresses occurring shortly before and during the time when measurements were made differ significantly from the average conditions that prevailed during the previous long stress period. The stresses that were varied between stress periods were pumping rates of the three municipal production wells, *WAFR* rates, and altitude of stream surfaces (table 12). The rates of *WAFR* varied widely during the 2-year measurement period, allowing analysis of a wide range of changes in upland recharge contribution to the valley fill through time.

Corrections for Effects of Pumping Cycles on Water Levels

Water levels in observation wells at the Dover well field showed short-term fluctuations that did not correlate with precipitation or river stage, but with the pumping schedule of the Dover production wells. Information on the short-term response of each observation well to the start or cessation of pumping of nearby production wells was used to adjust observed water levels to represent water levels corresponding to a standard pumping condition (Kontis, 1999). Measured and adjusted water levels in individual wells for the six measurement dates are shown in figure 39 (farther on); locations of these wells in relation to model cell location are given in table 17 (farther on). As shown in figure 39 the adjustments ranged from zero to more than 2 feet.

CALIBRATION PROCEDURES

Several procedures were used to enhance the calibration process and the interpretation of model results of both the Dover and Wooster models. These are (1) interpolation of model heads to a finer grid spacing, (2) calculation of model sensitivity to changes in model properties and (3) calculation and display of simulated flow directions.

Interpolation of Model Heads

Differences between observed and model heads in the calibration of ground-water flow models are commonly attributed to erroneous model values of hydraulic properties, which are then modified until the differences are judged to be sufficiently small. Part of the difference, however, may be the result of inadequate sampling of aquifer head. Ideally, the simulated head in a particular model cell should be compared with an observed value that is representative of the true mean aquifer head. This value is estimated from measurements in one or more observation wells located within the cell and open to the layer in question, but may be in error unless the number or location of the observation wells is such that the actual head configuration is adequately sampled. For such conditions, the potential adverse effects on model-fit calculations can be reduced by interpolating model heads to some finer scale (if the model-grid spacing is sufficient to define the essential water-level configuration). This procedure was followed in the calibration of the Dover and Wooster models.

The area encompassing model rows 15-29 and columns 15-32 of the Dover model (fig. 34) includes the municipal well field and is the area in which all water-level measurements available for model calibration were collected. To facilitate calibration, model heads within this area, the Dover-well field subregion, were generated at a uniform spacing of 50 ft by means of a one-dimensional cubic-spline interpolation (Davis and Kontis, 1970) applied first along model rows, then along columns. Because most potentiometric surfaces in stratified-drift aquifers are relatively smooth, other interpolation procedures could accurately represent the simulated surface such as, interpolation of hydraulic head at the exact location of observation wells by linear, triangular, or quadrilateral finite-element basis functions, as discussed by Hill (1992).

Goodness of Fit

The absolute difference (*AD*) between model head and observed head in a particular cell containing an observation well is

$$AD = |h_m - h_o| \ ,$$

where h_m is the model head calculated within the cell, and
h_o is observed water level or the average of all water-level measurements within the cell.

Goodness-of-fit was determined by computing two versions of the mean absolute difference (*MAD*) between model and observed values. The first version is a measure of the model fit for each stress period. That is, the *MAD* for the ith stress period for *N* observation wells is

$$MAD(i) = \frac{\sum_{n=1}^{N} |h_m - h_o|_n}{N}, \ i = 1, 2, \ldots 6 \text{ stress periods.} \quad (15)$$

The second version is a measure of the model fit for each observation well over all six stress periods. That is, the *MAD* for the *n*th observation well is

$$MAD(n) = \frac{\sum_{i=1}^{6} |h_m - h_o|_i}{6},$$
$$n = 1, 2, \ldots \ N \text{ observation wells.} \quad (16)$$

TABLE 12.—*Stress periods and hydraulic stresses applied to models of Rockaway River valley at Dover, N.J.*

[ft, feet; ft/s, feet per second; ft^3/s, cubic feet per second. For models 1–5 specific yield in layer 1 is 0.05 for till and 0.2 for stratified drift. For model 6 specific yield is 0.05 for till and 0.1 for stratified drift. Well locations shown in fig. 32; well 291 is at same location as well 290]

Stress period					Amount of water available for recharge (WAFR)		Pumping rate at wells (ft^3/s)		
Stress period no.	No. of time steps	End date	Duration (days)	River stage* (ft)	Rate ($10^7 ft^3/s$)	Inches	Well 286	Well 288	Well 291
***A.* Long-term average annual cycle**									
1	1	Dec. 30 (fall)	92	+0.3	1.06	10.11	2.63	0.74	1.41
2	1	Mar. 31 (winter)	90	+0.5	1.16	10.82	2.57	0.83	1.48
3	1	June 30 (spring)	91	+0.5	0.45	4.25	2.56	0.85	1.62
4	1	Sept. 30 (summer)	92	+0.1	0	0	2.48	0.83	1.63
***B.* Two-year simulation (September 23, 1983 through September 19, 1985)**									
1	5		237	+0.7	1.34	32.92	2.57	0.74	1.46
2	1	May 18, 1984	1	+0.7	1.34	0.14	2.72	0.37	1.90
3	2		48	+0.7	1.23	6.12	2.65	0.82	1.72
4	2	July 7, 1984	2	+2.4	24.10	5.00	2.72	0.37	1.90
5	3		74	+0.4	0.40	3.06	2.48	0.83	1.61
6	1	Sept. 20, 1984	1	0	0.40	0.04	2.72	0.37	1.90
7	5	Jan. 5, 1985	107	0	0.45	4.99	2.89	0.42	1.41
8	2		18	–0.1	0	0	2.89	0.42	1.41
9	1	Jan. 24, 1985	1	–0.1	0	0	2.72	0.37	1.90
10	5		123	+0.2	0.33	4.21	3.33	0.16	1.43
11	1	May 28, 1985	1	+0.2	0.33	0.03	2.72	0.37	1.90
12	5	Aug. 31, 1985	95	0	0.46	4.52	3.31	0	1.41
13	2		18	–0.1	0	0	3.31	0	1.41
14	1	Sept. 19, 1985	1	–0.1	0	0	2.72	0.37	1.90

* Above (+) or below (–) reference stage at all river cells.

Model Sensitivity

A measure of model sensitivity to a change in head is the quantity

$$\sigma = (\Delta h_{i,j,k} / \Delta h_s) 100, \quad (17)$$

where σ is sensitivity, in percent,

$\Delta h_{i,j,k}$ is the change in head in cell i, j, k due to a change in some model property or properties, and

Δh_s is the total range of head over a representative portion of an aquifer.

For instance, Δh_s can be taken to be the lateral range in head over the entire aquifer, or perhaps the difference in head between a pumping center and an adjacent area of little or no drawdown. In the Dover model, the head varies about 7 ft over the extent of the well-field subregion (fig. 34). Although the interpretation of this quantity is somewhat subjective, a σ of less than 2 percent is taken to be indicative of relative insensitivity, σ from 2 to 10 percent represents moderate sensitivity, and σ greater than 10 percent indicates a high degree of sensitivity.

If $\Delta h_{i,j,k}$ is interpreted to be the mean absolute difference between observed and simulated heads, then equation 17 can also provide a basis for evaluating the goodness of fit of different models as calculated, for example, by equations 15 or 16. A reasonable goal for most simulations is a σ of less than about 15 percent of the total range Δh_s. In addition, the differences between observed and simulated heads should be unbiased; that is, they should be randomly distributed. A comprehensive discussion of calibration and calibration error analysis is presented in Andersen and Woessner (1992).

Model Flow Paths

The direction of lateral flow at each cell was calculated from model flow-components by the relation

$$A_{i,j,k} = \tan^{-1}(QX_{i,j,k} / QY_{i,j,k}), \quad (18)$$

where $QX_{i,j,k}$ is the lateral flow parallel to row i, at node i, j, k, taken to be the average of the flows across the left and right face of the node (eqs. 10 and 11 of McDonald and Harbaugh, 1988);

$QY_{i,j,k}$ is the lateral flow parallel to column j, at node i, j, k, taken to be the average of the flow across the back and front faces of the node (eqs. 12 and 13 of McDonald and Harbaugh, 1988); and $A(i, j, k)$ is the angle of lateral-flow direction, at node i, j, k, relative to the orientation of model columns.

MODEL INPUT

The following paragraphs summarize procedures and assumptions that were used to estimate the spatial and temporal magnitude and distribution of the hydrogeologic characteristics and stress rates used in the simulations made with the Dover models, including streambed properties, stream-surface altitudes, pumping rates, storage properties, lateral and vertical hydraulic conductivities of aquifer and till material, and various properties that control recharge. Additional details are presented in Kontis (1999).

Streambed Properties

Vertical leakance (K/m) of a streambed with uniform hydraulic properties can be estimated from equation 9b for use in calculating streambed conductance (eq. 6), given measurements of streamflow loss, vertical head difference across the streambed, and streambed area. The average measured streamflow loss ($\Delta D'a,b$), over a reach of the Rockaway river adjacent to the Dover wellfield, was 0.67 ft^3/s, area of streambed (LW) was 104,000 ft^2, and the mean of the measured head differences ($\Delta\bar{h}$) over that reach was 2.7 ft (Dysart and Rheaume, 1999). Consequently, according to equation 9b, the resulting estimate of K/m was 0.21 (ft/d)/ft. Other estimates of K/m (table 10) were 0.28 (ft/d)/ft, obtained from a dissolved-oxygen tracer method, and 0.68 (ft/d)/ft, obtained from an analysis of the mass balance of environmental isotopes and from a vertical-temperature modeling method (Dysart and Rheaume, 1999). Vertical leakance values ranging from 0.2 to 0.6 (ft/d)/ft were used in the Dover simulations to represent the range of these estimates.

Stream-Surface Altitudes

Stream-surface altitude along the Rockaway River and its tributaries was determined from (1) periodic measurement of stage at several reference points near the Dover well field, (2) a field survey of stream-surface altitude along a 2,000-ft reach of the river north of the production wells, and (3) interpolation from topographic maps for locations elsewhere (Kontis, 1999). The altitude calculated for a convenient date in May, 1985 at each model cell containing a stream reach was taken as a reference stage. The rise and fall of stage relative to the reference stage for each of the four stress periods of the long-term average models and the 14 stress periods of the transient-state models is given in table 12.

Pumping Rates

Pumping rates used in Dover models (table 12) were derived from records of daily pumpage at the Dover well field (A. Du-Jack, Dover Water Dept., written commun., 1986). Seasonal average rates for 1984 were assumed to be representative of long-term average conditions and were used in the long-term average four-season simulations. In the 2-year transient-state simulation (September 1983-September 1985), the pumping rate for each stress period longer than 2 days was an average of daily pumpage during that period.

A different procedure was used to obtain pumping rates for the 1- and 2-day stress periods at the end of each long stress period (stress periods 2, 4, 6, 9, 11, and 14). As previously discussed, water levels that were measured when a nearby production well was idle, or had been turned on only a few hours earlier, were adjusted to approximate the water levels that would have occurred under an assumed standard pumping condition. Pumping schedules prevailing on several dates during the standard pumping condition, and water-level measurements from these dates were used as a basis for adjustment of water levels measured under nonstandard pumping conditions. The standard-pumping condition rates for the short-stress periods (table 12) represent the average of the rates for the 24-hour periods before each of these measurement sets and are the same for each short stress period (Kontis, 1999).

Hydraulic Properties of Earth Materials

Specific yields specified for five of the six model designs were 0.2 for valley-fill sediments and 0.05 for till, based on reported average values of specific yield as determined from laboratory analyses of similar materials. A specific yield of 0.1 was used for the valley fill of the sixth model.

The hydraulic conductivity estimates used in the initial simulations were developed from specific capacity tests, and extrapolated on the basis of surficial geology (fig. 31) and lithologic descriptions of well logs (Dysart and Rheaume, 1999). Vertical hydraulic conductivity estimates were based on vertical anisotropy values typical of the materials in question. These initial horizontal and vertical hydraulic conductivity estimates were modified during model calibration to improve the fit of simulated heads to adjusted observed

heads. The model cells of each layer were grouped into a series of zones (figs. 35, 36) each of which could be assigned a different hydraulic conductivity. The areal extent of the surficial deposits represented by layer 1 was reasonably well known but the hydraulic conductivity was not. The distribution and properties of deeper materials was poorly known, notably in a buried trough represented by zone 16 of layer 2 (fig. 36), which was the focus of two alternative model designs. In the first design, it was assumed the deposits in this zone to be coarse sand and gravel, and in the other, it was assumed the deposits to be sandy till with a hydraulic conductivity similar to that of upland till. Zones 11, 12, and 13 of layer 2 (fig. 36) were treated as sand and gravel in models 1, 2, 3, and 4, but as sandy till in models 5 and 6 to reflect the hydrogeologic interpretation of Canace and others (1993, pl. 2).

Vertical leakance between model layers was computed from equation 51 of McDonald and Harbaugh (1988). Vertical-hydraulic conductivity values, used in the vertical-leakance computation, were derived from the simulated horizontal hydraulic conductivity values for each layer and one of three assumed vertical anisotropy factors—1:100 for the upland cells and 1:10 and 1:20 for the valley-fill cells (table 16, farther on).

Properties that Control Recharge

WAFR.—*WAFR* during each stress period (table 12) was estimated from equation 11 as summarized in tables 13 and 14. The calculation procedure is similar to that of table 6, but the calculated quantity is conceptualized as *WAFR* rather than recharge. Storage of moisture as snow is usually small at Dover and was ignored in the calculation.

Land-Surface Elevation.—The array of land-surface altitudes (fig. 37) required to determine which of the recharge conditions of equations 13a-13c apply was obtained by estimating the average land-surface altitude within each of the unequally spaced model blocks (fig. 37) from available topographic maps, including maps with a 2-ft contour interval (U.S. Army Corps of Engineers, 1978; Geod Corporation, Oakridge, N.J., written commun., undated) and the USGS Dover, N.J. 15-min quadrangle map with a 20-ft contour interval, as explained in Kontis (1999).

Variable-Recharge Zones.—The division of the model area into subbasins or zones as required by the Variable-Recharge procedure (see item 2 under "Input Information") is shown in figure 38. Cells assigned to zone zero lie within topographically low areas from which any surface runoff resulting from seepage or rejected recharge (eq. 13) is assumed to flow to a stream and therefore is not available to recharge other model cells. The remaining cells, with zone numbers of 1 through 10, represent upland subbasins.

Reduction of WAFR in Urban Areas.—Much of the area adjacent to the Dover well field is urban (fig. 38), and has streets and other paved surfaces that drain to storm sewers, thereby disrupting natural recharge and runoff processes. Accordingly, the amount of water estimated to be available for recharge in urban areas was reduced to 50 to 75 percent of the amount estimated from equation 11 and shown in table 12, as discussed in Kontis (1999). In addition, runoff from the most highly urbanized upland areas (zones 3 and 10, fig. 38) was assumed to be unavailable to recharge the adjacent valley as unchanneled flow.

Disposition of Upland Runoff.—Surface runoff from each of the upland subbasins was treated as unchanneled surface runoff and applied as additional *WAFR* to specified cells along the valley floor adjacent to the subbasin (fig. 38), or to topographically low, nonurbanized areas within upland subbasins 2 and 5, where hillslopes are far removed from the coarse valley deposits.

MODEL CALIBRATION

Six models were developed that differ significantly in streambed leakance, hydraulic conductivity of till, and hydraulic conductivity of several zones of uncertain composition, as previously discussed and as specified in table 15. The hydraulic stresses and properties listed in table 12 were applied to each model. Hydraulic conductivity values for all areas not specified in table 15 were adjusted during calibration until reasonably close agreement between the simulated and the adjusted observed water levels was achieved. In addition, the calculated rates of *WAFR* (column 9, table 13) in some stress periods were varied somewhat during calibration, to match observed changes in water levels from one stress period to the next. The difference between the calculated rates of *WAFR* and the final rates (column 11, table 13) can be interpreted as the amount by which the precipitation or calculated evapotranspiration (columns 4 and 5 in table 13) would have to be increased (or decreased) over the duration of a stress period to account for the implemented change in the rate of *WAFR*.

The final distribution of hydraulic conductivity values resulting from the calibration of each of the six models is given in table 16. The calibrated hydraulic conductivity values for stratified drift in each zone, except for those zones in which hydraulic conductivity had been specified (table 15) and zone 14 of layer 1 (fig. 35), range from 0 to 43 percent more or less than the hydraulic conductivity of that zone averaged among all models. This range is well within the range of variation in hydraulic conductivity typical of stratified drift and is therefore plausible.

Goodness of Fit—Model Heads

The mean average deviation (*MAD*) statistics (eq. 15) for each of the six stress periods used in the calibrations are given for each model in table 17*A*. Except for stress period 4, the *MAD* of all models for 13 observation wells was no more

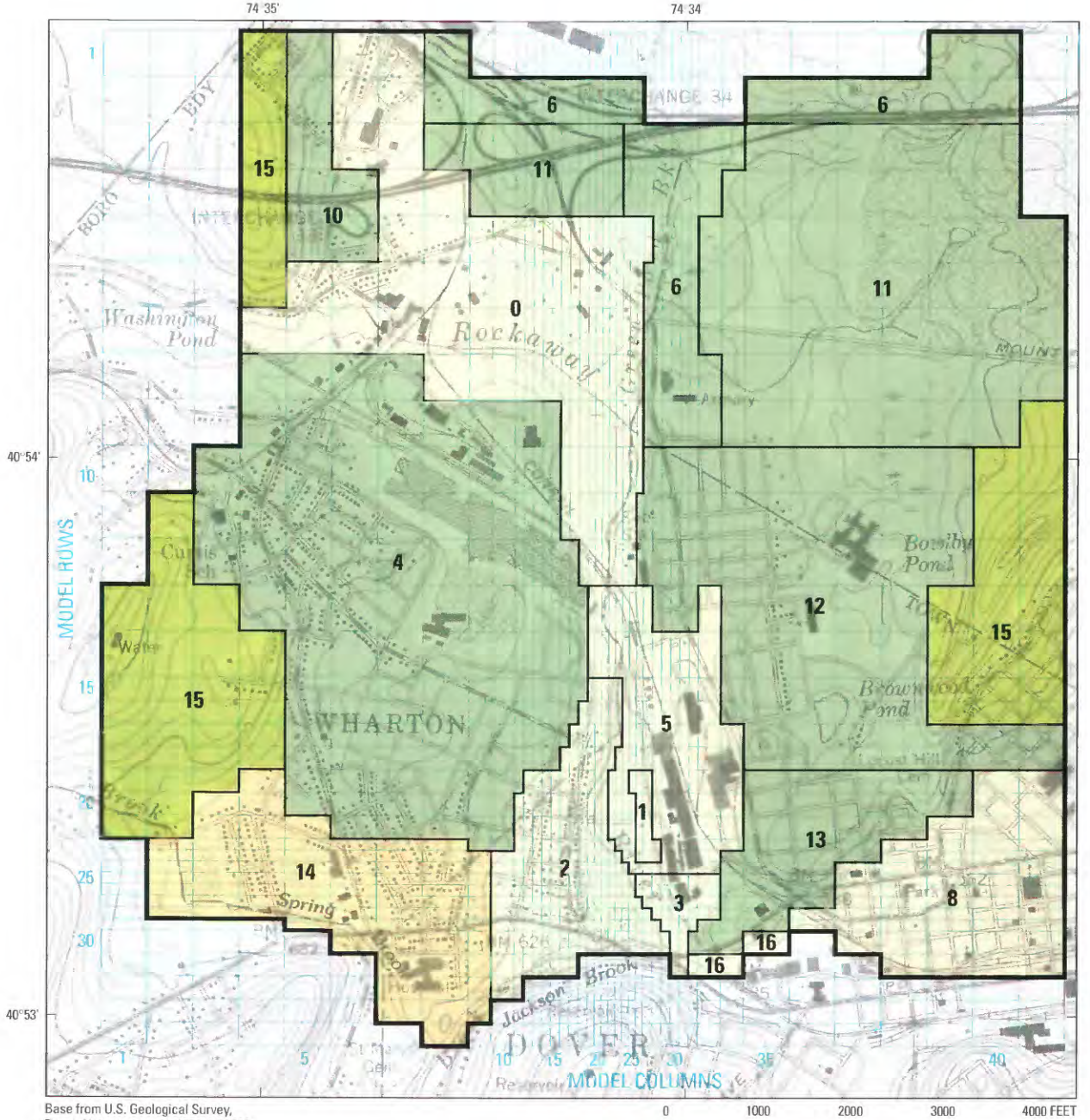

EXPLANATION

Material simulated and zone number

15	Bedrock
4	Moraine deposits—Chiefly till
	Sand and gravel:
8	Predominantly fluvial outwash and alluvium
14	Deltaic and lacustrine-fan deposits

Boundary of active model

Boundary of hydraulic-conductivity zones

FIGURE 35.—Location of Dover ground-water flow model and of hydraulic-conductivity zones in model layer 1 (from Kontis, 1999, fig. 36).

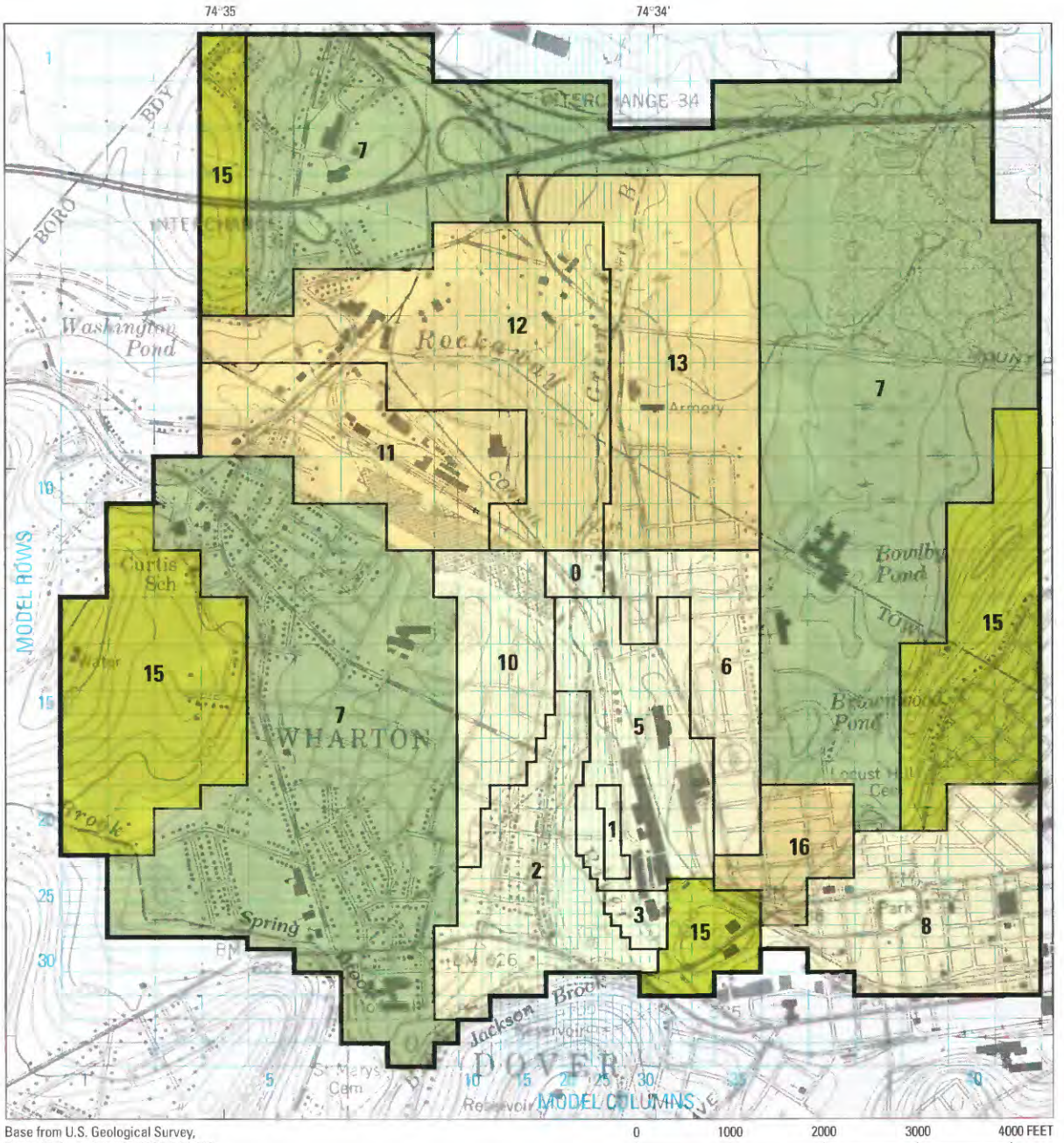

Base from U.S. Geological Survey, Dover, N.J. quadrangle, 1981, 1:24,000, contour interval 20 feet, National Geodetic Vertical Datum of 1929

0 1000 2000 3000 4000 FEET
0 500 1000 METERS

EXPLANATION

Material simulated and zone number

15	Bedrock
7	Till
8	Sand and gravel
13	Zones simulated as sand and gravel in some models and as till in other models

Boundary of active model

Boundary of hydraulic-conductivity zones

FIGURE 36.—Hydraulic-conductivity zones in model layer 2 of Dover models (from Kontis, 1999, fig. 37).

TABLE 13.—*Calculation of water available for recharge (WAFR) at Dover, N.J., September 23, 1983 through September 19, 1985*

[ft/s, feet per second]

Stress period			Precipitation, evapotranspiration, and soil moisture				*WAFR*			
No.	Dates	Duration (days)	Precipitation (inches)[1]	Evapotranspiration (inches)[2]	Soil-moisture depletion or addition (–) (inches)[3]	Accumulated soil-moisture deficit (cumulative total of col. 6) (inches)	Calculated amount available (col. 4+5+6) (inches)	Calculated rate for stress period (ft/s)[4]	Simulated rate for stress period (ft/s)[5]	Difference between calculated and simulated rates (inches)[6]
1	2	3	4	5	6	7	8	9	10	11
1	1983 Sept. 23–30	8	1.50	–0.66	0	0	0.84			
	October	31	5.91	–1.74	0	0	4.17			
	November	30	6.02	–1.09	0	0	4.93			
	December	31	8.13	0	0	0	8.13			
	1984 January	31	1.38	0	0	0	1.31			
	February	28	4.42	0	0	0	4.42			
	March	31	5.24	–1.58	0	0	3.66			
	April	30	6.90	–2.75	0	0	4.15			
	May 1–17	17	3.35	–1.99	0	0	1.36			
	sum	237					33.04	1.34×10^{-7}	1.34×10^{-7}	0
2	May 18	1	0	–0.12	+0.12	0.12	0	0	1.34×10^{-7}	0.14
3	May 19–31	13	6.77	–1.52	–0.12	0	5.13			
	June	30	2.90	–3.90	1.00	1.00	0			
	July 1–5	5	1.60	–0.66	–0.94	0.06	0			
	sum	48					5.13	1.03×10^{-7}	1.23×10^{-7}	1.0
4	July 6–7	2	5.0	–0.27	–0.06	0	4.67	22.5×10^{-7}	24.1×10^{-7}	0.33
5	July 8–31	24	4.24	–3.19	0	0	1.05			
	August	31	2.30	–3.73	1.43	1.43	0			
	Sept. 1–19	19	2.08	–1.56	–0.53	0.91	0			
	sum	74					1.05	0.15×10^{-7}	0.40×10^{-7}	1.9
6	Sept. 20	1	0	–0.08	+0.08	0.99	0	0	0.40×10^{-7}	–0.04
7	Sept. 21–30	10	0.35	–0.82	0.47	1.46	0			
	October	31	3.35	–1.74	–1.46	0	0.15			
	November	30	2.36	–1.09	0	0	1.27			
	December	31	3.65	0	0	0	3.65			
	1985 Jan. 1–5	5	0.88	0	0	0	0.88			
	sum	107					5.95	0.54×10^{-7}	0.45×10^{-7}	1.0

TABLE 13.—*Calculation of water available for recharge (WAFR) at Dover, N.J., September 23, 1983 through September 19, 1985*—Continued

[ft/s, feet per second]

Stress period			Precipitation, evapotranspiration, and soil moisture				*WAFR*			
No.	Dates	Duration (days)	Precipitation (inches)[1]	Evapotranspiration (inches)[2]	Soil-moisture depletion or addition (–) (inches)[3]	Accumulated soil-moisture deficit (cumulative total of col. 6) (inches)	Calculated amount available (col. 4+5+6) (inches)	Calculated rate for stress period (ft/s)[4]	Simulated rate for stress period (ft/s)[5]	Difference between calculated and simulated rates (inches)[6]
1	2	3	4	5	6	7	8	9	10	11
8	1985 Jan. 6–23	18	0.30	0	0	0	0.30	0.16×10^{-7}	0	0.30
9	Jan. 24	1	0	0	0	0	0	0	0	0
10	Jan. 25–31	7	0	0	0	0	0			
	February	28	1.96	0	0	0	1.96			
	March	31	1.59	–1.58	0	0	0.01			
	April	30	1.13	–2.75	1.62	1.62	0			
	May 1–27	27	6.05	–3.16	–1.62	0	1.27			
	sum	123					3.24	0.25×10^{-7}	0.33×10^{-7}	1.0
11	May 28	1	0.23	–0.12	0	0	0.11	1.06×10^{-7}	0.33×10^{-7}	0.08
12	May 29–31	3	0.46	–0.35	0	0	.11			
	June	30	7.46	–3.90	0	0	3.56			
	July	31	4.97	–4.12	0	0	0.85			
	August	31	2.67	–3.73	1.06	1.06	0			
	sum	95					4.52	0.46×10^{-7}	0.46×10^{-7}	0
13	Sept. 1–18	18	0.40	–1.48	1.08	2.14	0	0	0	0
14	Sept. 19	1	0	–0.08	0.08	2.22	0	0	0	0

[1] From record of daily precipitation at West Wharton, N.J. (National Oceanic and Atmospheric Administration, 1983–85).
[2] From table 14. For fractional months, evapotranspiration is proportioned linearly among number of days.
[3] If evapotranspiration (absolute value of column 5) exceeds precipitation (column 4), the difference represents a soil-moisture depletion (column 6). If precipitation exceeds evapotranspiration, the difference appears as a soil moisture addition in the present time period, but only to the extent needed to reduce to zero any accumulated soil-moisture deficit in column 7 of the previous time period. (In other words, a soil-moisture addition cannot exceed the magnitude of the accumulated soil-moisture deficit.)
[4] Obtained by dividing column 8 by column 3 and converting units to ft/s.
[5] Simulated rate is that which facilitated model calibration.
[6] Difference between calculated rate (column 9) and simulated rate (column 10), expressed in inches; can generally be interpreted as the amount by which evapotranspiration or precipitation would have to depart from values in columns 4 or 5 to account for this difference.

TABLE 14.—*Calculation of monthly evapotranspiration at Dover, N.J.*

Month	Evaporation (percent)[1]	Long-term mean values of evapotranspiration	
		Percent[2]	Inches[3]
1	2	3	4
January	2.6	0	0
February	3.1	0	0
March	5.8	6.33	1.58
April	10.1	11.00	2.75
May	13.3	14.51	3.63
June	14.3	15.59	3.90
July	15.1	16.46	4.12
August	13.7	14.95	3.73
September	9.0	9.82	2.46
October	6.4	6.97	1.74
November	4.0	4.36	1.09
December	2.5	0	0
		TOTAL	25.0

[1] Class A mean monthly pan evaporation at Hartford, Conn., the nearest station to Dover within the same climatic region cited by Lyford and Cohen (1988, table 2).

[2] Recalculated from monthly evaporation (column 2) assuming that monthly evapotranspiration values are actually zero from December through February (Lyford and Cohen, 1988, p. 41).

[3] Mean annual evapotranspiration is estimated to be about 25 inches, obtained as mean annual precipitation at Split Rock Pond, (50.1 inches, from National Oceanic and Atmospheric Administration, 1982) minus the estimated mean annual runoff at Dover (25.1 inches, from pl. 6 of Hely and others, 1961).

than 0.9 ft. In terms of the σ measure of fit (eq. 17), the *MAD* was less than 13 percent of the total range in head over the extent of the observation-well network.

Stress period 4 is characterized by a large rise in water levels and stream-surface altitudes in response to a 2-day rainfall of 5 in. (table 13). Simulated heads produced for this period by models 1 through 5 were 1.5 to 2 ft lower than the adjusted observed water levels (fig. 39). Model 6, which incorporated a specific yield of 0.1 rather than 0.2, gave a considerably better fit for stress period 4 and a generally better fit for the other stress periods (table 17). The *MAD* for model 6 was no more than 0.5 ft, and σ (eq. 17) was less than 7 percent for all stress periods.

A specific yield of 0.1 is at the low end of the range of published values for medium to coarse stratified drift as obtained from laboratory measurements (0.13 to 0.46, Morris and Johnson, 1967) and at the high end of the range of 0.03 to 0.13 typically derived from aquifer tests (Nwankwor and others, 1984). Although the distribution of simulated head is a function of many factors, the improved model fit obtained with the lower specific yield (model 6) supports the observation that for the analysis of the effects of water-table fluctuations in response to pumping, the lower values obtained from aquifer tests which generally last a few days at most can be more reliable than values based on laboratory measurements of core samples (Rasmussen and Andreason, 1959; Neuman, 1987).

The *MAD* statistics for each observation well, as computed by equation 16 over all six transient-stress periods (table 17*A*) average 0.6 ft for models 1 through 5 and 0.3 ft for model 6, and corresponds to σ values (eq. 17) of about 9 and 4 percent, respectively. Examples of model fit are also depicted in figure 39, which shows hydrographs of simulated heads in layer 1 of models 1 and 6 for each of the six stress periods, in cells containing observation wells. The figure also shows the corresponding measured and adjusted water levels.

Goodness of Fit—Interpolated Heads

As previously discussed, differences between observed and simulated heads can result not only from erroneous simulated hydraulic properties but also, in part, from model-grid discretization. The latter effect is illustrated in figure 40, which shows the model fit at two wells resulting from calibration of models 1 and 6 for six stress periods. The fit of simulated to observed heads was improved by about 1.4 ft at well S12 and about 0.5 ft at well S9, for each stress period, by interpolating the simulated model heads to a finer grid spacing. The effect is greater for well S12 than for S9, primarily because the head gradient at S12 is greater (see fig. 44). Calculation of model-fit statistics from interpolated model heads as well as actual model heads can therefore provide information as to whether discrepancies between observed and simulated heads are due, in part, to grid discretization or to assigned hydraulic properties, and whether adjustment of model properties is in order. Of the 24 individual comparisons between model fits using model heads and interpolated model heads shown in figure 40, 20 were improved by the interpolation process.

Simulated Stream Loss

The four methods that were used to estimate the streambed properties of the Rockaway River in the reach adjacent to the Dover well field (table 10) yielded values of stream loss (through induced infiltration) ranging from 0.67 to 1.8 ft^3/s (Dysart and Rheaume, 1999). Because the six models were calibrated to the same array of adjusted observed heads, differences between the models in simulated head distribution beneath the Rockaway River near the well field are minor. Consequently, a major difference between the models is the simulated induced infiltration. The simulated streamflow loss for the reach adjacent to the well field between upstream and downstream measurement sites is given in table 17*B* for each calibration stress period of models 1 through 6.

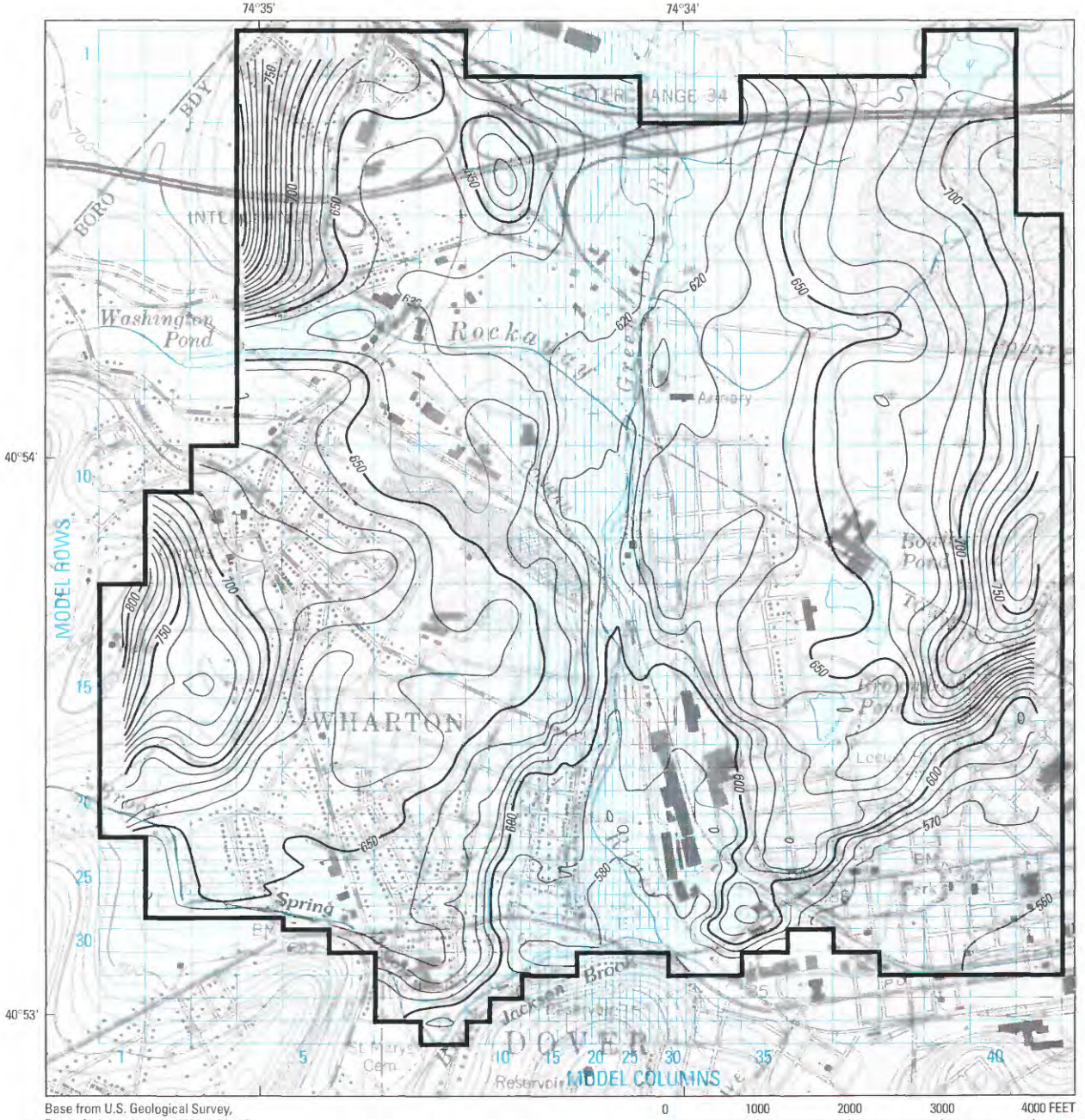

EXPLANATION

—700— —620— **Land-surface contour**—Shows altitude of land surface based on a data array of average land surface in each model cell as estimated from topographic maps. Contour interval 10 feet. Thicker index contours at 50-foot intervals. Datum is sea level

Boundary of active model

FIGURE 37.—Land-surface altitude array used by Variable-Recharge procedure in Dover models (from Kontis, 1999, fig.33).

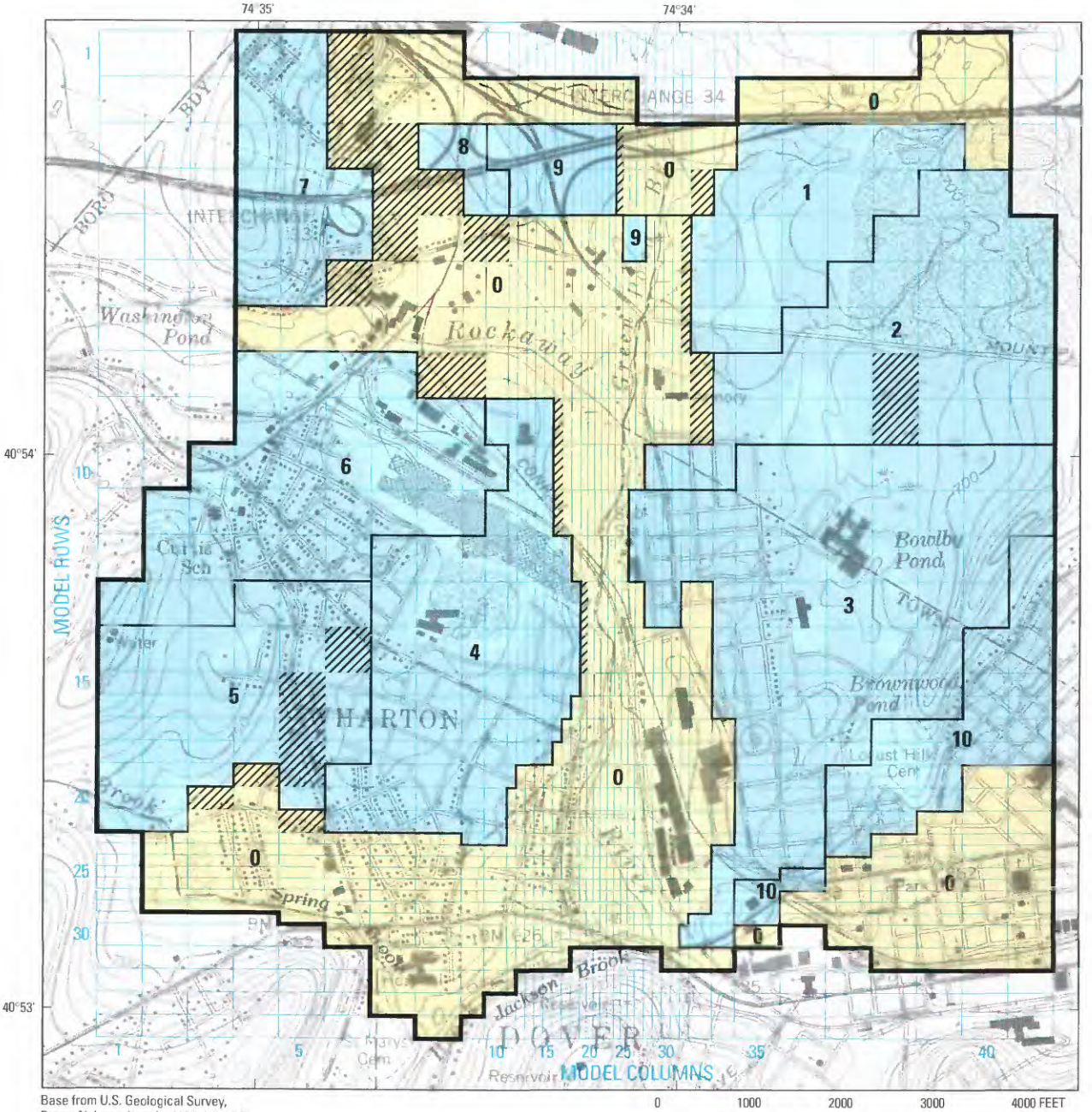

FIGURE 38.—Variable-Recharge zones and cells designated to receive unchanneled upland runoff in Dover models (from Kontis, 1999, fig. 34).

TABLE 15.—*Hydraulic characteristics that distinguish Dover ground-water flow models 1 through 6*

Model	Streambed leakance (*K/m*) (feet per day per foot)	Hydraulic conductivity values or range (feet per day)[1]			Specific yield of stratified drift
		Zone 16 of layer 2	Zones 11, 12, and 13 of layer 2	Upland till	
1	0.2	high (300)	high (375–400)	high (4)	0.2
2	0.2	low (4)	high (325)	high (4)	0.2
3	0.6	high (250)	high (300–350)	low (0.25)	0.2
4	0.6	low (4)	high (275–300)	low (0.25)	0.2
5	0.4	high (300)	low (25)	high (6)	0.2
6	0.4	high (300)	low (25)	high (6)	0.1

[1] Values in parentheses are the value, or range of values, of hydraulic conductivity used in specified model. Locations of zones are shown in figure 36.

The simulated streamflow loss is generally proportional to the simulated value of streambed leakance, and exhibits variation between stress periods due to the different rates of applied *WAFR* (table 13); thus, the streamflow losses for models 3 and 4, which incorporated a threefold increase in streambed leakance relative to models 1 and 2, are about three times those of models 1 and 2, and the streamflow losses of models 5 and 6 are about twice those of models 1 and 2 because the leakance was increased two-fold. The range of simulated streamflow loss, over time, in models 1 through 4 (0.49 to 1.84 ft^3/s, table 17*B*) approximates the estimated range of 0.67 to 1.8 ft^3/s of Dysart and Rheaume (1999).

RESULTS OF SIMULATIONS

The Dover models represent a much larger area than the well field subregion (fig. 34) to which they were calibrated. In this larger area, hydraulic property values were constrained only by geohydrologic plausibility. Models 1 through 5 fit the adjusted-observed heads with comparable accuracy (table 17). Decreasing the storage coefficient to 0.1 in model 6 gave a closer fit than did the value of 0.2 in model 5, but an equally good fit could probably have been obtained from the other models if a similarly small specific yield had been used. Thus, the process of model calibration to the local data could not distinguish which of the alternative specifications of models 1 to 5 is most nearly correct. Nevertheless, these models contain useful information on hydrologic relations at Dover as well as demonstrating application of the Variable-Recharge procedure for simulating the sources of recharge to a valley-fill aquifer.

Simulated-Head Configurations and Flow Paths

The head distribution in the uplands bordering the valley is a function of upland hydraulic conductivity. Under spatially uniform conditions and with a relatively low hydraulic conductivity of till (0.25 ft/d), simulated upland heads in layer 1 define a slightly subdued replica of land surface, whereas increased hydraulic conductivity values (4 to 6 ft/d) resulted in smoother and lower heads with gentler head gradients near the valley fill. These relations are illustrated by representative head profiles from models 1, 3, and 5 (fig. 41) and by maps of simulated head and flow directions from models 3 and 1 (figs. 42, 43). The results depicted in these illustrations represent long-term average end-of-summer conditions after 3 months without recharge (the initial condition for the two-year transient-state simulation).

Directions of simulated lateral flow in all models are generally from the uplands toward the valleys. Throughout the uplands, vertical flow is generally downward from layer 1 to layer 2, except in the vicinity of topographic depressions where it is upward. Within the Rockaway River valley, lateral flow is primarily downvalley and toward the production wells. Vertical flow is downward throughout the valley except near gaining-stream reaches and near the valley wall where it is upward.

Hydraulic factors within the valley, such as the rate of induced infiltration from the Rockaway River and the hydraulic properties of the stratified drift, greatly affect the size of the area from which ground water moves toward the production wells. The uplands too are an integral part of the valley flow system, and their hydraulic characteristics also affect the flow configuration. For example, the position of the groundwater divide that separates flow toward the well field from flow that bypasses the well field in layer 1 differs considerably between models 1 and 3 (figs. 42, 43), and the area that

TABLE 16.—*Hydraulic-conductivity values for Dover ground-water flow models 1 through 6*

[Horizontal hydraulic conductivity values in feet per day (ft/d). *K/m*, streambed leakance, in feet per day per foot]

Zone[a]	Material[b]	Ratio of vertical to horizontal hydraulic conductivity	Horizontal hydraulic conductivity and percent departure from average[c]					
			Model 1 (*K/m* = 0.2)	Model 2 (*K/m* = 0.2)	Model 3 (*K/m* = 0.6)	Model 4 (*K/m* = 0.6)	Model 5,6 (*K/m* = 0.4)	Average
Model layer 1								
0	SD	1:10	325 (18)	250 (9)	250 (9)	200 (27)	350 (27)	275
1*	do.	1:20	375 (14)	300 (9)	300 (9)	300 (9)	375 (14)	330
2*	do.	1:10	375 (23)	300 (2)	275 (10)	200 (34)	375 (23)	305
3*	do.	1:10	250 (9)	250 (9)	200 (13)	150 (35)	300 (30)	230
5*	do.	1:10	375 (17)	300 (7)	300 (6)	250 (22)	375 (17)	320
8	do.	1:10	150 (0)	150 (0)	150 (0)	150 (0)	150 (0)	150
14	do.	1:10	350 (56)	275 (22)	100 (56)	50 (78)	350 (56)	225
16	do.	1:10	250 (9)	250 (8)	200 (13)	200 (13)	250 (9)	230
4, 6, 10, 11, 12, 13	Till	1:100	4	4	0.25	0.25	6[d]	2.9
15	Bedrock	1:100	0.25	0.25	0.25	0.25	0.25[d]	0.25
Model layer 2								
0	SD	1:10	375 (12)	325 (3)	300 (10)	275 (18)	400 (19)	335
1*	do.	1:20	600 (3)	500 (14)	600 (3)	600 (3)	600 (3)	580
2*	do.	1:10	450 (14)	375 (5)	400 (1)	300 (24)	450 (14)	395
3*	do.	1:10	300 (7)	275 (2)	225 (20)	200 (29)	400 (43)	280
5*	do.	1:10	450 (6)	375 (12)	450 (6)	400 (6)	450 (6)	425
6	do.	1:10	400 (11)	325 (10)	350 (3)	300 (17)	425 (18)	360
10	do.	1:10	400 (16)	325 (6)	300 (13)	275 (20)	425 (23)	345
11	SD or till	1:10	400	325	300	275	25	—
12	do.	1:10	375	325	300	275	25	—
13	do.	1:10	400	325	350	300	25	—
8	SD	1:10	200	200	200	200	200	200
16	SD or till	1:10	300	4[e]	250	4[e]	300	—
7	Till	1:100	4	4	0.25	0.25	6[d]	2.9
15	Bedrock	1:100	0.25	0.25	0.25	0.25	0.25[d]	0.25

[a] Locations of zones for layers 1 and 2 are shown in figures 35 and 36, respectively; * denotes zones in Dover well-field area.
[b] SD, stratified drift.
[c] Values in parentheses are the difference, in percent, between the hydraulic conductivity of the indicated zone in a particular model and the hydraulic conductivity of that zone as averaged among all models.
[d] Ratio of vertical to horizontal hydraulic conductivity is 1:10.
[e] Ratio of vertical to horizontal hydraulic conductivity is 1:100.

contributes lateral flow from the eastern uplands to the production wells (fig. 43) is larger in model 3 than in model 1 (fig. 42), whereas the area contributing lateral flow to these wells from the western uplands is larger in model 1 than in model 3.

The head distribution within the Dover well field subregion in layer 1 as generated by model 6 (fig. 44) for each of the six transient-state-calibration stress-periods, is generally representative of that produced by all transient-state models. Simulated heads rose and fell in response to time-varying changes in the applied stresses (table 12), and flow patterns were generally the same in all stress periods with a few exceptions. One exception is the flow pattern at the end of the 2-day rainstorm (stress period 4) in the area south of the Dover well field. A nineteenfold increase in *WAFR* and a threefold increase in stream stage (1.7 ft) (table 12) relative to stress period 3 caused simulated heads to rise to land surface in several areas, resulting in outward seepage from some cells (eq. 13d) and conversion of these cells to specified head, equal to land-surface elevation (fig. 35), to represent local sites of discharge. These cells coincide with topographically low areas in the southern part of the well field subregion and form a sink in the flow system and an expanded area of rejected recharge.

TABLE 17.—*Mean absolute difference between interpolated model heads and corresponding adjusted observed heads at 13 observation wells in Dover well-field subregion, and simulated streamflow loss from Rockaway River adjacent to Dover well field*

[Difference values are in feet; streamflow losses are in cubic feet per second]

A. Mean absolute difference (MAD) values

1. MAD values for all wells in each calibration stress period, calculated by equation 15

Stress period		Model					
No.	End date	1	2	3	4	5	6
2	5-18-84	0.3	0.4	0.5	0.4	0.3	0.3
4	7-7-84	1.4	1.5	1.7	1.5	1.4	0.3
6	9-20-84	0.4	0.4	0.3	0.3	0.4	0.2
9	1-24-85	0.7	0.7	0.6	0.9	0.7	0.5
11	5-28-85	0.4	0.5	0.3	0.4	0.3	0.4
14	9-19-85	0.3	0.3	0.4	0.6	0.4	0.3

2. MAD values for each well over all stress periods, calculated by equation 16

Observation well	Model cell location in fig.34 (row, column)	Model					
		1	2	3	4	5	6
S1	(23, 24)	0.6	0.6	0.7	0.7	0.7	0.4
S2	(23, 26)	0.9	0.8	0.7	0.8	0.9	0.6
S3	(22, 27)	0.5	0.6	0.7	0.6	0.5	0.2
S4	(22, 25)	0.6	0.5	0.6	0.6	0.6	0.3
S5	(20, 27)	0.6	0.6	0.6	0.5	0.6	0.3
S6	(23, 18)	0.7	0.7	0.8	0.8	0.7	0.5
S7	(21, 21)	0.5	0.5	0.7	0.9	0.5	0.3
S8	(21, 19)	0.5	0.5	0.6	0.8	0.5	0.3
S9	(21, 24)	0.5	0.5	0.5	0.5	0.4	0.2
S10	(19, 23)	0.5	0.6	0.5	0.4	0.5	0.3
S11	(25, 28)	0.8	0.9	0.7	0.9	0.8	0.6
S12	(18, 23)	0.6	0.7	0.5	0.6	0.5	0.3
TW5	(22, 27)	0.6	0.6	0.6	0.6	0.5	0.2
	Average MAD	0.6	0.6	0.6	0.6	0.6	0.3

B. Simulated streamflow loss along Rockaway River[a]

Stress period		Model number and simulated value of K/m[b]					
		1[c]	2[c]	3[d]	4[d]	5	6
No.	End date	(0.2)	(0.2)	(0.6)	(0.6)	(0.4)	(0.4)
2	5-18-84	0.52	0.50	1.56	1.41	1.07	1.06
4	7-7-84	0.65	0.64	1.86	1.72	1.28	0.95
6	9-20-84	0.50	0.49	1.53	1.38	1.02	1.08
9	1-24-85	0.62	0.62	1.73	1.57	1.26	1.30
11	5-28-85	0.71	0.72	1.84	1.69	1.39	1.40
14	9-19-85	0.67	0.67	1.78	1.63	1.34	1.37

[a] Reach between upstream (row 17, column 25) and downstream (row 29, column 28) model cells (shown in fig. 35).

[b] K/m (in parentheses) is the simulated streambed leakance, in feet per day per foot.

[c] This value of streambed leakance corresponds to a streamflow loss of about 0.7 cubic feet per second, as estimated from paired streamflow measurements and the dissolved-oxygen tracer method (Dysart and Rheaume, 1999).

[d] This value of streambed leakance approximately corresponds to streamflow losses of 1.8 and 1.5 cubic feet per second, as estimated from vertical temperature modeling (Lapham, 1989) and mass balance of environmental isotopes (Dysart and Rheaume, 1999), respectively.

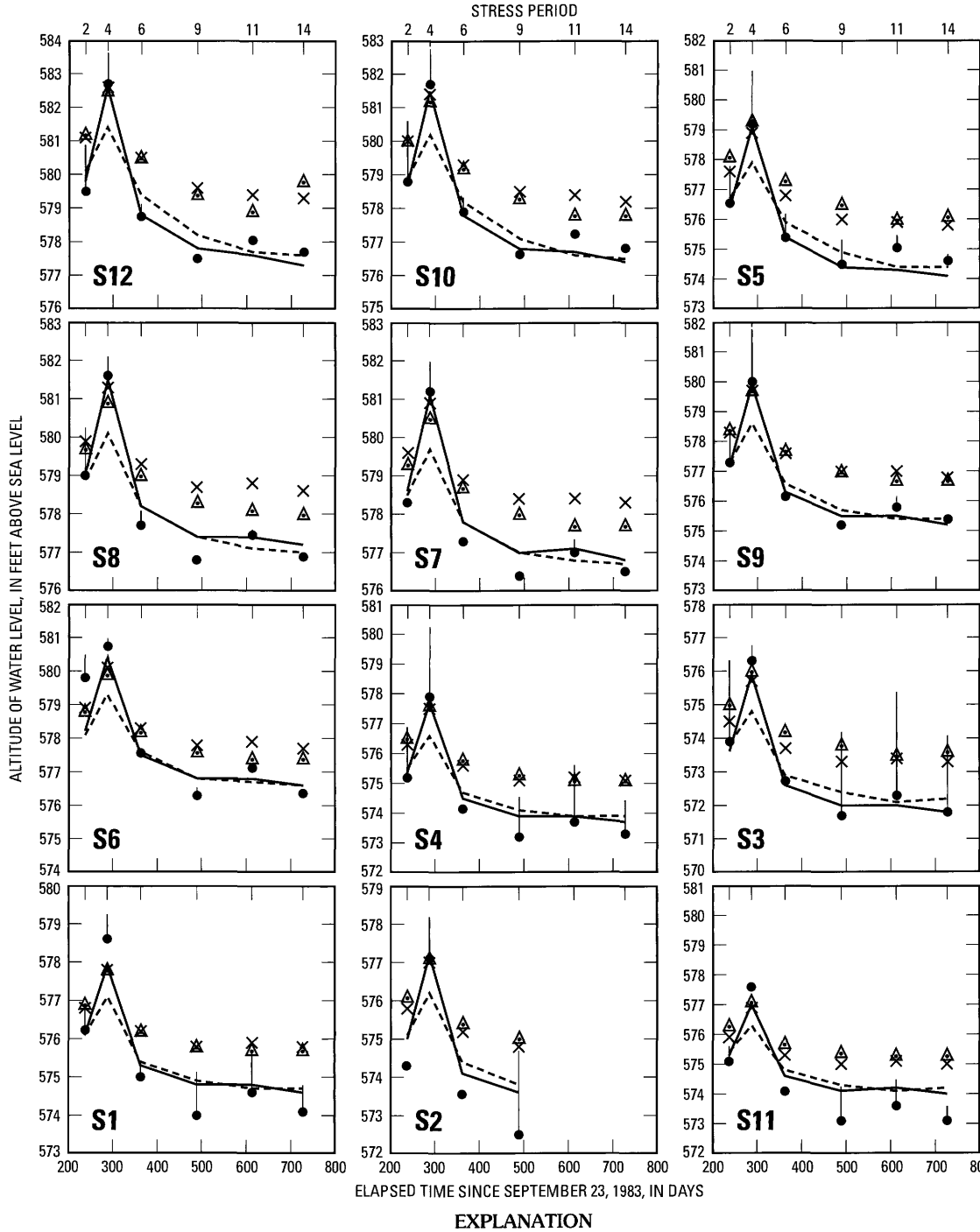

FIGURE 39.—Water levels in individual wells as observed, as adjusted, and as simulated by Dover models 1 and 6. Also shown is the sensitivity of model 1 to a change in streambed leakance (K/m) from 0.2 to 0.6 feet per day per foot and a change in hydraulic conductivity (K) within an abandoned reach of the Rockaway River valley (zone 16, layer 2 of fig. 36) from 300 to 4 feet per day per foot. The location of stress periods 2, 4, 6, 9, 11, and 14 are shown along the top of each panel (modified from Kontis, 1999, fig. 39).

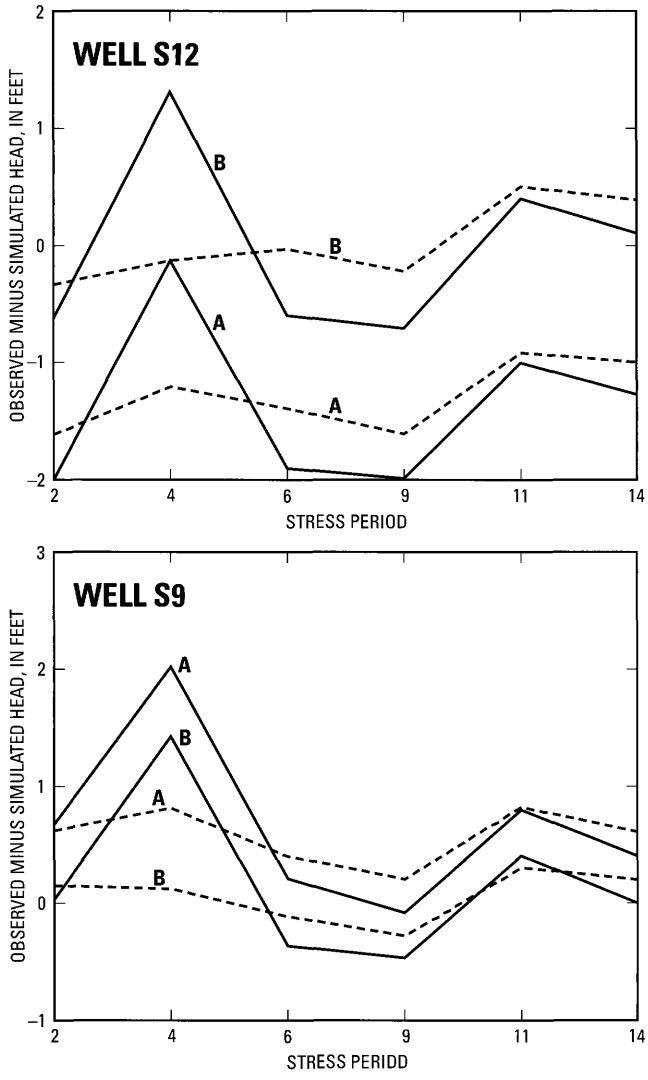

FIGURE 40.—Comparison of model fit for observation wells S9 and S12 as calculated from simulated heads at model grid spacing and from interpolated heads at a finer grid spacing, for six transient-state calibration stress periods. Model location of observation wells is given in table 17.

Water Budgets for Two Upland Settings

Inclusion of the uplands and use of the Variable-Recharge procedure in a model of a valley-fill aquifer is one way of simulating the lateral flow boundary along the valley wall. If the uplands are not explicitly modeled, the ground-water flow and unchanneled surface or shallow subsurface flow across the boundary between the uplands and the valley must be simulated at the perimeter of the valley fill by appropriate boundary conditions that can vary spatially and with time. If the uplands are included in the model and if the Variable-Recharge procedure is applied, then the flows across the valley-wall boundary depend on (1) the magnitude of WAFR, (2) hydrogeologic properties of the uplands and valley fill, and (3) characteristics that govern the magnitude and distribution of upland runoff (items 1 through 6 of the section "Input Information" under "Variable-Recharge Procedure"). The terms of equations 14a-14w are a convenient way of analyzing flow components of the upland water budget. Upland water budgets for models 1 and 3 for each calibration stress period (table 18) are discussed below, to demonstrate the kind of information that can be derived from the Variable-Recharge procedure and how the upland contribution to a valley-fill aquifer can vary under differing conditions. Models 1 and 3 together represent a wide range of upland hydraulic conductivity and are generally representative of the six models described previously.

Surface Runoff.—The partitioning of *WAFR* into surface runoff and areal recharge depends in part on the hydraulic properties of the uplands. In general, the altitude of the upland potentiometric surface is inversely related to hydraulic conductivity (fig. 41). The higher the potentiometric surface, the greater the probability that water levels will reach land surface in some areas, primarily in topographic depressions and on the lower slopes of hillsides, particularly in periods when the rate of *WAFR* is large. The Variable-Recharge procedure simulates surface runoff only from areas in which head is at or above land surface (eq. 13c) or the pseudo land-surface (eq. 13b); consequently, surface runoff will tend to be relatively high in upland areas of low permeability. This is evident in item 4 of table 18, where total surface runoff (*TSR*, eq. 14m) was substantially greater for model 3, in which hydraulic conductivity of till was 0.25 ft/d, than for model 1, in which hydraulic conductivity of till was 4 ft/d. An exception to this relation between surface runoff and hydraulic conductivity can occur during dry periods when the rate of *WAFR* is zero, as discussed below.

The number of seepage cells and the percentage of upland area in which seepage occurred differs among the six stress periods in both models in approximately the same rank order as the total *WAFR* rate (*TWAFR*, eq. 14j), as shown in items 1 to 3 of table 18. The percentage of upland area containing seepage cells ranged from 2 to 10 percent in model 1, and from 17 to 26 percent in model 3. The number of seepage cells for each stress period was considerably higher in model 3 than in model 1 and the total surface runoff in model 3 was 2 to 4 times that in model 1 (table 18, item 4), except for the two dry periods of zero *WAFR* (stress periods 9 and 14) when only outward seepage contributed to surface runoff. The total surface runoff for these dry periods was similar in both mod-

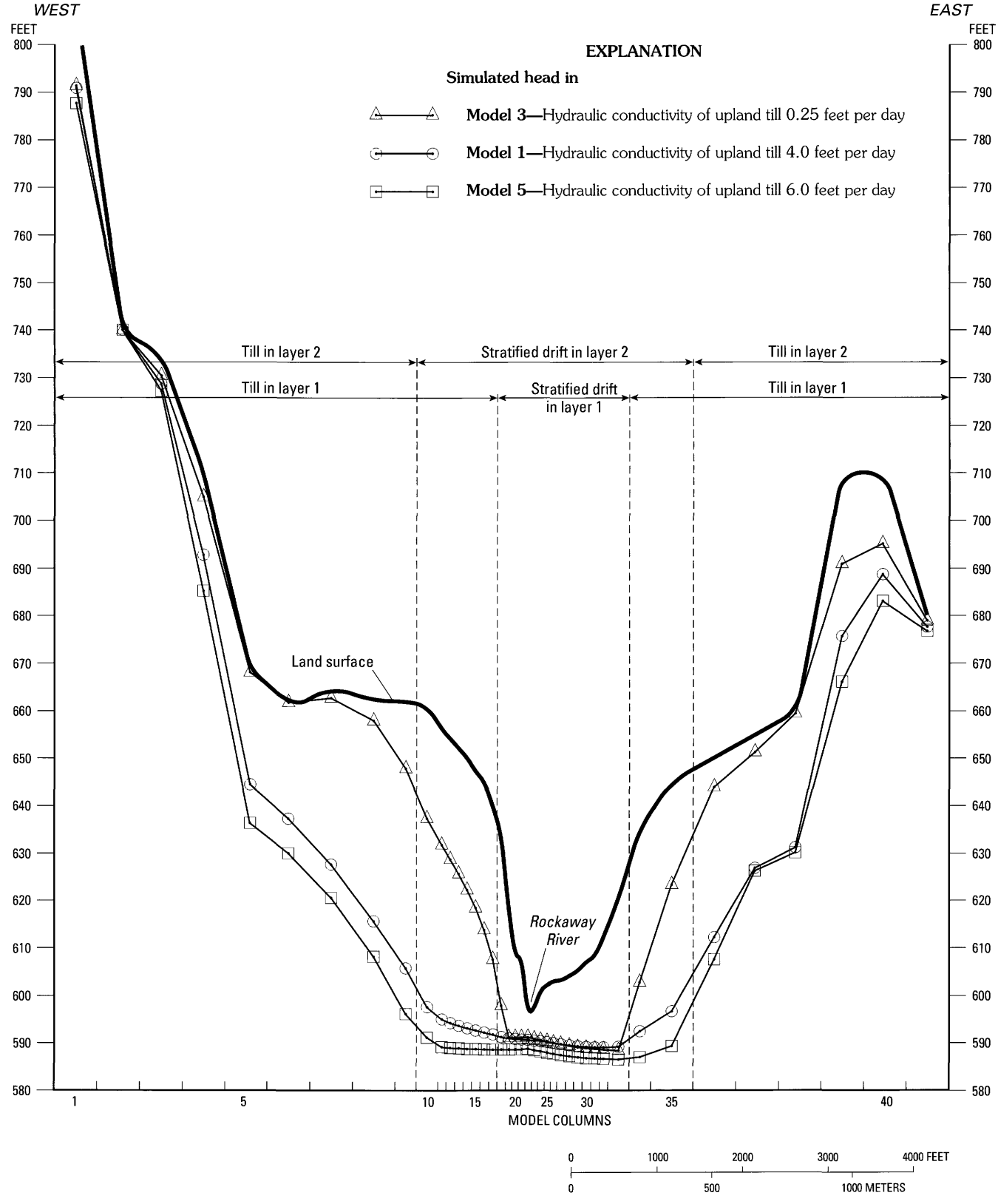

FIGURE 41.—Profiles of land-surface altitude and simulated water levels along model row 14 in layer 1 of Dover models 1, 3, and 5 at end of summer in long-term average transient-state simulation. Differences in water level are primarily a function of differences in hydraulic conductivity assigned to upland till (from Kontis, 1999, fig. 43).

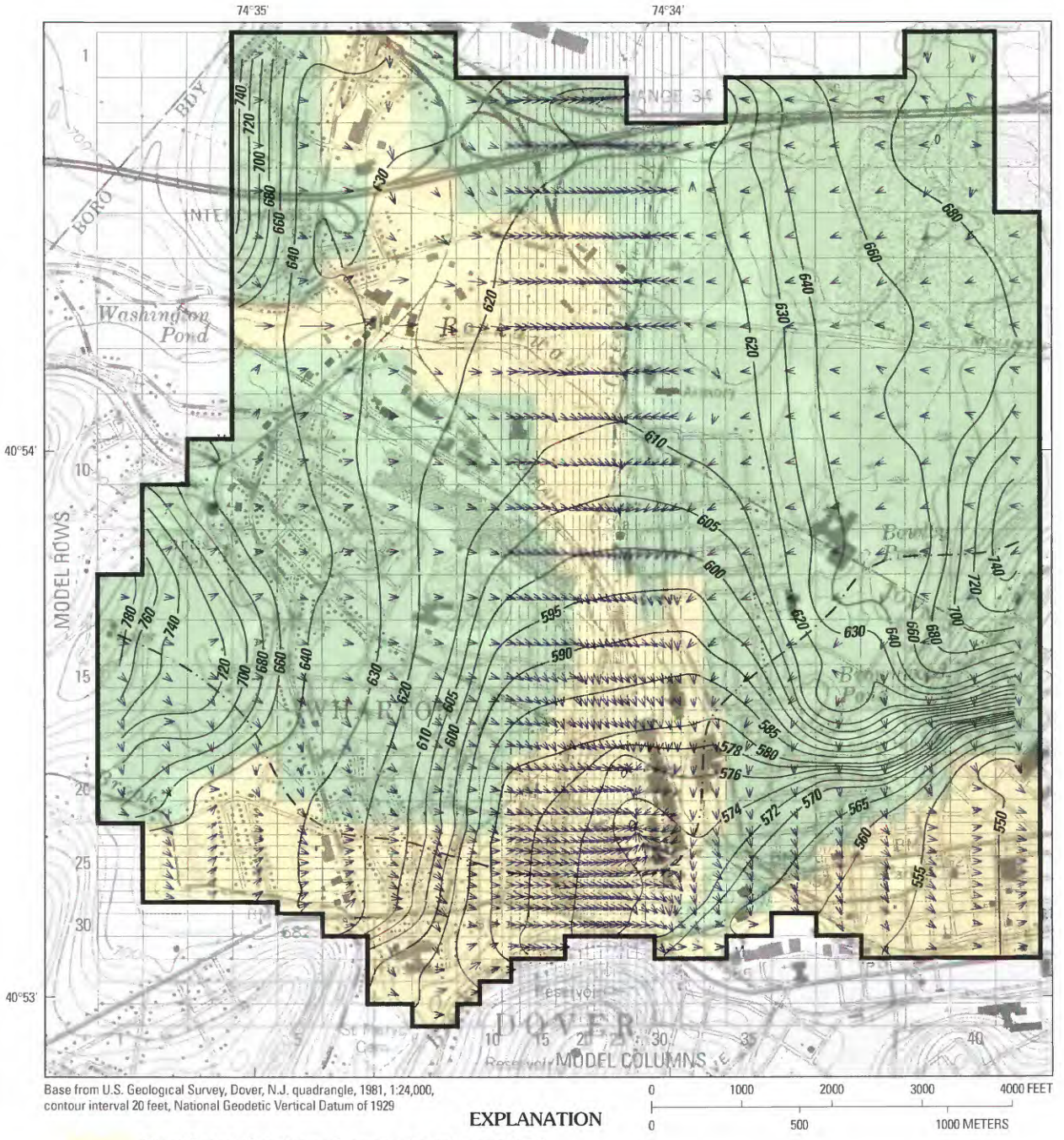

FIGURE 42.—Simulated head and flow direction in layer 1 of Dover model 1 at end of summer under long-term average conditions. Streambed leakage simulated as 0.2 feet per day per foot and hydraulic conductivity of upland till simulated as 4 feet per day (from Kontis, 1999, fig.44).

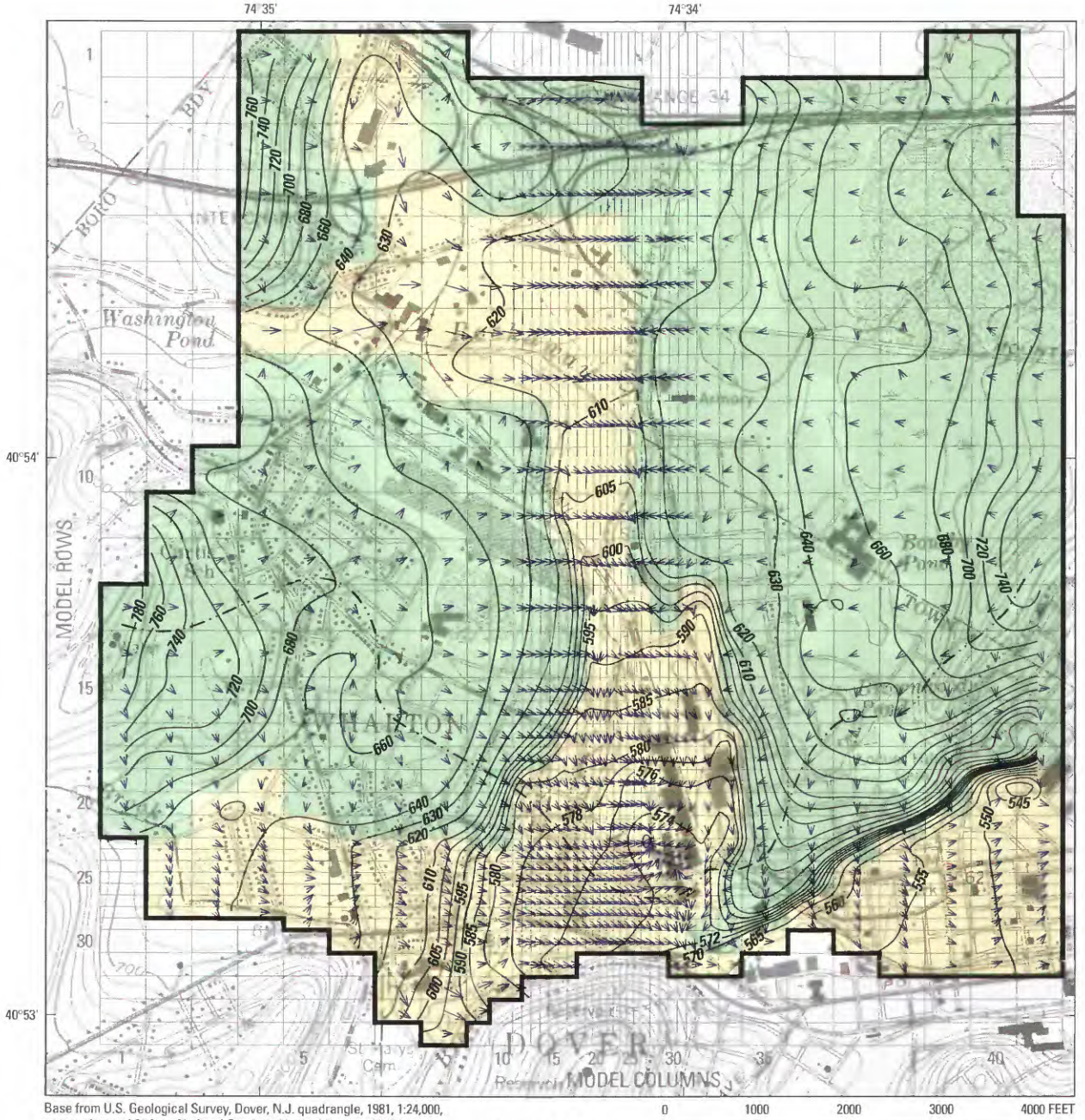

FIGURE 43.—Simulated head and flow direction in layer 1 of Dover model 3 at end of summer under long-term average conditions. Streambed leakage simulated as 0.6 feet per day per foot and hydraulic conductivity of upland till simulated as 0.25 feet per day (from Kontis, 1999, fig.45).

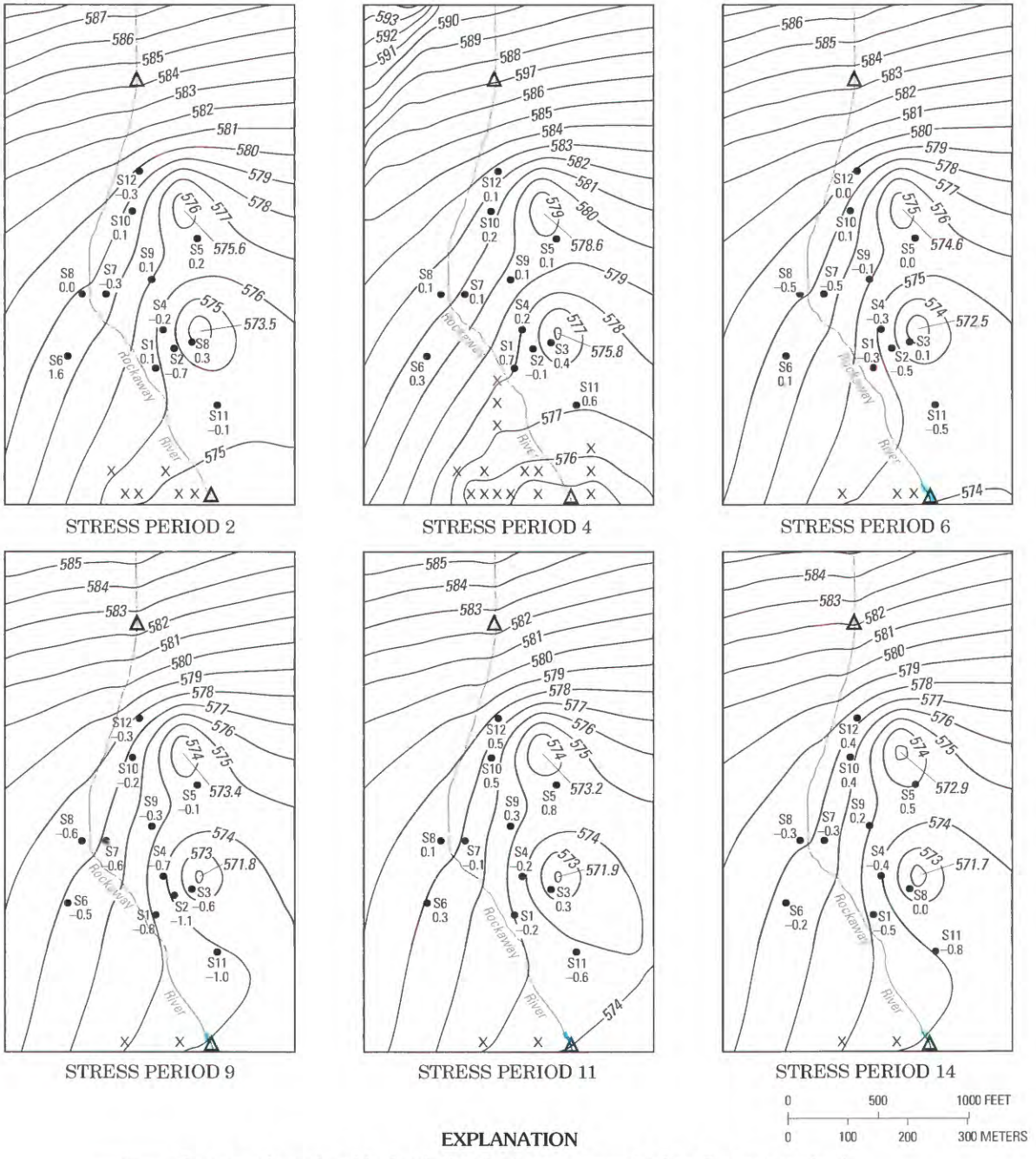

FIGURE 44.—Simulated heads in layer 1 of model 6 within the Dover well-field subregion for six transient-stress periods (location of subregion shown in figure 34). (From Kontis, 1999, fig.40).

TABLE 18.—*Water budgets for uplands and valley fill in Dover models 1 and 3, as simulated for fall 1983 through fall 1985*

[ft^3/s, cubic feet per second; ft/d, feet per day. Dash indicates negligible value]

Item no.	Budget component (terms of equation 14)	Model[a]	Stress period[b] 2	4	6	9	11	14
***A.* Uplands**								
1	Total flow rate of water available for recharge, *TWAFR* (ft^3/s)	1	6.2	124.1	1.8	0	1.5	0
		3	6.2	124.6	1.8	0	1.5	0
Surface runoff								
2	Number of seepage cells	1	21	32	15	8	6	6
		3	82	87	70	54	51	49
3	Seepage area of uplands (percent of upland area)	1	7	10	5	2	2	2
		3	26	26	24	19	18	17
4	Total surface runoff, *TSR* (ft^3/s)	1	1.6	44.8	0.5	0.18[c]	0.2	0.13[c]
		3	4.7	107.6	1.2	0.21[c]	0.8	0.18[c]
5	Proportion of total surface runoff available to recharge the valley fill	1	0.84	0.68	1.00	0.89	1.00	0.92
		3	0.72	0.49	0.75	0.57	0.75	0.60
6	Total available surface runoff, *TASR* (ft^3/s) (item 4 x item 5)	1	1.3	30.4	0.5	0.16	0.2	0.12
		3	3.4	52.7	0.9	0.12	0.6	0.11
Lateral ground-water flow (ft^3/s)								
7	Total net areal recharge, *TNR*	1	4.5	79.3	1.3	0	1.3	0
		3	1.5	17.0	0.6	0	0.7	0
8	Flow from or to (–) upland ponds, *Q*	1	0.30	—	0.4	0.5	0.5	0.5
		3	—	—	—	—	—	—
9	Flow from or to (–) upland storage, *St*	1	–0.4	–71.7	2.0	2.2	0.5	1.8
		3	–0.2	–15.6	0.65	1.3	0.3	1.1
10	Total lateral flow to valley, *TLF* (items 7 + 8 + 9)	1	4.4	7.6	3.7	2.7	2.3	2.3
		3	1.3	1.4	1.2	1.3	1.0	1.1
Unchanneled surface runoff								
11	Total available unchanneled runoff, *TAUR* (ft^3/s)	1	1.3	30.4	0.5	0.16	0.2	0.12
		3	3.4	52.7	0.9	0.12	0.6	0.11
12	Proportion of *TAUR* accepted as recharge to valley fill	1	0.46	0.28	0.80	1.00	1.00	1.00
		3	0.38	0.35	0.33	0.25	0.33	0.18
13	Total unchanneled recharge to valley, *TUR* (ft^3/s) (item 11 x item 12)	1	0.6	8.6	0.4	0.16	0.2	0.12
		3	1.3	18.6	0.3	0.03	0.2	0.02
***B.* Valley fill**								
Inflow (ft^3/s)								
14	Recharge from upland sources (items 10 + 13)	1	5.1	16.2	4.1	2.9	2.5	2.4
		3	2.6	20.0	1.5	1.3	1.1	1.1
15	Recharge from streams	1	2.8	4.1	2.5	3.4	3.8	3.7
		3	4.3	6.2	3.9	5.2	5.5	5.4
16	Direct recharge (areal)	1	2.4	47.0	0.7	0	0.6	0
		3	2.2	43.5	0.7	0	0.6	0
17	Boundary fluxes[d]	1	1.7	1.7	1.7	1.7	1.7	1.7
		3	1.7	1.7	1.7	1.7	1.7	1.7
18	Depletion of storage	1	0.2	—	2.2	1.2	0.5	1.3
		3	0.2	—	3.4	1.1	0.4	1.2
	Total[e]	1	12.1	68.9	11.2	9.2	9.0	9.1
		3	11.0	71.4	11.2	9.3	9.2	9.4
Outflow (ft^3/s)								
19	Pumping and boundary flux[d]	1	6.0	6.0	6.0	6.0	6.0	6.0
		3	6.0	6.0	6.0	6.0	6.0	6.0
20	Discharge to streams	1	3.2	1.8	3.6	2.7	2.3	2.4
		3	4.2	2.5	4.9	2.9	2.7	2.8
21	Seepage	1	2.7	7.6	1.5	0.4	0.4	0.3
		3	0.6	5.2	0.2	0.3	0.2	0.1
22	Accumulation of storage	1	0.1	52.8	—	—	0.3	0.3
		3	0.1	57.2	0.1	—	0.3	0.3
	Total[e]	1	12.0	68.3	11.2	9.1	9.0	9.0
		3	10.9	70.8	11.3	9.2	9.3	9.2
23	Percentage of valley-fill recharge derived from upland sources	1	43	24	37	31	27	27
		3	23	28	14	14	12	12

[a] Hydraulic conductivity of till: model 1, 4 ft/d; model 3, 0.25 ft/d.
[b] Dates are given in table 12.
[c] Surface runoff entirely from outward seepage.
[d] Locations of boundary fluxes are shown in figure 33*B*.
[e] Discrepencies between inflow and outflow and in calculation of some terms are due to round-off and model inaccuracies.

els even though the seepage area for model 3 was greater than in model 1; this is because the magnitude of seepage (eq. 13d) is related to the hydraulic conductivity of the upland material. Thus, the upland hydraulic conductivity of model 1 (4 ft/d) was sufficiently large that the total seepage for these dry periods was about the same as that from the larger seepage area of model 3, which had a much lower hydraulic conductivity (0.25 ft/d).

Total available surface runoff (*TASR*, eq. 14p) for most stress periods (table 18, item 6) was less than the total surface runoff because any surface runoff occurring in urban areas (upland zones 3 and 10, fig. 38) was assumed to be captured by sewers before reaching the valley. Also, the proportion of total surface runoff that was available for recharge to the valley aquifer (table 18, item 5) was smaller in model 3 than in model 1 because a disproportionate number of seepage areas in model 3 were in urban zones. Nevertheless, the total available surface runoff, *TASR*, for model 3 was about 2 to 3 times that of model 1, except during the dry stress periods 9 and 14.

Lateral Ground-Water Flow.—Water that does not run off recharges the uplands; thus, the total net recharge (*TNR*, eq. 14o and table 18, item 7) was greater in model 1 than in model 3. In addition, in model 1 there was flow into the till from upland ponds (fig. 35) in most stress periods ranging from 0.3 to 0.5 ft^3/s (table 18, item 8) because pond elevations were higher than the corresponding model 1 heads. Flow from the ponds to the upland till in model 3 was negligible because simulated heads were near pond elevation. The total net recharge in model 1 changed more than in model 3 from one stress period to the next (table 18, item 7), causing upland heads to generally rise and fall by larger amounts in model 1, over time, than in model 3. Thus, flow into or out of storage also was significantly greater in model 1 than model 3 (table 18, item 9).

Results for stress period 4 (the rainstorm event) illustrate how storage can affect the upland flow system. The chief effect of abundant recharge (*TNR*) in stress period 4 was flow into storage of about 71.7 ft^3/s in model 1 and 15.6 ft^3/s in model 3, rather than a large increase in lateral ground-water flow to the valley (*TLF*, eq. 14s, table 18, item 10). During time periods with little or no *WAFR*, by contrast, flow from storage and from external sources (ponds) was sufficiently large that the lateral ground water flow to the valley exceeded the applied rate of *WAFR*. This occurred in stress periods 6, 9, 11, and 14 of model 1 and stress periods 9 and 14 of model 3. The *TLF*, which ranged from 2.3 to 7.6 ft^3/s in model 1 and from 1.0 to 1.4 ft^3/s in model 3, represents the entire subsurface flow contribution to the valley fill from recharge in the uplands.

Unchanneled Surface Runoff.—The total available unchanneled runoff (*TAUR*, eq. 14r) that was applied to specified cells along the valley wall (fig. 38) in the form of additional *WAFR* is given in item 11 of table 18. No upland tributary streams were simulated in the Dover models (ε of equation 14h was specified to be zero for each upland zone), and all available surface runoff was assumed to be in the form of unchanneled surface runoff. The total amount of unchanneled runoff that was accepted as recharge (*TUR*, eq. 14u) in valley cells is given in table 18, item 13. As formulated in equations 13a-13c, recharge is a function of the relation of head to land surface (or pseudo land surface). In model 1, heads in the valley cells, relative to land-surface elevation, were such that less than half of the unchanneled runoff was accepted as recharge in stress periods 2 and 4 (table 18, item 12), whereas all or most of the unchanneled runoff was accepted as recharge in the stress periods of little or no *WAFR* (6, 9, 11, and 14). In model 3, by contrast, the water table in these same cells was sufficiently high that at least two thirds of the unchanneled runoff was rejected in all stress periods. Most of the rejected runoff occurred adjacent to upland zones 1, 2, and 5 (fig. 38) in valley cells that are characterized by swamps or topographic depressions and by surficial till (figs. 31, 35).

Areas characterized by seasonal saturation (rejection of recharge) could be expected to contain channels that conduct ephemeral runoff away. If application of the Variable-Recharge procedure indicates rejected recharge in a locality where no such channels exist or function, several model modifications can be made. The amount of unchanneled runoff that is applied to that locality can be reduced by decreasing the *WAFR* or the percentage of unchanneled runoff assumed to reach that locality, or by shifting the distribution of unchanneled runoff away from that locality. Alternatively, hydraulic properties could be modified in and downgradient from the locality to lower the heads there. If the locality is swampy, rejected recharge or seepage discharge during the growing season could be interpreted as intense evapotranspiration not accounted for by regional estimates of *WAFR* (eq. 11). Except for the rainstorm event (stress period 4), no field observations were available to confirm the rejected recharge suggested by the simulations. The likelihood of widespread rejected recharge for conditions represented by stress period 4, is supported, however, by observations of a generally high water table and standing water in low-lying areas (J. Dysart, USGS, oral commun. 1985).

Total Recharge from Upland Sources.—Only a part of the surface runoff was available for recharge in some stress periods because some was diverted to sewers in urban subbasins (table 18, item 5), and only a part of the available unchanneled runoff recharged the valley because some was rejected in local areas (table 18, item 12). The magnitude of individual components of runoff and recharge described by equations 14a-14w varied with upland hydraulic conductivity and the rate of *WAFR*. The interaction of these components was such that, except during the rainstorm event (stress period 4), the total upland-derived recharge (TR_{u-v}, eq. 14w) in model 1 (table 18, item 14) was 2 to 2.5 times larger than in model 3.

The amounts of inflow to the valley fill from upland sources, valley streams, direct recharge to the valley fill, boundary fluxes, and storage during periods of decreasing head are given in items 14 through 18 of table 18. These inflows were balanced by outflows from the valley fill to wells and boundaries, to streams, as outward seepage from valley areas where the water table reached land surface, and as flow into storage during periods of rising head, all as given in items 19 through 22 of table 18. The percentage of the simulated inflow to the valley fill that was derived from upland sources is given in item 23 of table 18. Except for the rainstorm event (stress period 4), the upland contribution to recharge to the valley fill in model 1 was about twice that in model 3, in ft^3/s (item 14 of table 18) and in percentage of valley-fill recharge (item 23 of table 18). The same contrast in upland contribution to valley-fill recharge was observed between models 2 and 4, which incorporated the same contrasts in hydraulic conductivity of till and in streambed leakance that distinguished models 1 and 3 (table 15).

The valley recharge from upland sources depicted in table 18 is the result of the complex interaction of various factors. Consider a simpler scenario in which all surface runoff from each upland subbasin is available to recharge the valley ($\rho = 1$ for all subbasins, eq. 14g), is unchanneled ($\varepsilon = 0$ for all subbasins, eq. 14h), and all of this upland runoff is accepted as valley recharge ($\gamma = 1$ for all subbasins, eq. 14u). Thus, total unchanneled recharge and total surface runoff would be the same and upland recharge to the valley (TR_{u-v}, eq. 14w) would consist of total surface runoff plus lateral ground-water flow. The upland recharge to the valley would also equal the total rate of *WAFR* (*TWAFR*, eq. 14j) plus or minus storage flow (S_t) and flow from or to external sources and sinks (Q). Under these conditions, dependence of upland-derived recharge on upland hydraulic conductivity would be through the S_t and Q components only. In a scenario that is the same but with steady-state conditions ($S_t = 0$) and no upland sources and sinks ($Q = 0$), the upland derived valley recharge would be simply *TWAFR* and, therefore, independent of upland hydraulic conductivity.

Significance of Upland Water Budgets.—The upland water budgets for models 1 and 3 in table 18 do not necessarily represent the most probable range of *WAFR* partitioning in the uplands at Dover into unchanneled runoff, lateral ground-water flow, diversion to sewers, etc; rather, they provide an example of (1) how the Variable-Recharge procedure can be used to estimate and allocate recharge from upland sources in a manner consistent with hydrologic concepts and (2) how recharge can vary as a function of simulated hydraulic properties and the rate of *WAFR*. The total upland contribution to valley recharge in models 1 and 3 (table 18, item 14) is the sum of individual flows which if distributed along the valley wall as the boundary condition (specified flux) of a transient-state model that does not explicitly include uplands, should result in essentially the same valley head-distributions as in models 1 or 3.

The study at Dover did not initially contemplate incorporating the uplands and the Variable-Recharge procedure; therefore, no data were collected in upland regions. Nevertheless, topographic data and plausible ranges of hydraulic properties allowed construction of models that estimate the upland contribution to the valley-fill aquifer for several scenarios. If head within the till had been measured at several localities and if information on the magnitude of runoff diversion to sewers had been obtained, the model would have been more constrained and, for some applications, would be more reliable than models that do not incorporate the uplands and rely on crude estimates of the upland-valley fill boundary fluxes.

SENSITIVITY ANALYSIS

The significance of several modeling procedures and assumptions regarding hydrogeologic characteristics was examined by sensitivity analysis. In particular, this section discusses the sensitivity of the six Dover models to changes in streambed leakance and to the hydraulic conductivity of layer 2 in zone 16, the buried channel of unknown composition (fig. 36). It also discusses the sensitivity of model 6 to each of four factors: (1) percentage of unchanneled upland runoff applied to valley cells adjacent to the valley wall, (2) addition of a third model layer representing till beneath the coarse valley-fill deposits, (3) local spatial variations in hydraulic properties of the Rockaway River streambed, and (4) several temporal pumping-rate distributions during a 24-hour period preceding the water-level measurements used in model calibration.

Streambed Leakance

The sensitivity of model 1 heads to a change in the streambed leakance (K/m) of streams in the Rockaway River valley is shown in figure 39. A threefold increase in streambed leakance of model 1, from 0.2 to 0.6 (ft/d)/ft, resulted in a rise in head throughout the Dover well field subregion. Depending on location and stress period, the head increase ranged from 0.5 to 1.7 ft, equivalent to a σ range (eq. 17) of 7 to 24 percent, and head in the aquifer beneath the streambed rose to near stream stage. On the other hand, a threefold decrease in model 3 streambed leakance, from 0.6 to 0.2 (ft/d)/ft, caused a larger change in head. Depending on location and stress period, heads dropped 1.2 to 4 ft, equivalent to a σ range (eq. 17) of 17 to 57 percent. Thus, model sensitivity to a decrease in streambed leakance, from the upper limit of the simulated range (0.6 ft/d/ft) to the lower limit (0.2 ft/d/ft), was about twice the sensitivity to an increase from the lower limit to the upper limit.

In a ground-water flow model in which the only head-dependent inflows and outflows are through streambeds, head response to a change in streambed leakance would be such

that the flow between stream and aquifer remained essentially unchanged. According to equation 6, for a given stream loss (*QRIV*) the difference in head between stream and aquifer is inversely related to streambed leakance. Therefore, a threefold change in streambed leakance would result in a compensating threefold change in the head difference between stream and aquifer. The decrease in aquifer head required to increase the head difference threefold is necessarily a larger number than the increase in head required to decrease the head difference threefold, however. Although the Dover models contain other head-dependent inflow and outflow mechanisms (flow from or to storage, and recharge or seepage as simulated by the Variable-Recharge procedure), this relation partly explains the asymmetric response in head to the imposed changes in streambed leakance. Similar results could be expected from a change in streambed leakance in any model whose head-dependent inflows and outflows are primarily through the streambed.

Increasing the streambed leakance resulted in a rise in aquifer head (fig. 39); thus, calibration of models 3 or 4 in which *K/m* was tripled relative to models 1 or 2 required modifications in other hydraulic properties to lower head. This was done by assigning somewhat lower hydraulic conductivity values to the sand and gravel units of models 3 and 4 than those of models 1 and 2, and lowering the hydraulic conductivity of the upland till from 4 ft/d to 0.25 ft/d (table 16). If the hydraulic conductivity of the uplands had not been reduced, additional reductions in hydraulic conductivity of the sand and gravel of models 3 and 4 would have been necessary to achieve calibration.

The simulated heads and flow directions in layer 1 under long-term average end-of-summer conditions within the Dover well field subregion are shown for models 1, 2, 3, and 4 in figure 45. The models differ primarily in the head configuration in the upland that occupies the northwest corner of the well field subregion, and also in the location of the groundwater divide south of the production wells (fig. 45). Because induced infiltration from the Rockaway River in models 3 and 4 is about three times that in models 1 and 2, the aquifer area from which water flows to the wells is reduced in models 3 and 4, so the divide is closer to the wells.

The tests described above show that simulated heads and flow patterns are potentially quite sensitive to streambed leakance. Because all six Dover models were calibrated to the same array of adjusted observed heads, however, the major difference between the models is in the rate at which water infiltrates from the river into the aquifer rather than in the simulated head or gradient beneath the river. Simulated streamflow losses near the well field were consistently proportional to the streambed leakance specified for each model (table 17*B*). That is, in models 3 and 4, which incorporated a threefold increase in streambed leakance relative to models 1 and 2, the streamflow losses were nearly three times those in models 1 and 2. Likewise, the simulated streamflow losses in models 5 and 6 were about twice those of models 1 and 2 because streambed leakance was twice as great in models 5 and 6.

The fact that all models could be calibrated with comparable accuracy (table 17*A*) indicates that model calibration to the array of measured heads in wells near the Dover well field was insufficient to define the magnitude of streambed leakance. Calibration to accurately measured streamflow loss as well as measured heads would allow the calibration process to define streambed conductance. Thus, if the actual streamflow loss from the Rockaway River in the well field reach were 0.5 to 0.7 ft^3/s, table 17*B* indicates that streambed leakance would be about 0.2 (ft/d)/ft, assuming homogenous conditions throughout the reach. Differences in induced infiltration among models 1 through 6 (table 17*B*) were necessarily balanced by differences in the extent of the cone of depression, and thus in capture of water derived from precipitation on the aquifer and bordering uplands (fig. 45). Thus, calibration to heads in a more extensive array of observation wells and streambed piezometers would constrain the extent of the losing stream reach and the cone of depression enough to indirectly constrain streambed leakance as well.

Hydraulic Conductivity of Bedrock Valley East of Dover Well Field

Zone 16 of layer 2 (fig. 36) represents the unconsolidated sediment that underlies surficial morainal till in the former Rockaway River gorge east of the Dover well field (fig. 32). Hydraulic conductivity of zone 16 in models 1 and 3 was assigned values of 300 and 250 ft/d, representative of coarse-grained deposits, to simulate possible continuity of deltaic sand and gravel through the gorge from the well field vicinity to the southeast corner of the model, and the hydraulic conductivity in models 2 and 4, was assigned a value of 4 ft/d, representative of sandy till, to simulate possible discontinuity in the coarse deposits.

When the hydraulic conductivity of zone 16 of layer 2 in model 1 was decreased from 300 to 4 ft/d, heads in the well field subregion increased (fig. 39). To achieve calibration of models 2 and 4, hydraulic conductivity values within the well field subregion had to be lower than required for models 1 and 3 (table 16), but the magnitude of the differences was moderate; thus, model calibration could not be used to determine if the coarse deposits are continuous through the bedrock gorge. Site-specific information would be needed to prove or disprove continuity.

Recharge from Unchanneled Surface Runoff

As previously discussed, in simulations of valley-fill systems in which only the valley fill is explicitly modeled, recharge that originates in the uplands and reaches the valley is usually represented as specified fluxes or as a head-depen-

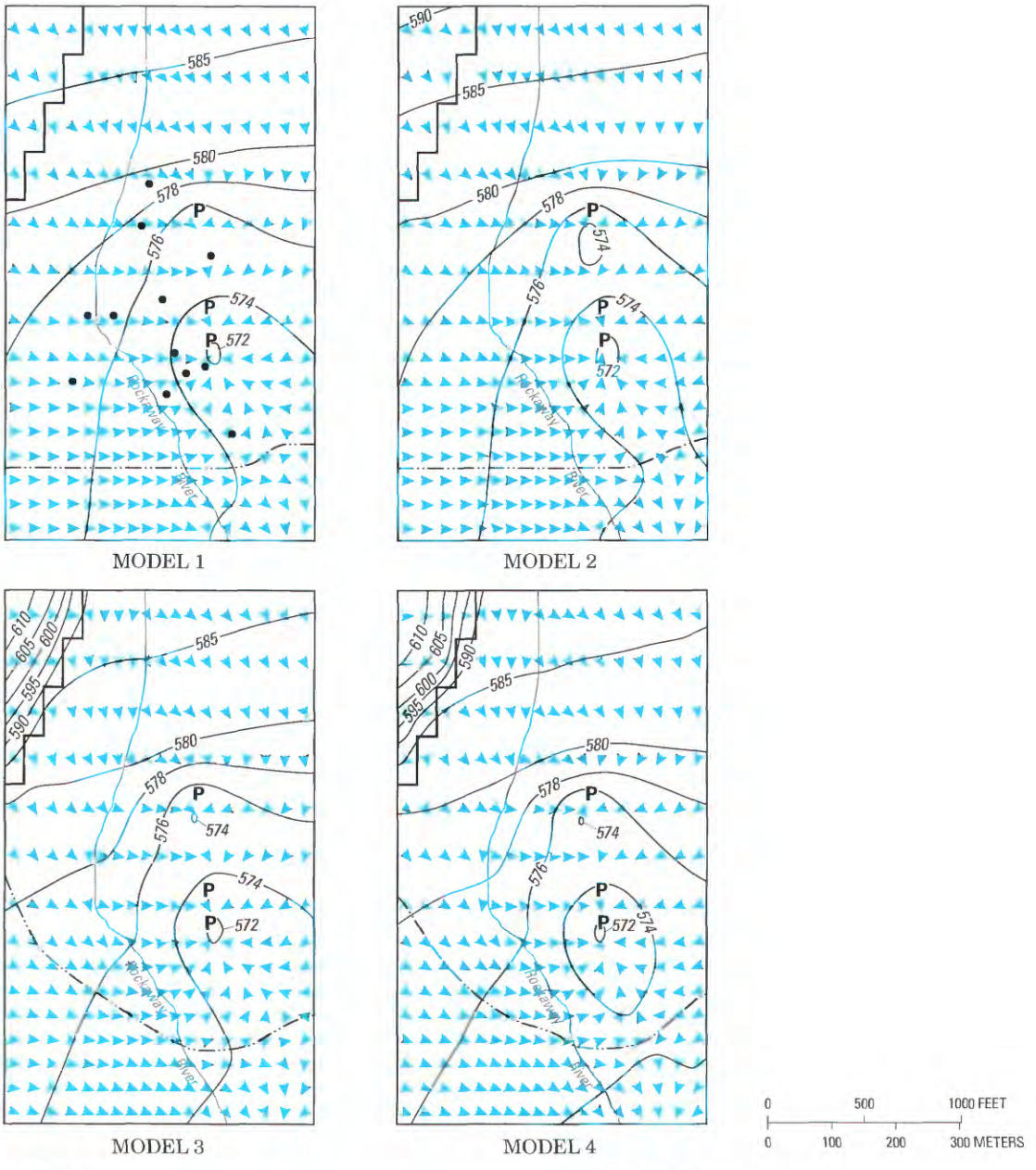

EXPLANATION

- Boundary between uplands and valley
- Inferred divide separating lateral flow toward and away from well field
- —580— Contour of simulated head, in feet
- Rockaway River
- Flow direction for active cells calculated from equation 18
- Observation well
- P Location of production well in layer 2

HYDRAULIC PROPERTIES

Model	Streambed leakance (ft/day/ft)	Hydraulic conductivity (ft/day)	
		Upland till	*Zone 16 of layer 2*
1	0.2	4	300
2	0.2	4	4
3	0.6	0.25	250
4	0.6	0.25	4

FIGURE 45.—Simulated heads and lateral flow directions within Dover well-field subregion in layer 1 of models 1–4 under long-term average end-of-summer conditions. The principal differences in the hydraulic properties of the four models are indicated. Location of zone 16 of layer 2 is shown in figure 36; location of well-field subregion is shown in figure 34.

dent boundary condition applied along the valley wall. This approach can be approximated with the Variable-Recharge procedure, when the uplands are explicitly simulated, by assigning a sufficiently low hydraulic conductivity to upland materials that the resultant upland heads in the upper model layer approach land surface, and therefore virtually all of the upland *WAFR* is rejected and becomes surface runoff that can be distributed to the valley. A measure of model sensitivity to variations in the amount of surface runoff applied at the valley wall was obtained through a series of 2-year transient-state simulations in which the hydraulic conductivity of the till and bedrock (zones 4, 6, 10-13 and 15; fig. 35) was set to 0.001 ft/d and the other hydraulic properties of model 6 (table 16) were used for the stratified drift. The streambed leakance value of 0.4 (ft/d)/ft was chosen to approximate the median of the estimated values at Dover (table 10). Five scenarios were implemented in which 0, 25, 50, 75 and 100 percent, respectively, of the simulated surface runoff was specified as available to recharge the valley fill in the form of unchanneled runoff. All surface runoff emanating from urban areas also was assumed available for unchanneled recharge. Consequently, valley cells bordering the urban upland zones (zones 3, 4, and 10; fig. 38) that previously did not receive unchanneled runoff were allowed to receive runoff from these zones.

The sensitivity of heads to these varying amounts of applied unchanneled runoff is summarized in figure 46, which shows water levels at six model cells containing observation wells; the corresponding adjusted-observed water levels are included for comparison. The zero-percent scenario is analogous to applying a zero-flow boundary condition along the edge of the valley wall (no upland contribution to the valley) resulting in water levels significantly lower than those predicted by model 6 (fig. 46). The stepwise increase in available unchanneled runoff from zero to 100 percent of surface runoff is analogous to a sequence of simulations in which the magnitude of the specified fluxes are correspondingly increased along the edge of the valley fill. As would be expected, water levels increased as the amount of unchanneled runoff at the edge of the valley wall increased. The difference in water levels between the two extremes (0 and 100 percent of available surface runoff) ranged from about 1 ft to about 4.5 ft, depending on the rate of *WAFR*, stress period, and location of the model cells. In terms of equation 17, the σ sensitivity values ranged from about 7 percent to 30 percent. Thus, significant model errors can occur if a zero-flow boundary condition is imposed at the valley wall when, in fact, there is an upland contribution to the valley fill.

For purposes of discussion, the scenario in which 100 percent of surface runoff was applied to the valley fill is designated as model 6x. Simulated water levels of model 6x were slightly lower than model 6 in stress period 2, considerably higher in stress period 4, and considerably lower for the remaining stress periods. This pattern can be explained by an analysis of the upland water budgets of the respective models (table 19). Upland heads in model 6x changed very little over time because net recharge to the uplands was negligible (table 19, item 3) and therefore flow from or to storage (table 19, item 5) or from or to upland ponds (table 19, item 4) also was virtually zero, resulting in negligible lateral ground-water flow to the valley fill (table 19, item 6). In addition, the low hydraulic conductivity of the uplands resulted in zero or negligible outward seepage, despite the high water table; thus, the upland water for each stress period in model 6x was entirely in the form of unchanneled runoff (table 19, item 7) equivalent to the rate of *WAFR* (table 19, item 1). As in models 1 and 3 (table 18), only a part of the unchanneled runoff applied to the valley became recharge (table 19, item 8); the rest was rejected, primarily in swamp or marsh areas. In model 6, unlike model 6x, a large fraction of the *WAFR* infiltrated the uplands in stress periods with non-zero *WAFR* (table 19, item 3), and flow from storage and ponds occurred (table 19, items 4 and 5). Thus, in model 6 lateral ground-water flow from the uplands to the valley occurred in all stress periods. In both models some unchanneled runoff was not accepted as recharge, whereas in model 6 all of the lateral ground-water flow was accepted, so the upland contribution to valley recharge was greater in model 6 than in model 6x for all stress periods except the high precipitation event of stress period 4 (table 19, item 10). In stress period 4, the amount of upland available runoff was significantly larger in model 6x (table 19, item 7) and even though only a part of this runoff was received as recharge (table 19, item 8) the amount of recharge to the valley fill of model 6x was 33 ft^3/s larger than in model 6 (table 19, item 9). The pattern of the hydrographs of figure 46 reflects that of the recharge from the uplands.

As discussed earlier, the amount of unchanneled upland runoff that recharges the valley fill depends in part on the hydraulic properties of the valley fill. A significant amount of the recharge rejected by cells designated to receive upland unchanneled runoff in model 6x (table 19, item 8) occurred in valley cells containing till deposits adjacent to Variable-Recharge upland zones 1 and 2 (fig. 38) that were simulated with a very low hydraulic conductivity. The effect of an increase of hydraulic conductivity in this area (till zone 6, fig. 35) from 0.001 ft/d to 10 ft/d, a value representative of sandy till, is illustrated in table 19, in the model 6xx entries. The increased hydraulic conductivity caused lower water levels in the cells receiving the runoff and therefore an increase of unchanneled recharge (table 19, items 9 and 10), ranging from 0.3 ft^3/s (stress period 11) to 1.8 ft^3/s (stress period 4).

Addition of a Third Model Layer

The relatively permeable materials of stratified-drift aquifers commonly overlie lacustrine deposits of low permeability, or till or bedrock. Flow to or from the materials of low permeability is generally assumed to be negligible. In the Dover simulations, this assumption was invoked for the

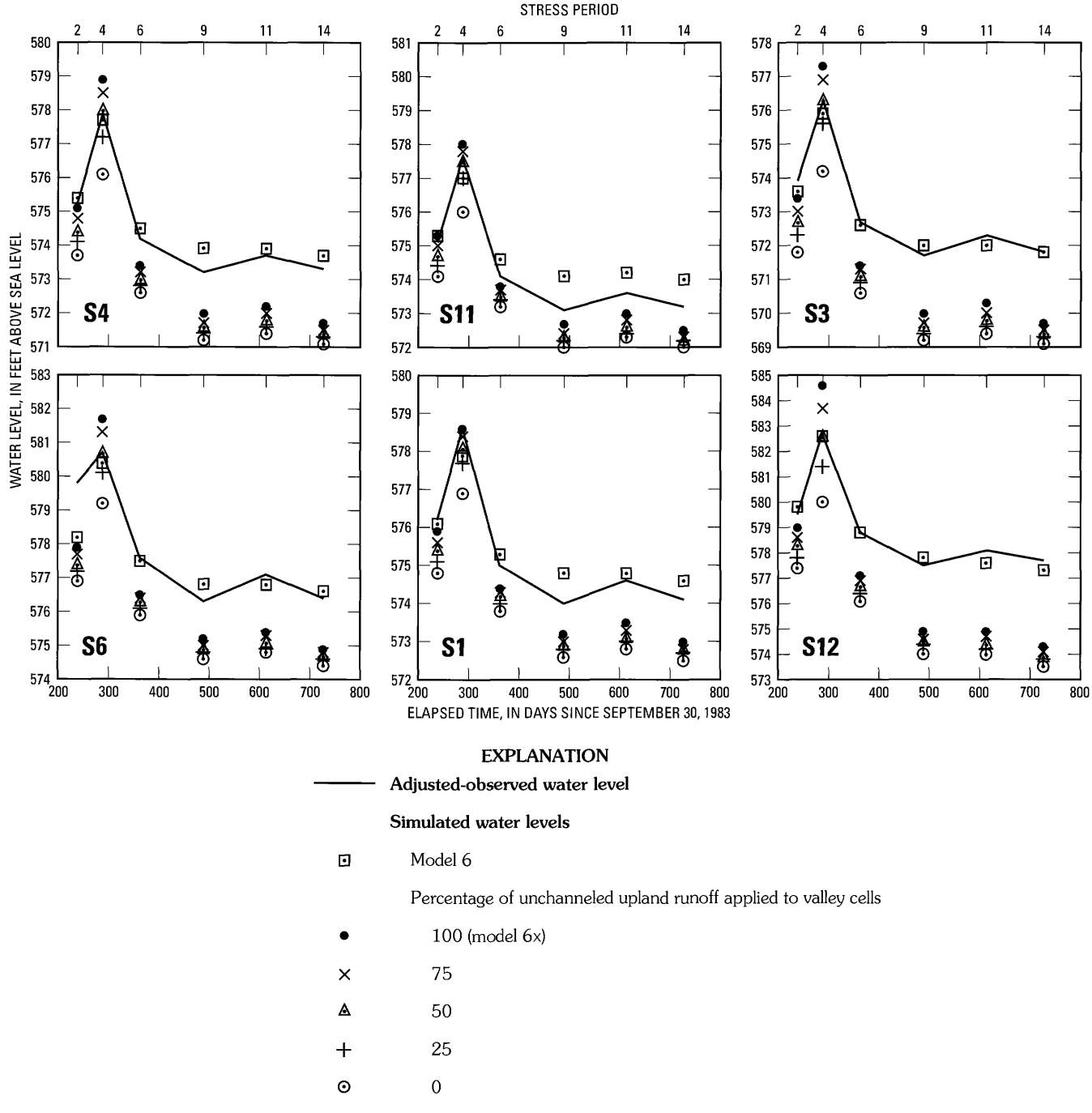

FIGURE 46.—Sensitivity of head in layer 1 of Dover model 6 to change in percentage of upland unchanneled runoff applied to valley cells along valley wall. Percentage of runoff applied was varied from 0 to 100. Also shown are the adjusted observed water levels and simulated water levels resulting from calibration of model 6. Simulated water levels represent cells that contain the indicated observation wells. Well locations are shown in figure 44.

boundary between the coarse stratified drift (layer 2) and a 35- to 45-ft-thick unit of silt and fine sand with some clay that overlies crystalline bedrock (fig. 33).

The effects of this assumption were investigated through five simulations that used the hydraulic properties of model 6 (table 16) and stresses for long-term average end-of-summer conditions (table 12) but added an additional lower layer with an assumed thickness of 35 ft. Four of these simulations (6a, 6b, 6c, 6d, table 20) assigned the additional layer the same horizontal hydraulic conductivity as till, 6 ft/d, equivalent to a transmissivity of 210 ft/d, except in areas of bedrock. The vertical hydraulic conductivity of the additional layer was

varied from 6 ft/d to 6 x 10^{-4} ft/d. As shown in table 20, the sensitivity of model heads to vertical hydraulic conductivity of the added layer ranged from 0.36 ft to 0.05 ft in simulations 6a through 6d. A horizontal hydraulic conductivity value of 0.25 ft/d, the assumed hydraulic conductivity of the bedrock, with a vertical hydraulic conductivity of 0.025 ft/d, resulted in heads virtually identical to those of model 6 (simulation 6e, table 20). The sensitivity to the additional layer according to equation 17 was 4 to 5 percent for simulations 6a, 6b, and 6c and less than 1 percent for simulation 6d. Thus, model 6 was moderately sensitive to the presence of an additional layer of moderate transmissivity except when the vertical hydraulic conductivity of the added layer was extremely low. At low transmissivity values (simulation 6e), model 6 was insensitive to an additional layer irrespective of the vertical anistropy. The significance of these results is discussed further in a similar sensitivity analysis of the Wooster, Ohio model.

Heterogeneity of Streambed Hydraulic Properties

In simulations of stream-aquifer interaction, the hydraulic properties of the streambed (eq. 10), at the scale of the model, are commonly assumed to be homogeneous, although depositional and erosional processes that govern the distribution and characteristics of streambed materials undoubtedly create some degree of heterogeneity. Model errors can arise if streambed leakance (K/m) is relatively homogeneous but the simulated value of K/m differs from its actual value, or if the actual streambed leakance varies spatially along the stream reach in question but is simulated with a constant value of K/m. A measure of model sensitivity to both types of error was obtained from twelve simulations, all of which used the hydraulic conductivity values of model 6 (table 16) and the long-term average stresses (table 12). In two simulations, the model-6 value of streambed leakance, 0.4 (ft/d)/ft, was increased, and then decreased, by 50 percent. In 10 other simulations, streambed leakance values of river cells along the reach of the Rockaway River adjacent to the Dover well field were assumed to have a uniform distribution over the range 0.2 (ft/d)/ft to 0.6 (ft/d)/ft according to the relation,

$$(K/m)_{i,j} = (K/m)_u(RN_{i,j} + 0.5), \qquad (19)$$

where, $(K/m)_u$ is the mean value of the uniform distribution, 0.4 (ft/d/)ft, and

RN is a random number, $0 \leq RN \leq 1$, so that $0.2 \leq (K/m) \leq 0.6$ for each river cell with model row and column coordinates i, j.

Thus, depending on the value of the random number RN, the value of K/m for a particular cell can take on any value between 0.2 (ft/d)/ft and 0.6 (ft/d)/ft with equal probability—that is, independent of the streambed leakance of adjacent cells. The set of values obtained by applying equation 19 to each of the cells along the simulated stream reach is termed a randomization. A longitudinal profile of streambed leakances for a particular randomization consists of random oscillations about the mean value of the distribution. The mean value of the oscillations (sample mean) for a particular randomization would probably differ from the mean value of the distribution, 0.4 (ft/d)/ft, but over a large number of randomizations the sample mean value would approach the mean value of the distribution.

Results of the twelve simulations are presented in figure 47, which shows simulated heads at the end of summer in layer 1 beneath the river reach in which streamflow loss was measured adjacent to the well field. As noted earlier, model sensitivity to changes in the simulated value of K/m can be highly asymmetric. Thus as shown in figure 47, when streambed leakance in all river cells was increased 50 percent, from 0.4 to 0.6 (ft/d)/ft, simulated heads were 0.1 to 1 ft higher than calibrated model-6 heads (a σ sensitivity range (eq. 17) of 1 to 14 percent); but when leakance was decreased 50 percent, from 0.4 to 0.2 (ft/d)/ft, simulated heads were 1.3 ft to more than 4 ft lower than the model-6 heads (a σ sensitivity range of 19 to 57 percent). Also, the simulated streamflow loss (table in fig. 47) was about 17 percent greater than in model 6 for a K/m of 0.6 (ft/d)/ft and about 40 percent less than in model 6 for a K/m of 0.2 (ft/d)/ft. Thus, simulated streamflow loss was much more sensitive to a uniform decrease in K/m than to an increase of equal magnitude. As this and previous examples have shown, if the streambed leakance is homogeneous, errors resulting from a K/m value that deviates from the actual value can be significant because all cells would be affected by a similar bias.

The simulations based on the 10 separate randomizations of K/m according to equation 18 resulted in head differences (relative to heads in model 6) of about 0.1 ft to 0.6 ft (fig. 47), a σ sensitivity range of 1 to 9 percent. The difference in streamflow loss for these simulations relative to that of model 6 ranged from +0.15 ft^3/s to -0.13 ft^3/s or about $\pm$10 percent. The range of these variations in simulated head and streamflow loss would increase somewhat if the number of randomizations were increased or if the upper and lower bounds of the allowed perturbations were increased. Nevertheless, the results demonstrate that if the streambed leakance is in fact heterogeneous within a reach, but is simulated as being homogenous, the resultant error would probably be relatively small if the streambed leakance value is representative of the mean of the heterogeneities. Model error could be relatively large, however, if the simulated streambed leakance value differs considerably from the mean value of the heterogeneous streambed leakances or if the magnitude of local heterogeneities are large.

TABLE 19.—*Water budgets for uplands and valley fill in Dover model 6 and sensitivity models 6x and 6xx, as simulated for fall 1983 through fall 1985*

[ft^3/s, cubic feet per second; ft/d, feet per day. Dash indicates negligible value. Minor discrepencies between total inflow and total outflow, and between some other terms and their components, are due to round-off errors and to inaccuracies in calculation by the model]

Item no.	Budget component (terms of equation 14)	Model[a]	Stress period[b] 2	4	6	9	11	14
***A.* Water budget for uplands**								
1	Total rate of water-available-for-recharge, *TR* (ft^3/s)	6, 6x	6.1	123.5	1.8	0	1.5	0
2	Total surface runoff, *TSR* (ft^3/s)	6	2.1	44.0	0.9	0.5[c]	0.5	0.4[c]
		6x	6.1	123.5	1.8	0	1.5	0
	Lateral ground-water flow (ft^3/s)							
3	Total net areal recharge, *TNR*	6	4.0	79.5	0.9	–0.5	1.0	–0.4
		6x	—	—	—	0	—	0
4	Flow from or to upland ponds, *Q*	6	0.7	0.1	0.8	1.0	1.0	1.0
		6x	—	—	—	—	—	—
5	Flow from (+) or to (–) upland storage, *St*	6	–0.4	–72.1	1.9	2.1	0.4	1.7
		6x	—	—	—	—	—	—
6	Total lateral flow to valley, *TLF* (items 3 + 4 + 5)	6	4.3	7.5	3.6	2.6	2.4	2.3
		6x, 6xx	—	—	—	—	—	—
	Unchanneled surface runoff							
7	Total available unchanneled runoff, *TAUR* (ft^3/s)	6	1.9	30.9	0.9	0.5	0.5	0.4
		6x	6.1	123.5	1.8	0	1.5	0
8	Proportion of *TAUR* that recharges the valley	6	.37	.25	.56	.80	.80	.75
		6x	.52	.33	.55	—	.53	—
		6xx	.67	.34	.78	—	.73	—
9	Total unchanneled recharge to valley, *TUR* (ft^3/s)	6	0.7	7.6	0.5	0.4	0.4	0.3
	(item 7 x item 8)	6x	3.2	40.6	1.0	—	0.8	—
		6xx	4.1	42.4	1.4	—	1.1	—
***B.* Water budget for valley fill**								
	Inflow (ft^3/s)							
10	Recharge from upland sources (*TLF* + *TUR*)	6	5.0	15.1	4.1	3.0	2.8	2.6
		6x	3.2	40.6	1.0	—	0.8	—
		6xx	4.1	42.4	1.4	—	1.1	—
11	Recharge from streams	6	4.5	4.7	4.4	5.6	6.0	5.9
		6x	5.4	4.4	5.5	6.3	6.5	6.4
		6xx	5.4	4.1	5.5	6.4	6.5	6.4
12	Direct recharge (areal)	6	2.4	43.7	0.7	0	0.6	0
		6x	2.1	37.2	0.6	0	0.5	0
		6xx	2.3	39.5	0.7	0	0.6	0
13	Boundary flux[d]	6, 6x, 6xx	0.5	0.5	0.5	0.5	0.5	0.5
14	Storage	6	0.2	—	2.2	0.9	0.3	0.9
		6x	0.1	—	2.4	1.3	0.3	1.3
		6xx	0.2	—	2.5	1.5	0.3	1.5
	Total inflow	6	12.6	64.1	12.0	10.0	10.2	9.9
		6x	11.4	82.7	10.0	8.2	8.6	8.2
		6xx	12.5	86.6	10.6	8.4	9.1	8.5
	Outflow (ft^3/s)							
15	Pumping and boundary flux[d]	6, 6x, 6xx	6.0	6.0	6.0	6.0	6.0	6.0
		6	5.1	4.1	5.5	3.8	3.7	3.7
16	Discharge to streams	6x	3.9	3.8	3.7	2.1	2.2	2.0
		6xx	4.7	4.2	4.4	2.5	2.8	2.4
		6	1.5	9.8	0.4	0.2	0.3	0.1
		6x	1.4	18.4	0.2	—	—	—
17	Seepage	6xx	1.7	19.9	0.2	—	—	—
		6	—	43.3	—	—	0.2	0.2
18	Storage	6x	—	54.2	—	—	0.3	0.1
		6xx	—	56.2	—	—	0.3	0.1

TABLE 19.—*Water budgets for uplands and valley fill in Dover model 6 and sensitivity models 6x and 6xx, as simulated for fall 1983 through fall 1985*—Continued

[ft^3/s, cubic feet per second; ft/d, feet per day. Dash indicates negligible value. Minor discrepencies between total inflow and total outflow, and between some other terms and their components, are due to round-off errors and to inaccuracies in calculation by the model]

Item no.	Budget component (terms of equation 14)	Model[a]	Stress period[b] 2	4	6	9	11	14
	Total outflow	6	12.7	63.2	12.0	10.0	10.2	10.0
		6x	11.3	82.4	9.9	8.1	8.5	8.1
		6xx	12.4	86.3	10.6	8.5	9.1	8.5
19	Percentage of valley-fill recharge derived from upland sources	6	40	24	35	30	27	26
		6x	29	49	10	—	9	—
		6xx	33	49	13	—	13	—

[a] In model 6x, hydraulic conductivity of till is 0.001 ft/d, and all upland surface runoff is applied to cells along the valley wall; otherwise it has the properties of model 6, where hydraulic conductivity of upland till is 6 ft/d. Model 6xx is same as model 6x except that hydraulic conductivity of zone 6, layer 1 (fig. 35) is increased from 0.001 to 10 ft/d to illustrate the effect on unchanneled recharge at valley wall.
[b] Dates are given in tables 12 and 13.
[c] Surface runoff entirely from outward seepage; hence negative *TNR* in item 3.
[d] Locations of boundary fluxes are shown in figure 34.

TABLE 20.—*Sensitivity of simulated head in Dover model 6 to variation in horizontal and vertical conductivity of lower layer added to model*

[ft, feet; ft/d, feet per day; ft^2/d, feet squared per day]

	Simulation 6a	6b	6c	6d	6e
***A.* Hydraulic properties of added lower layer (layer 3)**					
Horizontal hydraulic conductivity (ft/d)					
Bedrock	0.25	0.25	0.25	0.25	0.25
Upland till	6	6	6	6	0.25
Valley fill	6	6	6	6	0.25
Transmissivity (ft^2/d)[a]					
Bedrock	8.75	8.75	8.75	8.75	8.75
Upland till	210	210	210	210	8.75
Valley fill	210	210	210	210	8.75
Vertical hydraulic conductivity (ft/d)[b]	6	0.6	0.06	0.0006	0.025
***B.* Model response**					
Average increase in simulated head (ft) relative to head in two-layer model in 13 cells in layers 1 and 2 that contain observation wells, at end of summer under long-term average conditions	0.36	0.32	0.28	0.05	0.0

[a] Transmissivity calculated from hydraulic conductivity, assuming a layer thickness of 35 ft.
[b] Vertical leakance between layers 2 and 3, calculated as vertical hydraulic conductivity of layer 3 divided by layer thickness of 35 ft.

Temporal Distribution of Pumping Rates

The Dover 2-year transient-state models were discretized into 8 relatively long stress periods and 6 short stress periods (table 12). The short stress periods (1 to 2 days) coincide with dates when water levels used in model calibration were measured, and thus allow simulation of stresses that could have affected the measured water levels. As previously discussed, water-level measurements acquired under differing pumping conditions were adjusted to a standard pumping condition. The simulated pumping rates for short stress periods at the three production wells (table 12) were based on the pumpage, averaged over 24 hours, that was representative of the assumed standard pumping condition (Kontis, 1999). To obtain a measure of model sensitivity to changes in the magnitude and distribution of the short-stress-period pumping rates, several pumping scenarios for the last 24 hours of the 2-

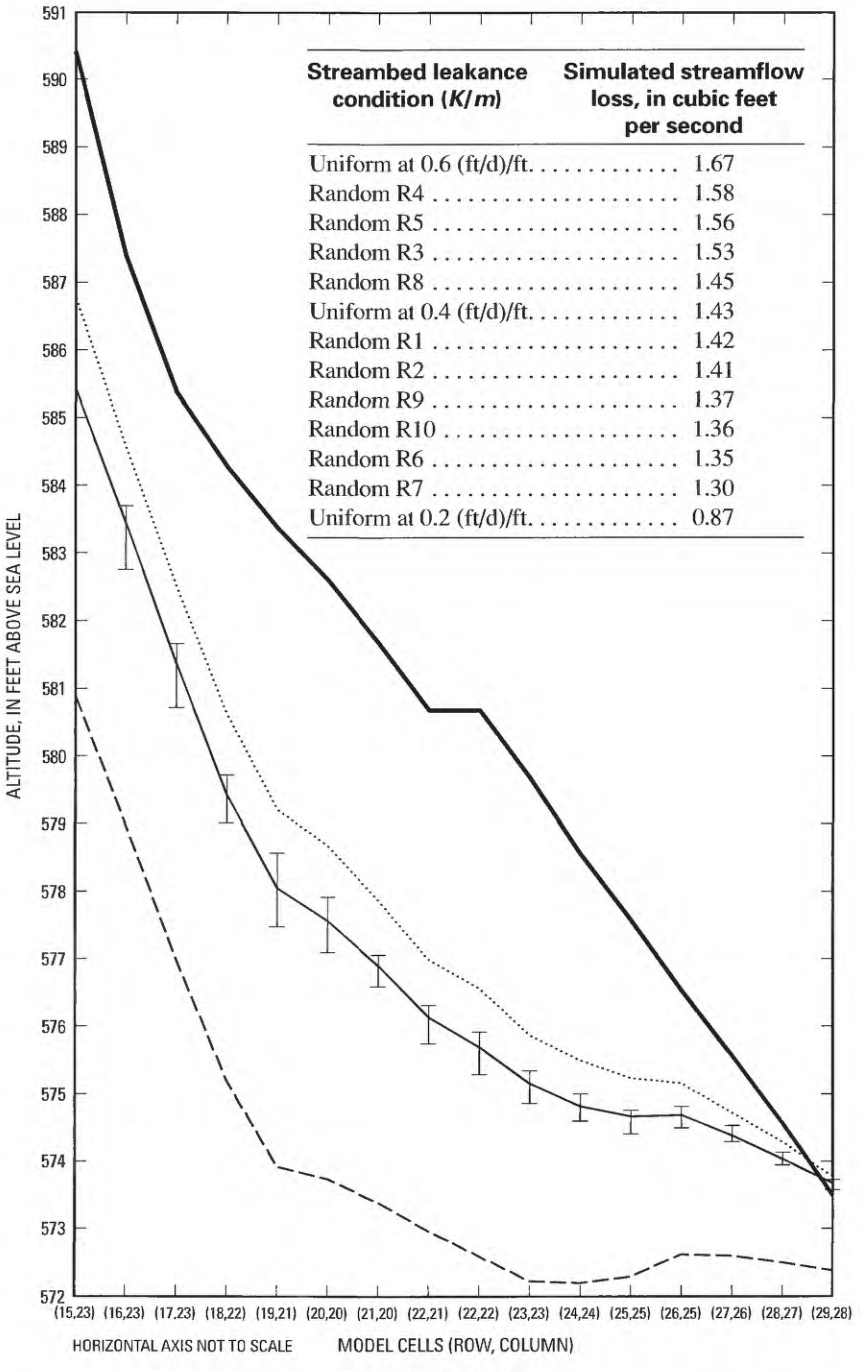

FIGURE 47.—Sensitivity of head in cells beneath the Rockaway River in layer 1 of Dover model 6 to a 50-percent increase and a 50-percent decrease in a uniform streambed leakance (K/m) of 0.4 foot per day per foot, and to 10 randomizations of streambed leakance within the range 0.4 foot per day per foot ±50 percent for long-term average end-of-summer conditions. Base of streambed is 5.1 feet below stream surface in all simulations.

year simulation (stress period 14) were simulated. For these simulations, the last 24 hours was divided into two 12-hour stress periods.

North-south and east-west profiles through the well field (fig. 48) show head in layer 2 of model 6 at the end of the 2-year simulation, for each scenario. The pumping rate of each well in scenario 5 was the same as in model 6, whereas the pumping rates in scenario 1 were set to zero so simulated heads would approximate ambient natural conditions. Thus, for any scenario in which simulated pumpage was less than specified for model 6, heads could be expected to fall somewhere between profiles for scenarios 1 and 5. The pumping rate in scenario 2 was half that of model 6. The pumping rates in scenarios 4 and 3 were those of model 6, but were applied only during the first and second 12-hour periods, respectively. The resultant heads from scenarios 2, 3, and 4 indicate that, although the average of pumping rates over each of the 24-hour periods were the same, heads differed substantially, depending on how the pumping was distributed through time. To the extent that the hydraulic properties of this model are representative of valley-fill systems in general, these results indicate that (1) model heads can be sensitive to changes in short-term pumping rates, and (2) if there are variations in pumping rate over the duration of a stress period, significant errors can occur even if the average pumping rate is correctly simulated. Consequently, the characteristics of the pumping-rate distribution prevailing before and during the measurement of water levels used in model calibration should be considered in designing model stress periods.

BURIED-VALLEY AQUIFER BENEATH KILLBUCK CREEK NEAR WOOSTER, OHIO

A finite-difference ground-water flow model was developed to represent Killbuck Creek valley and adjacent uplands near the city of Wooster in northeastern Ohio (fig. 1). The modeled area encompasses 30 mi^2 west of the city (fig. 49). Killbuck Creek valley in this vicinity is primarily agricultural. Two well fields, referred to herein as the north well field and the south well field (fig. 49), supply water for a population (in 1990) of about 23,000 (Breen and others, 1995).

HYDROLOGIC SETTING

Killbuck Creek valley is incised in interbedded shale, sandstone, and siltstone of the Cuyahoga and Logan formations that form the adjoining uplands (fig. 50*A*) and are capped by till of variable thickness. The uplands have a maximum relief of about 350 ft with relatively steep valley-wall slopes (fig. 49). Killbuck Creek valley contains an aquifer that is composed of stratified deposits of sand and gravel interbedded with discontinuous layers of silty clay, and is confined by an overlying surficial layer of silt, clay, and some fine sand partly of lacustrine and partly of alluvial origin (fig. 50*A*). The surficial confining layer is 20 to 30 ft thick and grades to permeable gravel and sand of alluvial-fan origin where tributaries enter the valley. Thus, the Killbuck Creek valley aquifer has characteristics of a buried aquifer (fig. 28 or 29), although the confining layer is thinner than those that overlie most buried aquifers. As discussed in the earlier section, "Simulation of Aquifer Types," the simulation of a buried aquifer is virtually the same as simulation of a valley-fill aquifer if the overlying fine-grained material is explicitly modeled. The stratigraphy of the valley sediments and the upland bedrock was represented, for simulation purposes, as three layers (fig. 50*B*).

Major surface-water features within Killbuck Creek valley include Killbuck Creek (drainage area of 115 mi^2), three tributaries—Little Killbuck, Clear Creek and Apple Creek—and several artificial ponds. Within the valley, the channels of Killbuck and Apple Creeks are incised mainly in silt and clay deposits, whereas the channels of Little Killbuck and Clear Creeks are incised mainly in alluvial-fan deposits.

The bedrock geology has been described by Conrey (1921) and Multer (1967), and the glacial geology by White (1967). Aspects of the hydrogeology are given in Beer (1894), Jones and others (1958), Miller (1976), Mayhew (1985), Springer (1987 and 1990), Breen (1988), and Breen and others (1995). An electrical-resistivity survey south of the south well field is described by Miller (1975). Springer and Bair (1990) analyzed ground-water flow at the north and south well fields using a combination of the Theis equation and image-well theory to compute drawdown from predevelopment potentiometric surfaces at uniformly spaced points (400 ft for the north well field and 250 ft for the south well field). Springer (1990) and Springer and Bair (1992) reported on a comparison of the various methods of delineating well-field protection areas. Additional information regarding the hydrogeology, including documentation of field data collected by the U.S. Geological Survey during the course of the study, and details regarding the ground-water flow model discussed herein, are presented in Breen and others (1995).

MODELING STRATEGY

A steady-state model representative of conditions prevailing during the fall of 1984 was developed. The plausibility of the steady-state model hydraulic properties was tested by a transient-state simulation of an 11-day recharge event that occurred in late February 1985. The simulated steady-state heads were used as the initial heads for the transient-state simulation.

Water levels in 13 observation wells near the north well field (fig. 49) were measured by the USGS from July 1984 through September 1985, at time intervals ranging from about 1 week to 2 months, and by Springer (1987) from April through December 1986, at about 1-month intervals. A series of test wells were drilled in the south well field area, under

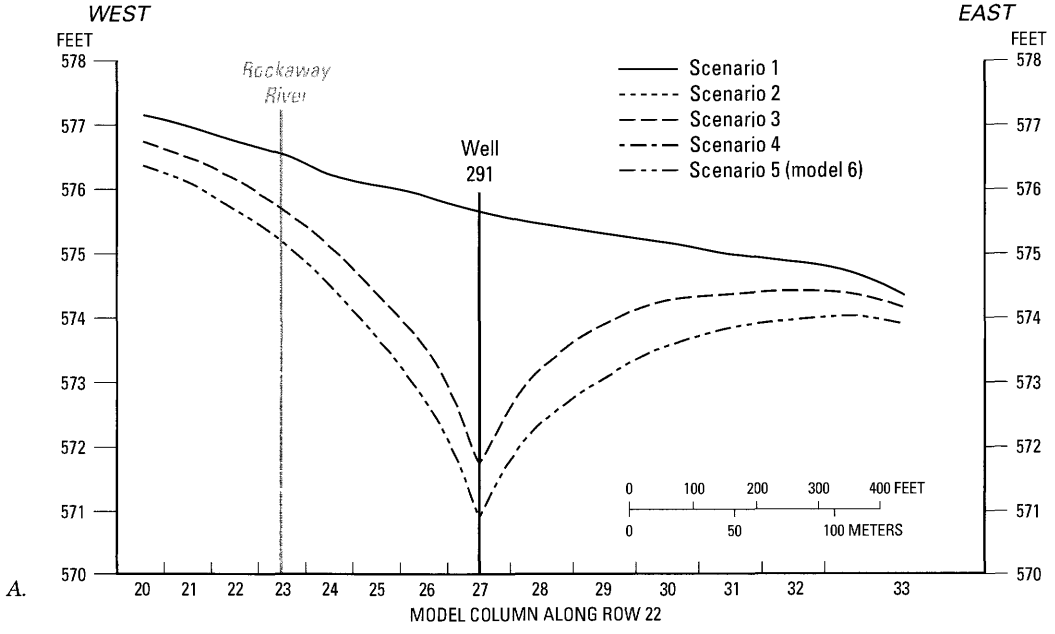

MODEL 6

Scenario	Stress period	Duration (hours)	Pumping rates (cubic feet per second)		
			Well 286	*Well 288*	*Well 291*
1	14	12	0	0	0
	15	12	0	0	0
2	14	12	1.36	0.19	0.95
	15	12	1.36	0.19	0.95
3	14	12	0	0	0
	15	12	2.72	0.37	1.90
4	14	12	2.72	0.37	1.90
	15	12	0	0	0
5	14	24	2.72	0.37	1.90

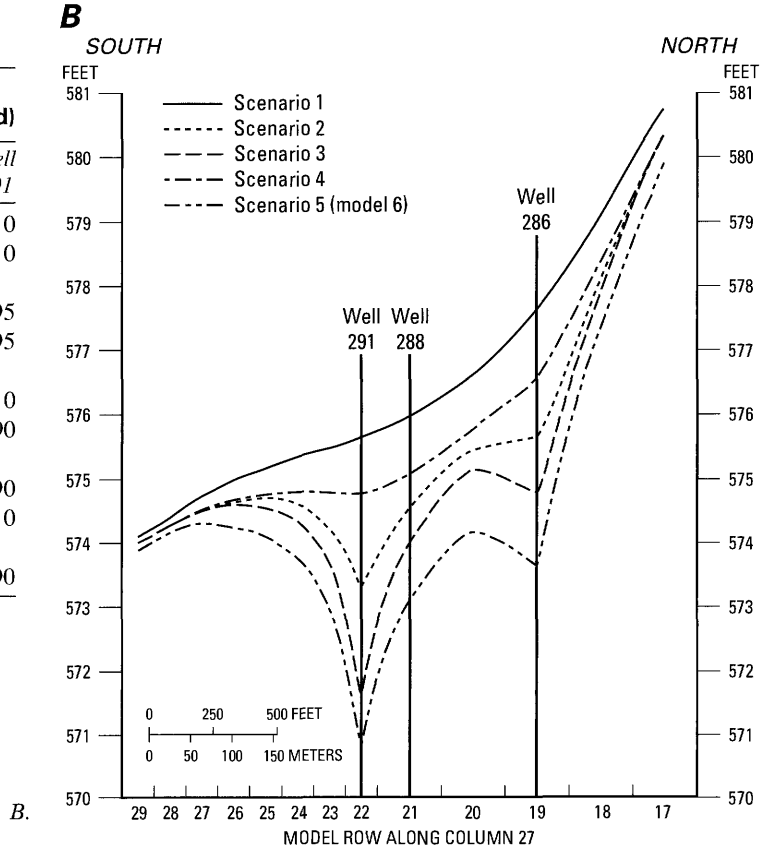

FIGURE 48.—Sensitivity of Dover model-6 head to changes in magnitude and distribution of pumping over the last 24 hours of 2-year transient-state simulation. *A*. East-west profile along model row 22. *B*. North-south profile along model column 27. Note that horizontal scales of *A* and *B* differ.

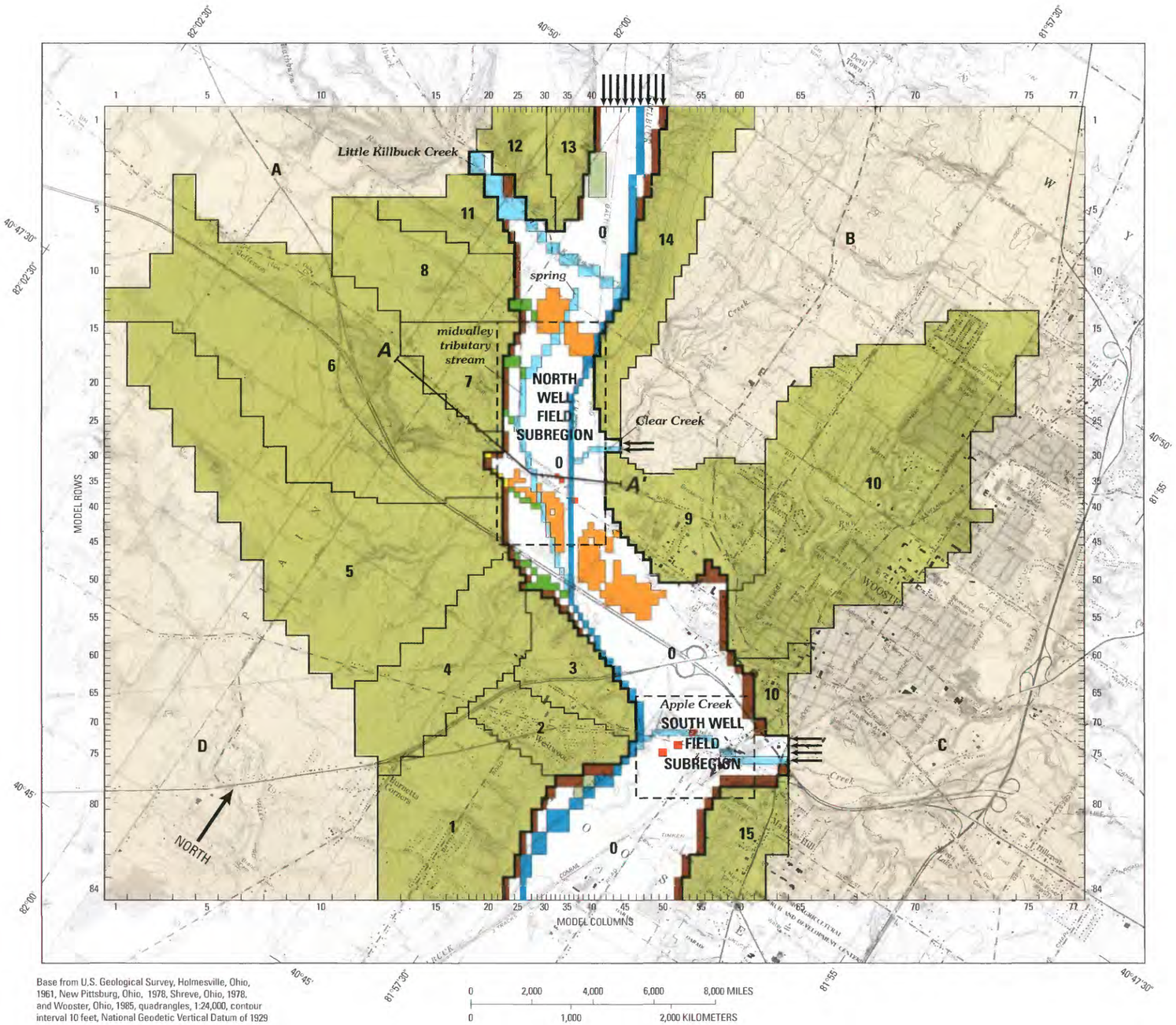

Base from U.S. Geological Survey, Holmesville, Ohio, 1961, New Pittsburg, Ohio, 1978, Shreve, Ohio, 1978, and Wooster, Ohio, 1985, quadrangles, 1:24,000, contour interval 10 feet, National Geodetic Vertical Datum of 1929

EXPLANATION

- Cells containing drains simulated with Drain Package
- Cells containing reaches of Killbuck Creek simulated with River Package
- Cells containing reaches of the Little Killbuck, Clear, and Apple Creeks and mid-valley tributary stream simulated with Stream Package
- Cells designated to receive recharge from unchanneled upland runoff
- Additional cells designated to receive recharge from unchanneled upland runoff from transient model 2
- Cells receiving channeled upland runoff and containing reaches of tributary streams simulated with Variable-Recharge procedure
- **Cells containing a pumping well**—Steady-state simulation
- **Constant-head cells**—Ponds
- **Upland Variable-Recharge zone**—Zones 1 through 15
- **Zone of inactive cells**
- **Cells receiving boundary fluxes from areas exterior to model**
- **Boundary of valley recharge zone**—Zone 0
- **Boundary of well field subregions**
- **Boundary of modeled area**—Ticks and numbers indicate model grid cell locations
- **Line of geologic section**
- **Zone boundary**

FIGURE 49.—Model grid, Variable-Recharge zones, and location of various features simulated by Wooster ground-water flow model (modified from Breen and others, 1995, pl. 1 and 2).

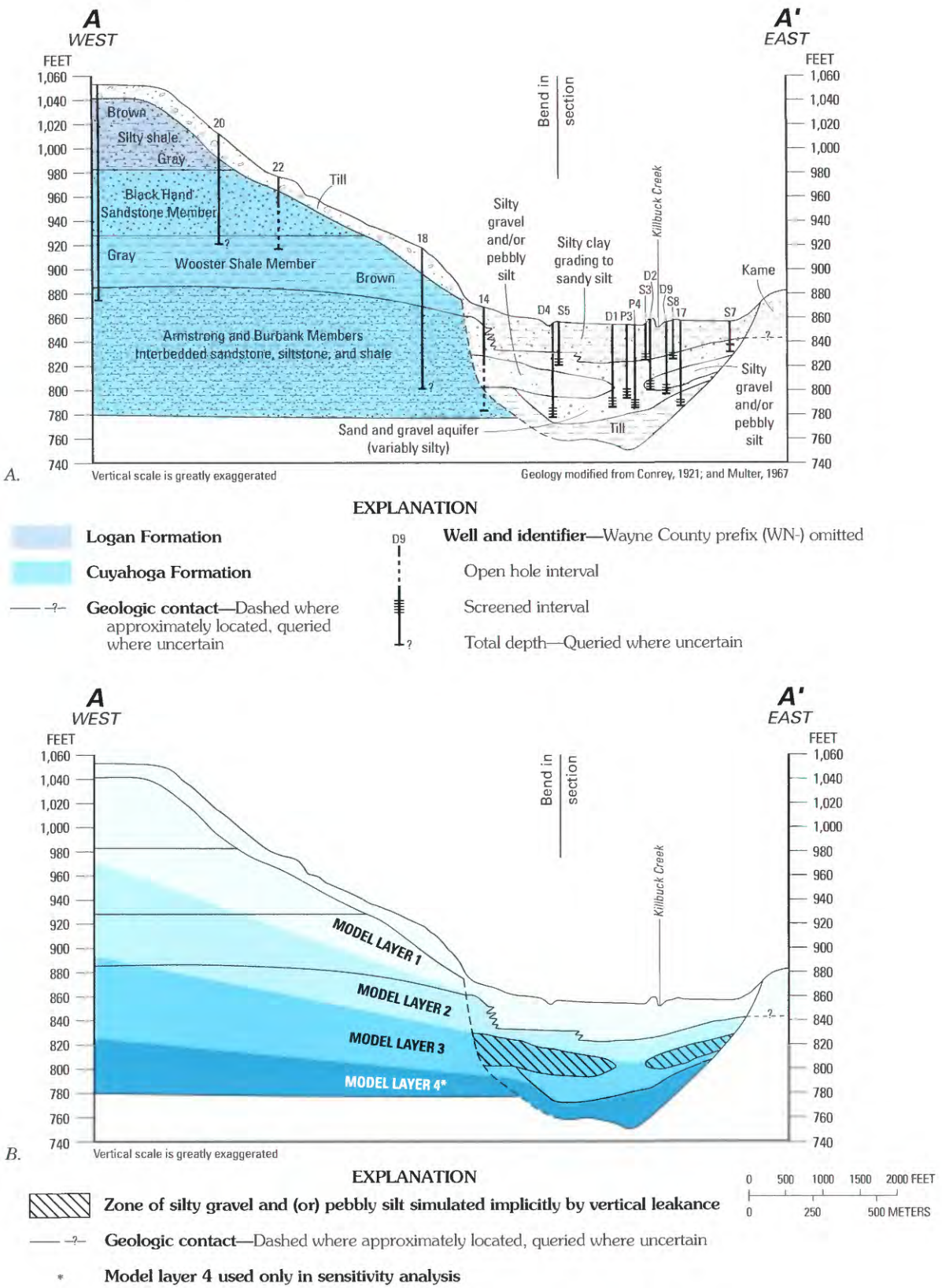

FIGURE 50.—Generalized section across Killbuck Creek valley showing geologic units and equivalent layers in ground-water flow model. Information on wells given in Breen and others (1995). Location of section is shown in figure 49. *A*. Geology, modified from Springer and Blair (1990) and Breen (1988, fig. 3); *B*. Model configuration, modified from Breen and others (1995, fig. 2).

the auspices of the city of Wooster, beginning in October 1983 (Mayhew, 1985). Water levels were measured in 25 of these wells from June through December 1986, at about 1-month intervals (Springer, 1987). Hydrographs of water levels in the north well field, examples of which are given in figure 51, show that water levels from October through December 1984 were relatively stable, indicating that the aquifer system was probably in a quasi steady-state condition. Therefore, the average value of water levels measured in each well during those three months was designated as representative of a fall 1984 steady-state condition. Water levels measured in the north well field in November 1986 were similar to the water levels of fall 1984 (fig. 51), indicating similar hydrologic conditions. Consequently, water levels measured in November 1986 by Springer in the vicinity of the south well field were used for calibration of the fall 1984 steady-state model. Other data that were available for calibration are described in Breen and others (1995) and include measurements of streamflow losses in Clear Creek, Little Killbuck Creek, and Killbuck Creek, water levels in piezometers finished a few feet below the Killbuck Creek streambed, and water levels in several wells in the uplands.

In response to rapid melting of 18 inches of snow in late February 1985, water levels rose several feet throughout the north well field (Breen and others, 1995, table 3). For example, the water level in deep well D2A rose about 11 ft over a six-day period (fig. 52). Killbuck Creek rose at least 7 ft, at two sites, over a 2- to 3-day period (Breen and others, 1995). Pre-snowmelt water levels were about 1 to 2 ft lower than the average water level during the fall of 1984 (fig. 51) indicating a period of little or no recharge in early winter of 1985. Nevertheless, the simulated heads from the fall 1984 steady-state model were used as initial conditions for a transient-state simulation of the 11 days from 23 February to 5 March 1985.

MODEL DESIGN AND PROCEDURES

The area in and around the Wooster waterworks (north well field) was the primary area of interest. As shown in figure 49, the model grid is oriented northwest—southeast along the trend of the valley in this vicinity. The model grid consists of 84 rows and 77 columns and has a non-uniform grid spacing that ranges from 150 to 750 ft. The area of fine grid-spacing corresponds with the location of the north well field production wells.

Geologic Discretization

The top layer (layer 1) of the model within the valley generally represents a confining unit that consists primarily of lacustrine silt and clay of relatively low permeability with small amounts of fine sand, but includes alluvial-fan deposits of relatively high permeability near Little Killbuck and Clear Creeks. In the uplands, layer 1 represents shale and sandstone overlain by till. Layers 2 and 3 within the valley represent material that ranges from silty clay to gravel (Breen, 1988). The upland extension of layers 2 and 3 consists of sandstone and shale (fig. 50). Both layers are confined by layer 1. Flow below layer 3 was assumed to be negligible; thus the bottom of layer 3 was taken to be a zero-flow boundary. The significance of this assumption is investigated by a sensitivity analysis, described further on.

Model Boundaries

The northern model boundary was placed about 6,000 ft north of the confluence of Little Killbuck Creek and Killbuck Creek and about 13,000 ft north of the north well field (fig. 49). As demonstrated by model sensitivity analysis, this boundary is sufficiently far from the north well field that inaccuracies in the applied boundary conditions have a minimal effect on the well field flow system. The southern model boundary was positioned beyond the south well field near the confluence of Killbuck and Apple Creeks but is only 4,000 ft south of the production wells (fig. 49). Simulations in which the applied boundary condition was varied showed that it can affect heads near the south well field.

Upland areas of the model were bounded by zero-flow boundaries along prominent topographic divides that were assumed to coincide with ground-water divides, or parallel to flow lines toward Killbuck Creek valley. Cells in zones A-D (fig. 49) were excluded from the active model. Ground water in zone D was assumed to drain to Killbuck Creek downstream from the study area and, therefore, has no effect on the active model. Zones A, B, and C are parts of the watersheds of large tributary streams that enter Killbuck Creek within the model area. Most of the ground water in the watersheds discharges to these streams; thus the hydraulic effect of flow in zones A, B, and C on the valley fill is primarily through the interaction of the tributary streams with the valley-fill aquifer. This interaction was simulated by the Stream Package of Prudic (1989).

MODEL INPUT

The input required for the ground-water-flow model includes properties of streams and drains, specification of pumping rates and boundary fluxes, hydraulic properties of earth materials, and data for the Variable Recharge procedure. For the transient-state model, stresses prevailing during the simulated period and the storage properties of the valley fill and uplands are required. These input data are further described in the following sections.

Streams and Drains

Little Killbuck Creek, Clear Creek, and Apple Creek were simulated with the Stream Package, as was an unnamed intermittent tributary, hereafter termed the midvalley tributary stream, whose source is a spring north of the well field (fig.

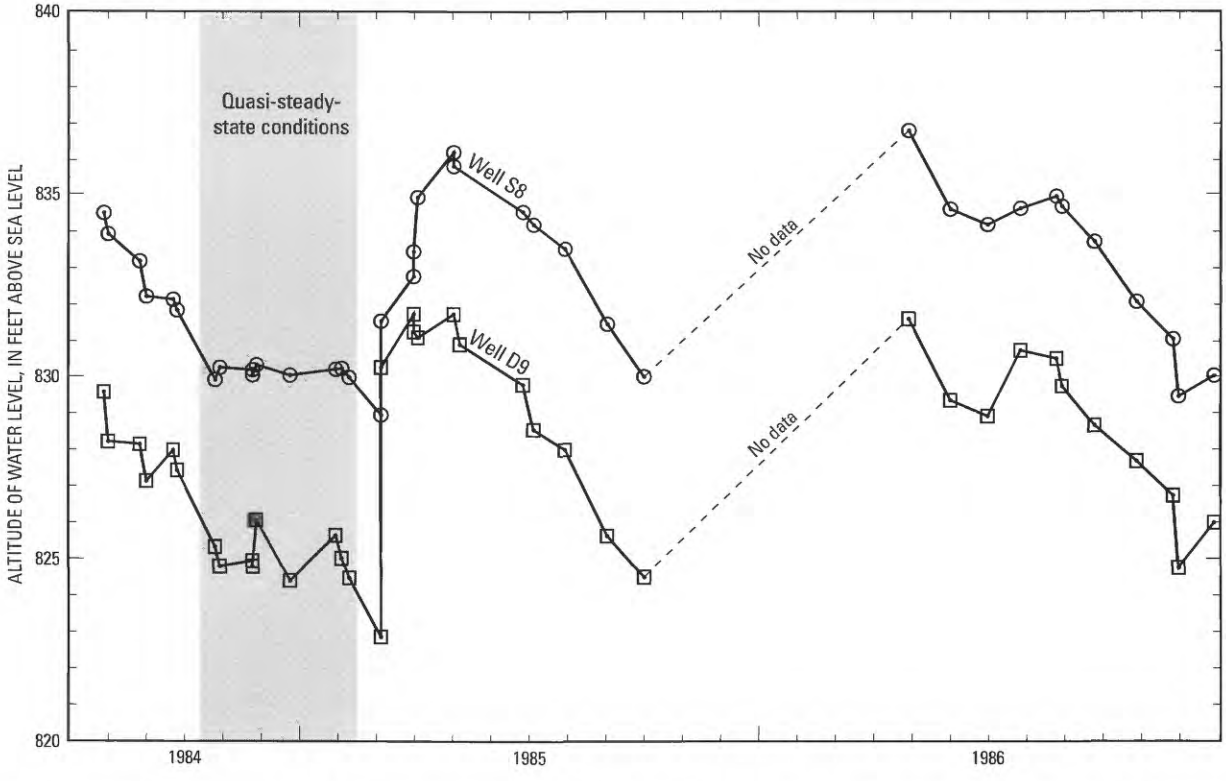

FIGURE 51.—Water levels in north well-field observation wells WN-D9 and WN-S8 from July 1984 to December 1986. Cell location of wells are given in table 23 (from Breen and others, 1995, fig. 3; data after April 1986 from Springer, 1987).

49). The input data, which are given in table 11 of Breen and others (1995), include (1) the quantity of flow in the upstream cell of each stream, (2) the terms of equation 6, and (3) the elevation of the top of the streambed.

The hydraulic interactions of layer 1 with Killbuck Creek and an extensive network of agricultural tile drains (fig. 49) were simulated by the River and Drain Packages (McDonald and Harbaugh, 1988), respectively. Development of data required by these procedures is discussed in Breen and others (1995). The simulated vertical leakance of Killbuck Creek, Apple Creek, the midvalley tributary stream, and the 6 tributaries simulated by the Variable-Recharge procedure ranged from 0.02 to 1 (ft/d)/ft, whereas streambed leakance of Little Killbuck Creek and Clear Creek ranged from 1 to 10 (ft/d)/ft.

Pumping Rates and Boundary Fluxes

Ground-water flow across the northern boundary of the model within the valley and ground-water flow emanating from the valleys of Clear and Apple Creeks were simulated by applying non-zero fluxes totaling 0.39 ft^3/s (fig. 49; see also table 8 of Breen and others, 1995). The fluxes were compiled by Darcy's law from representative hydraulic conductivity values, model-cell dimensions and an assumed head gradient perpendicular to the boundaries of 1 ft per model cell spacing. Under non-pumping conditions, there is probably a southerly underflow, within the valley, across the southern edge of the model (fig. 49). However, pumping from the south well field would induce flow from the south, resulting in a ground-water divide south of the well field. Consequently, for the steady-state simulation, the divide was assumed to be located near the southern edge of the model and to act as a zero-flow boundary. The pumping rates used in the steady-state simulation represent average rates for the north well field during the fall of 1984, and average rates for the south well field during the 1986 water year (Springer and Bair, 1990). These rates totaled 5.5 ft^3/s for the 5 wells in the north well field and 3 ft^3/s for the 3 wells in the south well field.

Hydraulic Properties of Earth Materials

Initial estimates of the hydraulic conductivity of the Killbuck Creek valley sediments were derived from a variety of sources, as summarized in Breen and others (1995). Analysis of well logs, primarily from the vicinity of the north and south well fields, indicates that the hydraulic conductivity of the clay, silt, sand, and gravel has a high degree of lateral and vertical variability. Aquifer tests within the north and south well field subregions indicate hydraulic conductivity values ranging from 200 to 1,000 ft/d (Breen and others, 1995). Hydraulic conductivity elsewhere along the margins of the valley, north of the north well field, and in the region between

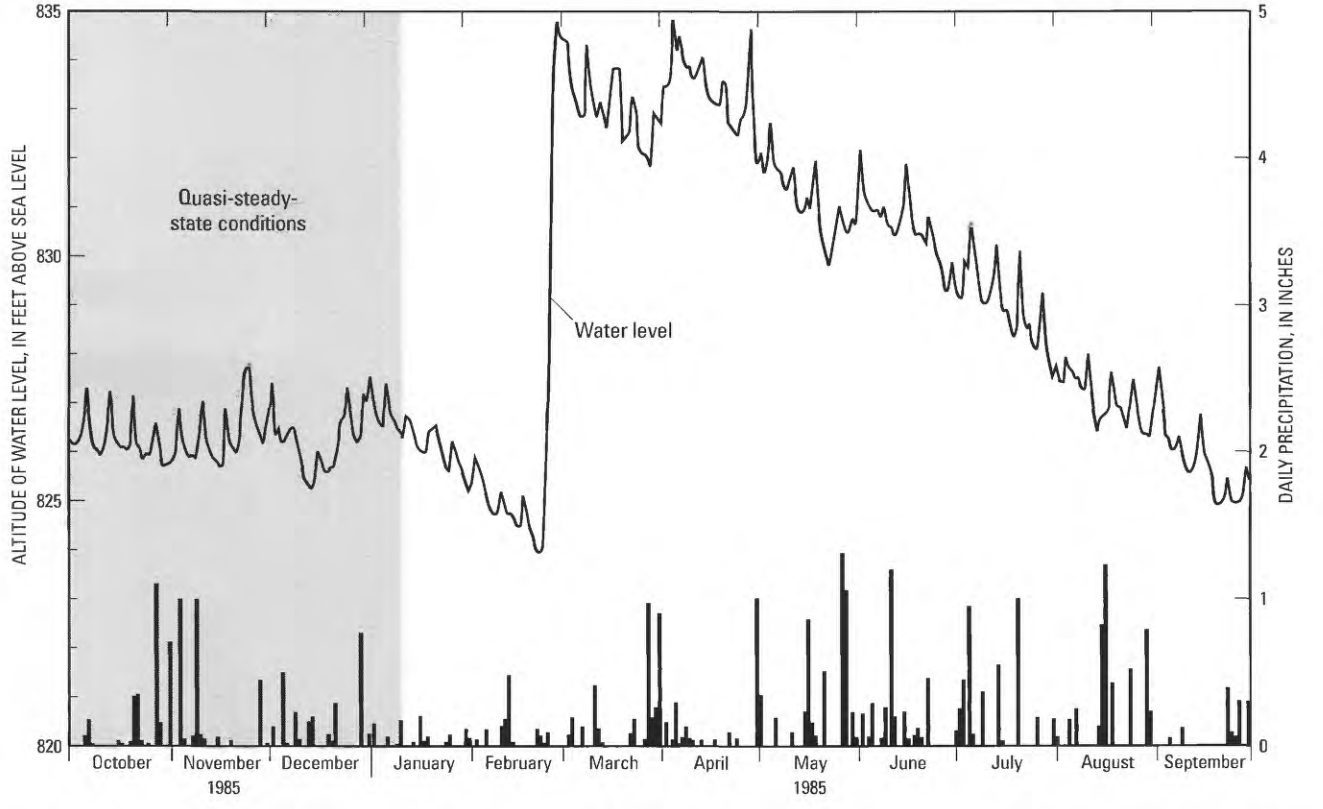

FIGURE 52.—Water levels in well D2A completed in the stratified drift of Killbuck Creek valley near Wooster, Ohio, and daily precipitation at Ohio Agricultural Research and Development Center at Wooster, Ohio, October 1984 through September 1985 (from Breen and others, 1985, fig. 4).

the north and south well fields was estimated from apparent resistivity measurements from an electrical resistivity survey (Jones and others, 1958) and from apparent-conductivity measurements from an electromagnetic survey conducted by the USGS in July 1986 as explained by Breen and others (1995). The spatial variability in apparent resistivity at shallow depths was used to group model cells in layer 1 into several zones of uniform resistivity and data from intermediate depths were applied similarly to layer 2 and 3. Hydraulic-conductivity and vertical-leakance zone maps were constructed for use as model input by assuming that the salinity of the ground water was uniform and that a qualitative correlation exists between apparent resistivity and hydraulic conductivity (Breen and others, 1995).

Properties that Control Recharge

As previously discussed, the Variable-Recharge procedure requires (1) the *WAFR* (eq. 11) expressed as a flow rate (eq. 12) for each of the active uppermost model cells, (2) an array of land-surface elevations, (3) a zone array that delineates upland subbasins and the valley fill, and (4) information that characterizes how the *WAFR* and upland surface runoff is to be distributed. These data were developed as follows.

WAFR.—Each of the terms for calculation of *WAFR* (eq. 11) was estimated for successive periods of a month or less, from 1 January 1984 through 5 March 1985 (table 21). The total *WAFR* for the steady-state period, October through December 1984, was 3.27 in. The equivalent flow rate (eq.12) for each model cell was 3.43×10^{-8} ft/s times the area of the cell.

Land-Surface Elevation.—The array containing land-surface elevation for each of the unequally spaced model cells was obtained by initially estimating average land-surface elevation within blocks of size 750 ft by 750 ft, from USGS topographic maps of the area (fig. 49), and applying a bicubic-spline interpolation method (Davis and Kontis, 1970; Kontis and Mandle 1980) to the uniformly spaced values to calculate land-surface elevation for each of the non-uniformly spaced model cells. A contour map of the resultant land-surface elevation is presented in figure 53.

Variable-Recharge Zones.—The division of the model area into subbasins or zones is shown in figure 49. Each of the upland subbasins numbered 1 through 15 are entirely within the model area whereas subbasins lettered A through D extend beyond the model boundaries. All surface runoff and ground-water flow in the explicitly simulated numbered subbasins was assumed to move toward upland tributary streams

TABLE 21.—*Calculation of water available for recharge (WAFR) at Wooster, Ohio, January 1984 through March 5, 1985*

[All values in inches except as noted]

Time period					Evapotranspiration		Soil-moisture depletion (+) or addition (–) (inches)[4]	Accumulated soil-moisture deficit (cumulative total of col. 7)	*WAFR*	
Month or dates		Duration (days)	Precipitation	Snow storage (–) or melt (+)[1]	Percent[2]	Inches[3]			Calculated amount available (col. 3+4+6+7)	Simulation-period totals
1		2	3	4	5	6	7	8	9	10
1984										
January		31	0.92	–0.92	0	0	0	0	0	
February		29	2.26	+0.92	0	0	0	0	3.18	
March		31	3.25	0	0	0	0	0	3.25	
April		30	3.97	0	11.0	–2.64	0	0	1.33	
May		31	5.38	0	15.2	–3.64	0	0	1.74	
June		30	1.66	0	18.2	–4.37	+2.71	2.71	0	
July		31	2.94	0	18.7	–4.49	+1.55	4.26	0	
August		31	5.09	0	16.5	–3.96	–1.13	3.13	0	
September		30	2.41	0	11.9	–2.86	+0.45	3.58	0	
October	steady-state simulation period	31	2.83	0	8.6	–2.06	–0.77	2.81	0	
November		30	3.54	0	0	0	–2.81	0	0.73	
December		31	2.54	0	0	0	0	0	2.54	**3.27**
1985										
January		31	0.96	–0.96	0	0	0	0	0	
February 1–22		22	1.20	–1.20	0	0	0	0	0	
February 23–March 5	transient-state simulation period	11	0.37	+2.16	0	0	0	0	2.53	**2.53**

[1] From records of daily precipitation at Ohio Agriculture Research and Development Center (OARDC), Wooster, Ohio. Location of gage is shown in figure 49.

[2] Class A pan average monthly evaporation for April–October (1956–70), in percent, at OARDC assuming that evapotranspiration from November through March is negligible (table 2 of Lyford and Cohen, 1988).

[3] Values obtained by multiplying percentages in column 5 by the mean annual evapotranspiration (24 inches) at Wooster, Ohio. Mean annual evapotranspiration at Wooster was estimated by subtracting estimated mean annual runoff of 13.2 inches (Lyford and Cohen, 1988) from mean annual precipitation (over 97-year period) of 37.2 inches (Statistics Laboratory, OARDC, written commun., 1984).

[4] If evapotranspiration (absolute value of column 6) exceeds precipitation (column 3), the difference represents a soil-moisture depletion (column 7). If precipitation exceeds evapotranspiration, the difference appears as a soil-moisture addition in the present time period, but only to the extent needed to reduce to zero any accumulated soil-moisture deficit in column 8 of the previous time period. (In other words, a soil-moisture addition cannot exceed the magnitude of the accumulated soil-moisture deficit).

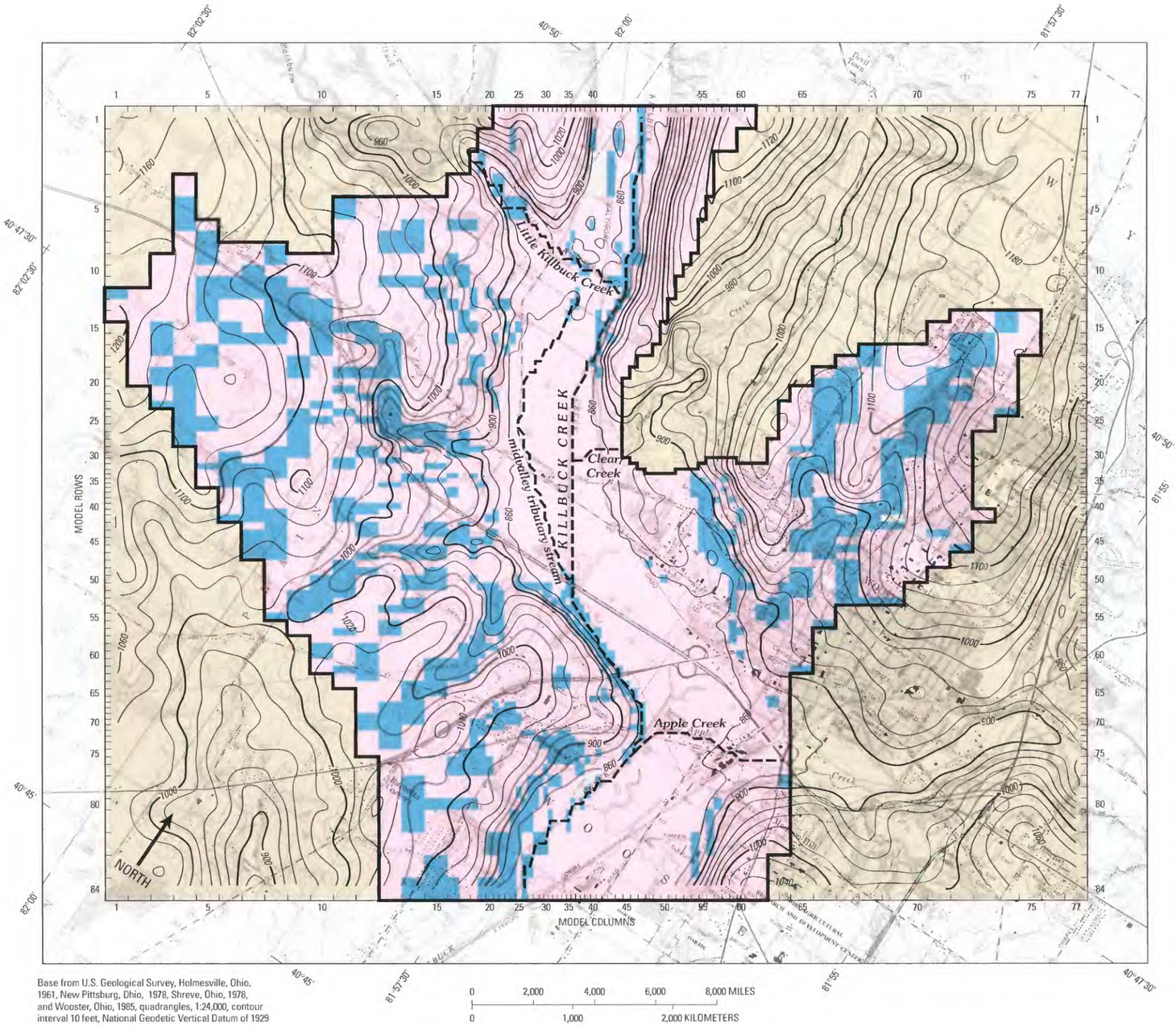

EXPLANATION

Model cell at which recharge was simulated

Model cell at which outward seepage was simulated

Inactive cells

—1000— —1040— **Contour of land-surface elevation**—Contour interval 20 feet. Thicker index contours at 100-foot intervals. Datum is sea level

Dashed lines drawn through cells at which a stream was simulated with the River or Stream Package—Stream cells colored pink represent a losing reach. Stream cells colored blue represent a gaining reach. Stream cells with no color represent a dry channel

Boundary of active model

25 30 **Boundary of modeled area**—Ticks and numbers indicate model grid cell locations

FIGURE 53.—Contours of land-surface elevation array used in Variable-Recharge procedure, locations of streams simulated by River or Stream Package, and distribution of recharge and outward seepage as simulated by Wooster steady-state model (from Breen and others, 1995, plate 3).

or to adjacent parts of the Killbuck Creek valley within the model area. Although upland subbasins A, B, and C containing Little Killbuck Creek, Clear Creek and Apple Creek, respectively, and subbasin D were not explicitly simulated, underflow within the Clear Creek and Apple Creek valleys was simulated by nonzero specified fluxes at the edge of Killbuck Creek valley (fig. 49). Underflow was applied also to the Little Killbuck Creek valley during the early stages of simulation, but was removed because the model was insensitive to the added underflow. Upland cells with zone numbers 1 through 15, together with all active cells in topographically low areas designated as zone 0, constitute the Variable-Recharge zone array (fig. 49).

Reduction of WAFR and Runoff in Urban Areas.—Urban areas contain features that reduce recharge and intercept unchanneled upland runoff; these features include paved surfaces, storm sewers, roadside ditches, and drainage systems around buildings. Much of zone 10 of the Wooster model (fig. 49) is urban. The Variable-Recharge procedure allows the rate of *WAFR* to be modified in each zone, and(or) the percentage of upland surface runoff that is available for recharge of the valley to be specified differently for each zone. The calculated *WAFR* rate in zone 10 was arbitrarily reduced by 50 percent, as was the percentage of surface runoff available for recharge (table 22, cols. 2, 3) to approximate probable reductions due to urban effects.

Disposition of Upland Runoff.—The percentage of surface runoff that reaches the valley as channeled flow must also be specified. The topographic expression of the subbasins may be used to estimate this quantity (Handman, 1986). Comparison of figure 49 with figure 53 indicates that upland zones 1, 2, 3, 9, and 11 through 15 have a few gullies notched into the side of Killbuck Creek valley, but no streams that extend out to Killbuck Creek or to major tributaries. The hillside gullies undoubtedly carry storm runoff at times, but apparently much of it infiltrates near the base of the hillside rather than forming permanent channels across the valley floor. Therefore, these zones were specified as having no channeled runoff. If modeling were to be carried out on a more detailed scale, a few of the hillside gullies might be simulated individually. Estimates of channeled runoff for zones 4 through 8 ranged from 50 percent to 87 percent of surface runoff (table 22, col. 4). These values are rough estimates based on the percentage of hillside area within each subbasin that slopes toward a tributary valley relative to the percentage that slopes toward the Killbuck Creek valley. The part of upland runoff that becomes unchanneled runoff is the difference between the available runoff and the channeled runoff. The unchanneled runoff is distributed as *WAFR* to valley cells adjacent to each upland zone. Locations of these cells are shown in figure 49, and the number of cells receiving runoff from each upland zone is given in table 22, column 5. For upland zones with channeled flow, the number of explicitly simulated tributary streams emanating from each zone and the number of model nodes containing a tributary are also specified (table 22, columns 6 and 7).

The tributaries designated to receive channeled runoff from the uplands (fig. 49) were simulated by the Variable-Recharge procedure in a manner similar to that of the Stream Package except that the streamflow in the upstream cells of each stream is calculated within the model (eq. 14h) and distributed according to information specified in table 22, column 6 rather than being specified as part of the model input.

Transient-State Simulation — Stresses and Storage

Changes in stresses from their steady-state values were applied to reflect average conditions over the 11-day snowmelt period of rapid recharge February 23 through March 5, 1985. These changes consisted of a 3-ft increase in elevation of all stream surfaces along Killbuck, Little Killbuck, Clear, and Apple Creeks and a 2-ft increase in elevation of the small tributary streams simulated with the Variable-Recharge procedure; these increases are approximations of conditions observed in the field. Other transient stresses were a *WAFR* rate of 2.2×10^{-7} ft/s, commensurate with the water equivalent of the 18-in snowmelt, elimination of pumpage from the south well field and application of southward fluxes along the valley portion of the southern edge of the model (Breen and others, 1995). Pumpage from the south well field was eliminated because no pumping occurred from this area during the period of simulation.

Storage coefficients estimated from aquifer tests (Breen and others, 1995) show a wide range for similar materials; therefore, storage properties used in the transient-stress simulation were selected from the range of specific storage discussed earlier in the section "Porosity and Storage Coefficient" and from tabulated values (Todd, 1970). In particular, the specific yield of layer 1 was 0.03, and storage coefficients of layers 2 and 3 were 3×10^{-4} for the valley fill and 5×10^{-5} for the uplands.

MODEL CALIBRATION

The steady-state and transient models were calibrated to measured values of head in piezometers and, where appropriate, estimates of streamflow gain or loss. Comparisons of simulated versus observed head and flow values indicate that the models resulted in head and flow patterns that matched observed conditions within the Killbuck Creek valley fairly well. The following section describes the calibration process, the calibrated data, and the comparisons between the modeled and actual hydrologic system.

Steady-State Model

The steady-state calibration process consisted of varying hydraulic properties over a plausible range of values until known values of head and streamflow loss and gains were

TABLE 22.—*Variable-Recharge procedure input data used to distribute water available for recharge (WAFR) and surface runoff in upland subbasins (zones) in Wooster steady-state simulation*

[*WAFR* is the calculated water available for recharge (equation 11). Zone locations are shown in figure 49]

Upland zone	Percentage of *WAFR* applied to zone	Percentage of upland runoff available to recharge valley	Percentage of upland runoff appearing as channeled flow	Number of valley nodes receiving unchanneled flow	Number of tributary streams or channels	Number of nodes per channel
1	2	3	4	5	6	7
1	100	100	0	7	0	0
2	100	100	0	11	0	0
3	100	100	0	9	0	0
4	100	100	75	5	1	6
5	100	100	80	8	1	12
6	100	100	87*	9	1	11
7	100	100	50	8	2	4 and 2
8	100	100	50	5	1	9
9	100	100	0	7	0	0
10	50	50	0	21	0	0
11	100	100	0	4	0	0
12	100	100	0	2	0	0
13	100	100	0	3	0	0
14	100	100	0	5	0	0
15	100	100	0	13	0	0

* This value was changed to 97 percent in transient-state model 2.

approximately replicated. The magnitude and distribution of the final set of hydraulic conductivity values and vertical leakance values are given in Breen and others (1995). Simulated hydraulic conductivity of valley-fill deposits in layer 1 ranged from 0.25 to 10 ft/d in areas characterized by clay, silt or fine sand and from 5 to 100 ft/d in alluvial gravel and sand deposits. Simulated transmissivity of layers 2 and 3 ranged from about 100 ft^2/d in areas containing silty clay to 20,000 ft^2/d in gravel deposits in the vicinity of the south well field. Simulated vertical leakance between layers 1 and 2 in areas of valley fill ranged from about 20 to 2 x 10^{-4} (ft/d)/ft and leakance between layers 2 and 3 ranged from about 1 to 1 x 10^{-4} (ft/d)/ft. The high values of vertical leakance were applied where deposits with relatively high permeability are in direct contact with one another. The hydraulic conductivity of each upland layer was taken to be 0.3 ft/d and vertical leakance between upland layers was about 1 x 10^{-4} (ft/d)/ft.

The north well field area of the model was calibrated with respect to the average of (1) measured water levels representative of the fall of 1984, in 13 observation wells screened at depths corresponding to model layers 2 or 3, and (2) measured water levels in 8 streambed piezometers screened in shallow deposits (layer 1). The south well field area was calibrated to water levels measured on November 25, 1986 (Springer, 1987) in 24 observation wells screened at depths representing layer 2 or 3. In addition, water-level measurements from nine widely scattered wells in the uplands, and estimates of streamflow gain and loss (Breen and others, 1995), were available for comparison with simulated values.

Goodness of fit.—The simulated head distributions for the north and south well field subregions, which contain the production wells, streambed piezometers, and observation wells used in the calibration, are shown by contours in figures 54 and 55. The contours are based on interpolation of the unequally spaced model heads at a uniform spacing of 100 ft, by a one-dimensional cubic-spline interpolation procedure (Davis and Kontis, 1970). The mean absolute difference (*MAD*) between observed heads and the corresponding interpolated model heads (eq. 15 with i = 1) is given in figures 54 and 55 for each model layer and subregion; the overall *MAD* for layers 2 and 3 in both subregions was 1.1 ft. The model fit for both layers, in terms of the σ statistic (eq. 17) for a Δh_s of 15 ft for the north well field and 6 ft for the south well field, was about 10 percent for the north well field and about 15 percent for of the south well field.

The interpolation of simulated heads at a finer spacing than the model-grid spacing can be advantageous in determining model fit, especially in regions with steep hydraulic head gradients, as was shown for the Dover simulation (fig. 40). Heads simulated by the model at the model-grid spacing and heads interpolated at a 100-ft uniform spacing are compared in table 23*A* with observed heads in a subset of wells in the vicinity of the north well field. The cone of depression in the north well field is sufficiently steep (fig. 54) that observed heads at many wells are represented more closely by the near-

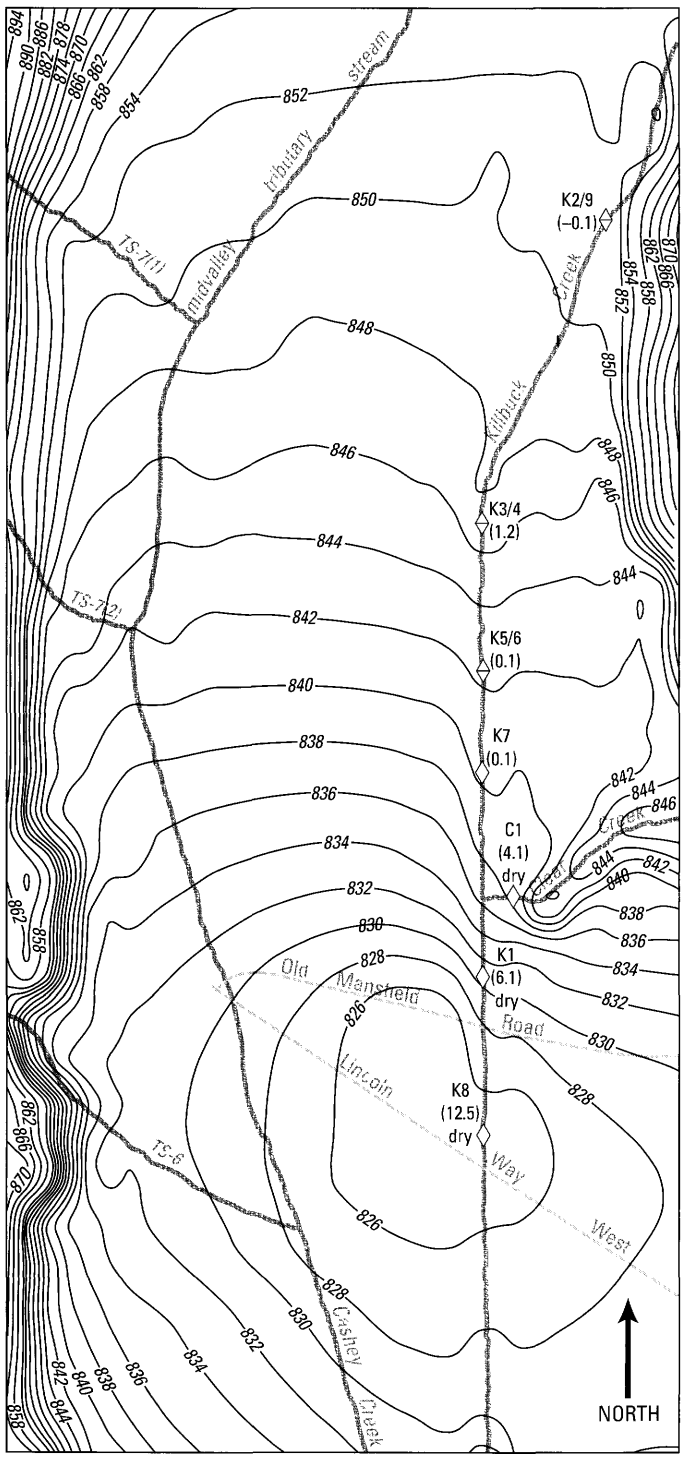

EXPLANATION

—848— **Contour of simulated steady-state head**—Contour interval, in feet, is variable. Datum is sea level

TS-7(1) **Tributary stream emanating from Variable-Recharge zone**—Number identifies zone and individual tributary within that zone (in parentheses). Because of finite-difference discretization, locations of simulated streams relative to contours are approximate

Well location and number

S13 Shallow drift well

D4 Deep drift well

14 Bedrock well

2.7 Lower number by each well is head difference, in feet, computed as the average of heads measured in well during fall 1984 minus the simulated head obtained by interpolating at 100-foot spacing the output from fall 1984 steady-state model

K7 **Streambed piezometer location and number**

K3/4 **Paired streambed piezometer location and number**

(0.1) Number in parentheses at each piezometer is head difference, in feet, computed as the head measured August 27–28, 1985, in piezometer minus the head in cell containing piezometer as simulated by fall 1984 steady-state model

dry **Well or piezometer was dry during measurement period**—and the adjacent head difference was computed as elevation of bottom of the screened interval minus the simulated head

0 400 800 1200 1600 FEET
0 400 800 METERS

A. MODEL LAYER 1 (Mean absolute difference 0.4 feet)

FIGURE 54.—Contours of steady-state heads in north well-field subregion of Wooster model for model layers 1, 2, and 3. Differences between interpolated model heads and observed heads representative of fall 1984 conditions, and the mean absolute difference between interpolated model heads and observed heads for each layer, are also given (from Breen and others, 1995, pl. 6).

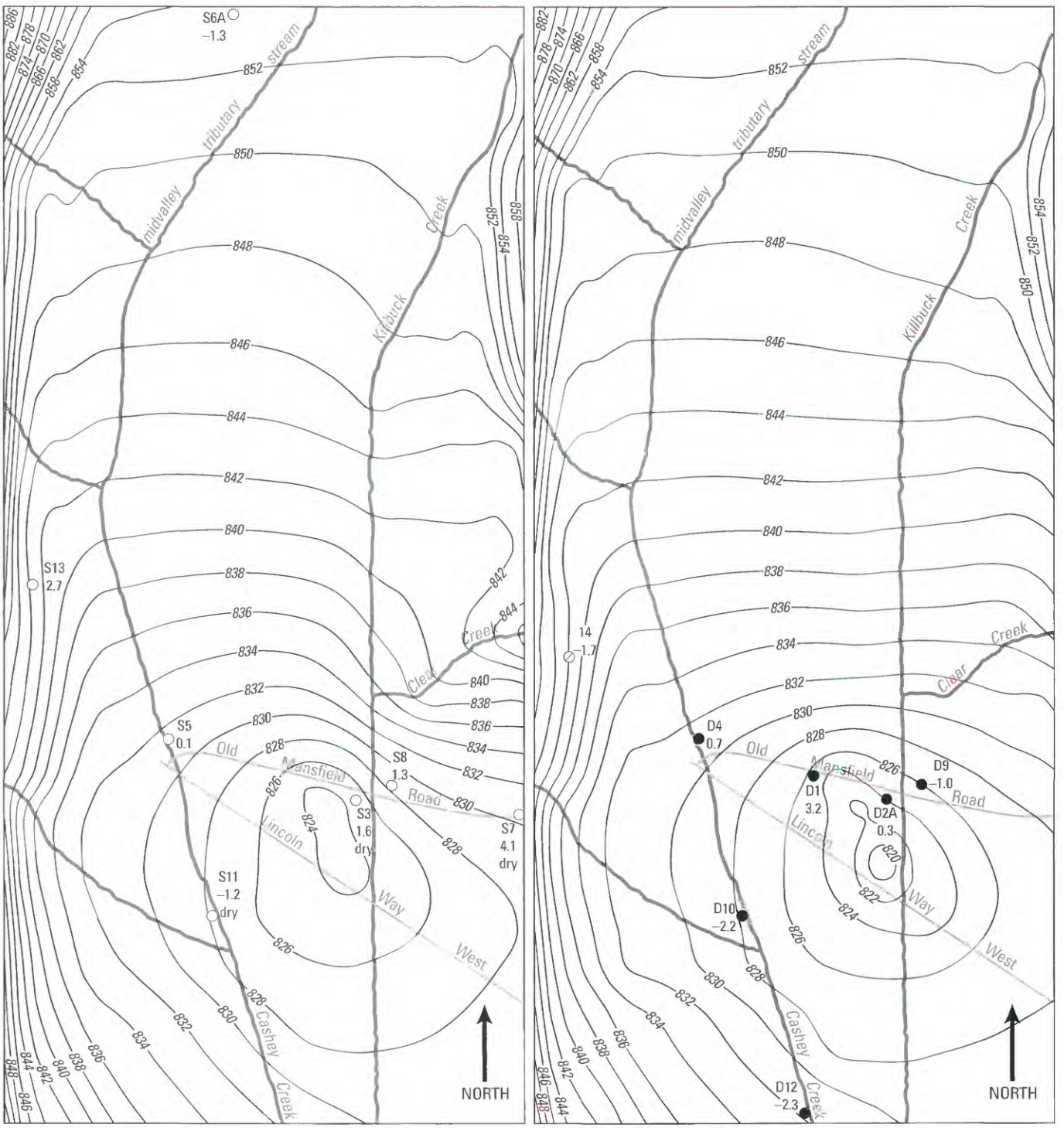

B. MODEL LAYER 2 (Mean absolute difference 1.4 feet)

C. MODEL LAYER 3 (Mean absolute difference 1.6 feet)

FIGURE 54.—Continued.

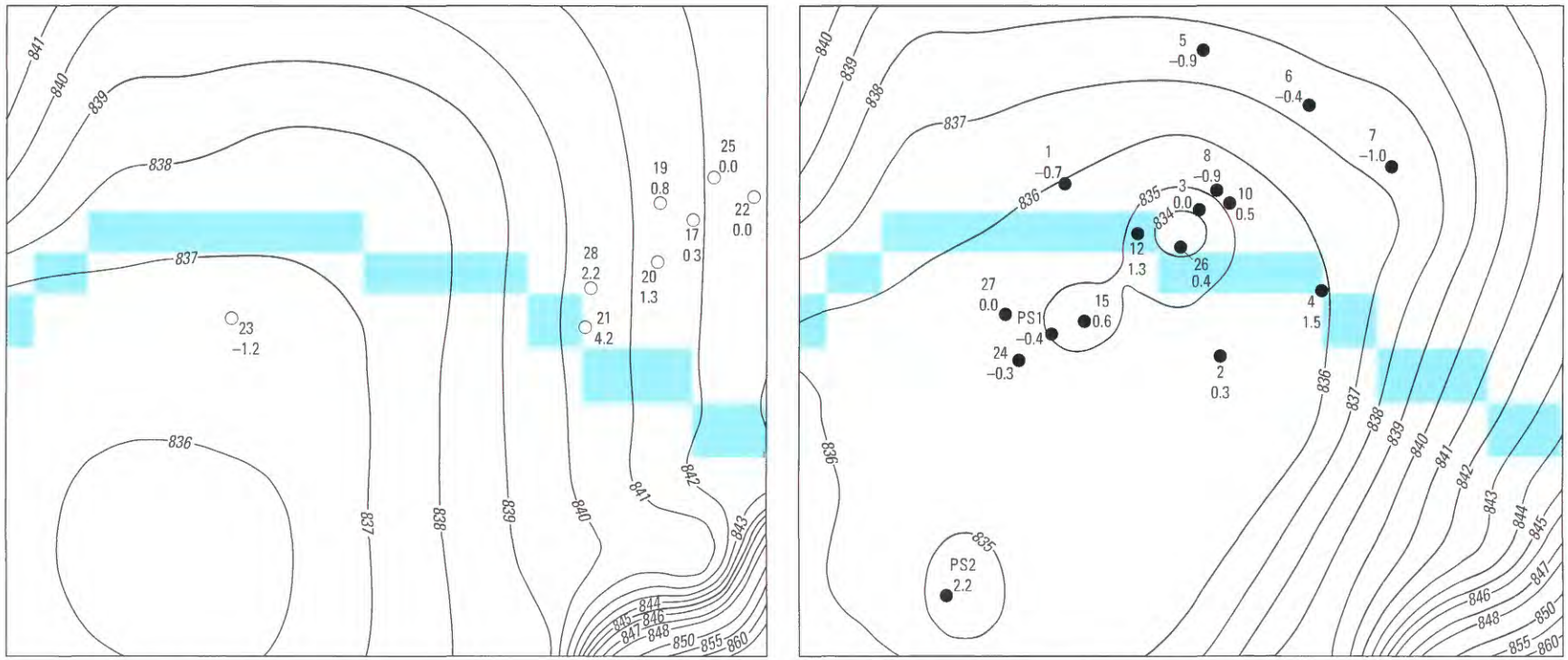

A. MODEL LAYER 2 (Mean absolute difference 1.3 feet)

B. MODEL LAYER 3 (Mean absolute difference 0.7 feet)

0 500 1,000 1,500 FEET

0 500 METERS

EXPLANATION

Model cells containing reaches of Apple Creek

—*839*— **Contour of simulated steady-state head**—Contour interval, in feet,is variable. Datum is sea level

○ 19 / 0.8 **Well screened in glacial drift**—Upper number is well identifier (from Springer, 1990, except where prefixed by PS, which denotes public-supply well). Lower number is difference, in feet, between head measured in fall 1984 and simulated head. Simulated head is head nearest to well location obtained through interpolation at 100-foot spacing between heads simulated by model for unequally spaced cells

○ Shallow well (in layer 2)

● Deep well (in layer 3)

FIGURE 55.—Contours of steady-state heads in south well-field subregion of Wooster model for model layers 2 and 3. Differences between interpolated model heads and observed heads representative of fall 1984 conditions, and the mean absolute difference between interpolated model heads and observed heads for each layer, are also given (from Breen and others, 1995, fig.5).

est interpolated heads than by the heads simulated for the model cells in which they are located; consequently, the *MAD* for the north well field decreased from about 2.2 ft to 1.5 ft when the interpolated heads were substituted for model-cell heads. The corresponding improvement for the south well field was relatively small because head gradients there are less steep (fig. 54).

The steady-state water-table configuration in layer 1 within the north well field subregion and its relation to simulated streams is shown in figure 54*A*; also shown are the locations of streambed piezometers, and the difference between simulated heads and piezometer measurements made on August 27-28, 1985. The *MAD* for the four piezometers that were not dry (fig. 54*A*) was about 0.4 ft. Observed and simulated heads for upland wells are given in table 23*B*; differences ranged from less than 1 ft to about 32 ft, with a *MAD* of about 11 ft. This corresponds to a σ model-fit statistic of about 11 percent for a Δh_s (eq. 17) of 100 ft.

Simulated streamflow loss.—The steady-state model indicated streamflow losses of about 1 ft^3/s from Little Killbuck Creek and 1.3 ft^3/s from Clear Creek where they cross alluvial sand and gravel after entering Killbuck Creek valley, in approximate agreement with streamflow measurements during periods of low flow (Breen and others, 1995). The model indicated losses from Killbuck Creek and Apple Creek near the well fields to be small, commensurate with the presence of silty clay beneath the channels. The total simulated flow to agricultural drains (fig. 49) for steady-state conditions was about 0.7 ft^3/s. Most of this flow (0.51 ft^3/s) was in the set of drains west of the midvalley tributary stream adjacent to upland zone 8. The only available measurement of drain discharge was made near streambed piezometer K2 (fig. 54*A*) on September 9, 1985, at the drain field east of the midvalley tributary stream adjacent to upland zone 14. The simulated discharge was essentially the same as the measured discharge of 0.1 ft^3/s (Breen and others, 1995). Simulated flow to the remaining drains, which are south of the north well field, was negligible.

Transient-State Model

Statistics on model fit for transient-state simulation of the period of rapid snowmelt (February 23 through March 5, 1985) in the north well field subregion are summarized in Breen and others, 1995. The *MAD* was 1.8 ft between simulated and measured heads on March 5, 1985, and 2.5 ft between the observed rise in head from fall 1984 to March 5, 1985 and the simulated rise. The poorest fit was in the vicinity of well S13 (fig. 54*B*), where the simulated head was more than 7 ft higher than the observed head. This well is near the valley wall, in an area that received unchanneled runoff from the adjacent upland subbasin (zone 6 of fig. 49). A probable explanation for the high simulated head is that unchanneled runoff was overestimated by the model. Accordingly, the transient-state simulation was repeated with a slightly redesigned model (transient-state model 2). In this model, (1) the total amount of available runoff from upland zone 6 was decreased by reducing the amount of surface runoff to be treated as unchanneled runoff from 13 percent to 3 percent (table 22), and (2) the valley area along the valley wall south of well S13 designated to receive unchanneled runoff was increased by 5 additional cells (fig. 49), thereby reducing the runoff applied to a particular model cell. These changes greatly reduced the recharge from unchanneled runoff near well S13 and lowered head in this vicinity by about 9 ft, which considerably improved model fit near well S13 and provided reasonably good fit elsewhere. Overall, the *MAD* between simulated and measured head in the north well field subregion was reduced to 1.3 ft, and the *MAD* between simulated and measured seasonal rise in head was reduced to 1.4 ft. The results of the transient-state simulations indicate that the general hydrogeologic characteristics of the steady-state simulation are probably representative of actual conditions, to the extent that the simulated storage properties and stresses related to the snowmelt event are valid.

RESULTS OF STEADY-STATE SIMULATIONS

The following sections contain steady-state model results as depicted by (1) contours of steady-state head and simulated flow directions in model layer 3, (2) a plot showing areas of recharge and outward seepage and their relation to topography, and gaining and losing reaches of streams, (3) a graphic representation of some of the budget terms of equation 14 that shows how the *WAFR* applied to the uplands was allocated to the model, (5) a tabulation of the water budget for the stratified drift, (6) a quantitative correlation between the amount of simulated surface runoff and recharge in the upland subbasins and the topography of the subbasins, and (7) an analysis of the sources of vertical recharge to the buried valley deposits.

Simulated Head Configuration and Flowpaths for layer 3

The distribution of steady-state head for layer 3 is shown in figure 56. The head contours are based on values interpolated to a uniformly spaced grid of 300 ft from the unequally spaced model heads by one-dimensional cubic-spline interpolation (Davis and Kontis, 1970), initially along model rows and then along model columns. The main characteristics of layer 1 and 2 heads are similar to those of layer 3. The lateral-flow vectors (eq. 18) in figure 56 indicate that flow in the uplands is toward topographic depressions and, generally, toward Killbuck Creek valley. Vertical flow in the uplands is downward, except in topographically low areas, and flow in the northern part of the valley, in the vicinity of Little Killbuck Creek, is toward Killbuck Creek. Flow in the north and south well field subregions is toward the production wells.

TABLE 23.—*Differences between observed and model-simulated heads near Wooster north well field and in uplands*

[ft, feet; mo, month; d, day; yr, year. Heads and differences are in feet. Records of wells are given in Breen and others (1995), except for those footnoted as data from Springer (1987)]

A. Simulated and interpolated heads at north well field

Well[1]	Model cell[2] (row, column)	Model layer	Absolute difference between average head measured in well in fall 1984 and simulated head in cell that contains the well, in: Original model grid	Supplementary grid of 100-ft spacing[3]
WN-S5	(33, 28)	2	1.3	0.1
WN-S6A	(15, 30)	2	1.6	1.3
WN-S8	(34, 37)	2	0.8	1.3
WN-S13	(28, 23)	2	4.9	2.7
WN-D1	(34, 32)	3	4.1	3.2
WN-D2	(35, 35)	3	0.4	0.3
WN-D4	(33, 28)	3	1.8	0.7
WN-D9	(34, 37)	3	1.3	1.0
WN-D10	(39, 29)	3	2.9	2.2
WN-D12	(45, 32)	3	2.6	2.3
WN-D14	(30, 23)	3	2.0	1.7
		Mean absolute difference†	2.15	1.53

[1] Local number. Prefix WN denotes Wayne County; D, deep well screened in sand and gravel at depths greater than 50 feet below land surface; S, shallow well screened in sand and gravel at depths less than 35 feet below land surface.
[2] Model-cell locations shown in figure 49.
[3] Heads in supplementary grid estimated by interpolation of heads in north well field area from model grid.
† As defined in equation 16, p.C82.

B. Upland wells

Well and date of measurement (mo-d-yr)		Model cell[1] (row, column)	Model layer	Head: Observed	Head: Simulated[2]	Absolute difference
WN-3[3]	12-20-84	(83, 61)	1	1,027.0	1,005.7	21.3
Golf Course[4]	11-02-86	(28, 65)	3	1,004.0*	1,033.3	29.3
Pig Farm[4]	11-25-86	(7, 23)	3	874.9	874.1	0.8
WN-15	11-29-84	(41, 19)	3	884.0	883.3	0.7
WN-16	11-29-84	(17, 14)	3	989.0	1,020.6	31.6
WN-18	9-23-85	(28, 21)	3	855.8	856.0	0.2
WN-19 (Gowins)	11-25-86	(14, 25)	3	853.3	859.7	6.4
WN-20	11-29-84	(21, 15)	3	981.0	980.1	0.9
WN-21 (Munson)[4]	11-25-86	(34, 19)	3	867.6	873.8	6.2
					Mean absolute difference†	10.8

[1] Model-cell locations shown in figure 49.
[2] Simulated value is head in model cell that contains the well, except as noted.
[3] Well is outside model area; comparison is for nearby cell (83, 61) in uplands with similar topography.
[4] From Springer (1987).
* Observed value is average of measurements at two wells.
† As defined in equation 16, p. C82.

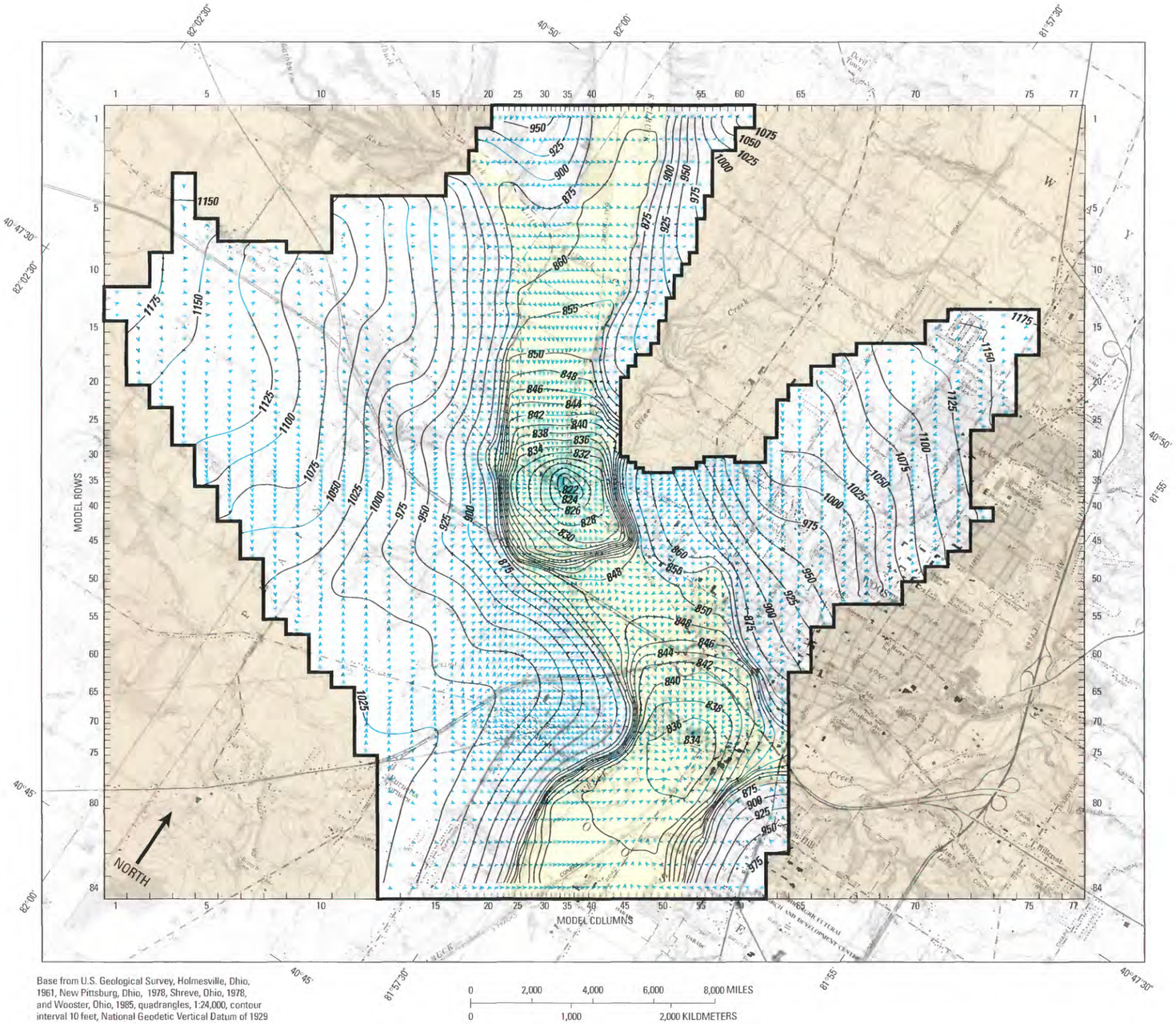

EXPLANATION

Valley fill

Inactive cells

— 975 — **Contour of simulated steady-state head in model layer 3**—Contour interval, in feet, is variable. Datum is sea level

Flow vector—Shows average direction of simulated lateral ground-water flow in each cell of model layer 3. Flow calculated by equation 18 and plotted at center of each model cell

Boundary of active model

25 30 **Boundary of modeled area**—Ticks and numbers indicate model grid cell locations

FIGURE 56.—Simulated steady-state head and lateral flow directions in Wooster model layer 3.

The flow vectors indicate, approximately, the segments of the uplands that contribute flow to the north and south well fields.

Distribution of Variable Recharge

The steady-state distribution of recharge and outward seepage resulting from application of the Variable-Recharge procedure is superimposed on land-surface contours in figure 53. Seepage cells in the uplands coincide with local and regional topographic lows and lower slopes of hillsides and constitute about 26 percent of the upland area, whereas recharge cells generally correspond to topographically high areas. Also shown are locations of gaining and losing reaches within the valley of Killbuck, Little Killbuck, Clear and Apple Creeks and the midvalley tributary. Cells within the valley that contain no recharge or seepage symbols are either constant-head cells (ponds) or reaches along the midvalley tributary that became dry. Outward seepage occurred in about 2.5 percent of the valley floor (excluding gaining reaches of streams), and was mostly in low-lying areas adjacent to discharge sites consisting of streams or ponds.

Distribution of Water Available for Recharge

The rate of *WAFR* for fall 1984 steady-state conditions, summed over the entire 12.2-mi^2 upland area (*TWAFR*, eq. 14a), was 10.45 ft^3/s and was distributed as shown in figure 57. The relation of simulated head in layer 1 to land-surface elevation and to the specified depth factor (df = 1.0 ft) which is described by equation 13, was such that total direct recharge to the uplands (*TDR*, eq. 14n) occurred at the rate of 5.70 ft^3/s, whereas 4.75 ft^3/s was rejected as recharge (*TREJ*, eq. 14k). Some water that infiltrated moved laterally through layer 1 of the uplands and seeped outward at the land surface (*TOS*, eq. 14l) at a rate of 2.87 ft^3/s; consequently, total upland surface runoff (*TSR*, eq. 14m), which is the sum of rejected recharge and seepage, was 7.62 ft^3/s. The total net recharge (*TNR*, eq. 14o) to layer 1 in the uplands was 2.83 ft^3/s—a rate equivalent to about 0.8 in of recharge during the simulation period of 92 days. Of the 2.83 ft^3/s of total net recharge to the uplands, about 1 ft^3/s (35 percent) entered the valley as lateral ground-water flow (*TLF*, eq. 14s) through the till-covered bedrock of layer 1 (fig. 50), and a net of 1.84 ft^3/s flowed downward to the underlying upland bedrock and thence to the valley (Q = –1.84 ft^3/s, eq. 14s).

The total upland surface runoff (7.62 ft^3/s) represents flow that was potentially available to recharge the valley, but urban development was assumed to divert 50 percent of the surface runoff from upland zone 10 (table 22), a loss that amounted to 0.53 ft^3/s. Thus, the total surface runoff available to recharge the valley (*TASR*, eq. 14p) was reduced to 7.09 ft^3/s. The manner in which the surface runoff from each upland zone was allocated to the valley is summarized in columns 4 and 5 of table 22 and is depicted in figure 58. A total of 3.20 ft^3/s was available as unchanneled runoff (*TAUR*, eq. 14r) and 3.89 ft^3/s was available as channeled runoff (*TACR*, eq. 14q) to the specified valley cells and tributaries (fig. 49).

Unchanneled valley recharge.—The relation of the simulated water table in layer 1 within the valley to land-surface elevation and to the pseudo-land surface (eq. 13) resulted in 1.74 ft^3/s of unchanneled recharge (*TUR*, eq. 14u) to valley cells along the valley wall and 1.46 ft^3/s of rejected recharge (fig. 58). This rejected recharge occurred primarily in areas where water levels were lower than land surface but above the pseudo land surface at a depth of 1 ft (eq. 13b). Most of this rejection occurred in the region adjacent to upland zone 1, west of Killbuck Creek (fig. 49). If the magnitude and distribution of the rejected recharge in a simulation is interpreted to be unrealistic, modifications can be applied to decrease the rejected recharge, as was noted in the discussion of the Dover simulations and of the Wooster transient-state simulation. In some situations, rejected recharge in the valley could be interpreted as representing ground-water evapotranspiration.

Channeled Valley Recharge.—The 3.89 ft^3/s of channeled runoff was distributed to the upstream cells of the six tributaries simulated by the Variable-Recharge procedure (fig. 49 and table 22). All of these streams except for the tributary emanating from upland zone 4 lost water to the surficial layer. Nevertheless, loss from these streams (*TCR*, eq. 14t) was only 0.15 ft^3/s because the small streambed leakance (0.1 (ft/d)/ft) and the narrow stream width (8 ft) resulted in a relatively small streambed conductance (eq. 6). Consequently, the component of upland channeled runoff that did not recharge the valley fill was relatively large (3.74 ft^3/s). Of this quantity, about 2 ft^3/s flowed to Killbuck Creek from the two tributary streams emanating from upland zones 4 and 5 (fig. 49), and the remaining 1.7 ft^3/s flowed from the four northernmost tributaries to the midvalley tributary; 1.5 ft^3/s was from the stream emanating from upland zone 6. The Variable-Recharge procedure does not provide for flow in the downstream reach of a tributary stream to be explicitly applied to another stream, but if flow from the four tributaries could have been applied to the midvalley tributary, some segments of the midvalley tributary depicted as dry on figure 53 would probably have been simulated as flowing. This additional 1.7 ft^3/s of streamflow represents potential recharge to the valley fill that was not accounted for in the simulation. The relatively small streambed conductance of the midvalley tributary indicates, however, that any additional recharge from stream loss would probably be small.

Ground-Water Budget

The simulated steady-state water budget for the stratified-drift aquifer at Wooster, Ohio is summarized in table 24. Total recharge to the stratified drift from all sources was about 12.5 ft^3/s. This recharge consisted of the following components: direct recharge (2.9 ft^3/s), unchanneled and

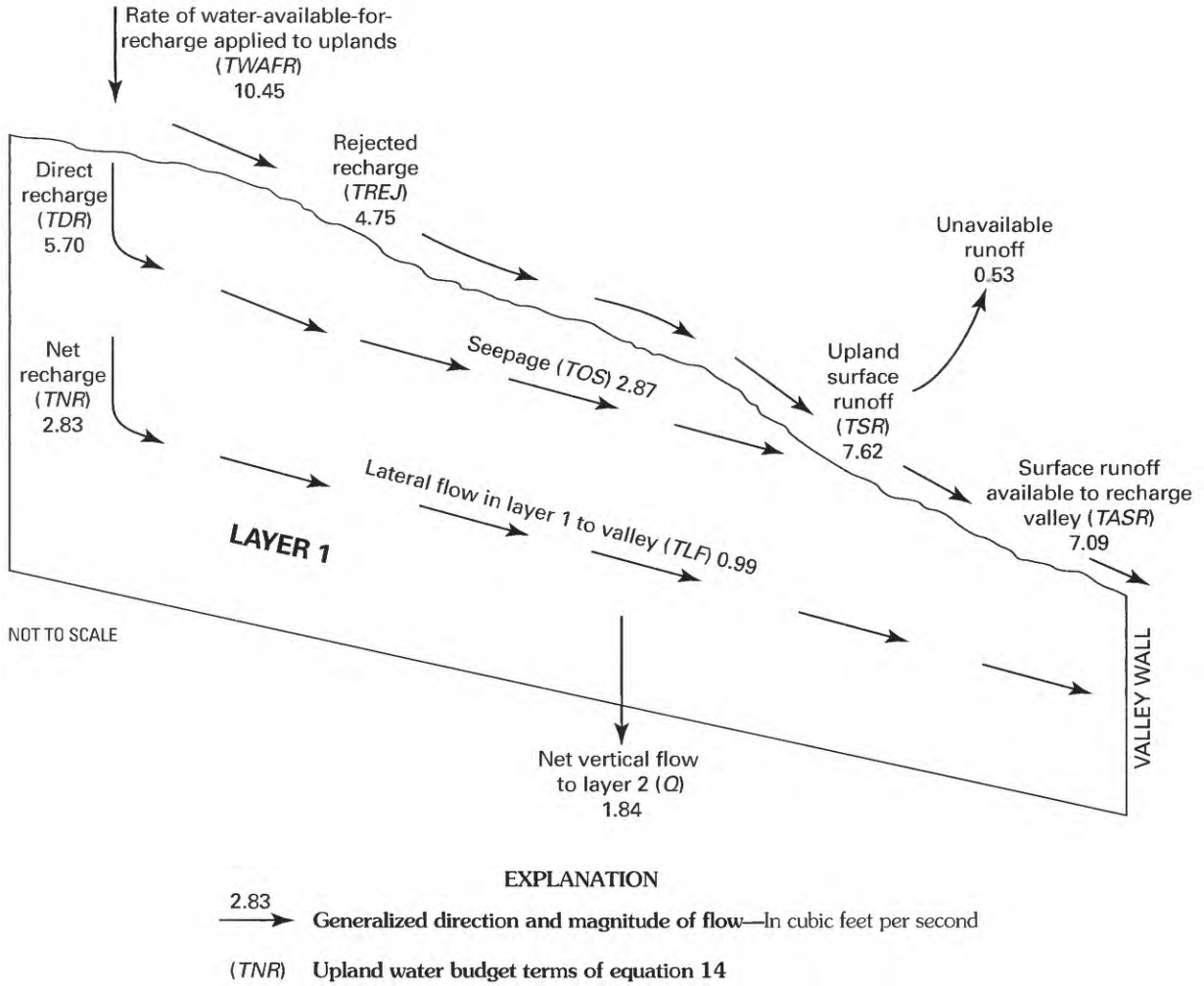

FIGURE 57.—Distribution of water available for recharge applied to uplands, as simulated by Variable-Recharge procedure in Wooster steady-state model of fall 1984 conditions (from Breen and others, 1995, fig. 8).

channeled recharge from upland sources (1.9 ft^3/s), losses from streams and ponds (4.4 ft^3/s); underflow from the upstream valley and from the deposits underlying Apple and Clear Creek (0.4 ft^3/s) and lateral ground-water flow from the uplands through all layers (2.8 ft^3/s). The total lateral ground-water flow from the uplands was equivalent to the net recharge to the uplands and represents about 23 percent of the total inflow to the stratified drift. Of the total inflow to the stratified drift from all sources, 7.9 ft^3/s (63 percent) was derived from sources in the uplands.

The simulated water budget for the entire model, including the vertical exchange between model layers and lateral ground-water flow into the valley, is given in figure 59. The quantity termed "Total Recharge to Valley at Land Surface" (9.28 ft^3/s) consists of all inflow terms of table 24 except lateral flow from the uplands and underflow, and the quantity termed "Total Discharge from Valley at Land Surface" consists of all outflow terms of table 24 except pumpage.

Net Recharge and Surface Runoff within Upland Subbasins

The Variable-Recharge procedure is a highly simplified approach to the simulation of the magnitude and distribution of upland recharge and surface runoff; it ignores many of the factors and processes that are the subject of hillslope and unsaturated-zone hydrology which govern the small-scale magnitude and distribution, in time and space, of infiltration and surface runoff. At best, the method can approximate actual processes at the scale of the model grid. A measure of how well these processes are approximated can be inferred by comparing simulated recharge and surface runoff with known information within individual upland subbasins. Simulated steady-state values of surface runoff, and net recharge of layer 1 for each of the 15 upland subbasins are given in table 25. In each of the upland subbasins 1, 4, 5, 6, 8, and 10 (fig. 49), the simulated steady-state surface runoff (*SR*, eq. 14d; table 25, column 4) represents more than 79 percent of the rate of *WAFR* (*WAFRZ*, eq. 14a; table 25, column 3); whereas

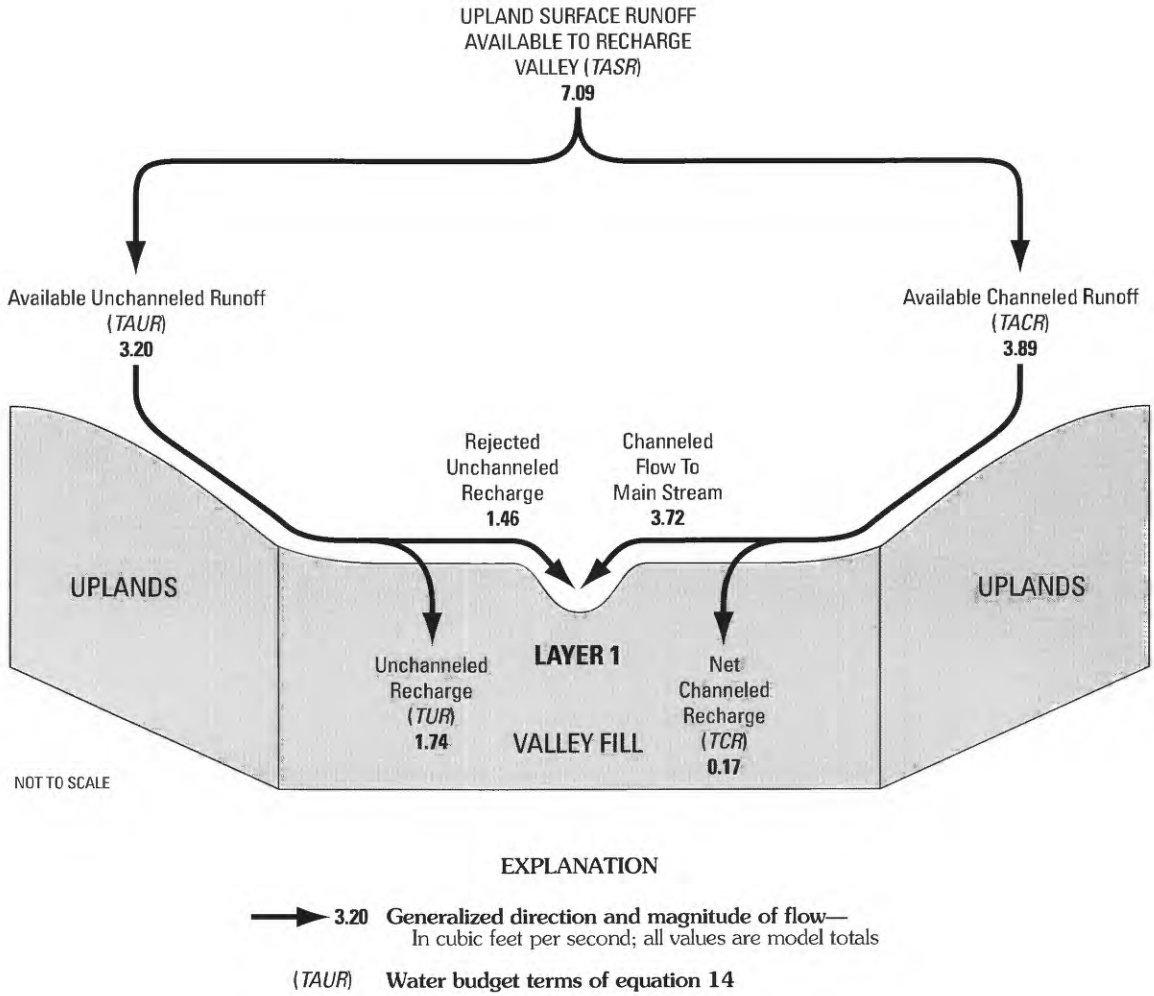

FIGURE 58.—Distribution of available upland surface runoff (unchanneled and channeled) and simulated recharge to the valley from upland sources in Wooster steady-state model of fall 1984 contitions (modified from Breen and others, 1995, fig. 9).

the net upland recharge in these subbasins (*NRZ*, eq. 14f; table 25, column 5) represents less than 21 percent of the rate of *WAFR*. Each of these subbasins contains at least one relatively large stream channel (fig. 49); thus a relatively large component of surface runoff is to be expected. Furthermore, the percentage of surface runoff that resulted from outward seepage (eq. 13c) in all of the subbasins ranges from 20 to 52 percent and averaged 42 percent. These values are consistent with the relation between ground-water outflow and percentage of drainage area underlain by stratified drift shown in figure 15. Although figure 15 is developed from Connecticut data, it indicates that in watersheds lacking stratified drift, about 35 percent of total runoff consists of ground-water outflow.

The simulated surface runoff in subbasins 12 through 15 represents only a small proportion of the rate of *WAFR*, whereas the net upland recharge in these basins is relatively large (table 25) and except for upland zone 12 all lack stream channels (fig. 49). The remaining subbasins (2, 3, 7, 9, and 11) contain relatively small stream channels, and simulated surface runoff and net upland recharge are roughly comparable. Thus, the simulated distribution of surface runoff and net upland recharge in most subbasins is generally commensurate with the topographic character of each subbasin.

Vertical Recharge of Buried Valley Deposits

The Killbuck Creek valley aquifer is capped by a fine-grained confining unit that is locally interrupted by permeable alluvial sand and gravel where tributaries enter Killbuck Creek valley. It is, therefore, reasonably typical of the delta-fed buried aquifers described in the section "Simulation of Aquifer Types", although the surficial position and relative thinness of the confining unit are atypical. Accordingly, the Wooster model can provide information as to the possible sources and spatial distribution of recharge to this type of aquifer. As discussed in Breen and others (1995), about 24 percent of the steady-state simulated recharge to or through

TABLE 24.—*Steady-state water budget for the stratified-drift aquifer at Wooster, Ohio*

[Asterisk denotes recharge from upland sources. Rates are in cubic feet per second]

Inflow	Rate	Percent of total	Outflow	Rate	Percent of total
Direct recharge	2.92	23.4	Seepage	0.71	5.7
Recharge from upland unchanneled sources	1.74*	14.0			
Recharge from upland channeled sources as simulated by Variable-Recharge procedure	0.17*	1.4	Discharge to channels of minor tributaries	0.02	0.2
Recharge from Little Killbuck, Clear, and Apple Creeks	2.99*	24.0	Discharge to Little Killbuck Creek	0.74	5.9
Recharge from Killbuck Creek	1.10	8.8	Discharge to Killbuck Creek	1.86	14.9
Recharge from constant heads (ponds)	0.32	2.6	Discharge to drains	0.67	5.4
Upstream underflow	0.22	1.8			
Clear Creek and Apple Creek underflow	0.17*	1.4			
Lateral flow from uplands	2.83*	22.7	Pumpage (north and south well fields)	8.50	68.0
Total	12.5	100	Total	12.5	100

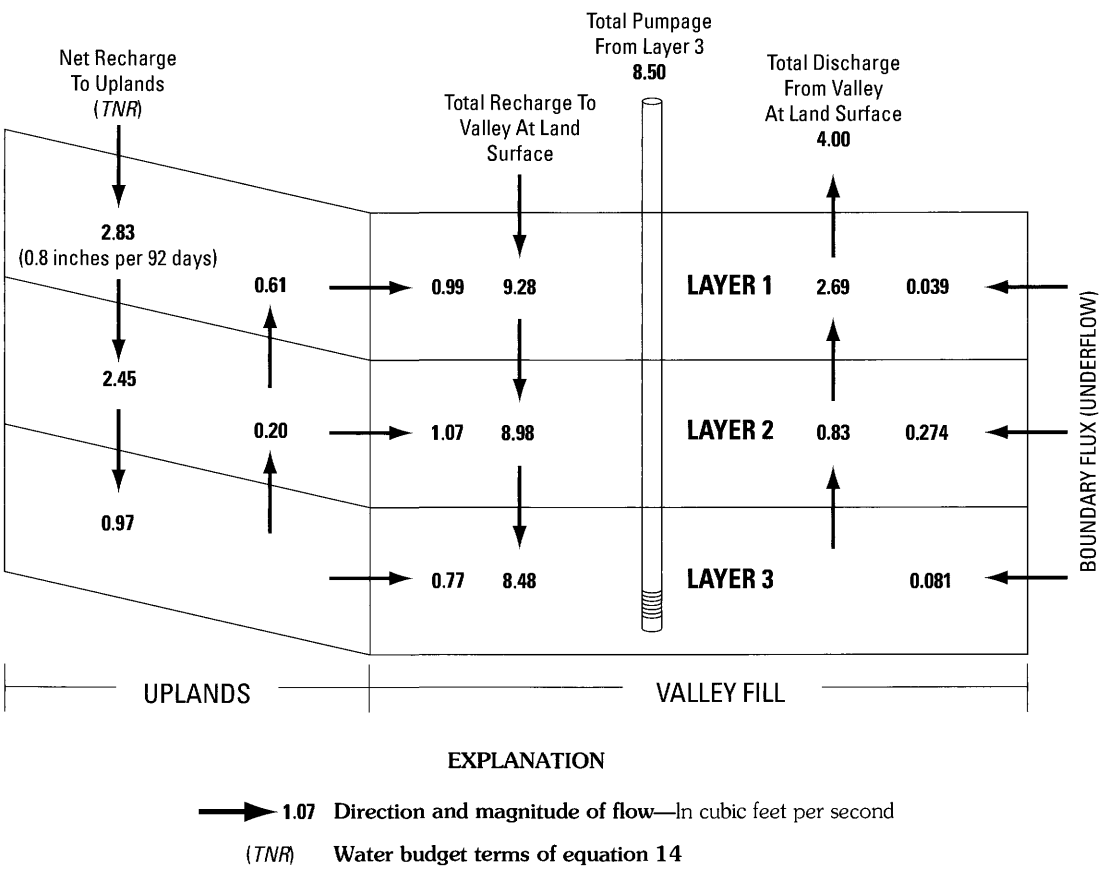

FIGURE 59.—Simulated ground-water budget for Wooster steady-state model of fall 1984 conditions (modified from Breen and others, 1995, fig. 13).

TABLE 25.—*Net recharge and surface runoff within upland subbasins in Wooster steady-state simulation*

[ft^3/s. cubic feet per second]

Upland subbasin (recharge zone)		Rates of recharge and runoff (ft^3/s)		
No.	Location[1]	Total water available for recharge	Surface runoff	Net upland recharge to layer 1
1	2	3	4	5
1	W, S	0.88	0.75	0.13
2	W, S	0.30	0.21	0.09
3	W, S	0.33	0.12	0.21
4	W, N	0.69	0.60	0.09
5	W, N	1.93	1.89	0.04
6	W, N	2.03	1.88	0.15
7	W, N	0.32	0.15	0.17
8	W, N	0.56	0.44	0.12
9	E, N	0.61	0.26	0.35
10	E, S	1.19	1.05	0.14
11	W, N	0.22	0.10	0.12
12	W, N	0.21	0.03	0.18
13	W, N	0.17	0.01	0.16
14	E, N	0.65	0.04	0.61
15	E, S	0.34	0.08	0.26
	Total	10.44	7.61	2.83[2]

[1] Location abbreviations:
W, zone west of valley; E, zone east of valley; S, zone south of ground-water divide separating north and south well fields; N, zone north of ground-water divide. Zone locations shown in figure 49.

[2] Disposition of net upland recharge is as follows:

to north well field	= 2.01 ft^3/s
to south well field	= 0.82 ft^3/s
Total	2.83 ft^3/s
to valley from western uplands	= 1.48 ft^3/s
to valley from eastern uplands	= 1.35 ft^3/s
Total	2.83 ft^3/s

the surficial confining layer occurred in only about 1 percent of the valley area, which is beneath major tributaries and in a few other localities along the valley wall where surficial materials grade to permeable sand and gravel with relatively high vertical leakance. The bulk of the recharge (76 percent), resulted from small vertical flows (less than about 0.01 ft^3/s per model cell) over large areas of the valley floor.

SENSITIVITY ANALYSIS

This section describes the response of the Wooster steady-state model to (1) variations in the horizontal and vertical hydraulic conductivity of the uplands, (2) streambed conductance of tributary streams simulated with the Variable-Recharge procedure, and (3) the addition of a fourth model layer.

Upland Horizontal Hydraulic Conductivity

A sensitivity analysis of the horizontal hydraulic conductivity of layers representing the uplands, similar to that described for the Dover models in the section "Water Budgets for Two Upland Settlings", was carried out for the Wooster model. The value of upland hydraulic conductivity for the calibrated steady-state model, designated as simulation D (table 26), was 0.3 ft/d. Additional simulations, designated as A, B, C, and E, were performed in which the hydraulic conductivity was specified as 0.03, 0.06, 0.1 and 1.0 ft/d, respectively. Sensitivity, in terms of changes in the upland budget-terms of equations 14a-14w and the manner in which the *WAFR* was distributed for each simulation, is given in table 26 and figure 60. Because the simulations were steady state and lacked upland sources and sinks, total lateral flow to the valley (*TLF*) was equal to total net recharge to the upland (*TNR*).

Response in uplands.—In the uplands, increased hydraulic conductivity results in generally lower water levels. Thus, when hydraulic conductivity was increased from 0.03 ft/d in model A to 1.0 ft/d in model E, water levels declined enough to allow an increase in infiltration and in total lateral flow from 0.8 ft^3/s in model A to 4.2 ft^3/s in model E (*TLF*, fig. 60, table 26, column 9) and a corresponding decrease in surface runoff from 9.7 ft^3/s to 6.3 ft^3/s (table 26, column 8). As upland water levels declined, the number of seepage cells decreased from 917 in model A to 364 in model E (table 26, column 5) and the area of outward seepage decreased from 33.7 percent to 15 percent of the upland area simulated (table 26, column 6). Despite this large decrease in the area of outward seepage, the volume of outward seepage increased from 0.8 ft^3/s in model A to 4.1 ft^3/s in model E (table 26, column 7) because the 33-fold increase in hydraulic conductivity in model E allowed much more flow through the remaining seepage cells, as computed by equation 13d. A similar increase in infiltration and seepage in response to increased hydraulic conductivity in the uplands was noted in the Dover models (table 18). Because infiltration in the uplands of Wooster model E greatly exceeded that in model A, total available unchanneled runoff from the uplands decreased about 50 percent, from 4.9 to 2.4 ft^3/s (*TAUR*, fig. 60 and table 25, column 12b). Total available channeled runoff decreased by only 19 percent, from 4.2 to 3.4 ft^3/s (*TACR*, fig. 60 and table 25, column 11b), because in upland subbasins that slope toward tributary streams, even though infiltration has increased at the expense of rejected recharge, much of the increased infiltration will flow laterally through layer 1 to discharge in seepage cells downslope, from which it is routed to the tributary and continues to reach the valley as channeled upland runoff. Total available surface runoff (*TASR*; table 25, column 10) was less than total surface runoff (*TSR*, column 8) for all simulations A through E, because the storm sewers in

TABLE 26.—*Simulated water budgets for Wooster steady-state condition showing distribution of upland water available for recharge and percentage of valley-fill recharge derived from upland sources as a function of upland hydraulic conductivity and vertical leakance*

[Water-budget terms (capital letters in parentheses) are defined by equations 14j through 14w. Water available for recharge rate (*TWAFR*, eq. 14j) is 10.45 ft^3/s for all simulations. Simulation ***D*** (italics) is calibrated steady-state model; simulation D* is same as simulation D except that streambed conductance of tributaries is 10 times greater. ft^3/s, cubic feet per second; ft/d, feet per day; (ft/s)/ft, feet per second per foot. Dashes indicate value not calculated]

Simulation	Upland horizontal hydraulic conductivity or vertical leakance	Total direct recharge (*TDR*) (ft^3/s)	Total rejected recharge (*TREJ*) (ft^3/s)	Seepage: Number of upland seepage cells	Seepage: Total upland seepage area (percent)	Seepage: Total outward seepage (*TOS*) (ft^3/s)	Total surface runoff (*TSR*) (ft^3/s)	Total lateral flow to valley (*TLF*)[a] (ft^3/s)	Total available runoff: Surface (*TASR*) Rate (ft^3/s)	Total available runoff: Channeled (*TACR*) Percent of *TASR*	Total available runoff: Channeled (*TACR*) Rate (ft^3/s)	Total available runoff: Unchanneled (*TAUR*) Percent of *TASR*	Total available runoff: Unchanneled (*TAUR*) Rate (ft^3/s)	Total recharge from runoff: Channeled (*TCR*) Rate (ft^3/s)	Total recharge from runoff: Unchanneled (*TUR*) Rate (ft^3/s)	Total recharge from upland sources[b] (TR_{u-v}) (ft^3/s)	Percent of valley recharge from all upland sources[c]
1	2	3	4	5	6	7	8	9	10	11a	11b	12a	12b	13	14	15	16
Simulation with varied horizontal hydraulic conductivity (col. 2)[d] and constant vertical leakance of 1.0×10^{-9} (ft/s)/ft																	
	ft/d																
A	0.03	1.6	8.9	917	33.7	0.8	9.7	0.8	9.1	46	4.2	54	4.9	0.18	3.0	4.0	62
B	0.06	2.4	8.1	887	32.9	1.2	9.3	1.2	8.7	47	4.1	53	4.6	0.18	2.8	4.2	—
C	0.10	3.3	7.2	854	32.1	1.6	8.8	1.6	8.3	49	4.1	51	4.2	0.18	2.5	4.3	—
D	***0.30***	***5.7***	***4.8***	***687***	***26.8***	***2.9***	***7.6***	***2.8***	***7.1***	***55***	***3.9***	***45***	***3.2***	***0.17***	***1.7***	***4.7***	***63***
D*	0.30	5.7	4.8	694	27.0	2.9	7.6	2.8	7.1	55	3.9	45	3.2	0.74	1.8	5.3	—
E	1.00	8.3	2.2	364	15.0	4.1	6.3	4.2	5.8	59	3.4	41	2.4	0.16	1.3	5.7	66
Simulation with varied vertical leakance (col. 2)[e] and constant horizontal hydraulic conductivity of 0.3 ft/d																	
	(ft/s)/ft																
F	0.1×10^{-9}	4.9	5.5	791	29.4	2.7	8.3	2.2	7.7	44	3.9	49	3.8	0.17	2.1	4.5	—
G	0.5×10^{-9}	5.4	5.0	712	27.4	2.8	7.8	2.7	7.2	54	3.9	46	3.4	0.17	1.8	4.7	—
D	***1.0×10^{-9}***	***5.7***	***4.8***	***687***	***26.8***	***2.9***	***7.6***	***2.8***	***7.1***	***55***	***3.9***	***45***	***3.2***	***0.17***	***1.7***	***4.7***	***63***
H	69.4×10^{-9}	6.9	3.6	538	23.1	3.7	7.4	3.1	6.9	57	3.9	43	3.0	0.17	1.7	5.0	—

[a] *TLF* equals net areal recharge to uplands (*TNR*).
[b] Columns 9 + 13 + 14; does not include recharge in valley from Little Killbuck, Clear, or Apple Creeks.
[c] Includes losses and underflow through alluvium along Little Killbuck, Clear, and Apple Creeks.
[d] Simulations A, B, C, D, and E differ only in horizontal hydraulic conductivity of the uplands. Simulation D* differs from model D in that streambed conductance of tributaries simulated by Variable-Recharge procedure is 1 (ft/d)/ft, 10 times that of simulation D [0.1 (ft/d)/ft].
[e] Simulations F, G, and H differ only in vertical leakance of uplands.

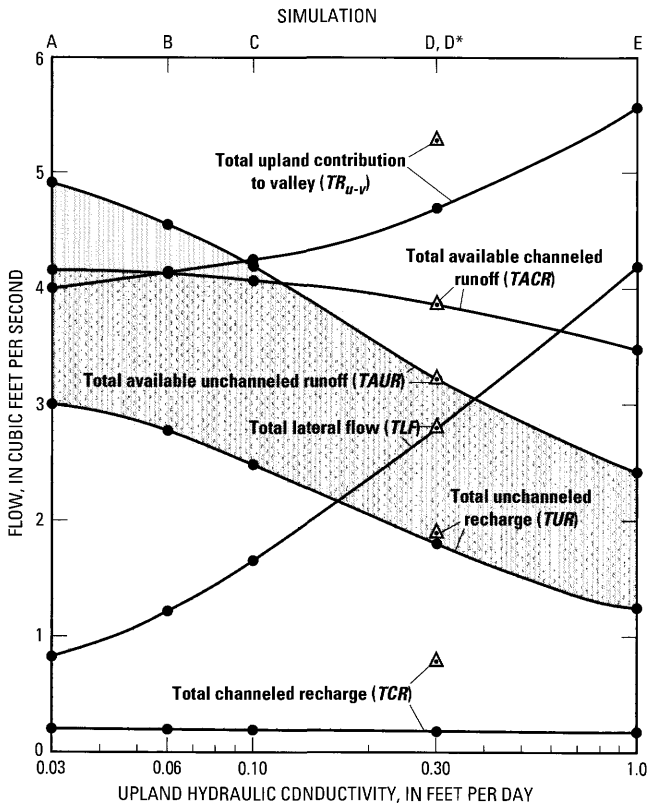

FIGURE 60.—Sensitivity of water-available-for-recharge components described in equation 14 to changes in upland hydraulic conductivity and to an increase in streambed leakance of upland tributary streams from 0.1 to 1.0 foot per day per foot, in Wooster steady-state model of fall 1984 conditions.

an urban area (zone 10, fig. 49) were assumed to intercept 50 percent of surface runoff (table 22).

Response in valley.—The increase in upland hydraulic conductivity from 0.03 ft/d in model A to 1 ft/d in model E caused heads in some areas within Killbuck Creek valley to increase substantially, as shown in figure 61. The head increases ranged from less than 1 ft (well N6, fig. 61) to about 7 ft (well N12, fig. 61), depending on location. This general increase in head was primarily the result of the substantial increase (3.4 ft^3/s) in total lateral ground-water flow from the uplands to Killbuck Creek valley (table 26, column 9), even though the increase in lateral flow was partially offset by decreases in available unchanneled and channeled runoff (table 26, columns 11 and 12). Some of the unchanneled runoff was rejected when it reached the valley floor, because of the low hydraulic conductivity and relatively high water table of layer 1 within the valley, and nearly all channeled runoff was similarly rejected. Therefore, the decrease in recharge from channeled and unchanneled runoff (*TCR* and *TUR*, fig. 60 and table 26, columns 13 and 14) that accompanied the increase in upland hydraulic conductivity was much smaller than the increase in recharge from lateral ground-water flow (*TLF*, fig. 60). Thus the total upland-derived recharge to the valley (TR_{u-v}, fig. 60 and table 26, column 15) increased from 4.0 ft^3/s to 5.7 ft^3/s, resulting in higher valley heads (fig. 61). If stream losses from Little Killbuck, Clear, and Apple Creeks and underflow from their watersheds are also considered to be upland-derived recharge, however, the proportion of total recharge to the valley fill that originates in the uplands increases only slightly, from 62 to 66 percent (table 26, column 16) in response to increased upland hydraulic conductivity, primarily because recharge to the valley from losing reaches of Little Killbuck Creek and Clear Creek diminish somewhat as valley heads increase.

Profiles of simulated head in model layers 1 and 2 along model row 55 (fig. 62*A*), for simulations B, D, and E, show the typical water-table response to increased upland hydraulic conductivity; that is, (1) a decrease in upland water-table elevation and gradient within recharge areas, (2) a similarity of water-table and land-surface elevation in discharge areas because the simulated water table is set to land surface elevation if outward seepage occurs (eq. 13d), and (3) an increase in valley heads. The pattern in the confined layer (fig. 62*B*) is similar in upland recharge areas and in the valley fill, but no predictable pattern is discernible in local upland discharge areas, perhaps because the upland heads respond regionally to hydraulic conductivity variations that are applied uniformly over the entire uplands.

Upland Vertical Leakance

Model sensitivity to changes in vertical hydraulic conductivity of upland materials was evaluated through several simulations in which vertical leakance in the uplands between layers 1 and 2 and layers 3 and 4 was varied. Upland water budgets for these simulations (termed simulations F, G, and H) together with that of the calibrated steady-state simulation (simulation D) are included in table 26. In general, if the vertical leakance between model layers is increased a smaller vertical head gradient is required to maintain a particular vertical flow rate, hence heads in the topmost layer will tend to decrease whereas heads in underlying layers will tend to increase. Thus, the water-table response (fig. 63*A*) to variations in vertical leakance, and therefore trends in water-budget terms (table 26), were similar to those obtained when

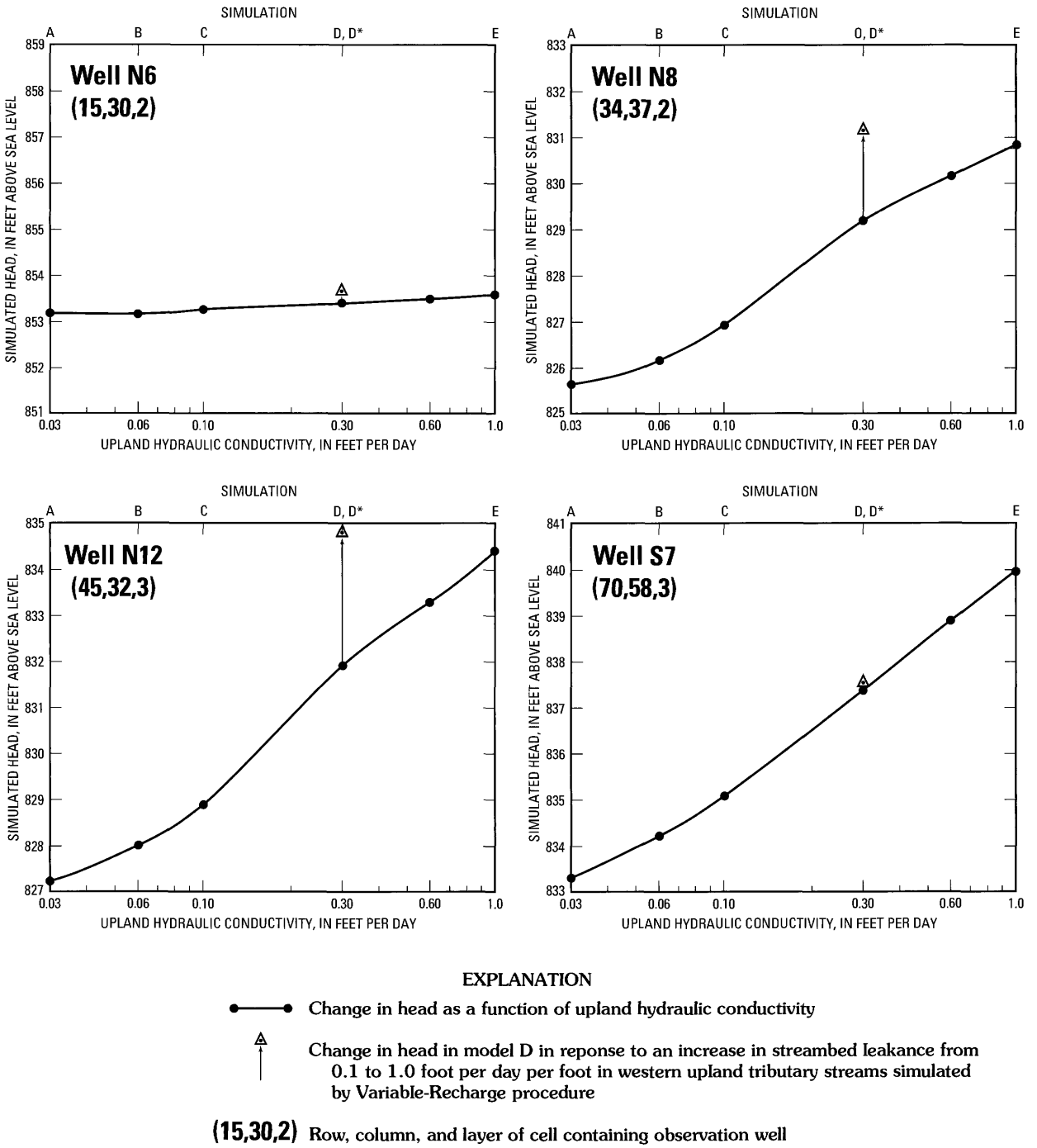

FIGURE 61.—Sensitivity of Wooster steady-state model heads in four valley cells to changes in hydraulic conductivity of uplands and to an increase in streambed leakance of small tributary streams flowing from western uplands.

upland hydraulic conductivity was varied; that is, upland water-table elevations and gradients in recharge areas decreased with an increase in vertical leakance.

The upland contribution to valley recharge increased from 4.5 to 5 ft^3/s (table 26, column 15) with increasing vertical leakance primarily because a decline in the upland water table enhanced net upland recharge and the resultant lateral ground-water flow to the valley (*TLF*; table 26, column 9); this in turn caused a rise in valley heads ranging from about 1 ft in the north well field to 3 or 4 ft in the south well field. Head changes were greater in the south well field than in the north well field because the increase in net recharge in upland subbasins adjacent to the south well field (and the consequent increase in lateral ground-water flow) was about twice that in

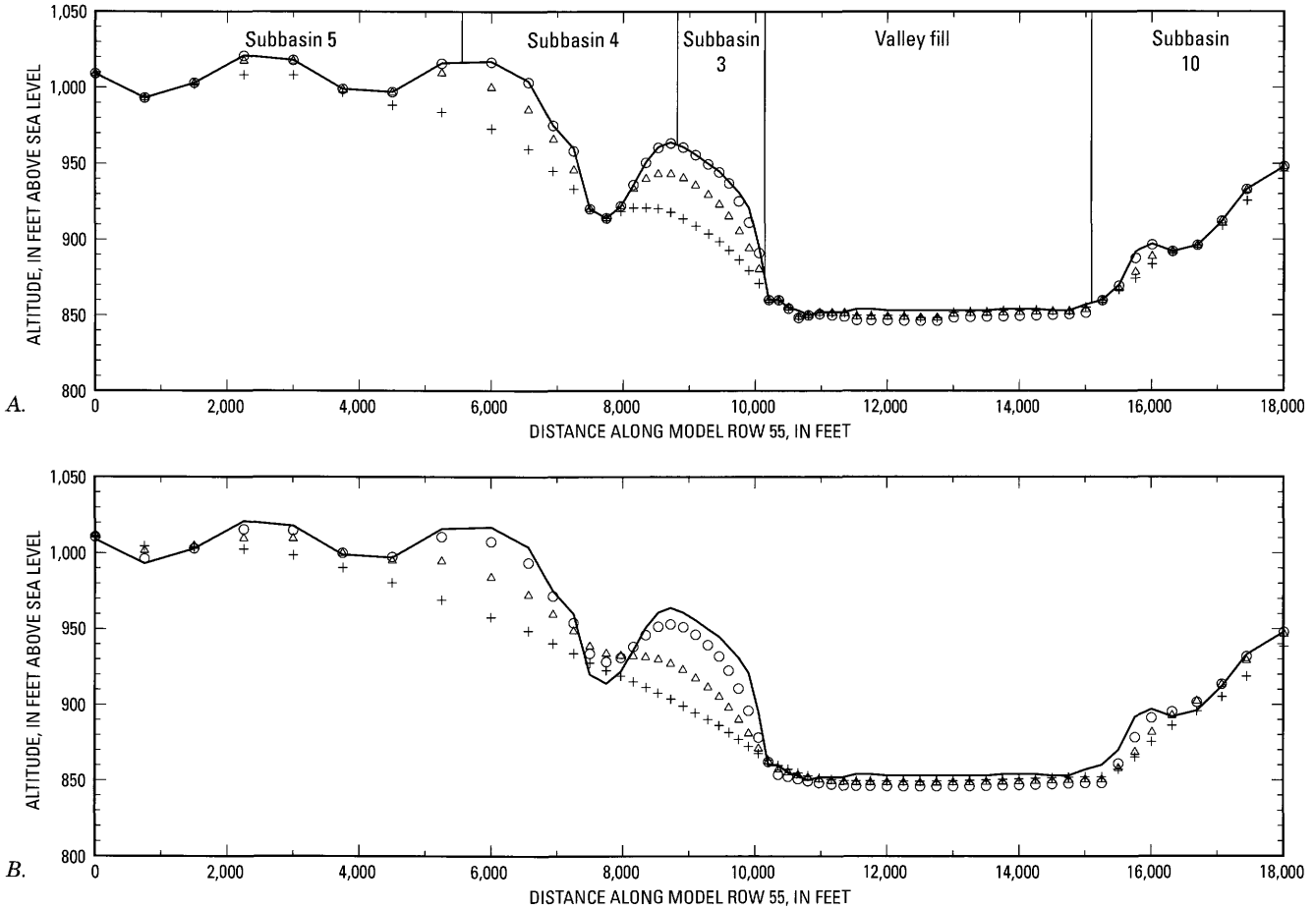

FIGURE 62.—Simulated steady-state heads along Wooster model row 55 as a function of upland hydraulic conductivity for (*A*) model layer 1 and (*B*) model layer 2. Simulations B, D, and E are described in table 26. Segments of the profiles coinciding with the valley fill and upland subbasins of figure 49 are indicated.

subbasins adjacent to the north well field. In general, order-of-magnitude increases in vertical leakance of upland materials had a smaller effect on the upland water-budget components (table 26) and on valley heads than did a comparable increase in horizontal hydraulic conductivity of upland materials.

The response in confined layer 2 to a uniform increase in vertical leakance was opposite to that of an increase in horizontal hydraulic conductivity; that is, water levels in recharge areas increased, rather than decreased, with increasing vertical leakance (fig. 63*B*, compare profiles for simulations F and H). As was noted in the sensitivity analysis of upland hydraulic conductivity, no predictable pattern is evident in the discharge areas. If variations in hydraulic properties were implemented locally, rather than regionally, the response would be more predictable; for example, if simulated confined heads in a particular discharge area were too high, a local increase in vertical leakance would result in lower heads in that area.

Streambed Leakance of Tributary Streams Simulated by Variable-Recharge Procedure

Simulation of the three largest upland subbasins (Little Killbuck, Clear and Apple Creeks) was impractical because

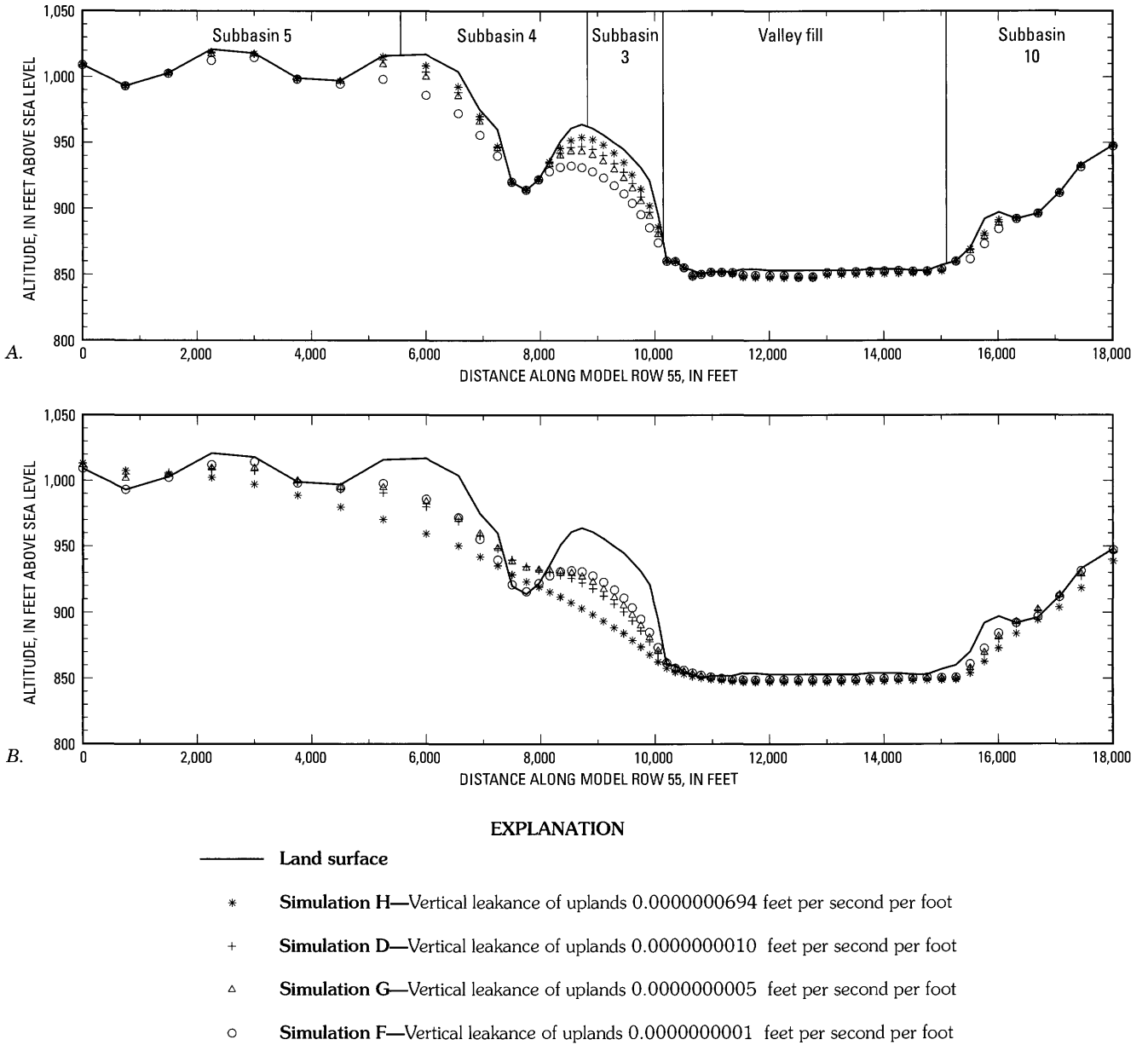

FIGURE 63.—Simulated steady-state heads along Wooster model row 55 as a function of upland vertical leakance between layers 1 and 2 for (*A*) model layer 1 and (*B*) model layer 2. Simulations D, F, G, and H are described in table 26. Segments of the profiles coinciding with the valley fill and upland subbasins of figure 49 are indicated.

the drainage areas were too big to incorporate into the model (fig. 49). Essentially all subbasin flow was assumed to enter the respective tributaries; thus, contributions from each subbasin to the valley consisted of streamflow losses as simulated by the Stream Package. The largest component of valley recharge (2.99 ft^3/s, table 24) came from these tributaries—primarily from Little Killbuck and Clear Creeks.

Six smaller streams emanating from the western uplands (fig. 49) were simulated as part of the Variable-Recharge procedure because their drainage basins could be readily incorporated within the model. The low streambed leakance and conductance assigned to these tributaries provided very little recharge to the valley fill (table 24). A simulation to determine head response to an increase in the streambed conductance of these streams was implemented with the same properties as the calibrated steady-state model (simulation D) except that streambed leakance was increased 10-fold from 0.1 to 1.0 (ft/d)/ft. The water budget for this simulation, designated as simulation D* (table 26 and fig. 60), shows that the streamflow losses from the tributaries and, therefore, the total channeled recharge (*TCR*) and total upland contribution to the valley (TR_{lt-v}) increased, relative to simulation D, by 0.6 ft^3/s.

In addition, the increased streambed leakance caused the three tributaries flowing from upland zones 7 and 8 (fig. 49) to lose all of their flow to the aquifer. This additional recharge caused heads in cells near the tributary streams (N6, N8, N12 of fig. 61) to rise by several tenths of a foot to several feet relative to simulation D, whereas the effect in cells far from the tributaries (S7 of fig. 59) was negligible. Thus, seepage losses from relatively small streams have the potential to strongly affect heads in nearby parts of an aquifer and their effects should be considered in designing flow models of aquifer systems containing such streams.

Addition of a Fourth Model Layer

Layer 3 of the Wooster model represents sand and gravel in Killbuck Creek valley that is underlain by 10 to 30 ft of clay-rich till containing boulders and lenses of silty sand and gravel; this unit, in turn, overlies bedrock. The model was bounded at the base of layer 3 on the assumption that the hydraulic effects of the underlying till on the flow system were negligible. This assumption was evaluated through several simulations in which a fourth model layer with a variety of hydraulic properties was added to the calibrated steady-state model. In one set of simulations (W_a, W_b, W_c, and W_d; table 27), the additional layer was assigned a uniform transmissivity of 10.5 ft^2/d (which may be interpreted as a layer 35 ft thick with the same horizontal hydraulic conductivity as the uplands of the three-layer model, 0.3 ft/d) while vertical hydraulic conductivity of the additional layer was varied over five orders of magnitude. The vertical leakance between layers 3 and 4 was taken to be the vertical hydraulic conductivity of layer 4 divided by the assumed thickness of 35 ft. A vertical hydraulic conductivity of 3×10^{-3} ft/d or greater in layer 4 caused model heads in layer 3 to increase by an average of about 0.5 ft within the north and south well fields, relative to those in the three-layer model (simulations W_a and W_b in table 27). Decreasing vertical hydraulic conductivity to 3×10^{-6} ft/d (simulation W_d) produced heads that were about equal to those in the three-layer model; the same result was obtained when transmissivity of layer 4 was reduced by 1 order of magnitude, with a vertical hydraulic conductivity of 3×10^{-2} ft/d (simulation W_e).

Two simulations in which the part of layer 4 beneath the upland was effectively impermeable (simulations W_f and W_g)

TABLE 27.—*Sensitivity of simulated head in Wooster model to variation in horizontal and vertical conductivity of lower layer added to the model*

[ft, feet; ft/d, feet per day; ft^2/d, feet squared per day]

	Simulation							
	Wa	Wb	Wc	Wd	We	Wf	Wg	Wh
***A.* Hydraulic properties of added lower layer (layer 4)**								
Horizontal hydraulic conductivity (ft/d)								
Bedrock beneath uplands	3×10^{-1}	3×10^{-1}	3×10^{-1}	3×10^{-1}	3×10^{-2}	3×10^{-4}	3×10^{-4}	3×10^{-1}
Valley fill	3×10^{-1}	3×10^{-1}	3×10^{-1}	3×10^{-1}	3×10^{-2}	3×10^{-1}	3.0	3.0
Transmissivity (ft^2/d)[1]								
Bedrock beneath uplands	10.5	10.5	10.5	10.5	1.05	0.0105	0.0105	10.5
Valley fill	10.5	10.5	10.5	10.5	10.5	10.5	105.0	105.0
Vertical hydraulic conductivity (ft/d)[2]	3×10^{-1}	3×10^{-3}	3×10^{-5}	3×10^{-6}	3×10^{-2}	3×10^{-6} (uplands) 3×10^{-1} (valley fill)	3×10^{-6} (uplands) 3×10^{-2} (valley fill)	3×10^{-2} (uplands) 3×10^{-1} (valley fill)
***B.* Model response for fall 1984 steady-state conditions[3]**								
Average increase in simulated head in north and south well-field regions relative to head in three-layer model (ft)	0.55	0.49	0.19	0.04	0.04	0.03	0.31	0.96

[a] Transmissivity calculated from an assumed layer thickness of 35 ft.
[b] Vertical leakance between layers 3 and 4 is assumed to be vertical hydraulic conductivity of layer 4 divided by layer thickness of 35 ft.
[c] Average increase in 21 cells containing observation wells open to model layer 3.

indicate the effect of the hydraulic properties of layer 4 within the valley fill only. Heads in simulation W_f were insensitive to the additional layer even though the valley part of layer 4 had the same hydraulic properties as in simulation W_a. Simulation W_g, in which transmissivity and vertical hydraulic conductivity of layer 4 within the valley were increased by 1 order of magnitude, caused heads in the well field regions to rise by only about 0.3 ft. Thus, the presence of relatively impermeable bedrock beneath the uplands reduced the sensitivity of head to the additional layer. This was further demonstrated in simulation Wh, wherein the average head in the well field regions increased by about 1 ft after the part of layer 4 beneath the uplands was assigned a transmissivity and vertical hydraulic conductivity comparable to the overlying upland material.

These differences in sensitivity result from the manner in which the additional layer is recharged—as a function of the hydraulic properties of the additional layer. If the part of layer 4 beneath the uplands is relatively permeable, some part of the upland recharge moves downward to layer 4 and laterally to the valley, and thus is available to replenish part of the water removed by pumping from the stratified drift overlying layer 4 in the valley. The magnitude of the vertical flow from layer 4 need not be large to have a measurable effect on heads within the overlying stratified drift; for example, the total recharge to the valley from the uplands through layer 4 in simulations Wa and Wh was only 0.3 and 0.5 ft^3/s, respectively.

An additional layer beneath the stratified drift in models in which the uplands are not explicitly simulated receives no lateral flow from the uplands; thus any upward flow to the overlying valley fill in response to pumping must be balanced by downward flow from nearby valley areas so that the net contribution to the valley fill from the additional layer would be nil. The additional layer in such simulations would therefore have a lesser effect on the valley-fill flow system than in a model in which the uplands are explicitly simulated.

These results suggest that the addition (or omission) of a layer with moderately low transmissivity (as in simulations Wa, Wb, and Wh, table 27) can, under some conditions of stress, have a significant effect on heads in systems in which the uplands are explicitly modeled. The potential effects of the location of the bottom boundary through which flow is assumed to be negligible can be readily determined by sensitivity analysis, given the relative ease with which an additional layer can be incorporated in a simulation, especially if the layer is assigned uniform transmissivity and vertical leakance.

SUMMARY AND CONCLUSIONS

REGIONAL HYDROGEOLOGY

The region designated as the glaciated Northeast encompasses the New England states, New York, and parts of Ohio, Pennsylvania, and New Jersey north of the limit of Wisconsin-age glaciation. Stratified drift was deposited primarily along meltwater channels and in bodies of ponded water in bedrock valleys scattered throughout the 122,000 square miles of the glaciated Northeast. Stratified drift with a saturated thickness of at least 10 ft and the potential for sustained yields of at least 10 gal/min to wells underlies a total area of about 15,400 mi^2, about 13 percent of the glaciated Northeast. More than 5,000 individual stratified-drift aquifers, each of which encompasses only a few square miles, have been mapped in the region. The widespread distribution of stratified drift within the region is depicted on a 1:1,500,000-scale map constructed from data digitized from larger-scale maps and processed with Geographic Information System techniques.

Aquifer Classification.— Stratified-drift aquifers can be classified into several categories on the basis of their hydraulic boundaries, relation to streams, and actual or potential sources of recharge. The following categories differ in their potential for ground-water development and in the design of ground-water flow models of each category.

1. Valley-fill aquifers: These are by far the most abundant type of stratified-drift aquifers and are found in valleys bordered by uplands of till-mantled bedrock. They are hydraulically connected to major streams, which are potential sources of induced recharge on a continuous basis.
2. Headwater aquifers: These are also in valleys bordered by uplands but are near watershed divides, lack major streams, and can sustain large seasonal groundwater withdrawals in late summer without significant depletion of low streamflow.
3. Hillside aquifers: These consist of stratified drift perched above stream grade along the sides of major valleys. They are commonly drained by springs and have thin saturated zones.
4. Sand-plain aquifers: These are thin, extensive sand deposits overlying fine sediment in areas that were once occupied by proglacial lakes. Most streams fully penetrate the sand and are incised into the underlying fine sediment. The streams serve as drains rather than sources of recharge.
5. Outwash-plain aquifers: These are thick, extensive sand-and-gravel beds that largely bury the underlying bedrock, but can be locally interrupted by hills of till or bedrock. Streams originate within the outwash.
6. Buried aquifers (isolated or delta-fed): These are deposits of sand and gravel that are buried totally or in part by fine-

grained sediment in valleys or lowlands. Delta-fed buried aquifers receive recharge from tributary streams through local surficial deltaic sand and gravel deposits along the valley walls. Isolated aquifers are recharged from adjacent fine-grained sediments and bedrock.

Bedrock and till are found throughout the region. They border the stratified drift aquifers and are an integral part of the flow systems that recharge those aquifers. Although the yield to individual wells from bedrock is relatively small, such wells provide from about 20 to 40 percent of the total amount of ground-water withdrawals in some states.

Hydrologic Characteristics.—Precipitation in the Northeast ranges from about 28 in. to more than 70 in. per year and increases with altitude. Mean annual snowfall ranges from about 35 in. in southern lowlands to more than 100 in. in mountainous regions. Mean annual air temperature ranges from about 40° to 50°F, depending on latitude and altitude. Mean annual runoff ranges from about 10 in. to more than 40 in. Mean annual evapotranspiration ranges from about 16 to 24 in. and fluctuates seasonally. It includes ground-water evapotranspiration, which presumably decreases as depth to the water table increases in stratified drift, although studies in the region have not provided a sound basis for site-specific estimation.

Under natural conditions, ground-water discharge from sand and gravel occurs primarily by seepage to streams and secondarily by ground-water evapotranspiration. During periods of low flow, streamflow consists chiefly of ground-water discharged from stratified-drift aquifers. Local variations in low flow can be attributed largely to three watershed properties—the annual amount of water available for recharge, the areal extent of the surficial sand and gravel, and the areal extent of lakes and swamps, where evapotranspiration consumes significant amounts of ground water that would otherwise become streamflow. Low flow per unit area from terrains underlain by medium to fine sand is much greater than that from terrains underlain by till or fine-grained sediments because the latter cannot transmit water rapidly, and because steep water-table gradients and high water tables in fine-grained sediments enhance ground-water evapotranspiration, which reduces streamflow. Narrow valleys underlain at shallow depth by highly permeable gravel may also have small low flows because ground water above stream grade drains rapidly to the streams.

Water-table fluctuations.—Regionwide, fluctuations in the water table display certain general patterns, depending on local geology and distance from streams. Water-table fluctuations in stratified drift near streams reflect fluctuations in stream stage in an attenuated manner, whereas in stratified drift distant from streams, seasonal water-table fluctuations are superimposed on long-term trends in precipitation. In till areas distant from streams, the water table approaches land surface each spring in response to spring recharge, whereas annual water-table minimums vary widely as a function of seasonal rainfall.

Sources of Recharge.—Recharge to stratified-drift aquifers can be derived from several sources, namely:

1. Precipitation directly on or above the aquifer.
2. Unchanneled surface runoff and shallow subsurface runoff from upland hillsides bordering the aquifer.
3. Seepage losses from channeled runoff in tributaries that flow from upland areas across the aquifer to a master stream.
4. Subsurface ground-water flow from bedrock and till bordering the aquifer.
5. Induced infiltration from major streams as a result of pumping.

Recharge from each of these sources can be separately estimated and(or) simulated in aquifer models. Sources 2-4 above collectively represent recharge from upland runoff, which in areas of high relief typically exceeds direct recharge from precipitation and constitutes more than half of the total recharge to the stratified drift under natural, non-pumping conditions. In areas of low relief, tributary streams are usually not sources of recharge under natural conditions.

Aquifer Properties.—Reported values of the horizontal hydraulic conductivity of stratified drift vary widely from less than 0.1 to several thousands of feet per day. Typical values range from several tens of feet per day for fine sand to several hundred feet per day for gravel, but several aquifers in the region—for example, some in the Susquehanna River Basin, the Oswego River basin, and the Schenectady aquifer of eastern New York —have considerably higher values. One of the least accurately known hydraulic properties of stratified drift is the vertical hydraulic conductivity. Reported values of the ratio of vertical to horizontal hydraulic conductivity range from about 1:2 to less than 1:1,000.

Aquifer transmissivity values for many individual sites have been reported in the literature cited in this report; these values range widely within localities as well as from one region to another, and no typical or predominant value is apparent. Transmissivity of highly productive aquifers can range from 5,000 ft^2/d (feet squared per day) to more than 50,000 ft^2/d. Most transmissivity values have been obtained from pumping tests of large-capacity wells, specific-capacity data for wells, and summation of hydraulic conductivity estimates empirically assigned to lithologic units from drillers logs. The most common methods of estimating the magnitude and distribution of hydraulic conductivity or transmissivity in localities remote from pumping wells are based on (1) qualitative descriptions of grain size and sorting and (2) extrapolations based on geomorphology and morphosequence distribution. The resulting estimates are likely to be approximate.

Estimates of hydraulic conductivity from empirical equations based on grain size vary, depending on the source of the samples and the effective grain size used to develop the equa-

tions. A regression of laboratory-determined hydraulic conductivity of clean, well-sorted samples from New England and recombined outwash fractions, against median grain size (*D50*, in millimeters), indicates that an approximate upper limit of hydraulic conductivity (UL), in feet per day, for sand-sized stratified drift can be estimated from the equation UL = 1500 $(D50)^{1.9}$. For a particular median grain size, hydraulic conductivity can be 1 to 2 orders of magnitude smaller than the upper limit, depending on the degree of sorting and silt content.

Stratified drift in small valleys is typically less than 50 ft thick, rarely exceeds 100 ft in thickness, and tends to be predominantly coarse grained. The total volume and relative proportion of fine-grained stratified drift tends to increase as valley width and depth increase, hence the total saturated thickness of unconsolidated sediment is not a reliable indicator of potential well or aquifer yield in large valleys. Nevertheless, water-yielding sand and gravel is widely distributed in broad lowlands and occurs near the top or bottom of the stratified drift in most localities in deep valleys. The hydraulic conductivity of particular aquifers typically ranges over several orders of magnitude, whereas saturated thickness generally ranges within 1 order of magnitude. Thus, variations in hydraulic conductivity have a greater effect on transmissivity than do variations in saturated thickness.

Streambed Properties.—Field observations indicate that the first few feet of alluvial deposits immediately below the beds of many streams are siltier and less permeable than underlying, coarse-grained stratified drift. These streambed deposits are the medium through which induced infiltration must flow. The land-surface area contributing recharge to wells is highly sensitive to the streambed leakance (defined as the ratio of streambed vertical hydraulic conductivity to streambed thickness) along stream reaches adjacent to production wells. Values of streambed leakance at several sites along major streams throughout the region have been calculated; most are about 1 (ft/d)/ft (foot per day per foot) or less. Alluvial fans of tributary streams in the Appalachian Plateau and probably in other regions of high relief are relatively permeable; streambed leakance in these areas commonly exceeds 1 (ft/d)/ft, and seepage losses from these tributaries may be controlled less by the streambed material than by the hydraulic properties of aquifer material.

Streambed-leakance values for moderately small streams, in which low flows are less than about 20 ft^3/s (cubic feet per second) and streambed hydraulic properties are homogeneous, can be estimated from paired streamflow measurements in losing reaches together with measurement of vertical head difference across the streambed. The accuracy of the estimated vertical leakance value depends on the measurement accuracy of (1) the streamflow loss, and (2) the vertical head differences across the streambed over the extent of the losing reach.

GROUND-WATER FLOW MODELING

Ground-water flow models of two stratified-drift aquifers (the Rockaway River valley near Dover, N.J. and the Killbuck Creek valley near Wooster, Ohio) and their adjacent uplands were developed to demonstrate several approaches to simulation of aquifers typical of the glaciated Northeast, and application of a new modeling technique, termed the Variable-Recharge procedure. The Dover, N.J. aquifer contains surficial sand and gravel bounded laterally by till-covered uplands of relatively low relief. The Wooster, Ohio aquifer contains sand and gravel overlain by silt and clay and bounded laterally by till-covered uplands of moderate relief. Both models centered on municipal well fields but also included extensive peripheral upland and valley areas for which little hydrologic information was available. The peripheral areas were included to demonstrate model response within the well fields to the manner in which peripheral areas were simulated and to demonstrate certain aspects of the Variable-Recharge procedure. The assigned hydrogeologic characteristics represent combinations of hydraulic properties and aquifer geometry that produced simulated heads that approximate the spatial and temporal distribution of a limited number of measured water levels, mainly within the well field areas. As in all ground-water flow models, other combinations of these properties could produce analogous results; thus, the resulting hydraulic properties for the well field areas are to be taken as approximations of actual hydrogeologic conditions. The hydraulic properties as simulated for areas outside the well fields, although plausible, cannot be confirmed without site-specific information.

Variable-Recharge Procedure.—The Variable-Recharge procedure was developed to simulate areal recharge to an aquifer as a function of water-table altitude relative to land surface and the contribution of flow from uplands to valley-fill aquifers when the uplands are explicitly modeled. The basic premise of the Variable-Recharge procedure is that infiltration of precipitation can occur only if the water table is below land surface. The amount of water that is available for recharge (*WAFR*), for a particular time period, is defined as precipitation minus evapotranspiration (from above the water table), plus snowmelt, minus snow held in storage, plus or minus changes in soil-moisture content. On an annual basis, *WAFR* equals runoff (or precipitation minus evapotranspiration). If the water table is at or near land surface, recharge may be rejected and *WAFR* becomes surface runoff. Furthermore, if the water table is at land surface within the volume represented by a finite-difference model cell, outward seepage can occur if ground water flows to the cell from surrounding areas. This seepage is treated as additional surface runoff in the Variable-Recharge procedure, and its magnitude is equivalent to the net flow to the cell from adjacent model cells. All recharge that infiltrates till or bedrock of the uplands and does not discharge by way of outward seepage

within the uplands is termed net upland recharge and becomes part of the upland ground-water flow system. That part of the net recharge that is not removed by sinks (for example, upland pumping) and does not become ground water in storage will recharge the valley fill as lateral ground-water flow from the uplands. All or part of the surface runoff from uplands may be applied to the valley fill as unchanneled and(or) channeled surface runoff. The unchanneled surface runoff is applied to specified regions along the valley wall as additional *WAFR* and the channeled surface runoff is distributed as streamflow in the upstream reaches of explicitly simulated tributary streams that flow onto the valley floor. The Variable-Recharge procedure can simulate flow from the uplands at the valley wall, and thus is one way of representing the boundary conditions that must be applied along the valley sides in models of stratified-drift aquifers.

Dover, N.J. model.—The Rockaway River valley-fill aquifer at Dover, N.J. and its adjacent uplands were simulated by a series of two-layer, 14-stress-period transient-state simulations of the period September 1983 through September 1985. The area from which data were available to calibrate the models was confined to a valley-fill subregion in and around the Dover municipal well field. The model area was extended to include the adjacent uplands and upvalley and downvalley segments in which knowledge of the hydraulic properties was limited, rather than limiting the areal extent of the models to the well field subregion and applying model boundary conditions along its periphery. Four field methods of estimating the water-bearing characteristics of the Rockaway River streambed indicated streambed leakance values ranging from 0.21 to 0.68 (ft/d)/ft.

Five models with differing hydraulic conductivity configurations were developed wherein the statistical model fit, in terms of simulated head within the Dover well field subregion, was virtually the same. Although the hydraulic properties of the Rockaway River streambed, the uplands, and the valley areas peripheral to the well field differed substantially among the five models, the hydraulic conductivity of the valley fill within the well field subregion of each model deviated from the average hydraulic conductivity of all five models by less than a few tens of percent. This degree of variation is within the typical range; therefore the model-calibration process based only on hydraulic head could not be used to infer which set of hydraulic properties for the peripheral areas or which streambed leakance value are most likely. Such inferences require precisely measured streamflow losses and(or) site-specific data from the peripheral areas.

A sixth model was constructed with a uniform specific yield of 0.1 rather than 0.2 for the stratified drift of the upper layer. The resultant model fit was significantly improved, especially in replicating changes in water levels in response to changes in stress. A specific yield of 0.1 is at the low end of the range of published values for coarse stratified drift as derived from laboratory measurements (0.1 to 0.35) and within the range of values typically derived from short-term aquifer tests (0.03 to 0.13). Although the model results are a function of many factors, the improved model fit obtained with the lower specific yield indicates that lower values obtained from aquifer tests may be more appropriate than values based on laboratory measurements in the analyses of aquifer response to short-term variations in stress such as pumpage or storm runoff.

The Dover simulations were highly sensitive to the magnitude of the streambed hydraulic properties. Models with the largest streambed leakance, K/m = 0.6 (ft/d)/ft, resulted in a much smaller area contributing flow to the production wells within each model layer than models with the smallest streambed leakance, K/m = 0.2 (ft/d)/ft, primarily because models with the higher value of streambed leakance received about three times the amount of induced infiltration from the Rockaway River. This threefold increase of streambed leakance also caused an increase in head, over the 2-year period simulated, of 0.5 to 1.7 ft within the Dover well field subregion. In contrast, decreasing streambed leakance threefold from 0.6 (ft/d)/ft to 0.2 (ft/d)/ft caused heads to decrease 1.2 to 4 ft. This asymmetric response occurs because the decline in head required to increase gradient threefold in response to a decrease in streambed leakance is inherently a larger number than the rise in head required to decrease gradient threefold in response to an increase in streambed leakance. Furthermore, if simulated heads fall below the base of a streambed in response to a decrease in streambed leakance, the aquifer is hydraulically decoupled from the stream, and streamflow loss is no longer a linear function of the head difference between stream-surface altitude and aquifer head but, rather, is limited to the product of streambed conductance and the fixed elevation difference between the stream surface and the base of the streambed. If streamflow loss is insufficient to balance discharges from the aquifer, water will be removed from storage, causing additional decreases in head.

A sensitivity analysis was implemented to determine the effects of random heterogeneities in the streambed properties of the Rockaway River by allowing the streambed leakance of each stream cell that lost water to the aquifer to take on any value between 0.2 and 0.6 (ft/d)/ft, with equal probability. The results of 10 separate simulations, each with a different random pattern of streambed leakance heterogeneity, indicated that the maximum head deviation relative to a homogeneous streambed leakance of 0.4 (ft/d)/ft was generally less than 0.5 ft—considerably less than the sensitivity displayed when the homogeneous streambed leakance was doubled to 0.6 (ft/d)/ft and halved to 0.2 (ft/d)/ft. The analysis indicates that simulating a streambed along a reach of moderate heterogeneity with a single streambed leakance value will result in relatively small model errors if the single value is close to the mean of the leakance values along the reach, whereas simulating the same streambed reach with a single leakance value that differs significantly from the mean of the leakance values

along the reach can produce relatively large model errors, especially if there are locally large deviations from the mean.

The 2-year Dover transient-state models were discretized into a series of long stress periods of several months followed by short stress periods of 24 to 48 hours. Representative pumping rates for the long stress periods were calculated by averaging the volume of water extracted over each stress period. The short stress periods were designed to represent stresses (recharge, stream-surface altitude, and pumping rates) prevailing immediately before and during the periods when the water levels used to calibrate the model were measured.

Wooster, Ohio model.—The stratified drift in Killbuck Creek valley near Wooster, Ohio and its adjoining uplands were simulated by a three-layer, steady-state ground-water flow model representing conditions in the fall of 1984. The model illustrates application of the Variable-Recharge procedure to simulate recharge from channeled and unchanneled upland runoff. Results indicate that about 75 percent of the vertical recharge to the sand and gravel within the valley consists of relatively low rates of downward flow through surficial fine-grained deposits that mantle most of the valley floor, while about 25 percent consists of relatively high rates of downward flow within small areas of coarse material near tributary streams, where surficial fine-grained sediments are apparently absent.

A water budget for uplands bordering Killbuck Creek valley, exclusive of three large tributary watersheds that were not explicitly simulated by the Variable-Recharge procedure, indicates that the rate of *WAFR* in these uplands was 10.45 ft^3/s in the fall of 1984. The simulated surface runoff from these uplands consisted of rejected recharge and outward seepage and was 73 percent (7.62 ft^3/s) of the *WAFR*; the remaining 27 percent (2.83 ft^3/s), equivalent to about 3.2 in./yr, infiltrated within the uplands and moved to the valley as lateral ground-water flow. Of the 7.62 ft^3/s of surface runoff, 41.9 percent (3.19 ft^3/s) was applied to the valley as unchanneled runoff, 32.6 percent (2.49 ft^3/s) was applied to the valley as channeled runoff, and 25.5 percent (1.94 ft^3/s) was assumed to flow through storm drains to Killbuck Creek. The available channeled runoff was applied as streamflow in the upstream cells of six tributary streams flowing from the western uplands. Streambed conductance was relatively low, so only 6.8 percent (0.17 ft^3/s) of the channeled runoff recharged the valley, whereas 54 percent (1.73 ft^3/s) of the unchanneled runoff recharged the valley along the valley wall. Total recharge to the valley fill was 12.5 ft^3/s, which included 4.74 ft^3/s from upland sources simulated by the Variable-Recharge procedure (channeled and unchanneled runoff plus ground-water flow from the uplands). Total recharge also included 3.16 ft^3/s from the three large tributaries not simulated by the Variable-Recharge procedure, which consisted of streamflow losses of 2.99 ft^3/s from valley reaches of these tributaries as well as underflow of 0.17 ft^3/s from sediments beneath two of the tributaries. Thus, the total contribution from the uplands was 7.9 ft^3/s, or about 63 percent of the total recharge to the valley fill.

The calibrated hydraulic properties of the steady-state simulation were tested by a transient-state simulation of a rapid snowmelt event that occurred from February 23 through March 5, 1985, and that caused water levels to rise considerably throughout the valley. Results of the transient-state simulation indicate that, if the simulated storage properties are characteristic of the aquifer materials, the hydraulic properties used in the steady-state simulation are a plausible representation of actual properties. The model properties in areas from which geologic and geophysical (electrical resistivity) information were available are probably a good approximation of the hydrogeologic system. The values assigned to areas where no information was available, such as along the valley walls, the northern part of the valley, and the area between the north and south well fields, are the result of the model-calibration process and, as such, are less reliable than the values based on field data.

MODELING CONSIDERATIONS

Several generalizations regarding the modeling of stratified-drift aquifers and application of the Variable-Recharge procedure are as follows.

Upland Hydraulic Properties.—Sensitivity analysis of the Dover and Wooster models showed that if the uplands have relatively low hydraulic conductivity the resultant shape of the water table will resemble the upland land surface. Consequently, if the land surface contains local undulations there will be numerous local flow systems. If the uplands have relatively high hydraulic conductivity the simulated water table will be a smoothed representation of the upland land surface and local flow systems will be attenuated. Where the uplands are relatively impermeable, surface runoff is relatively large and infiltration to the saturated zone is relatively small. Conversely, where the uplands are relatively permeable, surface runoff is relatively small and infiltration to the saturated zone is relatively large. In addition, changes in ground-water storage within the upland depend in part on the hydraulic conductivity of the upland material, as does flow from upland sources or to upland sinks that result from stress-induced changes in head. Consequently, the relative proportions of upland ground-water flow, unchanneled runoff, and channeled runoff for a given rate of *WAFR* vary as a function of upland hydraulic conductivity.

The extent to which unchanneled runoff recharges the valley depends on the head distribution, relative to land surface, in the valley areas adjacent to upland hillslopes; if the water table in these areas is high, the unchanneled runoff may be rejected. The amount of channeled runoff that recharges the valley depends on both the head distribution beneath the sim-

ulated streams that receive the runoff, in relation to stream stage, and on the streambed conductance. Unless the streams lose all of their flow to the valley fill, an increase or decrease in channeled runoff will not necessarily result in a commensurate increase or decrease in recharge to the valley. Nevertheless, sensitivity analysis indicates that the total upland contribution to the valley will generally increase with increasing upland hydraulic conductivity because infiltration of *WAFR* will increase and therefore ground water flow from the uplands to the valley will increase.

Steady-state recharge from the uplands to the Killbuck Creek valley increased by 40 percent (4.0 to 5.6 ft^3/s) as homogeneous upland hydraulic conductivities were increased from 0.03 to 1 ft/d. The increased recharge caused an increase in valley heads of as much as 7 ft. In a Dover simulation with relatively small hydraulic conductivity (0.25 ft/d) for upland till and consequently relatively large surface runoff, 12 to 28 percent of total recharge to the Rockaway River valley was derived from the uplands over a 2-year period, whereas in another simulation with a relatively large hydraulic conductivity (4 ft/d) for till and relatively small surface runoff, 24 to 43 percent of the valley recharge was derived from the uplands over the same time period. One reason for this difference is that much of the surface runoff that resulted from the low hydraulic conductivity of upland till could not infiltrate the valley fill because the water table was so high along the valley margins (primarily in swampy areas).

Flow at Valley Wall.—A scenario in which (1) the uplands are not explicitly simulated, and (2) the upland contribution to valley recharge is applied along the valley wall in the form of a specified-flux boundary condition, was approximated by assigning a small hydraulic conductivity (0.001 ft/d) to the uplands of one of the Dover models (model 6). The resulting simulated upland heads were at or near land surface; thus, virtually none of the *WAFR* infiltrated the uplands but, rather, became unchanneled surface runoff that was available to recharge the valley along the valley wall. The sensitivity of water levels in the valley to the magnitude of boundary fluxes could then be determined from five simulations in which 0, 25, 50, 75, and 100 percent of the upland surface runoff was distributed to the cells along the valley wall. As the percentage of applied unchanneled runoff was increased from zero to 100 percent, heads within the valley rose by about 0.5 ft in stress periods where the rates of *WAFR* (and therefore surface runoff) were relatively small and by more than 4 feet in stress periods with large rates of *WAFR* and surface runoff. Thus, if the valley-fill margin were assumed to be a zero-flow boundary in a simulation in which only the valley fill is explicitly modeled, substantial model error could occur, depending on the magnitude of *WAFR*.

Lower Boundary.—Ground-water flow models of stratified drift systems are generally designed on the assumption that the contact between coarse stratified drift and underlying till or bedrock is impermeable. The validity of this assumption was tested by simulating an additional layer beneath the coarse valley fill and assigning to that layer transmissivities of 10 to 200 ft^2/d, typical of low-permeability material. Sensitivity analysis indicated that a sufficiently large vertical leakance between that layer and the overlying valley fill can cause heads in the valley fill to rise several tenths of a foot or more under pumping conditions. Thus, to the extent that the range of hydraulic properties used in the sensitivity analyses are representative of real conditions, the assumption of an impermeable boundary beneath the valley-fill deposits could reduce simulated valley head on the order of 1 ft. A sensitivity analysis to determine the quantitative significance of simulating an additional layer rather than an impermeable bottom would require minimal effort and therefore warrants consideration in designing a model of a stratified-drift system.

Model Fit.—The simulated head in a model cell represents the average head in the cell, whereas water-level measurements within the cell represent conditions at the observation-well location. The steeper the head gradient and the larger the model cell, the greater the likelihood that the simulated head will not accurately represent head at the location of an observation well within the cell. Thus, a poor fit between an observed and simulated water level may be the result of model discretization rather than an erroneous representation of the hydrology. If so, interpolation of model heads at grid spacings smaller than the model grid, such that a simulated head represents a smaller area near each well, can improve calibration. Such interpolation of model heads significantly reduced the average departure of simulated heads from observed heads in parts of the Dover and Wooster models and would probably facilitate calibration of most other ground-water flow models.

Inclusion of Uplands.—Most flow models of valley-fill aquifer systems described in the hydrologic literature explicitly simulate only the valley fill. The contact between the uplands and the valley fill has been treated as a zero flow, specified flux, or head-dependent boundary at which estimates of upland-derived recharge to the valley are applied. If the upland contribution is accurately represented, the resultant flow model of the valley fill is suitable for most purposes. Inclusion of the uplands in a simulation of a valley-fill system and use of the Variable-Recharge procedure increases the amount of model input data and the overall complexity of the model, but once the Variable-Recharge procedure input data are developed, only a minimal effort is needed to generate data for transient-state simulations with multiple stress periods. Although the hydraulic properties of most uplands are poorly known, explicit simulation of the uplands and application of the Variable-Recharge procedure can provide useful information in investigations of aquifers that receive part of their recharge from the uplands, particularly where contributing areas to wells or variations in hydraulic interaction between the uplands and the valley fill, over time, are of interest.

REFERENCES CITED

Allen, R.V., and Barnes, C.R., 1985, Spatial and temporal snow cover distribution in New York State: Proceedings, Eastern Snow Conference, v. 49, p. 199-203.

Allen W.B., Hahn, G.W., and Brackley, R.A., 1966, Availability of ground water in the upper Pawcatuck River basin, Rhode Island: U.S. Geological Survey Water Supply Paper 1821, 66 p.

Alley, W.M., 1984, On the treatment of evapotranspiration, soil moisture accounting, and aquifer recharge in monthly water balance models: Water Resources Research, vol. 20, p. 1137-1149.

Anderson, H.R., 1968, Geology and ground-water resources of the Rahway area, New Jersey: New Jersey Department of Conservation and Economic Development Special Report 27, 72 p.

Anderson, M.P., 1989, Hydrogeologic facies models to delineate large-scale spatial trends in glacial and glaciofluvial sediments: Geological Society of America Bulletin, v. 101, p. 501-511.

Anderson, M.P., and Woessner, W.W., 1992, Applied groundwater modeling, simulation of flow and advective transport: San Diego, Academic Press, 381 p.

Appel, C.A., and Reilly, T.E., 1988, Selected reports that include computer programs produced by the U.S. Geological Survey for simulation of ground-water flow and quality: U.S. Geological Survey Water-Resources Investigations Report 87-4271, 64 p.

Archer, R.J., LaSala, A.M., Jr., and Kammerer, J.C., 1968, Chemical quality of streams in the Erie-Niagara Basin, New York: State of New York Conservation Department, Water Resources Commission, 104 p.

Ayotte, J.D., and Toppin, K.W., 1995, Geohydrology and water quality of stratified-drift aquifers in the Middle Merrimack River Basin, south-central New Hampshire: U.S. Geological Survey Water-Resources Investigations Report 92-4192.

Baker, J.A., Healy, H.G., and Hackett, O.M., 1964, Geology and ground-water conditions in the Wilmington-Reading area, Massachusetts: U.S. Geological Survey Water Supply Paper 1694, 80 p.

Baker, V.R., 1976, Hydrology of cavernous limestone terrane and the hydrochemical mechanisms of its formation, Mohawk River basin, New York: Empire State Geogram, v. 12, p. 2-65.

Ballaron, P.B., 1988, Ground-water flow model of the Corning area, New York: Susquehanna River Basin Commission Publication no. 116, 102 p.

Barksdale, H.C., O'Bryan, Deric, and Schneider, W.J., 1966, Effect of drought on water resources in the Northeast: U.S. Geological Survey, Hydrologic Investigations Atlas HA-243, 1 sheet.

Barnes, C.R., 1986, Method for estimating low-flow statistics for ungaged streams in the lower Hudson River Basin: U.S. Geological Survey Water Resources Investigations Report 85-4070, 22 p.

Bear, J., 1979, Hydraulics of ground water: New York, McGraw-Hill, 567 p.

Bedinger, M.S., 1961, Relation between median grain size and permeability in the Arkansas River valley, Arkansas: U.S. Geological Survey Professional Paper 424-C, p. C31-C32.

Beer, J.D., 1894, Report of the Wooster extension commission to the City of Wooster: Wooster, Ohio, 20 p.

Bennett, G.D., 1976, Introduction to ground-water hydraulics. A programmed text for self instruction: U.S. Geological Survey Techniques of Water-Resources Investigations Chapter B2, Book 3, 172 p.

Bent, G.C., 1995, Streamflow, ground-water recharge and discharge, and characteristics of surficial deposits in Buzzards Bay Basin, southeastern Massachusetts: U.S. Geological Survey Water Resources Investigations Report 95-4234, 56 p.

Berend, J.E., Rebhun, M., and Kahana, Y., 1967, Use of storm runoff for artificial recharge: Transactions American Society Agricultural Engr., vol. 10, no. 5, p. 678-684.

Bergeron, M.P., 1987, Effect of reduced industrial pumpage on the migration of dissolved nitrogen in outwash aquifer at Olean, Cataraugus County, New York: U.S. Geological Survey Water-Resources Investigations Report 85-4082, 38 p.

Bishop, G.D., and Church, M.R., 1992, Automated approaches for regional runoff mapping in the northeastern United States: Journal of Hydrology, v. 138, p. 361-383.

_____, 1995, Mapping long-term regional runoff in the eastern United States using automated approaches: Journal of Hydrology v. 168, p. 189-207.

Boulton, N.S., 1963, Analysis of data from non-equilibrium pumping tests allowing for delayed yield from storage: Institute of Civil Engineers Proceedings, [London], v. 26, p. 469-482.

Bouwer, H., and Rice, R.C., 1976, A slug test for determining hydraulic conductivity of unconfined aquifers with completely or partially penetrating wells: Water Resources Research, v. 12, no. 3, p. 423-428.

Bouwer, Herman, 1978, Groundwater Hydrology: New York, McGraw-Hill, 480 p.

Brackley, R.A., and Hansen, B.P., 1977, Water resources of the Nashua and Souhegan River basins, Massachusetts: U.S. Geological Survey Hydrologic Investigations Atlas HA-276, 1:48,000, 2 sheets.

Bradbury, K.R., and Muldoon, M.A., 1990, Hydraulic conductivity determinations in unlithified glacial and fluvial materials, *in* Nielsen, D.M., and Johnson, A.I., eds., Ground-Water and Vadose Zone Monitoring: Philadelphia, American Society for Testing and Materials, STP 1288, P. 138-151.

Bradley, Edward, 1964, Geology and ground-water resources of southeastern New Hampshire: U.S. Geological Survey Water Supply Paper 1695, 80 p.

Breen, K.J., 1988, Geochemistry of the stratified-drift aquifer in the Killbuck Creek valley west of Wooster, Ohio, *in* Randall, A.D., and Johnson, A.I, eds., Regional Aquifer Systems of the United States, Northeast Glacial Aquifers: American Water Resources Association Monograph Series, no. 11, p. 105-131.

Breen, K.J., Kontis, A.L., Rowe, G.L., and Haefner, R.J., 1995, Simulated ground-water flow and sources of water in the Killbuck Creek valley near Wooster, Wayne County, Ohio, U.S. Geological Survey Water Resources Investigations 94-4131, 104 p.

Burkham, D.E., 1970, A method for relating infiltration rates to streamflow rates in perched streams: U.S. Geological Survey Professional Paper 700-D, p. D266-D271.

Butler, S.S., 1957, Engineering hydrology: Englewood Cliffs, N.J., Prentice-Hall p. 157-165.

Caldwell, D.W., 1986, Preliminary hydrologic assessment of the town dump, Acworth, New Hampshire: [Report prepared for the Town of Acworth, New Hampshire, September 30, 1986], 12 p.

Caldwell, D.W., Faldetta, S., and Hanson, G.F., 1987, Geologic and hydrologic effects of a catastrophic flood in the Cold River, southwestern New Hampshire, *in* Westerman, D.S., ed., Guidebook for field trips in Vermont: New England Intercollegiate Geological Conference, 79th Annual Meeting, p. 21–28.

Canace, R.J., Hutchinson, W.R., Saunders, W.R., and Andres, K.G., 1983, Results of the 1980-81 drought emergency ground water investigations in Morris and Passaic counties, New Jersey: New Jersey Geological Survey Open File Report 83-3, 132 p.

Canace, R., Stanford, S.D., and Hall, D.W., 1993, Hydrogeologic framework of the middle and lower Rockaway River Basin, Morris County, New Jersey: New Jersey Geological Survey, Geological Survey Report GSR33, 68 p.

Carswell, L.D., and Bennett, G.D., 1963, Geology and hydrology of the Neshannock quadrangle, Mercer and Lawrence Counties, Pennsylvania: Pennsylvania Geological Survey, 4th series, Water Resources Report W-15, 90 p.

Carswell, L.D., and Lloyd, O.B., Jr., 1979, Geology and ground-water resources of Monroe County, Pennsylvania: Pennsylvania Geological Survey, 4th series, Water Resources Report 47, 61 p.

Carswell, L.D., and Rooney, J.G., 1976, Summary of geology and groundwater resources of Passaic County, New Jersey: U.S. Geological Survey Water Resources Investigations 76-75, 47 p.

Cervione, M.A., Jr., Grossman, I.G., and Thomas, C.E., Jr., 1968, Hydrogeologic data for the lower Thames and southeastern coastal river basins, Connecticut: Connecticut Water Resources Bulletin 16, 65 p.

Cervione, M.A., Jr., Mazzaferro, D.L., and Melvin, R.L., 1972, Water resources inventory of Connecticut, part 6, upper Housatonic River basin: Connecticut Water Resources Bulletin 21, 83 p.

Cervione, M.A., Jr., Melvin, R.L., and Cyr, K.A., 1982, A method for estimating the 7-day, 10-year low flow of streams in Connecticut: Connecticut Water Resources Bulletin 34, 17 p.

Church, M.R., Bishop, G.D., and Cassell, D.L., 1995, Maps of regional evapotranspiration and runoff/precipitation ratios in the northeast United States: Journal of Hydrology, v. 168, p. 283-298.

Coates, D.R., 1966, Glaciated Appalachian Plateau: Till shadows on hills: Science, v. 152, p. 1617-1619.

Coates, D.R., 1971, Hydrogeomorphology of Susquehanna and Delaware basins, *in* Morisawa, Marie, ed., Quantitative geomorphology, some aspects and applications: Binghamton, N.Y., Publications in Geomorphology, State University of New York, p. 272-306.

Collings, M.R., Wiesnet, D.R., and Fleck, W.B., 1969, Water resources of the Millers River basin in north-central Massachusetts and southwestern New Hampshire: U.S. Geological Survey Hydrologic Investigations Atlas HA-293, 4 sheets.

Cooper, H.H., Jr., Bredehoeft, J.D., and Papadopulos, I.S., 1967, Response of a finite diameter well to an instantaneous change of water: Water Resources Research, v. 3, no. 1, p. 263-269.

Conrey, G.W., 1921, Geology of Wayne County: Ohio Geological Survey Bulletin 24, 155 p.

Cosner, O.J. and Harsh, J.F., 1978, Digital-model simulation of the glacial-outwash aquifer, Otter Creek— Dry Creek Basin, Cortland County, New York: U.S. Geological Survey Water-Resources Investigations 78-71, 34 p.

Cotton, J.E., 1975, Availability of ground water in the upper Connecticut River basin, northern New Hampshire: U.S. Geological Survey Water-Resources Investigations Report 53-75, 1:125,000, 1 sheet.

_____, 1989, Hydrogeology of the Cocheco River basin, southeastern New Hampshire: U.S. Geological Survey Water-Resources Investigations Report 87-4130, 47 p.

Crain, L.J., 1966, Ground-water resources of the Jamestown area, New York, with emphasis on the hydrology of the major stream valleys: New York State Water Resources Commission Bulletin 58, 167 p.

_____, 1974, Ground-water resources of the western Oswego River basin, New York: New York State Department of Environmental Conservation, Basin Planning Report ORB-5, 137 p.

Cressy, G.B., 1966, Land Forms *in* Thompson, J.H., ed., Geography of New York State: Syracuse University Press, 543 p.

Cross, W.P., 1949, The relation of geology to dry-weather streamflow in Ohio: Trans. Am. Geophys. Union vol. 30, p. 563-566.

Crowl, G.H., and Sevon, W.D., 1980, Glacial border deposits of Late Wisconsinan age in northeastern Pennsylvania: Pennsylvania Geological Survey, 4th ser., General Geological Report G-17, 68 p.

Crowell, K.S., 1978, Ground-water resources of Columbiana County, Ohio: Columbus, Ohio Department of Natural Resources, Division of Water, 1:62,500, 1 sheet.

Cruff, R.W., and Thompson, T.M., 1967, A comparison of methods of estimating potential evapotranspiration from climatological data in arid and subhumid environments: U.S. Geological Survey Water Supply Paper 1839-M, 28 p.

Cummins, J.W., 1959, Buried river valleys in Ohio: Ohio Department of Natural Resources, Ohio Water Plan Inventory Report No. 10, 1:625,000, 2 sheets.

Davis, T.M., and Kontis, A.L., 1970, Spline interpolation algorithms for track-type survey data with application to the computation of mean gravity anomalies: Bay St. Louis, Miss., U.S. Naval Oceanographic Office Technical Report 226, 50 p.

de Lima, V.A., 1991, Stream-aquifer relations and yield of stratified-drift aquifers in the Nashua River Basin, Massachusetts: U.S. Geological Survey Water-Resources Investigations Report 88-4147, 47p.

de Lima, V.A., and Olimpio, J.C., 1989, Hydrogeology and simulation of ground-water flow at Superfund-site wells G and H, Woburn, Massachusetts: U.S. Geological Survey Water Resources Investigations Report 89-4059, 99 p.

Delaney, D.F., and Maevsky, Anthony, 1980, Distribution of aquifers, liquid-waste impoundments, and municipal water supply sources, Massachusetts: U.S. Geological Survey Open-File Report 80-431, 1:250,000, 1 sheet.

Delaney, D.F., and Gay, F.B., 1980, Hydrology and water resources of the coastal drainage basins of northeastern Massachusetts from Castle Neck River, Ipswich to Mystic River, Boston: U.S. Geological Survey Hydrologic Investigations Atlas HA-589, 1,250,000, 4 sheets.

Denny, C.S., 1982, Geomophology of New England: U.S. Geological Survey Professional Paper 1208, 18 p.

Dethier, B.E., 1966, Precipitation in New York State: Ithaca, N.Y., Cornell University Agricultural Experimental Station Bulletin 1009, 78 p.

Diaz, H.F., 1995, Climate change at high elevations discussed at workshop: EOS, vol. 76, no. 50, p. 516.

Dickerman, D.C., 1984, Aquifer tests in the stratified drift, Chipuxet River basin, Rhode Island: U.S. Geological Survey Water Resources Investigations Report 83-4321, 39 p.

Dickerman, D.C., and Ozbilgin, M.M., 1985, Hydrogeology, water quality, and ground-water development alternatives in the Beaver-Pasquiset ground-water reservoir, Rhode Island: U.S. Geological Survey Water Resources Investigations Report 85-4170, 104 p.

Dickerman, D.C., Trench, E.C.T., and Russell, J.P., 1990, Hydrogeology, water quality, and ground-water development alternatives in the lower Wood River ground-water reservoir, Rhode Island: U.S. Geological Survey Water Resources Investigations Report 89-4031, 109 p.

Dingman, S.L., 1978, Synthesis of flow-duration curves for unregulated streams in New Hampshire: Water Resources Bulletin, v. 14, no. 6, p. 1481-1502.

_____, 1981, Elevation - a major influence on the hydrology of New Hampshire and Vermont, USA: Hydrologic Sciences Bulletin, v. 26, no. 24, p. 399-413.

_____, 1994, Physical hydrology: Englewood Cliffs, N.J., Prentice Hall, 573 p.

Driscoll, F.G., 1986, Groundwater and wells: St. Paul, Minn., Johnson Division, 1089 p.

Dunne, T., and Black, R.D., 1970, Partial-area contributions to storm runoff in a small New England watershed: Water Resources Research, v. 6, no. 5, p. 1296-1311.

Dysart, J.E., 1988, Use of Oxygen-18 and deuterium mass-balance analysis to evaluate induced recharge to stratified drift aquifers, *in* Randall, A.D., and Johnson, A.I., editors, Regional Aquifer Systems of the United States, Northeast Glacial Aquifers: American Water Resources Association Monograph Series, No. 11, p. 133-156.

Dysart, J.E., and Rheaume, S.J., 1999, Induced infiltration from the Rockaway River and water chemistry in a stratified-drift aquifer at Dover, New Jersey: U.S. Geological Survey Water Resources Investigations 96-4068.

Environment Canada, 1989, Climatological station catalogues (Quebec; Atlantic Provinces): Downsview, Ontario, Environment Canada. [These publications describe each precipitation station; companion publications give 1951-80 precipitation records.]

ESRI, 1991, Surface modeling with tin: Redlands, Calif., Environmental Systems Research Institute, Arc/Info user's guide NSTR3.4M8/91

Exarhoulakos, K., Heeley, R.W., and Motts, W.S., 1992, Geologic features of a Mesozoic basin in western Massachusetts and their significance in

numerical model development: National Ground Water Association, Proceedings of the Focus Eastern Conference, 15 p.

Ferris, J.G., Knowles, D.B, Browne, R.H., and Stallman, R.W., 1962, Theory of aquifer tests: U.S. Geological Survey Water Supply Paper 1536-E, 174 p.

Fidler, R.E., 1975, Digital model simulation of the glacial-outwash aquifer at Dayton, Ohio, U.S. Geological Survey Water-Resources Investigations 18-75, 25 p.

Fisher, D.W., Isachsen, Y.W., and Rickard, L.V., 1970, Geologic map of New York: New York State Museum and Science Service, Map and chart series 15, scale 1:250,000, 5 sheets.

Franke, O.L., and Reilly, T.E, 1987, The effects of boundary conditions on the steady-state response of three hypothetical ground-water systems—results and implications of numerical experiments: U. S. Geological Survey Water Supply Paper 2315, 19 p.

Franke, O.L., Reilly, T.E., and Bennett, G.D., 1987, Definition of boundary and initial conditions in the analysis of saturated ground-water flow systems - an introduction: U.S. Geological Survey Techniques of Water-Resources Investigations, Book 3, chapter B5, 15 p.

Freeze, R.A., and Cherry, J.A., 1979, Groundwater: Englewood Cliffs, N.J., Prentice Hall, 604 p.

Frimpter, M.H., 1972, Ground-water resources of Orange and Ulster Counties, New York: U.S. Geological Survey Water Supply Paper, 1985, 80 p.

_____, 1974, Ground-water resources, Allegheny River basin and part of Lake Erie Basin, New York: New York State Department of Environmental Conservation Basin Planning Report ARB-2, 98 p.

_____, 1980, Probable high ground-water levels in Massachusetts: U.S. Geological Survey Water Resources Investigations Report 80-1205, 19 p.

Gardner, W.R., 1964 Relations of root distribution to water uptake and availability: Agronomy Journal, v. 56, p. 41-45.

Geraghty and Miller, 1968, Preliminary investigation of ground water conditions on the Burough of Wharton, New Jersey: Port Washington, N.Y., Geraghty and Miller, Inc., 10 p.

_____, 1969, Appraisal of ground-water conditions in the town of Dover, New Jersey: Port Washington, N.Y., Geraghty and Miller, Inc., 12 p.

_____, 1972, Construction and testing of production well 5 in the Princeton Avenue well field, town of Dover, New Jersey: Port Washington, N.Y., Geraghty and Miller, Inc., 10 p.

Gerath, R.F., Fowler, B.K., and Haselton, G.M., 1985, The deglaciation of the northern White Mountains of New Hampshire, *in* Borns, H.W., Jr., and others, eds., Late Pleistocene history of northeastern New England and adjacent Quebec: Geological Society of America Special Paper 197, p. 1-12.

Giese, G.L., and Hobba, W.A., Jr., 1970, Water resources of the Champlain-Upper Hudson basins in New York State: Albany, N.Y., New York State Office of Planning Coordination, 153 p.

Gill, H.E., and Vecchioli, John, 1965, Availability of ground water in Morris County, New Jersey: New Jersey Department of Conservation and Economic Development Special Report 25, 56 p.

Gonthier, J.B., Johnston, H.E., and Malmberg, G.T., 1974, Availability of ground water in the lower Pawcatuck River basin, Rhode Island: U.S. Geological Survey Water Supply Paper 2033, 40 p.

Gordon, Allison, 1993, Hydrogeology of and simulated ground-water flow in the valley-fill aquifers of the upper Rockaway River basin, Morris County, New Jersey: U.S. Geological Survey Water Resources Investigations Report 93-4145, 74 p.

Grady, S.J., and Handman, E.H., 1983, Hydrogeologic evaluation of selected drift deposits in Connecticut: U.S. Geological Survey Water-Resources Investigations Report 83-4010, 51 p.

Grady, S.J., Weaver, M.F., and Bingham, J.W., 1992, Hydrogeology, groundwater availability and water quality in the Titicus River valley, Ridgefield, Connecticut: U.S. Geological Survey Water-Resources Investigations 87-4144, 43 p.

Guswa, J.H., and LeBlanc, D.R., 1985, Digital models of ground-water flow in the Cape Cod aquifer system, Massachusetts: U.S. Geological Survey Water Supply Paper 2209, 112 p.

Haeni, F.P., 1978, Computer modeling of ground-water availability in the Pootatuck River valley, Newtown, Connecticut, with a section on quality of water by E.H. Handman: U.S. Geological Survey Water Resources Investigations Report 78-77, 64 p.

Haeni, F.P. 1995, Application of surface-geophysical methods to investigations of sand and gravel aquifers in the glaciated Northeast United States, U.S. Geological Survey Professional Paper 1415A, 70 p.

Hall, F.R., 1968, Base-flow recessions, a review: Water Resources Research, v. 4, no. 5, p. 973-983.

Hamon, W.R., 1961, Estimating potential evapotranspiration: Proceedings, American Society of Civil Engineers, v. 87, no. HY-3, p. 107-120.

Handman, E.H., 1986, Delineating recharge areas for stratified drift aquifers in Connecticut with geologic and topographic maps: U.S. Geological Survey Water Investigations Report 83-4230, 35 p.

Handman, E.H., Haeni, F.P., and Thomas, M.P., 1986, Water resources inventory of Connecticut, part 9, Farmington River Basin: Connecticut Water Resources Bulletin 29, 91p.

Hansen, B.P., and Lapham, W.W., 1992, Geohydrology and simulated ground water flow, Plymouth-Carver area of southeastern Massachusetts, U.S. Geological Survey Water Resources Investigations Report 90-4204, 69 p.

Hayes, G.S., 1972, Average water content of snowpack in Maine: U.S. Geological Survey Hydrologic Investigations Atlas HA-452, 1:1,000,000, 1 sheet.

Hazen, Allen, 1892, Some physical properties of sands and gravels, with special reference to their use in filtration: Massachusetts State Board of Health, Twenty-fourth Annual Report.

Heald, M.T., 1956, Cementation of Triassic arkoses in Connecticut and Massachusetts: Geological Society of American Bulletin, v. 67, p. 1133-1154.

Heath, R.C., 1964, Ground water in New York: New York Conservation Department Bulletin GW-51, 1 sheet, scale 1:1,000,000.

Heath, R.C., Mack, F.K., and Tannenbaum, J.A., 1963, Ground-water studies in Saratoga County, New York: New York State Water Resources Commission Bulletin, GW-49, 128 p.

Hely, A.G., Nordenson, T.J., and others, 1961, Precipitation, water loss, and runoff in the Delaware River Basin and New Jersey: U.S. Geological Survey Hydrologic Investigations Atlas HA-11, 1:500,000, 6 sheets.

Hendrick, R.L., and deAngelis, R.J., 1976, Seasonal snow accumulation. melt and water input—a New England model: Journal of Applied Meteorology, v. 15, no. 7, p. 717-727.

Hill, M.C., 1992, A computer program (MODFLOWP) for estimating parameters of a transient, three-dimensional ground-water flow model using nonlinear regression: U.S. Geological Survey Open-File Report 91-84, 358 p.

Hill, M.C., and Pinder, G.F., 1981, An investigation of the hydrologic system and a computer simulation of the phreatic aquifer in northern Long Valley, New Jersey: Princeton, N.J., Princeton University Dept. of Civil Engineering, Final report to the Environmental Commission of Roxbury Township, N.J., 81-WR-11, 159 p.

Hill, M.C., Lennon, G.P., Brown, G.A., Hebson, C.S., and Rheaume, S.J., 1992, Geohydrology and simulation of ground-water flow in the valley-fill deposits in the Ramapo River valley, New Jersey: U.S. Geological Survey Water Resources Investigations Report 90-4151, 92 p.

Hodges, A.L., Jr., 1966, Ground water favorability map of the Batten Kill, Walloomsac and Hoosic River basins, Vermont: Montpelier, Vermont Department of Water Resources, 1:125,000, 1 sheet.

Hodges, A.L., Jr., Butterfield, David, and Ashley, J.W., 1976a, Ground-water resources of the Barre-Montpelier area, Vermont: Montpelier, Vermont Department of Water Resources, 27 p.

_____, 1976b, Ground-water resources of the White River Junction area, Vermont: Vermont Department of Water Resources, 27 p.

Hodges, A.L., Jr., Willey, R.E., Ashley, J.W., and Butterfield, D., 1977, Ground water resources of the upper Winooski River basin, Vermont: U.S. Geological Survey Water Resources Investigations Report 77-120, 27 p.

Hoffman, J.L., 1989, Simulated drawdowns, 1972-1995 in the Pleistocene buried valley aquifers in southwestern Essex and southeastern Morris counties, New Jersey: New Jersey Geological Survey Open-File Report 89-1, 26 p.

Hollowell, J.R., 1971, Hydrology of the Pleistocene sediments in the Wyoming Valley, Luzerne County, Pennsylvania: Pennsylvania Geological Survey, 4th series, Water Resources Report 28, 77 p.

Hollyday, E.F., 1969, An appraisal of the ground-water resources of the Susquehanna River basin in New York: U.S. Geological Survey unnumbered open-file report, 52 p.

Hunt, O.P., 1967, Duration curves and low-flow frequency curves of streamflow in the Susquehanna River Basin, New York: State of New York Conservation Department, Bulletin 60, 52 p.

Hurr, R.T., 1966, A new approach for estimating transmissibility from specific capacity: Water Resources Research, v. 2, no. 4, p. 657-664.

Hutchinson, W.R., 1981, Computer simulation of the glacial/carbonate aquifer in the Pequest valley, Warren County, New Jersey: New Brunswick, N.J., Rutgers University, Ms. thesis, 115 p.

Hvorslev, M.J., 1951, Time lag and soil permeability in ground-water observations: Vicksburg, Miss., U.S. Army Corps of Engineers, Waterways Experiment Station, Bulletin no. 36, 50 p.

Iorio, A.L., 1972, Precipitation regimes of the Upper Delaware basin and Catskill region: Albany, N.Y., Upper Delaware River Regional Resources Planning Board and New York State Department of Environmental Conservation, Water Management and Planning.

Jacob, C.E., 1938, Ground-water underflow in Croton valley, New York: National Research Council, Transactions of the American Geophysical Union, 19th Annual Meeting, p. 419-430.

_____, 1947, Drawdown test to determine the effective radius of artesian well: Transactions, American Society of Civil Engineers, v. 112, p. 1047-1070.

_____, 1949, Report on estimated capacity of the first ten water supply wells completed in the Conneaut Marsh-French Creek area for the Keystone Ordnance Works, near Geneva, Pa.: U.S. Geological Survey, open-file report.

_____, 1963, Determining the permeability of water-table aquifers, *in* Bentall, Ray (compiler), Methods of determining permeability, transmissibility, and drawdown: U.S. Geological Survey Water Supply Paper 1536-I, p. 245-271.

Johnson, K.E., and Marks, L.Y., 1959, Ground-water map of the Wickford quadangle, Rhode Island: Rhode Island Water Resources Coordinating Board, Ground Water Map 1, 1:24,000, 1 sheet.

Johnson, A.I., 1967, Specific yield—compilation of specific yields for various materials: U.S. Geological Survey Water Supply-Paper 1662-D, 74 p.

Johnson, C.D., Tepper, D.H., and Morrissey, D.L., 1987, Geohydrologic and surface-water data for the Saco River valley glacial aquifer from Bartlett, New Hampshire to Fryeburg, Maine, October 1983 through January 1986: U.S. Geological Survey Open-File Report 87-44, 80 p.

Johnson, M.L., 1970, Runoff from eight watersheds in northeastern Vermont: Baltimore, Md., Johns Hopkins University, Ph.D dissertation, 188 p.

Johnston, H.E., and Dickerman, D.C., 1974a, Availability of ground water in the Blackstone River area, Rhode Island and Massachusetts: U.S. Geological Survey Water Resources Investigations 4-74, 1:24,000, 2 sheets.

_____, 1974b, Availability of ground water in the Branch River basin, Providence County, Rhode Island: U.S. Geological Survey Water-Resources Investigation 18-74, 39 p.

Johnston, R.H., 1964, Ground water in the Niagara Falls area, New York, with emphasis on the water-bearing characteristics of the bedrock: New York State Water Resources Commission Bulletin GW-53, 93 p.

_____, 1971, Base flow as an indicator of aquifer characteristics in the coastal plain of Delaware: U.S. Geological Survey Professional Paper 750D, p. D212-215.

Johnstone, Don, and Cross, W.P., 1949, Elements of applied hydrology: New York, Ronald Press, 276 p.

Jones, H.P., Henry, T.B., and Williams, L.G. 1958. Water improvements report for Wooster Ohio: Toledo, Ohio, Jones, Henry and Williams Engineers, 201 p.

Kammerer, J.C., and Hobba, W.A., Jr., 1967, The geology and availability of ground water in the Genesee River basin, New York and Pennsylvania: U.S. Army Corps of Engineers, Genesee River Basin Comprehensive Study, v. 5, Appendix I, 102 p.

Kantrowitz, I.H., 1970, Ground-water resources of the eastern Oswego River basin, New York: Albany, N.Y., New York State Water Resources Commission Basin Planning Report ORB-2, 129 p.

Knisel, W.G., Jr., 1963, Baseflow recession analysis for comparison of drainage basins and geology: Journal of Geophysical Research, vol. 68, no. 12, p. 3649-3653.

Knox, C.E., and Nordenson, T.J., 1955, Average annual runoff and precipitation in the New England-New York area: U.S. Geological Survey Hydrologic Investigations Atlas HA-7, 1:1,000,000, 3 sheets.

Kontis, A.L., 1999, Modeling ground-water flow in the Rockaway River valley, *in* Dysart J.E. and Rheaume, S.J., Induced infiltration from the Rockaway River and water chemistry in a stratified-drift aquifer at Dover, New Jersey: U.S. Geological Survey Water Resources Investigations Report 96-4068, 112p.

Kontis, A.L., 2001, Computer program for simulation of variable recharge with the U.S. Geological Survey modular finite-difference groundwater flow model (MODFLOW): U.S. Geological Survey Open-File Report 00-173.

Kontis, A.L., and Mandle, R.J., 1980, Data-base system for Northern Midwest regional aquifer system analysis: U.S. Geological Survey Water-Resources Investigations Report 80-104, 23 p.

Koteff, Carl, 1974, The morphologic sequence concept and deglaciation of southern New England, *in* Coates, D.R. (ed.), Glacial Geomorphology: Binghamton, N.Y., State University of New York, Publications in Geomorphology, p. 121-144.

Koteff, Carl, and Pessl, Fred, Jr., 1981, Systematic ice retreat in New England: U.S. Geological Survey Professional Paper 1179, 20 p.

_____, 1985, Till stratigraphy in New Hampshire; Correlations with adjacent New England and Quebec, *in* Borns, H.W., Jr., and others, eds., Late Pleistocene history of northeastern New England and adjacent Quebec: Geological Society of America Special Paper 197, p. 1-12.

Krug, W.R., Gebert, W.A., Graczyk, D.J., Stevens, D.L., Rochelle, B.P., and Church, M.R., 1990, Map of mean annual runoff for the northeastern, southeastern, and mid-Atlantic United States, water years 1951-80: U.S. Geological Survey Water Resources Investigations Report 88-4094, 11 p.

Krumbein, W.C., and Monk, G.D., 1942, Permeability as a function of the size parameters of unconsolidated sand: Transactions of the American Institute of Mining and Metalurgical Engineers, v. 151, p. 153-163.

Kruseman, G.P., and deRidder, N.A., 1990, Analysis and evaluation of pumping-test data: Wageningen, the Netherlands, International Institute for Land Reclamation and Development, 377 p.

Ku, H.F.H., Randall, A.D., and MacNish, R.D., 1975, Streamflow in the New York part of the Susquehanna River basin: New York State Department of Environmental Conservation Bulletin 71, 130 p.

Lang, S.M., Bierschenk, W.H., and Allen, W.B., 1960, Hydraulic characteristics of glacial outwash in Rhode Island: Rhode Island Hydrologic Bulletin number 3, 38 p.

Langbein, W.B., and others, 1949, Annual runoff in the United States: U.S. Geological Survey Circular 52, 14 p.

Langbein, W.B., and Iseri, K.T., 1960, General introductions and hydrologic definitions: U.S. Geological Survey Water-Supply Paper 1541-A, 29 p.

Lapham, W.W., 1988, Yield and quality of ground water from stratified-drift aquifers, Taunton River basin, Massachusetts: U.S. Geological Survey Water-Resources Investigations Report 86-4053, 69 p.

_____, 1989, Use of temperature profiles beneath streams to determine rates of vertical ground-water flow and vertical hydraulic conductivity: U.S. Geological Survey Water Supply Paper 2337, 34 p.

LaSala, A.M., Jr., 1964, Geology and ground-water resources of the Bristol-Plainsville-Southington area, Connecticut: U.S. Geological Survey Water-Supply Paper 1578, 70 p.

_____, 1967, New approaches to water-resources investigations in upstate New York: Ground Water, v. 5, no. 4, p. 6-11.

_____, 1968, Ground-water resources of the Erie-Niagara basin, New York: New York State Conservation Department Basin Planning Report ENB-3, 114 p.

Lee, Richard, 1969, Latitude, elevation and mean temperature in the Northeast: Professional Geographer, v. 21, p. 227-231.

Leggette, R.M. and Jacob, C.E., 1938, Report on the water resources of Croton Valley, New York below Croton Dam: Albany, N.Y., U.S. Geological Survey Open File Report, 44 p.

Likens, G.E., Borman, F.H., Pierce, R.S., Eaton, J.S., and Johnson, N.M., 1977, Biogeochemistry of a forested ecosystem: New York, Springer-Verlag, 146 p.

Lins, H.F. and Michaels, P.J., 1994, Increasing U.S. streamflow linked to greenhouse forcing: EOS, Transactions American Geophysical Union, v. 75, no. 25, p. 281.

Lloyd, O.B., Jr., and Carswell, L.D., 1981, Groundwater resources of the Williamsport region, Lycoming County, Pennsylvania: Pennsylvania Geological Survey, 4th series, Water Resources Report 52, 69 p.

Lloyd, O.B., Jr., and Lyke, W.L., 1995, Ground-water atlas of the United States, segment 10: U.S. Geological Survey Hydrologic Investigations Atlas 730-K.

Lohman, S.W., 1939, Ground-water in north-central Pennsylvania: Pennsylvania Geologic Survey, 4th series, Bulletin W-6, 219 p.

_____, 1972, Ground-water hydraulics: U.S. Geological Survey Professional Paper 708, 70 p.

Lyford, F.P. and Cohen, A.J., 1988, Estimation of water-available-for-recharge to sand and gravel aquifers in the glaciated Northeastern United States, *in* Randall, A.D., and Johnson, A.I., (eds.), Regional Aquifer Systems of the United States, Northeast Glacial Aquifers: American Water Resources Association Monograph Series, no. 11, p. 37-61.

Lyford, F.P., Dysart, J.E., Randall, A.D., and Kontis, A.L., 1984, Glacial aquifer systems in the Northeastern United States—a study plan: U.S. Geological Survey Open-File Report 83-928, 31 p.

Mack, F.K., Pauszek, F.H. and Crippen, J.R., 1964, Geology and hydrology of the West Milton area, Saratoga County, New York: U.S. Geological Survey Water Supply paper 1747, 110 p.

Mack, T.J. and Lawlor S.M., 1992, Geohydrology and water quality of stratified-drift aquifers in the Bellamy, Cocheco, and Salmon Falls River Basins, Southeastern New Hampshire: U.S. Geological Survey, Water Resources Investigations Report 90-4161, 85 p.

MacNish, R.D., and Randall, A.D., 1982, Stratified-drift aquifers in the Susquehanna River basin, New York: New York State Department of Environmental Conservation Bulletin 75, 68 p.

Maevsky, Anthony, 1976, Ground-water levels in Massachusetts, 1936-74: Massachusetts Hydrology Data Report 17, 107 p.

Male, J.W., and Ogawa, Hisashi, 1982, Low flow of Massachusetts streams: Amherst, Mass., University of Massachusetts, Water Resources Research Center Publication 125, 152 p.

Martinec, J., 1975, Subsurface flow from snowmelt traced by tritium: Water Resources Research, vol. 11, no. 3, p 496-498.

Masch, F.O. and Denny, K.J., 1966, Grain-size distribution and its effect on the permeability of unconsolidated sands: Water Resources Research, v. 2, no. 4., p. 665-667.

Matalas, N.C., and Jacobs, Barbara, 1964, A correlation procedure for augmenting hydrologic data: U.S. Geologic Survey Professional Paper 434-E, 7 p.

Mayhew, G.H., 1985, Contamination investigation of the south well field for the city of Wooster, Ohio: Massilon, Ohio, Ohio Drilling Company, 17 p.

Mazzaferro, D.L., 1980, Ground-water availability and water quality in Farmington, Connecticut: U.S. Geological Survey Water Resources Investigations Report 80-751, 57 p.

_____, 1986a, Ground-water availability and water quality at Southbury and Woodbury, Connecticut: U.S. Geological Survey Water-Resources Investigations Report 84-4221, 105 p.

_____, 1986b, Ground-water yields for selected stratified-drift areas in Connecticut: Connecticut Geological and Natural Survey, Connecticut Natural Resources Atlas Series: Ground-water yields, 1:125,000, 1 sheet.

_____, 1989, Estimation of the recharge area of a pumped, stratified-drift aquifer in Connecticut by simulation modeling: U.S. Geological Survey Water Resources Investigations Report 87-4124, 100 p.

Mazzaferro, D.L., Handman, E.H., and Thomas, M.P., 1979, Water resources inventory of Connecticut, part 8, Quinnipiac River basin, Connecticut: Connecticut Water Resources Bulletin 27, 88 p.

McDonald, M.G., and Harbaugh, A.W., 1988, A modular three-dimensional finite difference ground-water flow model: U.S. Geological Survey Techniques of Water Resources Investigations, Book 6, Chapter A1, 586p.

McGuiness, J.L., and Bordne, E.F., 1972, A comparison of lysimeter-derived potential evapotranspiration with computed values: U.S. Department of Agriculture Technical Bulletin 1452.

Meade, D.B., 1978, Ground-water availability in Connecticut: Connecticut Geological and Natural History Survey, Natural Resources Atlas Series, 1:125,000, 1 sheet.

Meinzer, O.E., and Stearns, N.D., 1929, A study of ground water in the Pomperaug River basin, Connecticut: U.S. Geological Survey Water Supply Paper 597-B, p. 73-146.

Meisler, H.E., 1976, Computer simulation model of the Pleistocene valley-fill aquifer in southwestern Essex and southeastern Morris counties, New Jersey: U.S. Geological Survey Water Resources Investigations Report 76-25, 70 p.

Melvin, R.L., 1974, Hydrogeology of southeastern Connecticut: Connecticut Department of Finance and Control, Office of State Planning and Finance, 6 sheets.

Melvin, R.L., de Lima, V.A., and Stone, B.R., 1992, The stratigraphy and hydraulic properties of till in southern New England: U.S. Geological Survey Open-File Report 91-481, 53 p.

Miller, L.E., 1975, City of Wooster, Ohio survey for ground water supply potential, electrical resistivity methods in parts of Wooster and Franklyn Townships: Toledo, Ohio, Jones and Henry Engineers Ltd., 12 p.

_____, 1976, Aquifer performance evaluation and ground-water production potential of the city of Wooster, Ohio: Toledo, Ohio, Jones and Henry Engineers Ltd., 15 p.

Miller, L.M., and Associates, 1981, Pumping test analysis of the south well field-well no. S-2, Wooster, Ohio: Toledo, Ohio, Jones and Henry Engineers, Ltd., 15 p.

Miller, T.S., 1988a, Potential yields of wells in unconsolidated aquifers in upstate New York—Finger Lakes sheet: U.S. Geological Survey Water Resources Investigations Report 87-4122, 1:250,000.

_____, 1988b, Potential yields of wells in unconsolidated aquifers in upstate New York—Niagara sheet: U.S. Geological Survey Water Resources Investigations report 88-4076, 1:250,000.

Modica, Edward, Reilly, T.E., and Pollock, D.W., 1997, Patterns and age distribution of ground-water flow to streams: Ground Water, vol. 35, no. 3, p. 523-537.

Moench, A.F., 1995, Combining the Neuman and Boulton models for flow to a well in an unconfined aquifer: Ground Water, v. 33, no. 3, p. 378-384.

Moody, D.W., Chase, E.B., and Aronson, D.A., (compilers), 1986, National Water Summary 1985: U.S. Geological Survey Water Supply Paper 2300, 506 p.

Moore, J.E., and Jenkins, C.T., 1966, An evaluation of the effect of groundwater pumpage on the infiltration rate of a semipervious streambed: Water Resources Research, v. 2, no. 4, p. 691-696.

Moore, R.B., 1990, Geohydrology and water-quality of stratified drift aquifers in the Exeter, Lamprey, and Oyster River Basins, southeastern New Hampshire: U.S. Geological Survey Water Resources Investigation Report 88-4128, 60 p.

Moore, R.B., Johnson, C.D., and Douglas, E.M., 1994, Geohydrology and water quality of stratified-drift aquifers in the Lower Connecticut River Basins, Southwestern, New Hampshire: U.S. Geological Survey Water Resources Investigations Report 92-4013, 325 p.

Morris, D.A., and Johnson, A.I., 1967, Summary of hydrologic and physical properties of rock and soil materials, as analyzed by the hydrologic laboratory of the U.S. Geological Survey 1948-60: U.S. Geological Survey Water Supply Paper 1839-D, 39 p.

Morrissey, D.J., 1983, Hydrology of the Little Androscoggin River valley aquifer, Oxford County, Maine: U.S. Geological Survey Water Resources Investigations Report 83-4018, 79 p.

Morrissey, D.J., Randall, A.D., and Williams, J.H., 1988, Upland runoff as a major source of recharge to stratified drift in the glaciated Northeast, in Randall, A.D., and Johnson, A.I., eds., Regional Aquifer Systems of the United States, Northeast Glacial Aquifers: American Water Resources Association Monograph Series, no. 11, p. 17-36.

Multer, H.G., 1967, Bedrock geology of Wayne County: Ohio Geological Survey, Report of Investigations 61, 1 sheet.

Mustonen, S.E., and McGuinness, J.L., 1968, Estimating evapotranspiration in a humid region: U.S. Department of Agricultural Technical Bulletin 1389, 123 p.

Myette, C.F., Olimpio, J.C., and Johnson, D.G., 1987, Area of influence and zone of contribution to Superfund-site wells G and H, Woburn, Massachusetts: U.S. Geological Survey Water Resources Investigations Report 87-4100, 21 p.

Myette, C.F., and Simcox, A.C., 1989, Water resources and aquifer yields in the Charles River Basin, Massachusetts: U.S. Geological Survey Water-Resources Investigations Report 88-4173, 53 p.

National Oceanic and Atmospheric Administration, 1966-84, Climatological data New York and Climatological data New England: National Climatic Data Center, Asheville, N.C.

National Oceanic and Atmospheric Administration, 1981, Divisional normals and standard deviations of temperature °F and precipitation (inches), 1931-80: Asheville, N.C., National Climate Center, Climatography of the United States no. 85, 196 p.

_____, 1982, Monthly normals of temperature, precipitation and heating and cooling degree days, 1951-1980: U.S. National Oceanic and Atmospheric Administration, Climatography of the United States no. 81, New Jersey, 7 p.

_____, 1983-85, Climatological data New Jersey: Asheville, N.C., National Climatic Data Center, (1983) v. 95, no. 13; (1984) v. 96, no. 13; (1985) v. 97, no. 13.

_____, 1985a, Climatic summaries for selected sites, 1951-80: Climatography of the United States, no. 20 [Separate publication for each state].

_____, 1985b, Climatological Data Annual Summary, New England, New Jersey, New York, Pennsylvania and Ohio: National Climatic Data Center, Asheville, N.C., v. 97, no. 13.

Nemickas, Bronius, 1976, Geological and ground-water resources of Union County, New Jersey: U.S. Geological Survey Water-Resources Investigations 76-73, 103 p.

Neuman, S.P., 1972, Theory of flow in unconfined aquifers considering delayed response of the water table: Water Resources Research, v. 8, no. 4, p. 1031-1044.

_____, 1975, Analysis of pumping test data from anisotropic unconfined aquifers considering delayed gravity response: Water Resources Research, v. 11, no. 2, p. 329-342.

_____, 1987, On methods of determining specific yield: Ground Water, v. 25, no. 6, p. 679-684.

_____, 1988, Reply to discussion by Z. Sen of "On methods of determining specific yield": Ground Water, vol. 26, no. 5, p. 651-653.

Newman, W.A., Berg, R.C., Rosen, P.S., and Glass, H.D., 1990, Pleistocene stratigraphy of the Boston Harbor drumlins, Massachusetts: Quaternary Research, v. 34, p. 148-159.

Norris, S.E., 1970, The effect of stream discharge on streambed leakance to a glacial outwash aquifer: U.S. Geological Survey Professional Paper 700-D, p. 262-265.

Norris, S.E., and Spieker, A.M., 1962, Seasonal temperature changes in wells as indicators of semiconfining beds in valley-train aquifers: U.S. Geological Survey Professional Paper 450B, p. 101-2.

_____, 1966, Ground-water resources of the Dayton area, Ohio: U.S. Geological Survey Water Supply Paper 1808, 167p.

Norvitch, R.F. and Lamb, M.E.S., 1966, Records of selected wells, springs, test holes, materials tests, and chemical analyses of water in the Housatonic River basin, Massachusetts: U.S. Geological Survey open-file report, 40 p.

Norvitch, R.F., Farrell, D.F., Pauszek, F.H., and Peterson, R.G., 1968, Hydrology and Water Resources of the Housatonic River basin, Massachusetts: U.S. Geological survey Hydrologic Investigations Atlas HA-281, 1:125,000, 4 sheets.

Nwankwor, G.I., Cherry, J.A., and Gillham, R.W., 1984, A comparative study of specific yield determinations for a shallow sand aquifer: Ground Water, v. 22, no. 6, p. 764-772.

Olcott, P.G., 1995, Ground-water atlas of the United States, Connecticut, Maine, Massachusetts, New Hampshire, New York, Rhode Island, Vermont: U.S. Geological Survey Hydrologic Investigations Atlas 730-M, 28 p.

Olimpio, J.C., and deLima, V.A., 1984, Ground-water resources of the Mattapoisett River Valley, Plymouth County, Massachusetts: U.S. Geological Survey Water Resources Investigations Report 84-4043, 83 p.

Olmsted, F.H., and Hely, A.G., 1962, Relation between ground water and surface water in Brandywine Creek Basin Pennsylvania: U.S. Geological survey Professional Paper 417-A, 21 p.

Olney, S.L., 1983, An investigation of the relationship between the coefficient of permeability and effective grain size of unconsolidated sands: Boston, Boston University, Ms. thesis, 61 p.

Ohio Drilling Company, 1971, Ground-water potential, Northeast Ohio: Massilon, Ohio, Ohio Drilling Co., Report to Ohio Department of Natural Resources, 360 p.

Osberg, P.H., Hussey, A.M., and Boone, G.M., 1984, Bedrock geologic map of Maine, scale 1:500,000.

Palmer, W.C., 1965, Meteorologic drought: U.S. Weather Bur., Res. Pap. 45, 58 pp.

Palmer, A.N., Rubin, P.A., and Palmer, M.V., 1991, Interaction between karst and glaciation in the Helderberg Plateau, Schoharie and Albany Counties, New York, *in* Ebert, J.R., ed., Field Trip Guidebook: New York Geological Association, 63rd Annual Meeting, P. 161-190.

Paulson, Q.F., 1965, Geologic factors affecting discharge of the Sheyenne River in southeastern North Dakota: U.S. Geological Survey Professional Paper 501D, p. D177-D181.

Perlmutter, N.M., 1959, Geology and ground-water resources of Rockland County, New York: New York State Water Power and Control Commission Bulletin GS-42, 133 p.

_____, 1962, Ground-water geology and hydrology in the Maynard area, Massachusetts, with a section on an aquifer test in deposits of glacial outwash, *by* N.J. Lusczynski: U.S. Geological Survey Water-Supply Paper 1539-E, 69 p.

Pessl, F., Jr., and Schafer, J.P., 1968, Two-till problem in Naugatuck-Torrington area, western Connecticut, Trip B-1, *in* Orville, P.M., ed.,

Guidebook for field trips in Connecticut: New England Intercollegiate Geological Conference, 60th Annual Meeting, New Haven, Conn., Connecticut Geological and Natural History Survey Guidebook no. 2, p. 1-25.

Pettyjohn, W.A., and Henning, R., 1979, Preliminary estimate of groundwater recharge rates, related streamflow and water quality in Ohio: State of Ohio Water Resources Center, The Ohio State University, Project Completion Report No. 552, 323 p.

Pluhowski, E.J. and Kantrowitz, I.H., 1964, Hydrology of the Babylon-Islip area, Suffolk County, Long Island, New York: U.S. Geological Survey Water-Supply Paper 1768, 119 p.

Poth, C.W., 1963, Geology and hydrology of the Mercer quadrangle, Mercer, Lawrence, and Butler Counties, Pennsylvania: Pennsylvania Geological Survey, 4th series, Water Resources Report W-16, 149 p.

Potter, S.T., and Gburek, W.J., 1987, Seepage face simulation using PLASM: Ground Water, v. 25, no. 6, p. 722-732.

Prescott, G.C., Jr., 1966, Surficial geology and availability of ground water in the Lower Penobscot River basin, Maine: U.S. Geological Survey Hydrologic Investigations Atlas HA-225, 3 p., 1:62,500, 1 sheet.

_____, 1973, Ground-water favorability and surficial geology of the lower St. John River valley, Maine: U.S. Geological Survey, Hydrologic Atlas HA-485, 1:62,500, 1 sheet.

Prickett, T.A., 1965, Type-curve solution to aquifer tests under water table conditions: Ground Water, v. 3, no. 3, p. 5-14.

Prill, R.C., Johnson, A.I., and Morris, D.A., 1965, Specific yield—laboratory experiments showing the effect of time on column drainage: U.S. Geological Survey Water-Supply Paper 1662-B, 55 p.

Prudic, D.E., 1986, Ground-water hydrology and subsurface immigration of radionuclides at a commercial radioactive-waste burial site, West Valley, Cattaragus County, New York: U.S. Geological Survey Professional Paper 1325, 83 p.

Prudic, D. E., 1989, Documentation of a computer program to simulate stream-aquifer relations using a modular, finite difference, groundwater flow model: U.S. Geological Survey Open-File Report 88-729, 113 p.

Quinn, A.W., and others, 1948, The geology and ground-water resources of the Pawtucket quadrangle, Rhode Island: Rhode Island Industrial Commission, Rhode Island Geologic Bulletin 3, 85 p.

Rahn, P.H., 1968, The hydrology of an induced streambed infiltration area (Connecticut): Ground Water, v.6, no. 3, p.21-32.

Randall, A.D., 1964, Geology and ground water in the Farmington-Granby area, Connecticut: U.S. Geological Survey Water Supply Paper 1661, 129 p.

Randall, A.D., 1970, Movement of bacteria from river to municipal well—a case history: Journal American Water Works Association, v. 62, no. 11, p. 716-720.

_____, 1972, Records of wells and test borings in the Susquehanna River basin, New York: New York State Department of Environmental Conservation Bulletin 69, 92 p.

_____, 1977; The Clinton Street-Ballpark aquifer in Binghamton and Johnson City, New York: New York State Department of Environmental Conservation Bulletin 77, 87 p.

_____, 1978, Infiltration from tributary streams in the Susquehanna River basin, New York: U.S. Geological Survey Journal of Research, v. 6, no. 3, p. 285-297.

_____, 1979, Ground water in Dale Valley, New York: U.S. Geological Survey Water Resources Investigations Report 78-120, 85 p.

_____, 1986, Aquifer model of the Susquehanna River valley in southwestern Broome County, New York: U.S. Geological Survey Water Resources Investigations Report 85-4099, 38 p.

Randall, A.D., (2001), Hydrogeologic framework of stratified-drift aquifers in the glaciated northeastern United States, U.S. Geological Survey Professional Paper 1415-B.

Randall, A.D., and Johnson, A.I., 1988, The northeast glacial aquifers RASA project—an overview of results through 1987, *in* Randall, A.D., and Johnson, A.I., eds., Regional Aquifer Systems of the United States, Northeast Glacial Aquifers: American Water Well Association Monograph Series, no. 11, p. 1-15.

Randall, A.D., Francis, R.M., Frimpter, M.H., and Emery, J.M., 1988a, Region 19, Northeastern Appalachians, *in* Back, William, Rosenshein, J.S., and Seaber, P.R., (eds.), Hydrogeology: Boulder, Colo., Geological Society of America, The Geology of North America, v. 0-2, p. 177-187.

Randall, A.D., Snavely, D.S., Holecek, T.J., and Waller, R.M., 1988b, Alternative sources of large seasonal ground-water supplies in the headwaters of the Susquehanna River basin, New York: U.S. Geological Survey Water Resources Investigations Report 85-4127, 121 p.

Randall, A.D., Thomas, M.P., Thomas, C.E., Jr., and Baker, J.A., 1966, Water resources inventory of Connecticut, part 1, Quinnebaug River basin: Connecticut Water Resources Bulletin 8, 99 p.

Rasmussen, W.C., and Andreasen, G.E., 1959, A hydrologic budget of the Beaverdam Creek basin, Maryland: U.S. Geological Survey Water-Supply Paper 1472, 106 p.

Rau, J.L., 1969, Hydrogeology of the Berea and Cussewago Sandstones in northeastern Ohio: U.S. Geological Survey Hydrologic Investigations Atlas HA-341, scale 1:250,000, 2 sheets.

Razack, Moumtaz, and Huntley, David, 1991, Assessing transmissivity from specific capacity in a large and heterogeneous alluvial aquifer: Ground Water, vol. 29, no. 6, p. 856-861.

Razem, A.C., 1983, Simulations of non-steady flow in a glacial outwash aquifer, southern Franklin County, Ohio: U.S. Geological Survey Water-Resources Investigations Report 83-4022, 17 p.

Reilly, T.E., Buxton, H.T., Franke, O.L., and Wait, R.L., 1983, Digital model study of the effects of sanitary sewers on ground-water levels and streams, Nassau and Suffolk Counties, part 1--Geohydrology, modeling strategy, and regional evaluation: U.S. Geological Survey Water-Resources Investigations Report 82-4045, 45 p.

Reilly, T.E. and Harbaugh, A.W., 1993, Simulation of cylindrical flow to a well using the U.S. Geological Survey modular finite-difference ground-water flow model: Ground Water, v. 31, no. 3, p. 489-494.

Reisenauer, A.E., 1977, Ground-water model application to the Chemung River basin 208 study area, New York State: Richland, Wash., Batelle Pacific Northwest Laboratories, 57 p.

Reynolds., R.J., 1987, Hydrogeology of the surficial outwash aquifer at Cortland, Cortland County, New York: U.S. Geological Survey Water Resources Investigations Report 85-4090, 43 p.

Reynolds, R.J. and Brown, G.A., 1984, Hydrogeologic appraisal of a stratified-drift aquifer near Smyrna, Chenango County, New York: U.S. Geological Survey Water Resources Investigations Report 84-4029, 53 p.

Reynolds, R.J., and Garry, J.D., 1990, Hydrogeology of the valley-fill aquifer, Owego, Tioga County, New York: U.S. Geological Survey Water Resources Investigations Report 89-400, 1:24,000, 8 sheets.

Richards, D.B., McCoy, H.J., and Gallaher, J.T., 1987, Groundwater resources of Erie County, Pennsylvania: Penna. Department of Environmental Resources, Water Resources Report 62, 101 p. plus maps.

Riser, D.W., and Madden, T.W., Jr., 1994, Evaluation of methods for delineating areas that contribute water to wells completed in valley-fill aquifers in Pennsylvania: U.S. Geological Survey Open-File Report 92-635, 82 p.

Roberts, C.M., and Brashears, M.L., Jr., 1945, Progress report on the groundwater resources of Providence, Rhode Island: Rhode Island Industrial Commission, Rhode Island Geologic Bulletin 1, 35 p.

Robinson, T.W., 1958, Phreatophytes: U.S. Geological Survey Water-Supply Paper 1423, 84 p.

Rogers, R.J., 1989, Geochemical comparison of ground water in areas of New England, New York, and Pennsylvania, Ground Water, v. 27, no. 5, p. 690-712.

Rorabaugh, M.I., 1964, Estimating changes in bank storage and ground-water contribution to streamflow: International Association of Scientific Hydrology Publication 63, p. 432-441.

Rose, H.G., and Smith, H.F., 1957, A method for determining permeabilities and specific capacity from effective grain size: Water Well Journal, v. 11, no. 3, p. 10-11.

Rosenshein, J.S, Gonthier, J.B, and Allen, W.B., 1968, Hydrologic characteristics and sustained yield of principal ground-water units Potowomut-Wickford area, Rhode Island: U.S. Geological Survey Water Supply Paper 1775, 38 p.

Rutledge, A.T., 1993, Computer programs for describing the recession of ground-water discharge and for estimating mean ground-water recharge and discharge from streamflow records: U.S. Geological Survey Water Resources Investigations Report 93-4121, 45 p.

Ryder, R.B., Cervione, M.A., Jr., Thomas, C.E., Jr., and Thomas, M.P., 1970, Water resources inventory of Connecticut, part 4, southwestern coastal river basins: Connecticut Water Resources Bulletin 17, 54 p.

Ryder, R.B., Thomas, M.P., and Weiss, L.A., 1981, Water Resources Inventory of Connecticut, part 7, Upper Connecticut River basin: Connecticut Water Resources Bulletin 24, 78p.

Sammel, E.A., Baker, J.A., and Brackley, R.A., 1966, Water resources of the Ipswich River basin, Massachusetts: U.S. Geological Survey Water Supply Paper 1826, 82 p.

Schicht, R.J., and Walton, W.C., 1961, Hydrologic budgets for three watersheds in Illinois: Illinois State Water Survey Report of Investigations 40, 40 p.

Schiner, G.R., and Gallaher, J.T., 1979, Geology and ground-water resources of western Crawford County, Pennsylvania: Pennsylvania Geological Survey, 4th series, Water Resources Report 46, 103 p.

Schneider, W.J., 1957, Relation of geology to streamflow in the uppper Little Miami basin: Ohio Jour. of Science, v. 57, no. 1, p. 11-14.

Schneider, W.J., 1965, Areal variability of low flows in a basin of diverse geologic units: Water Resources Research, vol. 1, p. 509-515.

Shepherd, R.G., 1989, Correlations of permeability and grain size: Ground Water, v. 27, no. 5, p. 633-638.

Shepps, V.C., White, G.W., Droste, J.B., and Sitler, R.F., 1959, The glacial geology of northwestern Pennsylvania: Pennsylvania Geological Survey, 4th series, Bulletin G32, 59 p., 1:125,000, 1 sheet.

Silvey, W.D., and Johnston, H.E., 1977, Preliminary study of sources and processes of enrichment of manganese in water from University of Rhode Island supply wells: U.S. Geological Survey Open-File Report 77-561, 33 p.

Sklash, M.G., and Farvolden, R.N., 1982, The use of isotopes in the study of high-runoff episodes in streams, *in* Perry, E.C., Jr. and Montgomery, C.W. (eds.), Isotope studies in hydrologic processes: DeKalb, Ill., Northern Illinois University Press, p. 65-73.

Smith, R.C., and White, G.W., 1953, The ground-water resources of Summit County, Ohio: Columbus, Ohio Department of Natural Resources, Division of Water, Bulletin 27, 130 p.

Snavely, D.S., 1983, Ground-water appraisal of the Pine Bush area, Albany County, New York: U.S. Geological Survey Water Resources Investigations Report 82-4000, 47 p.

Socolow, R.S., Frimpter, M.H., Turtora, Michael, and Bell, R.W., 1994, A technique for estimating ground-water levels at sites in Rhode Island from observation-well data: U.S. Geological Survey Water-Resources Investigations Report 94-4138, 43 p.

Soller, D.R., 1993, Map showing the thickness and character of Quaternary sediments in the glaciated United States east of the Rocky Mountains: U.S. Geological Survey, map I-1970A, B, C, D, scale 1:1,000,000.

Springer, A.E., 1987, A hydrogeologic evaluation of the ground water resources of Wooster, Ohio: Wooster, Ohio, The College of Wooster, senior thesis, 78 p.

_____, 1990, An evaluation of well field protection area delineation methods as applied to municipal wells in the stratified-drift aquifer at Wooster, Ohio: Columbus, Ohio, Ohio State University, Ms. thesis, 167 p.

Springer, A.E., and Bair, E.S., 1990, The effectiveness of semianalytical methods for delineating well field protection areas in stratified-drift buried-valley aquifers: Ground Water Management, v. 1, p. 413-429.

_____, 1992, Comparison of methods used to delineate capture zones of wells: 2. Stratified-drift buried-valley aquifer: Ground Water, v. 30, no. 6, p. 908-917.

Stanford, S.D., 1989, Surficial geology of the Dover Quadrangle, New Jersey: New Jersey Geological Survey, New Jersey Geologic Map Series 89-2, 1:24,000, 1 sheet.

Stanford, S.D., Witte, R.W., and Harper, D.P., 1990, Hydrogeologic character and thickness of the glacial sediment of New Jersey: New Jersey Geological Survey Open-File Map 3, 1:100,000, 2 sheets.

Stekl, P.J., and Flanagan, S.M., 1992, Geohydrology and water quality of stratified-drift aquifers in the Lower Merrimack and Coastal River Basins, Southeastern, New Hampshire: U.S. Geological Survey Water-Resources Investigations Report 91-4025, 93 p.

Stephenson, D.A., Fleming, A.H., and Mickelson, D.M., 1988, Glacial deposits, *in* Back, William, Rosenshein, J.S., and Seaber, P.R., (eds.), Hydrogeology: Boulder, Colo., Geological Society of America, The Geology of North America, v. O-2, p. 301-314.

Stewart, D.P., and MacClintock, P., 1969, The surficial geology and Pleistocene history of Vermont: Vermont Geological Survey Bulletin 31, 251 p.

Stone, E.L., and Kalisz, P.J., 1991, On the maximum extent of tree roots: Forest ecology and management vol. 46, p. 59-102.

Stout, B.B., 1956, Studies of the root system of deciduous trees: Black Rock Forest Bull. 15, 45 pp.

Sun, Ren Jen, (ed.), 1986, Regional aquifer-system analysis program of the U.S. Geological Survey—Summary of projects, 1978-84: U.S. Geological Survey Circular 1002, 264 p.

Sun, Ren Jen, and Weeks, J.B., 1991, Bibliography of Regional Aquifer-System analysis program of the U.S. Geological Survey, 1978-91: U.S. Geological Survey Water Resources Investigations Report 91-4122, 92 p.

Sun, Ren Jen, and Johnston, R.H., 1994, Regional Aquifer-System Analysis Program of the U.S. Geological Survey, 1978-1992: U.S. Geological Survey Circular 1099, 126 p.

Talkington, R.W., and O'Brien J.B., 1991, The geologic and hydrogeologic setting of the artesian Tolan Farm well, Montague, Massachusetts: Proceedings of the Focus Conference on Eastern Regional Ground Water Issues, book 7, p. 443-455.

Tasker, G.D., 1972, Estimating low-flow characteristics of streams in southeastern Massachusetts from maps of ground-water availability, *in* Geological Survey Research, 1972: U.S. Geological Survey Professional Paper 800D, p. D217-D220.

Taylor, L.E., 1988, Ground-water resources of the Chemung River basin, New York and Pennsylvania: Susquehanna River Basin Commission Publication 115, 226 p.

Tepper, D.H., Morrissey, D.J., Johnson, C.D., and Maloney, T.J., 1990, Hydrogeology, water quality, and effects of increased municipal pumpage of the Saco River valley glacial aquifer—Bartlett, New Hampshire to Fryeburg, Maine: U.S. Geological Survey Water Resources Investigations Report 88-4179, 113 p.

Theim, Gunther, 1906, Hydrologic Methods: Leipzig [Germany], J.M. Gebhart, 56 p.

Theis, C.V., 1935, The relation between the lowering of the piezometric surface and the rate and duration of discharge of a well using ground-water storage: Transactions of the American Geophysical Union, v. 16, p. 519-524.

Theis, C.V., Brown, R.H., and Meyer, R.R., 1963, Estimating the transmissibility of aquifers from the specific capacity of a well, *in* Bentall, Ray (compiler), Methods of determining permeability, transmissibility, and drawdown: U.S. Geological Survey Water Supply Paper 1536-I, p. 332-336.

Thomas, C.E., Jr., Randall, A.D., and Thomas, M.P., 1966, Hydrogeologic data for the Quinebaug River basin, Connecticut: Connecticut Water Resources Bulletin no. 9, 84 p.

Thomas, C.E., Jr., Bednar, G.A., Thomas, M.P., and Wilson, W.E., 1967, Hydrogeological data for the Shetucket River basin, Connecticut: Connecticut Water Resources Bull. No. 12.

Thomas, C.E., Jr., Cervione, M.A., Jr., and Grossman, I.G., 1968, Water resources inventory of Connecticut, part 3, lower Thames and southeastern coastal river basins, Connecticut: Connecticut Water Resources Bulletin 15, 105 p.

Thomas, H.A., 1981, Improved methods for National Water Assessment, report, contract WR15249270, U.S. Water Resour. Counc., Washington, D.C.

Thomas, M.P., 1966, Effect of glacial geology upon the time distribution of streamflow in eastern and southern Connecticut: U.S. Geological Survey Professional Paper 550-B, p. B209-B212.

Thomas, M.P., Bednar, G.A., Thomas, C.E., Jr., and Wilson, W.E., 1967, Water resources inventory of Connecticut, part 2, Shetucket River basin: Connecticut Water Resources Bulletin 11, 96 p.

Thompson, W.B., and Borns, H.W., Jr., editors, 1985, Surficial geologic map of Maine: Maine Geological Survey, 1:500,000, 1 sheet.

Thornthwaite, C.W., 1948, An approach toward a national classification of climate: Geological Review, v. 38., p. 55-94.

Thornthwaite, C.W., and Mather, J.R., 1955, The water balance: Publ. Climatol. Lab. Climatol. Drexel Inst. Technol., no. 8, vol 1, p. 1-104.

_____, 1957, Instructions and tables for computing potential evapotranspiration and the water balance: Publ. Climatol. Lab. Climatol. Drexel Inst. Technol., no. 10, vol. 3, p. 185-311.

Todd, D.K., (ed.), 1970, The water encyclopedia: Port Washington, N.Y., Water Information Center, 559 p.

_____, 1980, Groundwater Hydrology, second edition: New York, John Wiley and Sons, 535 p.

Tolman, A.L., Tepper, D.H., Prescott, G.C., Jr., and Gammon, S.C., 1983, Hydrogeology of significant sand and gravel aquifers - northern York and southern Cumberland Counties, Maine: Maine Geological Survey Open-File Report 83-1, 4 pl.

Toppin, K.W., 1987, Hydrogeology of stratified-drift aquifers and water quality in the Nashua regional planning commission area, south-central New Hampshire: U.S. Geological Survey Resources Investigations Report 86-4358, 101 p.

Trainer, F.W., 1988, Plutonic and metamorphic rocks, *in* Back, William, Rosenshein, J.S., and Seaber, P.R., eds., Hydrogeology: Boulder, Colo., Geological Society of America, The Geology of North America, v. O-2, p. 367-380.

Trainer, F.W., and Salvas, E.H., 1962, Ground-water resources of the Massena-Waddington area, St. Lawrence County, New York, with emphasis on the effect of Lake St. Lawrence on ground water: New York State Water Resources Commission Bulletin GW-47, 227 p.

Turcan, A.N., Jr., 1963, Estimating the specific capacity of a well: U.S. Geological Survey Professional Paper 450-E, p. E145-E149.

U.S. Army Corps of Engineers, 1978, Passaic River basin study: New York District, U.S. Army Engineers, multiple map sheets, 1:2,400 scale.

U.S. Environmental Data Service, 1968, Climatic atlas of the United States: Washington, D.C., U.S. Department of Commerce, Environmental Science Services Administration, 80 p.

U.S. Geological Survey, 1990, National Water Summary 1987—Hydrologic events and water supply: U.S. Geological Survey Water-Supply Paper 2350, 553 p.

U.S. Geological Survey, 1997, Water Resources Data Massachusetts and Rhode Island, Water Year 1996: U.S. Geological Survey Water-data report Ma-RI-96-1, 367 p. [Similar reports published for Maine, New Hampshire and Vermont, Connecticut, New York, New Jersey, Pennsylvania, and Ohio for each year since 1961.]

van der Heijde, P.K.M., El-Kadi, A.I., and Williams, S.A., 1988, Groundwater modeling—an overview and status report: U.S. Environmental Protection Agency, EPA/600/2-89/028, 242 p.

Vecchioli, John, and Nichols, W.D., 1966, Results of the drought-disaster test-drilling program near Morristown, N.J.: New Jersey Department of Environmental Protection, Water Resources Circular 16, 48 p.

Walker, A.C., 1979a, Ground-water resources of Portage County: Ohio Department of Natural Resources, Division of Water, County groundwater resource map, 1:62,500, 1 sheet.

_____, 1979b, Ground-water resources of Stark County: Ohio Department of Natural Resources, Division of Water, County ground-water resource map, 1:62,500, 1 sheet.

Waller, R.M., and Finch, A.J., 1982, Atlas of eleven selected aquifers in upstate New York: U.S. Geological Survey Open-File Report 82-553, 255 p.

Walton, W.C., 1962, Selected analytical methods for well and aquifer evaluation: Illinois State Water Survey Bulletin 49, 81 p.

_____, 1970, Groundwater resource evaluation: New York, McGraw-Hill, 664 p.

_____, 1987, Groundwater pumping tests, design and analysis: Chelsea, Mich., Lewis Publishers, 201 p.

Wandle, S.W., Jr., and Randall, A.D., 1994, Effects of surficial geology, lakes and swamps, and annual water availability on low flows of streams in central New England, and their use in low flow estimation: U.S. Geological Survey Water-Resources Investigations Report 93-4092, 57 p.

Weaver, M.F., 1987, Availability of ground water from selected stratified-drift aquifers in southwestern Connecticut: Connecticut Water Resources Bulletin 33B, 63 p.

Weigle, J.M., and Kranes, Richard, 1966, Records of selected wells, springs, test holes, materials tests, and chemical analyses of water in the lower Merrimack River valley in New Hampshire: New Hampshire Basic-Data Report 2, U.S. Geological Survey open-file report, 44 p., 1 pl.

Weiss, E.J., and Razem, A.C., 1980, A model for flow through a glacial outwash aquifer in southeast Franklin County, Ohio: U.S. Geological Survey Water Resources Investigations 80-56, 27 p.

Weiss, L.A., Bingham, J.W., and Thomas, M.P., 1982, Water resources inventory of Connecticut, part 10, lower Connecticut River basin, Connecticut: Connecticut Water Resources Bulletin 31, 85 p.

Wenzel, L.K., 1942, Methods for determining permeability of water-bearing materials, with special reference to discharging-well methods: U.S. Geological Survey Water Supply Paper 887, 192 p.

Wetterhall, W.S., 1959, The ground-water resources of Chemung County, New York: New York State Water Power and Control Commission Bulletin GW-40, 58 p.

White, W.N., 1932, A method of estimating groundwater supplies based on discharge by plants and evaporation from soil: U.S. Geological Survey Water Supply Paper 659-A, p. 1-105.

White, G.W., 1967, Glacial geology of Wayne County, Ohio: State of Ohio, Division of Geological Survey, Report of Investigations no. 62, 39 p.

_____, 1982, Glacial geology of northeastern Ohio: Ohio Geological Survey Bulletin No. 68, 75 p.

Willey, R.E., and Butterfield, D., 1983, Ground-water resources of the Rutland area, Vermont: U.S. Geological Survey Water Resources Investigations Report 82-4057, 38 p.

Williams, J.H., 1991, Tributary stream infiltration in Marsh Creek valley, north-central Pennsylvania: U.S. Geological Survey Water Resources Investigations Report 90-4052, 39 p.

Williams, J.H., Taylor, L.E., and Low, D.J., 1993, Hydrogeology and groundwater quality of the glaciated valleys of Bradford, Tioga and Potter Counties, Pennsylvania: Pennsylvania Geological Survey Water Resources Report.

Williams, J.H. and Morrissey, D.J., 1996, Recharge of valley-fill aquifers in the glaciated Northeast from upland runoff, *in* Ritchie, J.D. and Rumbaugh, J.O. (eds.), Subsurface fluid-flow (ground-water and vadose

zone) modeling: Philadelphia, American Society for Testing and Modeling, STP 1288, p. 97-113.

Williams, J.R., 1968, Availability of ground-water in the northern part Ten-mile and Taunton River basins southeastern Massachusetts: U.S. Geological Survey Hydrologic Investigations Atlas HA-300, 1:31,680, 1 sheet.

Williams, J.R., Farrell, D.F., and Willey, R.E., 1973, Water resources of the Taunton River basin, southeastern Massachusetts: U.S. Geological Survey Hydrologic Investigations Atlas HA-460, 3 sheets.

Williams, J.R., and Tasker, G.D., 1974a, Water resources of the coastal drainage basins of southeastern Massachusetts, Plymouth to Weweantic River, Wareham: U.S. Geological Survey Hydrologic Investigations Atlas HA-507, 2 sheets.

_____, 1974b, Water resources of the coastal drainage basins of southeastern Massachusetts, Weir River, Hingham, to Jones River, Kingston: U.S. Geological Survey Hydrologic Investigations Atlas HA-504, 1:48,000, 2 sheets.

Wilson, W.E., Ryder, R.B., and Thomas, C.E., Jr., 1968, Hydrogeology of southwestern Connecticut, *in* New England Intercollegiate Geological Conference Guidebook for Field Trips in Connecticut: State Geological and Natural History Survey of Connecticut, Guidebook 2, no. 3, p. 1-33.

Wilson, W.E., Burke, E.L., and Thomas, C.E., Jr., 1974, Water resources inventory of Connecticut, part 5, lower Housatonic River basin: Connecticut Water Resources Bulletin 19, 79 p.

Wiltshire, D.A., Lyford, F.P., and Cohen, A.J., 1986, Bibliography on ground-water in the glacial-aquifer systems in the northeastern United states: U.S. Geological Survey Circular 972, 26 p.

Winslow, J.D., Stewart, H.G., Jr., Johnston, R.H., and Crain, L.J., 1965, Ground-water resources of eastern Schenectady County, New York with emphasis on infiltration from the Mohawk River: New York State Water Resources Commission Bulletin 57, 148 p.

Wolf, S.H., Celia, M.A., and Hess, K.M., 1991, Evaluation of hydraulic conductivities calculated from multiport-permeameter measurements: Ground Water, v. 29, no. 4, p. 516-525.

Wright Associates, Inc., 1982, Special groundwater study of the upper Delaware River basin, study area 3, volume 1: Middletown, Penna., Report prepared for the Delaware River Basin Commission, 5 chapters.

Wyrick, G.G., and Borchers, J.J., 1981, Hydrologic effects of stress-relief fracturing in an Appalachian valley: U.S. Geological Survey Water-Supply Paper 2177, 51 p.

Yager, R.M., 1986, Simulation of ground-water flow from the Susquehanna River to a shallow aquifer at Kirkwood and Conklin, Broome County, New York: U.S. Geological Survey Water Resources Investigations Report 86-4123, 70 p.

_____, 1993, Estimation of hydraulic conductivity of riverbed and aquifer system on the Susquehanna River in Broome County, New York: U.S. Geological Survey Water-Supply Paper 2387, 49 p.